Sheffield Hallam University

A Sheffield Hallam University thesis

REFERENCE

ProQuest Number: 10701004

ProQuest 10701004

Published by ProQuest LLC (2017). Copyright of the Dissertation is held by the Author.

ProQuest LLC.
789 East Eisenhower Parkway
P.O. Box 1346
Ann Arbor, MI 48106 – 1346

Interactions at the Clay/Polymer/Water Interface

Nigel Ivor Edward Shewring

A thesis submitted in partial fulfilment of the
requirements of Sheffield Hallam University for the
degree of Doctor of Philosophy

December 1998

Colaborating Organisation:

Schlumberger Cambridge Research
High Cross
Madingley Road
Cambridge CB3 0EL

DECLARATION

The work carried out in this thesis was carried out by me in the Chemistry Department in the University of Durham, in the Materials Research Institute in Sheffield Hallam University and at Sclumberger Cambridge Research, Cambridge, between October 1992 and December 1998. I declare that this work has not been accepted in substance for any other degree, and is not being concurrently submitted for candidature for any other degree. The work is original except where indicated by reference.

Signed _____

Date   _____

<u>ACKNOWLEDGEMENTS</u>

ABSTRACT

The thesis investigates the behaviour of aqueous montmorillonite suspensions and also the interactions between montmorillonite as a free standing film and in highly dispersed aqueous suspension with water soluble polymers used as additives in water based drilling fluids.

FTIR microscopy and FTIR ATR spectroscopy have been employed to study in-situ dehydration of fully dispersed aqueous montmorillonite suspensions. The IR spectrum of the dispersed bentonite shows significant differences from that of a dry bentonite powder, which have been attributed to the hydration of the exchangeable cation. Drying, or concentrated salt solution causes the differences to disappear and this is attributed to the exchangeable cation settling back to its ditrigonal cavity in the silicate sheet of the mineral under these conditions.

The adsorption of various molecular weights of neutral polyacrylamide (PAM) onto montmorillonite has been studied using FTIR transmission, ATR spectroscopy and XRD. Shifts seen in the NH_2 stretching and bending bands have been interpreted as being due to H-bonding with the outer co-ordination sphere of exchangeable cations. KCl has shown to have some influence on this system.

Another neutral polymer used extensively in water based drilling fluids is polyalkylglycol (PAG). The adsorption of two molecular weights of this polymer from aqueous solutions of various concentrations have been monitored both in the presence and absence of KCl. The physical form of the montmorillonite (either as a free standing film or as a dispersed suspension), the concentration of the polymer solution, the polymer molecular weight and the presence of KCl all have significant effects on the adsorption of polymer.

The stabilisation of montmorillonite films by PAG and PAG/KCl solutions has been monitored by ATR spectroscopy, and the dehydration of these films by polymer has been monitored using FTIR spectroscopy and XRD. The interaction of PAG is thought to be via hydrogen bonding with the innermost co-ordination sphere of the exchangeable cations which thus presents a hydrophobic surface to solvent molecules, preventing the film from collapse.

Since all water based drilling fluids are multi-component systems, techniques previously used have been employed to study the competitive adsorption of the polyalkylglycol and polyacrylamide components. Preferential adsorption of the PAG is seen in these systems either due to the mass transport effects (PAG is considerably smaller than PAM) or due to PAG removing all but the inner cation hydration sphere, and presenting a hydrophobic surface for the PAM, and therefore preventing its adsorption.

TABLE OF CONTENTS

1. OIL WELL DRILLING FLUIDS

1.1. Introduction

The overall aim of the research described in this thesis was to undertake a study into the interactions occurring between water soluble polymers and clay mineral surfaces in aqueous media. This is particularly relevant to water based drilling fluids where polymers interact both with the clay mineral component of the fluid in suspension and also with the drilled formation which can often be shales which comprise a significant proportion of clay mineral.

The purpose of the research explained throughout the course of this study is to understand the interactions between the various components within the drilling fluids and also with the drilled surface of the well bore. Features such as the nature of the interaction between clay and polymer in aqueous drilling fluid; the conformation adopted by a polymer, either freely interacting with solvent or adsorbed to the clay component of the fluid and where a polymer interacts with the clay mineral, can have significant bearing on the properties of the fluid, in particular its rheological behaviour and help to establish the depletion of polymer in the fluid.

In addition, the adsorption behaviour of polymer from the fluid solution onto the surface of aggregated, clay mineral platelets can be established and so evaluation of wellbore stabilisation / destabilisation by drilling fluids can be demonstrated. Studies of this nature can also ascertain the functions performed by individual components or groups of components in the multicomponent drilling fluid system.

There has been significant research in this particular field [1, 2, 3, 4]. However, without first explaining the underlying principles and the problems which have elevated the importance of this particular research into water based oil well drilling fluids, it would be impossible to rationalise the methodology, techniques and particular materials used.

Hence, a considerable portion of the introduction is devoted to the industrial importance of oil well drilling fluids; their properties, uses and formulations. This is accompanied by a discussion of the structure and properties of clay minerals, a principal constituent of both drilling fluid and drilled formation. The remainder of the introduction is concerned with a relevant discussion of the literature regarding the adsorption from aqueous solution of water soluble polymers and in particular their adsorption onto a clay mineral adsorbate.

The particular techniques used to provide information on molecular interactions in these polymer-mineral systems yields results which will help to correlate the behaviour of water based oil well drilling fluids with the behaviour of some of their individual components or mixtures of components.

1.2 The Nature of Oil Well Drilling Fluids

Oil well drilling fluids or 'muds' are used extensively in the drilling of wells for oil. There are many different formulations and the optimum formulation for a particular borehole is chosen for its ability to aid production under a given set of circumstances.

1.2.1. Functions of oil well drilling fluids

The improvement in production afforded by the drilling fluid depends on the ability of the mixture to fulfil five typical criteria [5]

1.   The removal and suspension of drilled solids.

It is essential that cuttings produced during drilling are immediately removed to prevent their inhibition of further drilling by settling on the cutting surface. A circulating fluid must have the ability to suspend such cuttings and bring them back to the surface whilst minimising disintegration of the solids.

2.   Cool and lubricate the drill bit and string

Damage to the drill bit due to friction produced between itself and the wellbore can be reduced by the presence of a circulating drilling fluid which will help to dissipate heat produced. In addition, drag between the drill string and the wellbore will also be reduced by the lubricating drilling fluids.

3.   Confine underground fluid deposits to their respective penetrated formations

Underground formation fluids can often be highly pressurised and these high formation pressures must be controlled to prevent the inflow of fluids into the wellbore. This is generally achieved by the density control of the fluid itself, i.e. by controlling the weighting agents [5] and polymer molecular weight.

4.   Stabilise the wellbore

Drilled wellbores are quite naturally unstable. However stabilisation of the wellbore can be enhanced by the formation of a thin, low permeability filter cake, from drilling fluid solids, which seals pores in permeable penetrated rock. Chemically unstable formations such as shales which are unstable in water due

3

to their clay mineral constituents readily hydrating and dispersing may be stabilised by polymers in the drilling fluid. This is a point discussed in greater detail later in this thesis.

5.   Assist in formation evaluation

Since a drilled well is intended for the commercial production of oil it is important that the drilling fluid used does not interfere with information obtained regarding the underground deposits and prevent commercial recovery.

Oil well drilling fluids or 'muds' are used extensively in the drilling of wells for oil. There are many different formulations and the optimum formulation for a particular borehole is chosen for its ability to aid production under a given set of circumstances.

1.2.2.   Properties of oil well drilling fluids

The formulation of an oil well drilling fluid will provide it with the properties necessary to achieve the previously mentioned functions. These properties are:

1.   Density

The density of a drilling fluid obviously has a large bearing on the pressure it exerts down a borehole. Hence, the density is critical in confining fluids to the pores in their formation, it also helps to enhance borehole stability by virtue of its pressure. The density of a mud also enables it to suspend and transport cuttings to the surface

2.   Rheology

The flow properties of a mud are extremely important, particularly in the transport of cuttings from the drilled face. The very nature of a drilling fluid

(being a solid-in-liquid suspension) means it will exhibit non-Newtonian behaviour. This means that the fluid will exhibit shear thinning and a tendency to develop a gel structure at low shear rates all factors which must be accounted for when formulating the mud.

3.   Filtration

The formation of a filter cake which prevents the continuous loss of mud to the formation is dependent upon the mud containing some particles of a size just smaller than that of the pores.

1.3.   Composition of oil well drilling fluids

There are two common, distinct types of drilling mud [5, 6]; either water-based or oil-based, each depending on the nature of the continuous liquid phase.

1.3.1.   Oil-based drilling fluids

The most commonly used type of oil-based mud is that of the invert emulsion [6]. These muds have oil as the continuous phase in ratios between 95:5 and 50:50 with an internal calcium chloride brine phase. In addition to the two phases, water emulsifying surfactants, weighting and filtration control agents are added in varying proportions to change the properties.

There are many advantages in using an invert emulsion oil-based drilling fluid

- They are extremely adept at inhibiting shale hydration since the continuous phase is not water and so will help to maintain borehole stability.

- Their non-polar nature offers good protection against drill bit corrosion.

- They have a very low lubricity coefficient which helps to reduce torque and drag.

Although oil based drilling fluids are preferred by the industry [7], principally due to their formation stabilisation, they are expensive to formulate and their environmental impact can be quite detrimental. As a result, extensive research has been undertaken to improve the performance of water-based drilling fluids.

1.3.2.   Water-based drilling fluids

Historically, water itself was the first drilling fluid to be used [5] but the properties, discussed earlier, which are currently demanded of commonly used water based muds are now provided by the presence of dispersed solids (principally barite and drilled cuttings of which the clay mineral bentonite is the chief constituent) dissolved salts (including sodium, potassium and calcium chlorides) and water soluble polymers, oligomers and surfactants (such as polyacrylamides and polysaccharides).

Whilst being relatively inexpensive and easy to use these muds are able to easily hydrate and disperse clay mineral containing shales and will as a result reduce borehole stability. They are also particularly sensitive to salt contamination by drilling through underground deposits of soluble salts. Since increases in ionic strength will cause flocculation of the clay mineral constituent there will be a corresponding deterioration in the fluid loss control and flow properties of the mud. However these muds are considerably more environmentally acceptable than the toxic oils used in oil based muds and as a result significant research has been undertaken to improve water based mud formulations. Attempts have been made [4, 7, 8, 9] to reduce their destabilisation of the borehole by shale inhibition and minimising formation damage, to improve their fluid loss control and to have high viscosities at low shear rate. Thus, attempts have been made to provide a water based drilling fluid with the properties of an oil based drilling fluid and hence reduce the detrimental environmental impact.

Consequently the research described in this thesis will examine the interaction of the clay mineral bentonite either as a free standing film or as a fully dispersed aqueous suspension with aqueous polymer and oligomer additives commonly found in water based drilling fluids. It is essential that the two separate bentonite systems are considered since the first enables simulation of adsorption on the wellbore whilst the latter enables simulation of adsorption on suspended solids within the mud.

2. CLAY MINERALS

It is often found in clay mineralogy, that there are some terms which are defined differently by researchers in different fields. To avoid confusion and as a guide to the nomenclature within this thesis, I shall define the term 'clay' as a natural mineral, very fine grained (<2 μm) and comprised almost entirely of aluminosilicate materials.

Clay minerals are abundantly distributed being composed of three of the earth's most common elements; silicon, aluminium and oxygen. They exist as small crystals which are created by the weathering of igneous rock and are carried to sedimentary basins by weathering processes [10]. They are commonly encountered whilst drilling for oil in sedimentary formations and as such become cuttings and are readily distributed throughout the drilling fluid.

Clay minerals have great chemical importance and numerous properties and as such find numerous industrial applications. In addition to being widely found in oil well drilling fluids, clay minerals are one of the most commonly used natural materials being found in applications as diverse as industrial fillers [11], water treatment [12] and the manufacture of ceramic products [12].

It is instructive to consider some of the more important properties of clay minerals with reference to their chemical composition and structure since an understanding of these gives an insight into their behaviour, particularly in aqueous solution which is of relevance in this thesis.

2.1. Structure of aluminosilicate clay minerals

Layered clay minerals are essentially constructed from two types of sheet-like structures which are known as their basic building units.

2.1.1. The tetrahedral sheet

The fundamental building block for this sheet is a silicon oxide tetrahedral unit in which four oxygen atoms (or hydroxyl groups to balance the structure) are arranged at the four corners of a regular tetrahedron and at the centre sits a silicon atom. These tetrahedra have a chemical composition SiO_4^{4-} (figure 2.1.1a) and are able to undergo polymerisation by linking the oxygen atoms to form an hexagonal network of chemical composition $Si_4O_6(OH)_4$ (figure 2.1.1c). The tetrahedra are arranged such that the apices all point in the same direction and each of the three remaining basal oxygen atoms of the tetrahedron are shared with three adjacent silica tetrahedra. All tetrahedron bases lie in the same plane and consequently a flat, infinitely repeating, two dimensional sheet is produced (figure 2.1.1b).

In actuality, the ideal hexagonal silicate sheet is slightly distorted in most clay minerals to a di-trigonal surface symmetry [12]. This is due to the misfit of a large tetrahedral sheet with a smaller octahedral layer.

2.1.2. The octahedral sheet

The second unit which is found in the structure of clay minerals is an octahedral sheet (figure 2.1.2b). The fundamental building unit of which consists of either aluminium, magnesium or iron ions located at the centre of an octahedral arrangement of oxygen atoms or hydroxyls (figure 2.1.2a).

Figure 2.1.1 The tetrahedral layer silicate sheet and its various components.
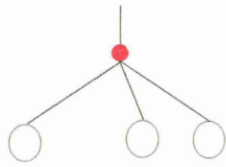
a) structural model of a single silica tetrahedron.
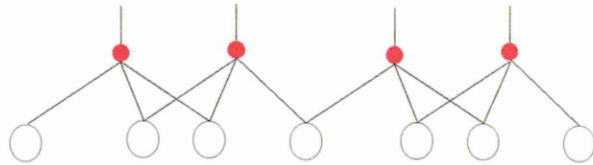
b) structural model of the silica tetrahedral sheet.
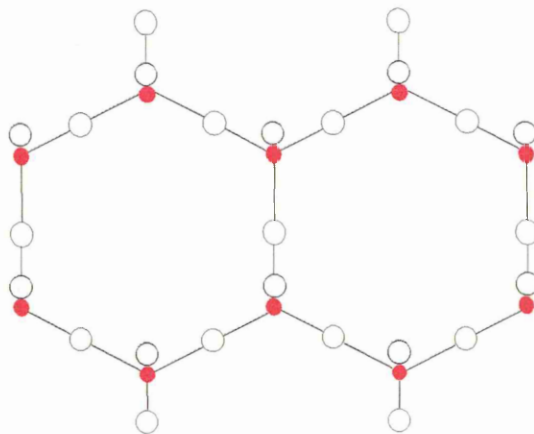
c) plan view (down the c dimension) of the silica tetrahedral sheet showing the hexagonal network.

○   Oxygen

●   Silicon

These octahedral units are polymerised into a two dimensional sheet in which oxygen atoms are shared between neighbouring octahedra giving an arrangement in which the metal ions are surrounded by two parallel planes of closely packed oxygen atoms or hydroxyls. When the metal ions are aluminium, the chemical structure is $Al_2(OH)_6$ and only two thirds of the available sites in the structure are filled with metal ions. When magnesium is the metal ion present, however, its structure is $Mg_3(OH)_6$ and all three sites are filled with metal ions. The hydroxyl species is formed in the sheet when a proton binds to an oxygen atom to satisfy valence requirements.

2.1.3.   Layer silicates

Since the octahedral and tetrahedral sheets have very similar dimensions and analogous symmetry, it is possible for oxygen atoms to be shared between the two distinct sheets. As a result the oxygen atom apices which protrude from the tetrahedral sheet are shared with metal ions in the octahedral sheet (figure 2.1.3) to produce the clay platelet.

The clay layers which are produced by the superimposition of octahedral and tetrahedral sheets are mostly stacked parallel to each other. van der Waals forces of attraction exist between silicate layers in adjacent clay platelets and hold the structure together. These bonds are easily cleaved by mechanical shear and will readily allow polar molecules to enter between the layers.

The combination between tetrahedral and octahedral layers forms the basis on which clay platelets are formed. Indeed the ratio of tetrahedral and octahedral layers and the type of interlayer cation (see later) govern the classification of clay minerals.

Figure 2.1.2 The octahedral layer alumina sheet and its various components.
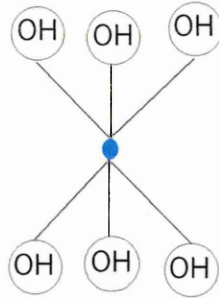
a) structural model of a single alumina octahedron.
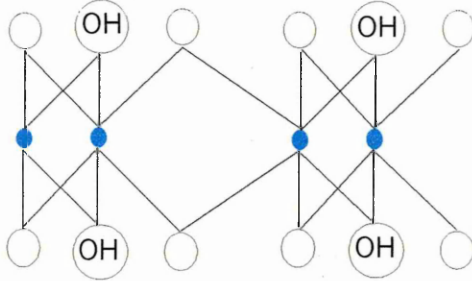
b) structural model of the alumina octahedral sheet.

Figure 2.1.3 Structural model of the combined tetrahedral and octahedral sheets in a 2:1 layer silicate.

○ Oxygen   OH Hydroxyl

● Silicon   ● Aluminium, Magnesium, Iron
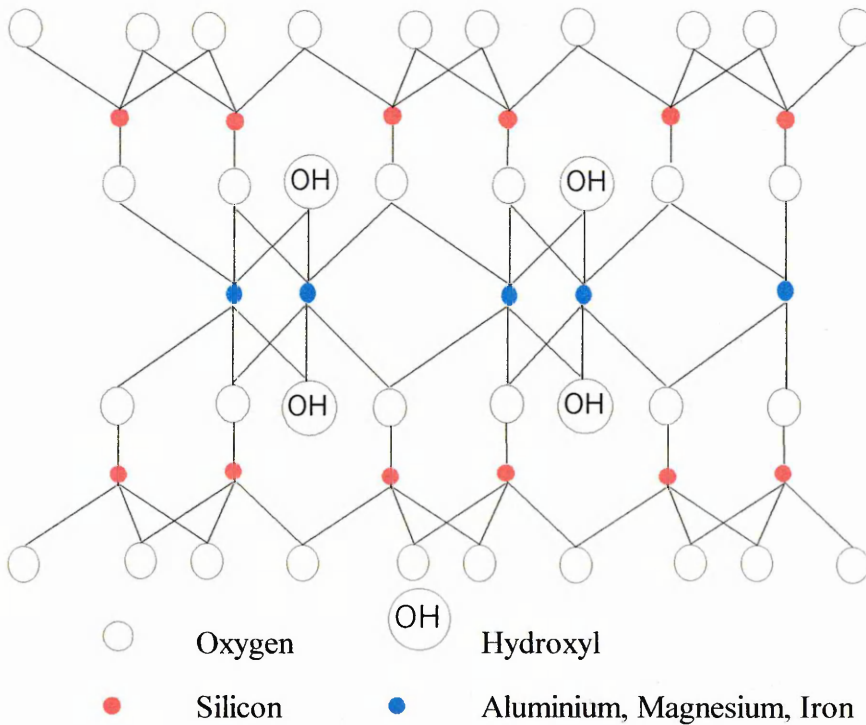
Most clay minerals fall into one of two clay types depending upon the stacking arrangements of the component sheets. For example, when one tetrahedral sheet is superimposed upon one octahedral sheet, a 1:1 clay is formed such as the kaolin group of minerals. It is also possible for the two tetrahedral sheets to sandwich either side of one octahedral sheet to form a 2:1 clay mineral as is observed in the smectite or mica groups of minerals.

A detailed structural classification of the various clay minerals will not appear in this thesis and as such the reader is referred to several excellent descriptions by Grim [12, 13] and van Olphen [14].

It will, however, be important to discuss the structure and properties of the clay mineral used exclusively in the studies presented throughout this thesis; that particular mineral being montmorillonite, a member of the 2:1 smectite group of minerals.

2.2.   Structure of montmorillonite minerals

The structure of montmorillonite has been the subject of intense investigation but these have not fully explained its reactivity. The most popular, commonly accepted structure is that proposed by Hofmann et al [15] and modified by Magdefrau and Hofmann [16] and Hendricks [17] (figure 2.2a). This structure is the one described previously for a 2:1 layer silicate mineral in which two silica tetrahedral sheets sandwich an alumina octahedral sheet. This is the structure widely accepted as being the structure of pyrophyllite, a non-swelling 2:1 smectite clay mineral [13].

This proposal, however, did not fully explain the observed properties of montmorillonite. In particular, it failed to explain the linear swelling behaviour

and high ionic exchange capacity of montmorillonites. As a result Edelman and Faverjee [18] proposed an alternative, less commonly accepted structure (figure 2.2b) in which some apical oxygen atoms at the tetrahedral silicate layer surface were replaced with hydroxyl groups so that some hydroxyl groups exist at the layer surface. The structure is balanced by inverting 20% of the silica tetrahedra. This structure has been used recently by Plee et al [19] to explain pillaring. This model contains no isomorphous substitution and as such the cation exchange capacity relies upon the dissociation of hydroxyl groups. This is found, experimentally, not to be the case and it must be noted that layer surface hydroxyl groups are very rare.

2.2.1. Cheto and Wyoming types of montmorillonite

Two broad groups of montmorillonite the so called Cheto-type and Wyoming-type were identified by Grim and Kulbicki [20]. This conclusion was based on the results which showed that various samples of montmorillonite did not yield the same crystalline phases upon heating. Guven [21] also subdivided these groups by virtue of their chemical composition and thermal behaviour. Other differences between these two groups include properties such as optical refraction [22] and X-ray diffraction intensities of glycol complexes [23]. However Solomon and Hawthorne [24] considered there to be only slight structural differences between the two types of montmorillonite. Bukka et al [25] have shown that it was possible to distinguish between the Cheto and Wyoming types of montmorillonite using FTIR spectroscopy of partially deuterated samples of the two types. They used the Hofmann model to explain how the ratios of two -OD structural stretching bands is related to the Mg/Al weight ratio for the two types of clay mineral and hence allows for their classification.

Figure 2.2 The structural models proposed for montmorillonite.
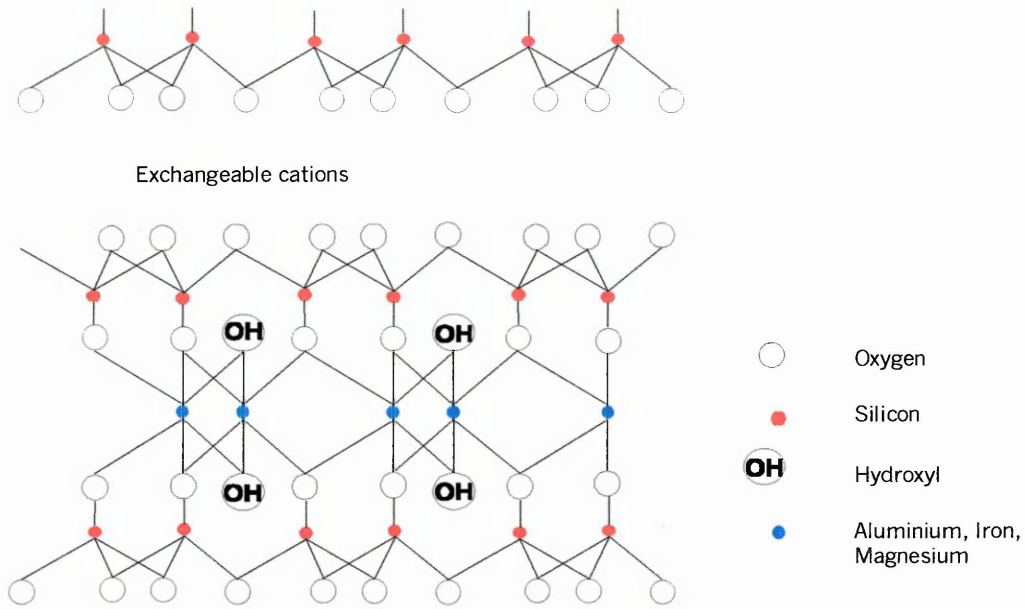
a) Structural model for montmorillonite proposed by Hofmann et al [15].
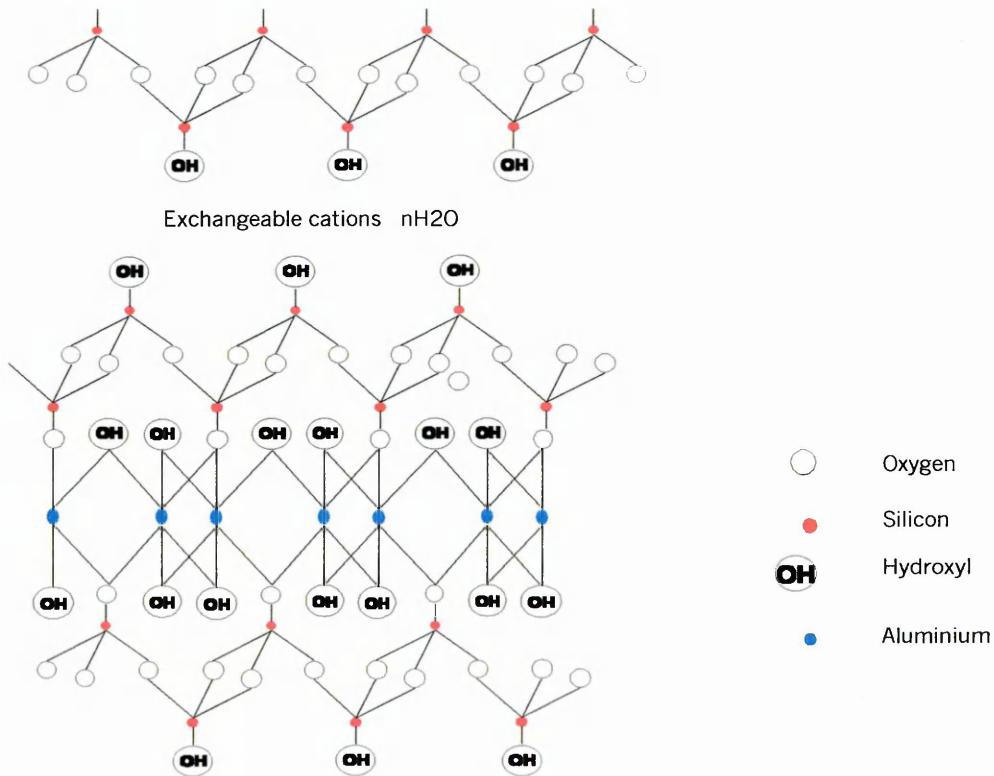
b) Structural model for montmorillonite proposed by Edelman and Faverjee [18].

Due to some of the flaws in the Edelmann and Faverjee model and the general acceptance of the Hofmann model it will be the latter which will be used for discussion in this thesis.

2.3. Chemical composition

Calculations of chemical composition [14] have shown that montmorillonites have the typical formula

$$(Al_{2-x}Mg_xFe_z)^{VI}(Si_{4-y}Al_y)^{IV}O_{10}(OH)_2\ M^+_{x+y}.n\ H_2O$$
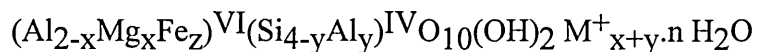
The exchangeable cation is represented by M^+ and the octahedral layer in which the isomorphous replacement predominates is represented by VI and the tetrahedral layer by IV. There are traces of Fe in the octahedral layer.

2.4 Properties of montmorillonite minerals.

Several properties of montmorillonite clay minerals have been alluded to previously in this chapter. It is instructive to briefly describe some of these properties and the underlying principles behind them.

2.4.1. Surface Area

Montmorillonite has a very large surface area, it has been calculated using the glycerol adsorption method, to be of the order 750 m^2g^{-1} [26]. This is due not only to it having an external surface area determined by its geometrical shape, but also having a large 'internal' surface area as a result of its plate-like arrangement.

2.4.2. Charges on clays

The high reactivity of clay minerals is predominantly due to the presence of electrical charge on their surfaces. There are two types of charge on clay mineral which arise by slightly altering the overall electrical neutrality of what is essentially a balanced ionic structure.

2.4.2.1. Edge charges

These arise from the fracture of clay crystal platelets, often by the shear energy in a circulating aqueous dispersion. Obviously, breaking the crystal causes a charge imbalance at the broken edge creating positive charge on the alumina layer and negative charge on the silica layer. This is due to the tendency for aluminium to donate electrons and silicon to accept electrons.

The nature of this charge is therefore pH dependent. Hence, in acid conditions the protons in solution will neutralise the negative charge on the silica layer leaving a predominantly positive charge on the clay edge. Conversely, in alkaline conditions hydroxide ions will neutralise the positive charge on the alumina layer leaving an overall negative charge on the silica layer. At a pH of approximately 6.3 there is a roughly equal concentration of positive and negative charges.

2.4.2.2. Isomorphous substitution

Modification of the overall neutrality of the clay structure can be achieved by replacing one metal ion within the clay sheet by another of similar size and of the same co-ordination but of lower charge. Hence for montmorillonite, within the octahedral sheet it is possible to replace Al^{3+} by Mg^{2+} or to a lesser extent,

Fe^{2+}, whilst in the tetrahedral sheet it is possible (but less common) to substitute Al^{3+} for Si^{4+}. Since metal ions of lower charge are introduced to the clay platelet, there is an excess of electrons and an overall negative charge produced. These charges are not affected by changes in pH but the position and extent of substitution within the layers will affect the properties of the clay mineral.

2.4.3. Exchangeable cations (counter cations).

Since the isomorphous substitution is predominantly in the octahedral sheet of the clay particles it is here that the excess negative charge exists. In order to retain overall neutrality, metal ions reside at the surface of the clay mineral platelets. They are unable to approach the negatively charged sites closely enough to lose their ionic character or to significantly affect the mineral surface.

2.4.4. Cation exchange and Cation Exchange Capacity (CEC).

In aqueous solution it is possible for the exchange of one particular type of exchangeable cation for another. Hence if a clay is placed in an aqueous electrolyte solution an equilibrium ion exchange occurs between the metal ions on the clay surface and the dissociated metal ions of the electrolyte of the type:

$$\textbf{Clay-X}^+ \; + \; \textbf{Y}^+ \;\; \Leftrightarrow \;\; \textbf{Clay-Y}^+ \; + \; \textbf{X}^+$$

The extent of exchange of cation Y^+ for cation X^+ depends on the relative concentrations of X^+ and Y^+ cations, the nature of the clay and since some cations are adsorbed more strongly than others, the nature of the cations. The preference of these cations to adsorb to the surface follows the lyotropic series, i.e.: $H^+ > Al^{3+} > Ba^{2+} > Sr^{2+} > Ca^{2+} > Mg^{2+} > NH_4^+ > K^+ > Na^+ > Li^+$
Side reactions are also important, as with any equilibrium process, and may allow the equilibrium to be driven predominantly to one side.

The mineral used extensively in the work published within this thesis is Wyoming bentonite which occurs naturally with small amounts of potassium and calcium counter cations but predominantly sodium. It is an important feature of clays that they are able to exchange cations and be prepared in a homoionic exchanged form

The cation exchange capacity (CEC) is a measure of the quantity of exchangeable cations and is generally expressed in milliequivelents of each cation per 100g of clay. Montmorillonite has the largest cation exchange capacity of all the clay minerals having a CEC between 80 and 150 meq/100g [13, 14].

Grim explained [13] that in montmorillonite :

- 80% of CEC is due to isomorphous substitution (pH independent).

- 15-20% of CEC is due to broken edge charge (pH dependent).

- In addition, there may be a small remaining percentage of the cec which may be attributed to the ionisation of surface hydroxyls as described in the model of Faverjee and Edelman, but this is somewhat unlikely. This is also pH dependent.

A range of values for the cation exchange capacity must be stated because the exchangeable cations, and hence the CEC, are sensitive to both pH (as indicated above) and the valency of the exchangeable cation. This is because divalent cations have a higher affinity for edge charges than monovalent cations [27] which will effect the CEC capacity.

There are many methods for evaluating the cation exchange capacity but one of the most commonly used techniques is the methylene blue adsorption test [28].

2.5. Hydration of clay minerals.

Due to its highly hydrophilic nature and the ease of cleavage of adjacent clay platelets (platelets are bound only by van der Waals forces), water is readily adsorbed to the clay mineral. In this we are concerned only with water that is relatively strongly held by the clay and which would be lost by heating to between 100 and 150°C. This must be distinguished from structural water which is released by the decomposition of the octahedral lattice OH sites at much higher temperatures (up to 800°C). It is the low temperature water which is important since it is this which provides a clay with its important properties.

2.5.1. Clay surface hydration

As explained previously, the cations which are present at the surface of the clay mineral to neutralise the negative charge (present in the layer due to isomorphous substitution) are physically unable to get close enough to the clay platelet surface to fully satisfy the negative charge and as a result polar water molecules are able to access the surface and weakly hydrogen bond to form an oriented layer. There is only weak H-bonding attraction between the surface and the adsorbing water because, in montmorillonite, the negative charge generated due to isomorphous substitution in the octahedral layer is delocalised (smeared out) between the surface oxygen atoms resulting in a low layer charge (in montmorillonite this has been shown to be between 0.5 and 1 charge units per unit cell [12, 13]). A second oriented layer will also form but due to thermal fluctuations, as more layers are added they will be less oriented and will approach the orientation adopted by bulk water.

2.5.2. Cation hydration.

When salts are dissolved in water they dissociate to give positively and negatively charged ions. Their charge attracts polarised water molecules and in the case of cations the water molecules orient themselves such that the electronegative oxygen atom points towards the positively charged ion and as a result a hydration sphere forms around the interlayer cation. Usually another, outer hydration sphere of water will form commonly known as the second solvation shell. Hence in an anhydrous mineral, the exchangeable cation will exist in the interlayer region between clay platelets neutralising the layer charge. However, as the clay becomes hydrated and the interlayer cation is solvated it will form inner and outer hydration spheres.

The two most important factors governing the quantity of water adsorbed into the interlamellar space of the clay mineral are:

1.   The surface area of the clay (montmorillonite has an accessible external and internal surface area)

2.   The size and charge on the exchangeable cation

Table 2.5 Size and charge of typical exchangeable cations.

ion	dehydrated radius (Å)	charge density (charge/Å^2)	hydrated radius (Å)
Na^+	0.98	0.088	5.6
K^+	1.33	0.045	3.8
Ca^{2+}	1.06	0.176	9.6

Although Ca^{2+} is able to hydrate easily (it has a high charge density), it is a divalent ion and is able to bind two clay sheets together by forming bridges between areas of negative charge and so satisfying its valency. As a result, these clays do not swell easily.

The K^+ ion does not hydrate very well (as can be seen from its values of charge density and hydrated radius in table 2.5. Consequently, its dimensions, which allow it to fit into the di-trigonal cavities in the tetrahedral silicate layer, allow it to neutralise the negative layer charge more effectively and allow the platelets to approach each other more closely. Hence, a more stable arrangement is obtained which reduces the hydration and swelling of the clay.

The Na^+ (and Li^+) ions are able to hydrate quite easily (Li^+ in particular has a high charge density) and being monovalent are only associated with one interlayer sheet. Thus the clay platelets are able to hydrate and swell quite easily.

2.6.   Structure of water near the clay surface

The behaviour of water and the accompanying swelling of montmorillonite has received much experimental and theoretical study [29]. The two commonly used treatments for the description of water adsorbed at the clay-water interface are the spectroscopic and thermodynamic approaches.

2.6.1.   The spectroscopic treatment

Sposito and Prost [29] review the literature describing the structure of water at the clay-water interface in terms of the information which can be obtained from

the experiments used to probe the water. These experiments are split into two sections in which one of two structures is obtained.

1.   The vibrationally averaged structure (V structure)-The spatial arrangement of the water molecules is established by their vibrational motions. This can be probed by, amongst others, infrared spectroscopy, neutron scattering and nuclear magnetic resonance spectroscopy.

2.   The diffusionally averaged structure (D structure)-The water structure obtained comprises the vibrational, rotational and translational molecular motions of the water molecules and as a result is more ordered since it observes only the most probable configurations of the water molecules. These structures are obtained by X-ray and neutron diffraction techniques.

Infrared spectroscopy and X-ray diffraction techniques are the two principal techniques which have been used to obtain the results, on montmorillonite hydration and polymer adsorption on montmorillonite, described in this thesis and as such a detailed description of their theory and their operation will be found in chapter 4.

2.6.1.1. Infrared spectroscopy

It has, for a long time, been established by infrared spectroscopy that there are two distinct environments of water in the interlamellar regions of montmorillonite. Prost [30] and Sposito and Prost [29] established these two environments as:

1.   Water molecules which are directly co-ordinated to the exchangeable cations (i.e. the first, strongly bound, inner hydration sphere of the cations). This water is extremely difficult to remove.

2.   physisorbed water which is easily removed (at temperatures below 105°C and corresponds to water molecules which exist in external regions, for

example occupying interstitial micropores, interlamellar spaces between cations or polar sites on external surfaces.

Prost [30] suggested that the first stage of water adsorption is the solvation of the exchangeable cations by water molecules. The successive hydration corresponds to c-axis spacings which correspond to either one or two layers of adsorbed water. The second stage of hydration is suggested to depend on the ability of the cations to solvate themselves and so involves the formation of successive solvation spheres of water molecules. After the cations are fully solvated any further water adsorbed by the montmorillonite will condense in the micropores and in the interstitial regions.

Sposito and Prost [29] highlighted the hydration of Li-montmorillonite. In this particular structure the surface charge originates almost entirely from the isomorphous substitutions in the octahedral sheet and as a result it is delocalised around the oxygen atoms which compose the di-trigonal cavity. Consequently, there is a preferred orientation of the water molecules in which the lone pair of the oxygen of water points towards the Li^+ cation and one of the protons of water points towards the structural OH group at the base of the di-trigonal cavity (figure 2.6.1.1). This is the preferred conformation since the proton will sit at the centre of the lone pairs of surface oxygen atoms which surround the di-trigonal cavity. If the surface charge had originated in the tetrahedral layer of the mineral then it would not be delocalised but localised on surface oxygen atoms so that conventional hydrogen bonding between water molecule and surface would occur. Small angle neutron scattering reported by Sposito and Prost [29] indicate that swelling of Li montmorillonite goes to the limit of separation, i.e. to individual platelets.

Farmer [31] discussed the restricted environments of water molecules co-ordinated to metal cations relative to that in bulk water. This was additional

evidence to support work by Russell and Farmer [32] in which they established that the OH stretching and bending bands of montmorillonite decreased in frequency on dehydration.

Johnston et al [33] observed the correlation between the water content of thin bentonite films having various exchangeable cations and the wavenumber position of the H-O-H bending mode of water in transmission. They also discovered that on lowering the water content of the clay the bending vibration is shifted to lower wavenumber values accompanied by a significant increase in the molar absorptivity. They assume that, at low water contents, the spectra are dominated by water molecules in the inner hydration sphere of the exchangeable cation and hence the polarisation of this cation.

Figure 2.6.1.1. The structure of montmorillonite showing the interaction of the metal cation with water and the interaction between the water molecules and the structural OH group.
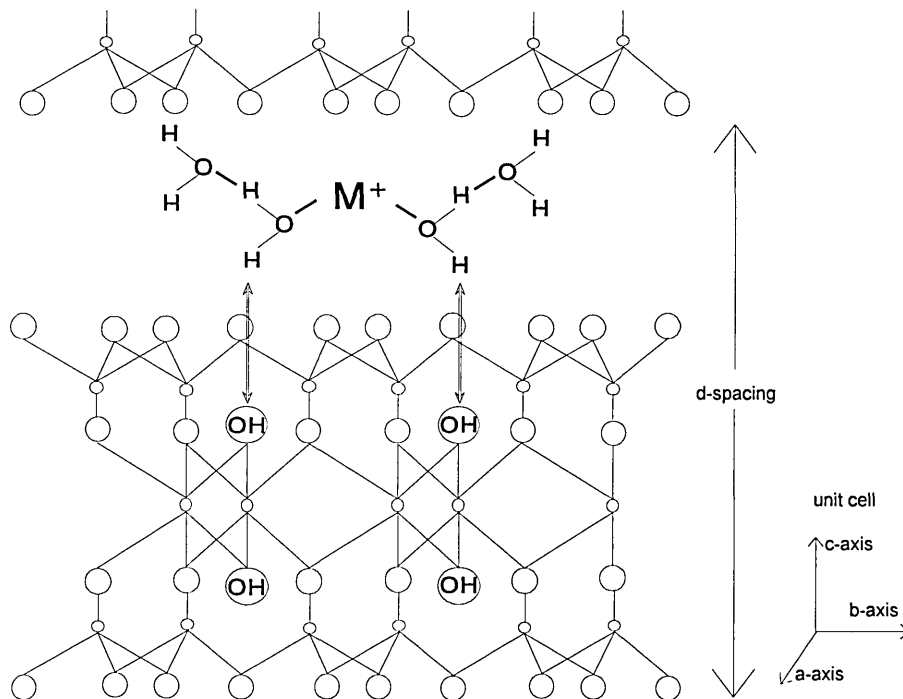
Bishop et al [34] also note this shift and also attributed it to the hydration energies of the cations and hence their polarising power. Poisignon et al [35] discovered that the molar absorptivities of the OH stretch and H-O-H bending modes of water in montmorillonite are strongly dependent on the hydration energies of the counter cation, the water content and the surface charge density of the mineral.

Bishop et al [34] used mid and near infrared techniques to assign the complex appearance of water in the infrared spectra of various homoionic montmorillonites. They assigned the bands observed at 3610, 3550, 3450 and between 3400 and 3350 cm^{-1} using previously determined band positions for bulk water [36] and alkali halide saturated water [37].

Eisenberg and Kauzmann [36] assigned band positions for bulk water at 3439 and 3600 cm^{-1} to the symmetric (ν_1) and anti-symmetric (ν_2) stretching modes of bulk water respectively. Similarly, Shulz [37] assigned band positions for alkali saturated water at 3460 and 3612 cm^{-1} to the ν_1 and ν_2 vibrations respectively. Hence, Bishop suggested that the 3610 cm^{-1} band of water is assigned to the anti-symmetric v(OH) vibration of water bound in the inner hydration sphere of the cation in accordance with the band found between 3610 and 3630 cm^{-1} in montmorillonite by Farmer and Russell [38]. Bands observed by Bishop at 3550 cm^{-1} and between 3400 and 3350 cm^{-1} were seen to be strongly dependent on the polarising power of the exchange cation and the moisture content of the clay. Cations with high polarising power cause the vibrations of the water molecules to be restricted and so they have reduced energy vibrations and are found at lower wavenumber positions. At low water contents, only the band at 3550 cm^{-1} was seen, whereas at high water contents both bands are seen, in keeping with the results of Prost [30] on hectorite. The implication is that the bands are due to symmetric stretching modes (due to their direction of movement, the symmetric stretch will be more sensitive than the

anti-symmetric stretching mode to the cation) of inner sphere hydrated cations and bulk hydrogen bonded water. Although Low [39] predicted that water molecules bound to the clay mineral surface would have higher energy O-H stretching vibrations than bulk water, Sposito and Prost [30] have suggested that the surface bonded water molecules do not have a higher O-H stretching vibration than any other H-bonded interlayer water molecules.

It was previously found Eisenberg and Kauzman and Shulz [36, 37] that there exists at ~3230 cm^{-1} an overtone of the water bending vibration at ~1630 cm^{-1}. So the remaining band at 3450 cm^{-1} which is observed at high water contents was assigned to the anti symmetric vibrations of outer sphere water molecules.

Sposito et al [40] have used the infrared technique to probe the hydration and detachment of Na^+ from homoionic bentonite at low water contents to determine the extent of cation dissociation from the clay surface. The increase in intensity of M-OH structural bending modes (in the region 950-750 cm^{-1}) on deuteration was attributed to the movement of solvated Na^+ out of di-trigonal cavities in the silicate surface. This is assumed to be caused by the removal a Na^+ ion from the cavity and so, the removal of the suppressing repulsive force on the vibration of the M-OH bond in the bottom of the cavity which allows its infrared absorbance to increase.

Infrared hydration studies of montmorillonite by Shewring et al [41] (discussed in further detail in this thesis) have shown that there is a shift in the Si-O stretching vibration at 1086 cm^{-1}, seen in dilute montmorillonite suspensions, to low wavenumber on dehydration and increasing the electrolyte concentration. This was attributed to the settling of the Na^+ exchangeable cation into the di-trigonal cavities on its desolvation. Migration of exchange cations into the hexagonal holes in the silicate layer surface has also been used to describe the

dehydration of water (from the cation hydration atmosphere) from montmorillonite clay at 200°C [42].

Other studies of the silicate stretching frequency by Lerot and Low [43] attempted to study the shifts in frequency which might correspond to changes in crystal symmetry during hydration. No shifts in frequency were observed but an increase in band intensity of the with increasing water content was interpreted as disorientation of the layers as the clay swells. Gan and Low [44] also attempted to study the ν(Si-O) band at 1040 cm^{-1} seen in the transmission spectra of various cation exchanged homoionic montmorillonites, but noted no shift in frequency on increasing electrolyte concentration. More recently, studies by Yan et al [45] have revealed a dependence of the frequency of Si-O stretching modes of montmorillonite and the H-O-H bending mode of water on the water content (M_w/M_c) in aqueous gels. They tentatively attribute this to the water in the interlayer region adopting a structure like that of bulk water with increasing M_w/M_c; A structure it cannot adopt in the confined space between clay platelets. They suggest that shifts in ν(Si-O) are coupled to the ν(H-O-H) and since the silica tetrahedra are exposed to water, that shifts in both will occur as the platelet separation changes. These results could quite easily be explained in terms of hydration of the exchange cation and the change in ν(Si-O) as the silicate lattice relaxes when the cation migrates away from the di-trigonal cavity. Additionally, shifts to higher wavenumber of ν(H-O-H) with increasing M_w/M_c could easily be due to increases in the amount of 'adsorbed' water around the exchange cation, as defined by Bishop et al [34].

2.6.1.2. X-ray diffraction

The coherent scattering of X-rays by hydrated montmorillonites has received much attention [46]. It should be noted that it is the aluminosilicate layers which

act as diffracting planes and not the atoms which comprise water molecules (as in neutron scattering). However, the interlayer spacing (or basal spacing or the (001) d-spacing) helps to determine the structure of water molecules in the interlayer region.

Pons et al [47] described the structure of water on Na-montmorillonite as an adsorbed oriented monolayer strongly bound to the surface oxygen atoms with essentially bulk liquid water subject to the constraints imposed by the surface. Bradley et al [48] first established that water molecules adsorb onto montmorillonite in steps of one, two, three and four layers of water corresponding to step-wise increases in the basal spacing as a function of water content. Only d-spacings which correspond to integral layers of water molecules between platelets were observed by Mooney et al [49]. These d-spacings correlated with the shape of desorption isotherms and heats of desorption, further evidence that discrete layers of water exist between the layers. Any differences were explained in terms of ionic hydration effects. Glaeser and Méring [50] have also shown that the interlayer spacing of Na-montmorillonite increases in a step-wise manner on increasing the relative humidity of the equilibrating atmosphere. The K^+ ion was seen to behave in a similar way to the Na^+ exchangeable cation with increasing water content showing spacings at ~9.5, 12.5 and 15.5Å. However, the basal spacing of Ca^{2+} exchanged clay are more stable due to the hexa co-ordinated octahedral hydrated Ca^{2+} cation. Ormerod and Newman [51] measured the basal spacing and water sorption on Ca-montmorillonite concurrently. At low water contents single water sheets develop but at vapour pressures between 0.35 and 0.95, basal spacings between 15.7 and 19Å and water contents of 12-16 molecules of water per cation indicate that there is a strongly bound inner layer of water and at least the same amount again of weakly bound water.

Sposito and Prost [29] reviewed small angle X-ray scattering studies of montmorillonite gel systems at ambient temperatures. These revealed that K-montmorillonite exists as parallel plates with and without water interspersed; Cs-montmorillonite exists as thick aggregates with either none or a monolayer of water between the layers and Ca-montmorillonite exists as quasi-crystals consisting of 4-5 platelets with three monolayers of water molecules between adjacent crystals. Other work by Ben-Rhaiem et al [52] has discussed the formation of quasi-crystals (not to be confused with tactoids) on dehydration of Ca-montmorillonite as described by Quirk and Aylemore [53].

Norrish [54] showed the effect of electrolyte on the interlayer spacings of montmorillonite. On reduction of electrolyte concentration he too observed a step-wise increase in the interlayer spacing up to 20Å as expected. However, below a certain value of ionic strength, c, the basal spacing jumped to 40Å and increased steadily, varying as $1/\sqrt{c}$. The value of interlayer spacings quoted by Norrish are actually the probability of a particular interlayer separation, since the spaces are represented by a statistical distribution.

The type of exchangeable cation is important to the swelling mechanism. Studies on mixed K^+/Na^+ ion exchanged clays [55] revealed that the swelling is strongly inhibited in clays with 44% or less Na^+ exchange fractions. Hence Na-montmorillonites may or may not undergo complete dissociation. However, Li-montmorillonite does undergo unlimited swelling. Swelling to infinite separation is not seen for divalent cations. Ca-montmorillonite, for example, does not fully disperse probably due to the bridging properties of cations such as Ca^{2+} between two adjacent platelets [46].

MacEwen et al [46] explained that the swelling of montmorillonites relies upon surface charge density and the surface charge delocalisation in addition to the

nature of the counter cation. Indeed, Slade et al [56] precisely controlled the swelling between 15.5 and 18.5Å by varying the concentration of equilibrium salt and found that various Na montmorillonites with relatively lower layer charge and whose layer charge predominately originates from the octahedral layer swell relatively easily. By comparison, Na montmorillonites with high surface charge density and whose charge predominantly originates from the tetrahedral layer do not exhibit extensive swelling. However, if the counter cation was Li^+, the montmorillonites would swell regardless of the size and origin of their layer charge. Na Wyoming montmorillonite used in these studies have low layer charge which is delocalised over the di-trigonal cavities of the silicate surface due to isomorphous substitution in the octahedral layer and can be seen to swell easily. Slade and Quirk [57] followed the swelling of Mg-, Ca- and La-montmorillonites over a range of salt concentrations depending upon the magnitude and origin of the layer charge, the higher the layer charge, the lower salt concentration at which the clay swelled.

The expansion of Na-montmorillonite in decreasing concentrations of electrolyte solution is not a reversible process having different isotherms during desorption and adsorption [46]. Laird et al [58] explained this hysterisis in terms of intrinsic processes during swelling due to the rigidity of the clay-water system and extrinsic processes due to the formation of rigid quasi-crystals. It is seen that work must be done to overcome the rigidity in the system.

The X-ray analysis of the swelling of Na-montmorillonite has also revealed that the b-dimension increases continuously as it swells [59]. In fact, studies [59] have shown a linear dependence between the swelling of montmorillonite and the b-dimension of montmorillonite at low water contents. Odom and Low [60] have suggested that, "epitaxy exists between water and montmorillonite ... the b-dimension affects the structure of water ...all properties depend on it [the b-

dimension]". This is evidence which supports the thermodynamic approach to swelling, explained in section 2.6.2. of which P. F. Low is a strong advocate.

The spectroscopic approach to swelling relies on the DLVO theory of double layer formation as established by Langmuir [61], Derjaguin [62] and Verwey and Overbeek [63]. The generally accepted view of swelling is that it occurs in two distinguishable stages:

1.   Intracrystalline swelling.

This is caused by the hydration of exchangeable cations in the interlayers of montmorillonite which can be seen spectroscopically since on the infrared time scale the exchangeable cations are translationally stationary. This occurs at less than three monolayers of water adsorbed.

2.   Osmotic swelling.

Osmotic swelling is the second stage of swelling and results from the large differences between ion concentrations close to the clay surface and in the pore water. Two important features of the swelling are the large spacings observed between individual layers and also that the forces between the layers are osmotic and result from the balance of electrostatic forces, van der Waals forces and the osmotic pressure exerted by the interlayer cations.

2.6.2.   Thermodynamic approach to clay hydration

This particular treatment of the swelling of clay minerals was first muted in 1956 by Hemwall and Low [64] and involves a macroscopic description of the clay water system in which all observed changes with respect to bulk water are

attributed to the water phase and not the clay phase which is considered separately.

Later, Low and Margheim [65] and Low [66] described how conventional DLVO double layer theory [61, 62, 63] does not adequately describe the swelling of montmorillonites. In their theory they discuss how that the cations in the Stern layer, closely associated to the silicate surface of the platelet, are hardly dissociated from this position on hydration (the details of the Stern layer are discussed later in this chapter). This prevents the formation of significant double layers which implies that the interaction between repulsive double layers on adjacent platelets could not be the mechanism for swelling. Miller and Low [67] showed that there exists around a platelet of montmorillonite a very well developed Stern layer in which most of the exchangeable cations reside. The electrostatic potential at the boundary of this layer(the outer Helmholz plane) is not affected by electrolyte, pH or the clay itself and it is postulated that there is a critical value of the potential which depends on the exchangeable cations, and above which cations cannot leave the layer. Adjustments are made by the layer to maintain the critical value.

It is possible to define the swelling pressure for a clay mineral as the net repulsive force per unit area at a particular separation [65] and is determined by measuring the externally applied force which is required to maintain a constant separation of the platelets on hydration. An empirical formula was developed [65] which related the swelling pressure Π, to the ratio of the mass of water to mass of clay, m_w/m_c, in the system.

$$\ln(\Pi + 1) = \alpha\left[(m_c/m_w) - (m_c/m_w)^p\right] \quad \text{eqn 2.6.2a}$$

Where α is a parameter which is characteristic of the clay and $(m_c/m_w)^p$ is the value of (m_c/m_w) when $\Pi = 0$.

Viani et al [68] determined that the swelling pressure between adjacent sodium montmorillonite platelets is related, empirically, to the inverse of the interlayer separation, λ, by:

$$\ln(\Pi + 1) = k\left[\left(\frac{1}{\lambda}\right) - \left(\frac{1}{\lambda^0}\right)\right]$$ eqn 2.6.2b

Where λ^0 is the separation between surfaces when $\Pi = 0$. At the separations studied (between 20-100Å) they predict that double layer forces would be too weak to account for the observed swelling pressures.

Mulla and Low [69] refer to several papers, of which Low was author or co-author, in which studies have been made the thermodynamic and hydrodynamic properties of water in the montmorillonite-water system including, amongst others, the specific volume, specific heat capacity, heat of compression, specific expansibility, and viscosity compared with that of bulk water and also the frequency of O-D stretching vibration. He established that all of these properties obeyed the general equation

$$J_i = J_i^o \exp[\beta_i \, m_c/m_w]$$ eqn 2.6.2c

where J_i is the magnitude of any property i, of the system

J_i^o is the magnitude of the same property for bulk water

m_c/m_w is the mass ratio of montmorillonite to water

β_i is a constant which is characteristic of the property and the

montmorillonite.

He claimed that since the O-D stretching vibration is dependent on intermolecular bonding of water molecules then all properties J_i must depend on the arrangement and interaction of the interlayer water molecules which in turn is influenced by the particle surfaces. This relates to the theory [65, 66] that differences between interlayer water and bulk water are related to the differences in intermolecular bonding which are influenced by the montmorillonite surface. Low [70] suggests that water bonds in the interlayer

are "more extensible and compressible but less breakable or bendable than those in bulk water" but is unable to suggest what the detailed nature of the bonds and their arrangement might be.

Sun et al [71] describe the non-specific nature of the interaction between water and clay mineral surfaces (i.e. that it does not depend on characteristics such as surface area, surface charge density, cation exchange capacity and b dimension of the unit cell). This led to several postulates, the two most credible of which are:

 i) that there is insufficient space in the interlayer region for the water to attain a structure characteristic of bulk water, or that,

ii) the solid silicate surface affects the vibrational, rotational and translational motion of the water molecules thus allowing intermolecular interactions at significant distances.

This agrees well with the assumption [71] that long range interactions between water and the clay mineral surface influence the structure and physical properties of interlayer water.

Several papers [67, 72, 73] have discussed the assumptions used in DLVO theory with respect to clay minerals and the convenient nature with which this theory has been applied by researchers. In particular, they highlight the absence of any term to allow for hydration of the platelet surfaces and the assumption that no hydration forces exist.

It must be noted that P. F. Low is not alone in his belief that the swelling of clay minerals is due to the hydration of the mineral and the subsequent arrangement and bonding of water molecules in the interlamellar region. For example,

Israelichvelli and Adams [74] observed an extra short-range repulsive force between smooth mica sheets in aqueous electrolyte solution and ascribed it to hydration effects. Similarly, Pashley [75] attributed short range repulsive forces between mica sheets in electrolyte solution to hydration of the counter ions. Israelichvelli and Pashley [76] found periodicity in the hydration force on bringing mica sheets together and attributed it to the layer by layer displacement of a co-ordinated water structure. At high concentrations of electrolyte, Pashley and Quirk [77] concluded that the forces of repulsion between mica surfaces could not be explained by DLVO theory and that the extra repulsive force must be due to hydration of the cations. Although there is agreement with the ideas of P. F. Low, much of this work does not disregard the double layer contribution to the swelling mechanism (which is particularly relevant at large separations where the influence of the layer surface on water structure will be limited) and state that it is the counter ions that hydrate and not the surfaces.

The thermodynamic data showed that water in clay-water systems varies significantly from bulk water and gave very different results from those obtained by infrared spectroscopic methods. This is not an unlikely result, since infrared radiation will probe the vibrational motion of the interlayer water whereas the thermodynamic properties will measure the time-averaged behaviour of water (including the vibrational, rotational and translational molecular motions). This being the case, thermodynamic data would be expected to show few differences from data obtained by X-ray diffraction. However, differences exist between the thermodynamic data and X-ray diffraction data which may be evidence [29] that thermodynamic properties are more sensitive to structural changes in the liquid phase than diffraction patterns. This may then support the theory of Low [70] that H-bonding of adsorbed water in sodium montmorillonite is more wide ranging than in bulk water, even at high water content.

2.6.3   Computer simulations.

Monte Carlo and molecular dynamic simulations of the clay-water systems have not reduced the confusion surrounding which approach to clay hydration and swelling should be used.

Skipper et al [78] revealed that model Na smectite adsorbed water which forms inner and outer sphere complexes with the Na^+ cation. The interlayer water was not organised around the cation but, due to competing hydrogen bonding with itself and to the surface it exhibits lower self diffusion coefficient than bulk water. Skipper et al [79] used the model Na Wyoming type montmorillonite and found that Na^+ cations associated with tetrahedral substitution sites formed inner sphere surface complexes and that the Na^+ associated with octahedral substitution sites were found at two sites:

i) Outer sphere complexes bound to di-trigonal cavities

ii) Highly solvated species in the diffuse layer.

Between the platelets, interlayer water exists whose structure becomes less organised on increasing hydration, but still remains more organised than in bulk water. Recent studies [80] of increasing layer hydrates of K montmorillonite have shown that the water and cation mobilities are lower than in bulk water. This was attributed to the restricted geometry.

In contrast to these findings, Delville [81] reported that stepwise increases in the interlayer spacing revealed an oscillatory distribution of the local density of water molecules in the interlayer region. This was attributed to solvent structure and the transition between successive water layers. Delville concluded that there is a link between water organisation and the distribution of Na counter cations and that this accounted for the swelling mechanism. The DLVO theory of swelling was rejected because, at some interlayer separations, there was a zero

density of Na^+ in the interlayer region and so swelling pressure must have been due to factors other than hydrated Na^+ cations in the diffuse layer. Delville was unable to find any significant periodicity in the water content of the pore; the swelling energy; or the solvation forces, as would be expected if there was strong organisation of water molecules at the clay surface and subsequent layering. This was attributed to the ability of water to overlap and fill available space which is not possible in hard sphere models. Similar stepwise increases in interlayer spacing have been reported elsewhere [82]. These, however, have been attributed to the formation of hydrogen bonds between water protons and the oxygens on the silicate surface and the adsorption of water in the hexagonal cavity of the clay surface.

Since the experiments and results presented in this thesis have been obtained by spectroscopic techniques, then DLVO theory will be used to interpret them. This does not imply that the theories of Low and his co-workers are in any way flawed, it is mainly a reflection on the relative ease of interpreting results by the two theories.

2.7.   Interactions between clay particles in aqueous suspension.

Clay minerals exist in aqueous suspensions as fundamental crystallographic units of individual platelets. Brownian motion causes these platelets to approach each other and depending on the nature of the dominant force between them, the platelets will either repel each other and continue to exist as individual units, or they will attract and form flocs, and the system will be flocculated.

2.7.1. Attractive van der Waals forces

Short range van der Waals forces arise from the instantaneous alignment of electric dipoles on neighbouring atoms. Since clays have very large numbers of neighbouring atoms these forces are additive and can become quite important. Although they are relatively short range compared to the range of the electrical double layer (the cumulative force decays as $1/d^3$ where d is the distance of separation [83]) if the platelets come close enough to each other the force will be strong enough to cause aggregation. Figure 2.7.1 shows the typical form of the potential energy curve.

Figure 2.7.1. Typical potential energy curve for van der Waals attractive forces

Energy

Repulsive

+tive

Distance of
separation (d)

0

Attractive

-tive

$\propto 1/d^3$
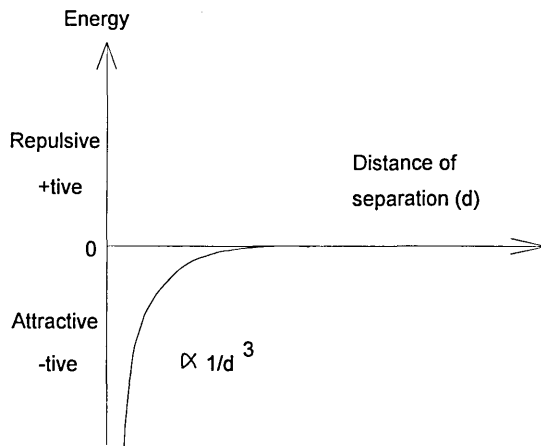
2.7.2 Repulsive electrical double layer forces

Figure 2.7.2a shows a typical representation of the ion distribution next to the clay surface. This representation is based on the Stern model which describes the electric potential which must be overcome for two like charged surfaces to come together. This electric potential (figure 2.7.2b) is not just the charge itself, but is derived from the assembly of the charged surface and the exchangeable

cations. Within this model the solid surface has a fixed charge (which for montmorillonite is negative due to isomorphous substitution as explained previously). In the solution, next to the solid surface, is a strongly adsorbed monolayer of exchangeable cations this layer is called the Stern layer and the potential drops across the Stern layer from its original value to a value known as the Stern Potential. The outer limit of the stern layer is defined by a plane commonly known as the Outer Helmholz plane. Due to the adsorption of water to the tightly bound Stern layer of cations there also exists a plane of shear which defines the surface of the envelope of water surrounding the Stern layer. The electrical potential at this point is known as the zeta potential. It is the zeta potential which determines the stability of the clay suspension (it is in turn dependent upon the Stern potential).

Figure 2.7.2a Diagrammatic representation of the electrical double layer
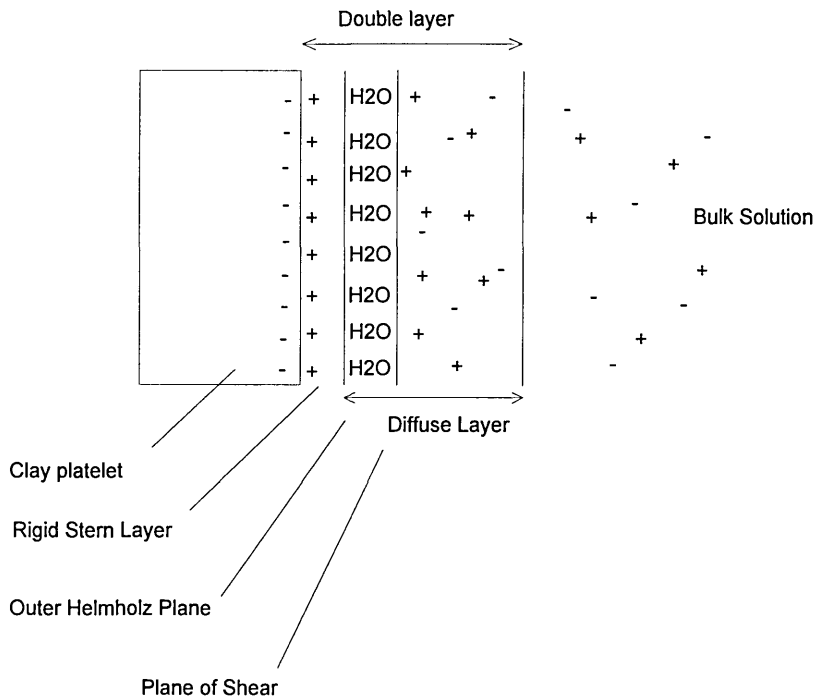
Beyond the plane of shear, a diffuse layer of mobile exchangeable cations is formed whose concentration decays exponentially away from the surface until it reaches a concentration which corresponds to that of the bulk solution. The potential similarly drops across this region.

Figure 2.7.2b The electrical potential surrounding the clay platelet

Energy

Repulsive

+tive

$\propto e^{-d}$

0

Attractive

-tive

distance of
separation (d)
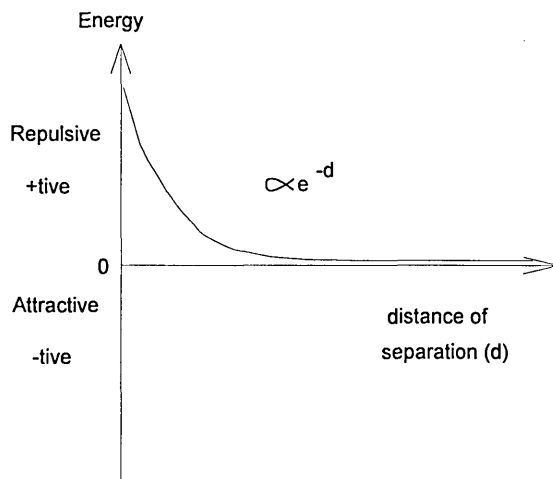
2.7.3. Flocculation of montmorillonite by electrolyte

In order for flocculation to occur, the attractive van der Waals forces must be greater than the repulsive forces due to the electrical double layer. However, the diffuse layer can be contracted by increasing the electrolyte concentration (number of cations) until it is the same in the bulk as it is at the surface of the clay platelet (figure 2.7.3a).

Figure 2.7.3a The effect of increasing electrolyte concentration on the electrical potential surrounding the clay platelet.
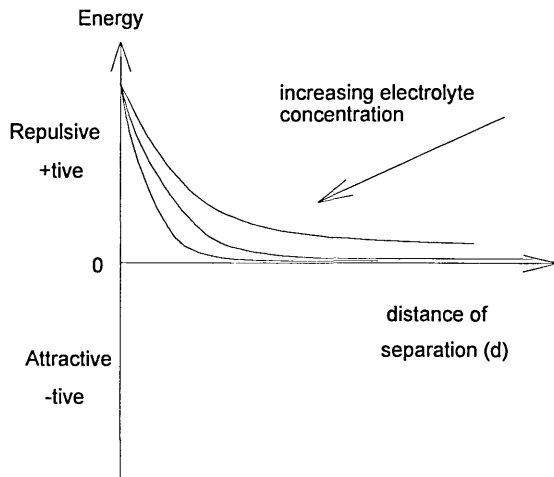
The diffuse layer will contract and will enable platelets to approach each other more closely. Since attractive van der Waals forces are unaffected by salt concentration and predominate at short ranges, it is possible that they will cause the plates to attract and to flocculate (figure 2.7.3b-d).

Figure 2.7.3. The effect of increasing electrolyte on the overall interaction energy (thick line)
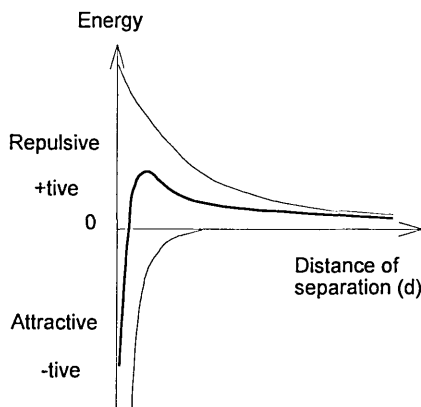
b) No electrolyte, overall interaction energy is repulsive
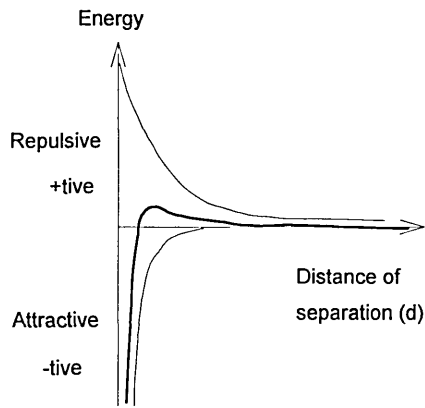
c) Low electrolyte concentration (~0.002%), limited flocculation
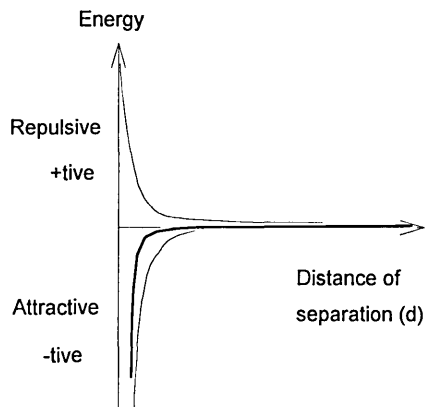
d) High electrolyte concentration (2%), extensive flocculation

The valency of cations in addition to a high concentration of counter cations in solution, is also important in causing flocculation and flocculation follows the order:

$$Ca^{2+} > K^+ > Na^+ > Li^+$$
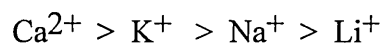
Hence, monovalent cations are less likely to cause flocculation. However, divalent cations are able to cause flocculation by a bridging mechanism in which its valency of two is satisfied by negative charge on two sheets causing the layers to stay closer together, a feature not available to monovalent cations.

2.7.4. Mechanisms of flocculation

Three possible particle-particle associations are possible for montmorillonite platelets and are shown schematically in figure 2.7.4.

1.   Edge-Face (EF) in which positively charged edges are attracted to negative surface charges.

2.   Edge-Edge (EE) in which the positive and negatively charged edges are attracted to each other.

3.   Face-Face (FF) in which two faces are attracted. This flocculation gives the largest association in terms of area of contact.

All three mechanisms are possible but the FF mechanism will predominate since the negative basal surfaces of the clay govern flocculation. This leads to dense flocs forming which will have the most stable orientation possible and will easily sediment out of solution.

Figure 2.7.4. The three possible particle-particle associations

Face-to-Face   Face-to-Edge   Edge-to-Edge
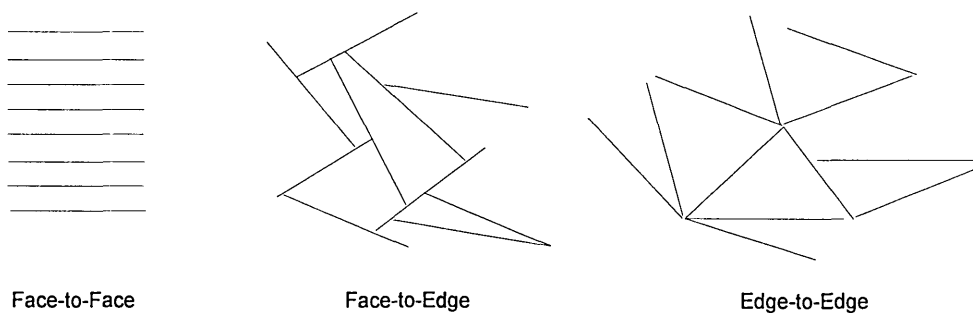
2.7.5.   Aggregation-Dispersion

Van Olphen [14] distinguishes between flocculation, as obtained by EF and EE flocculation mechanisms, and aggregation which is due to the parallel aggregation of thicker particles by the FF flocculation mechanism. The term dispersion is then applied to the reversal of the aggregation mechanism, for example, by mechanical shear or chemical forces (such as hydration) which breaks down a dense stack of platelets into smaller particles. It is possible therefore for dispersed or aggregated suspensions to be also flocculated or deflocculated.

2.7.6.   Flocculation-Deflocculation

Deflocculation is the reverse procedure of the EF and EE flocculation mechanisms. The most commonly used mechanism for deflocculation involves the reversal of edge charge since this is easily achieved by increasing pH to give the edges an overall negative charge. It is also possible by peptisation as outlined by Van Olphen [14] which is the adsorption of excess polyanions such as silicate and phosphate at the clay edges leaving an overall negative charge. It is, however, also possible to reverse the charge on the clay surface by the adsorption of organic cations such as long chain quaternary cations. Deflocculants are commonly found in drilling fluids in order to reduce particle-particle interactions, i.e. in order to reduce the drilling fluid viscosity. Commonly found deflocculants, or thinners, as they are known in drilling fluids, are polyacrylic acid and ferrochrome lignosulphate [6] whose adsorption by the clay mineral increases the repulsion between platelets by increasing the overall negative charge on them.

2.7.7. Polymer stabilisation of colloidal dispersions.

There is another common cause of flocculation used in colloid chemistry and is often encountered in clay chemistry and that is polymer flocculation. Napper [84] discusses the theory of the effects that polymers have on colloidal dispersions and describes them roughly in terms of the concentration of polymer in solution (figure 2.7.7. after Napper [84]).

Figure 2.7.7 Effect on dispersion stability on addition of increasing polymer concentrations

Bridging Flocculation

increase polymer concentration

Steric Stabilisation

increase polymer concentration

Depletion Flocculation

increase polymer concentration

Depletion Flocculation
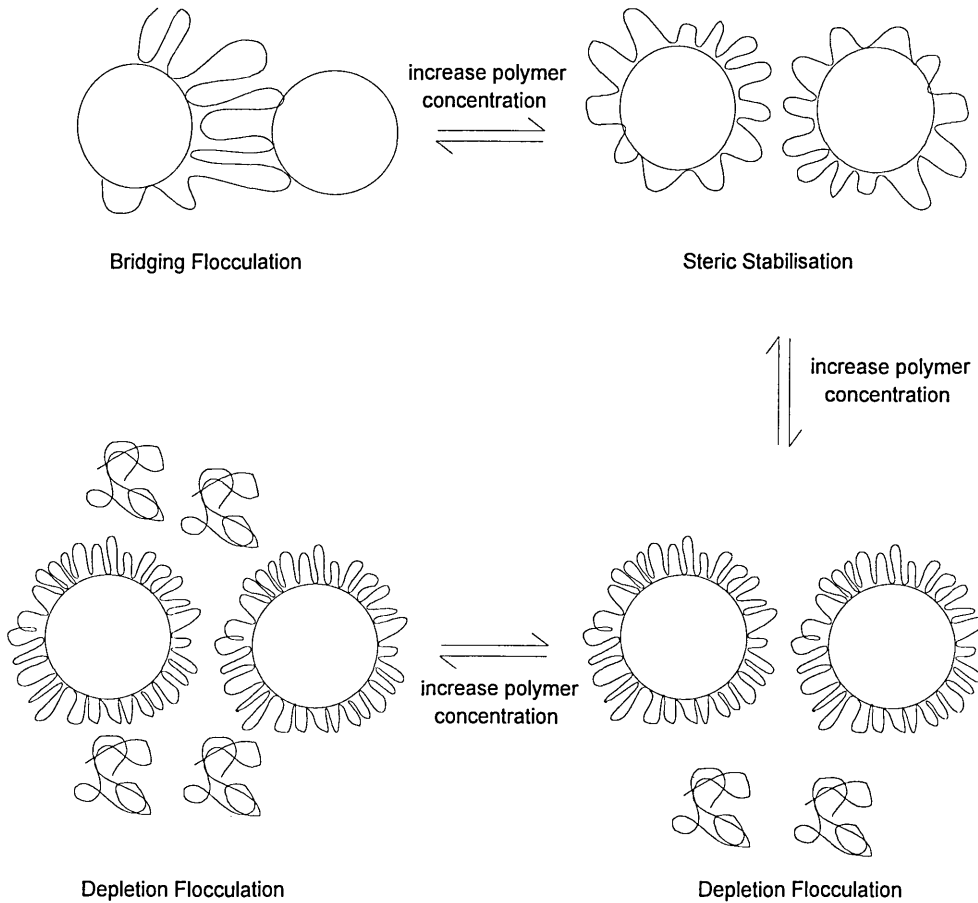
2.7.7.1. Bridging Flocculation.

At relatively low concentrations, polymer segments on one particular chain are adsorbed to the surface of more than one colloidal particle. This links the particles and forms rapidly sedimenting flocs or aggregates.
Bridging is possible because there is incomplete surface coverage at such low concentrations which allows a polymer chain attached to one particle to adsorb to another during Brownian collisions.

The best bridging flocculants are high molecular weight polyelectrolytes because the spatial extension of a polymer increases with molecular weight and charge (chapter 3). The flocculation mechanism requires that the spatial extension of the adsorbed polymer loops or chains must be greater than the electrostatic double layer which extends from the colloid surface so as to overcome colloid repulsion. Addition of electrolyte improves the effect of lower charge, lower molecular weight flocculants by collapsing the electrostatic double layer and making flocculation easier.

The commonest modes of interaction are electrostatic or hydrogen bonding. However in clays, it is possible for a negatively charged polymer to flocculate the negatively charged platelet. This is by a mechanism which involves the bridging effect of Ca^{2+} which binds to both the clay surface and the negatively charged polymer (a bridge within a bridge).

2.7.7.2. Steric stabilisation

As the polymer solution concentration increases more polymer is able to adsorb to the particles and saturation surface coverage can be obtained.

The best steric stabilisers are copolymers in which the anchor component is insoluble in the solvent but adsorbs strongly to the particle and a chain component which is soluble and extends in solution. Bridging flocculation is prevented by having complete surface coverage and by the repulsive interaction between stabilising chain components on each particle. Sterically stabilised particles may flocculate if the anchoring is not adequate, if the surface coverage is incomplete or if the thickness of the adsorbed layers is so thin that the van der Waals attractive forces can act between the particles. Bridging heteroflocculation is possible by the addition of a low concentration of a second adsorbing polymer to a sterically stabilised dispersion.

2.7.7.3. Depletion flocculation

At higher polymer concentrations, polymer molecules exist both adsorbed to particles and as free polymer in solution. In such circumstances, if the colloidal particles become closer together than the polymer diameter then the polymer will be excluded leaving pure solvent in the interparticle region. If the polymer has a high affinity for the solvent and the particles approach each other more closely solvent will be forced from the interparticle region bringing the particles closer together and enhancing flocculation.

2.7.7.4. Depletion stabilisation

If the polymer concentration is increased further, depletion stabilisation will immediately follow depletion flocculation. this is because work must be done to de-mix polymer and solvent which have a high affinity for each other and to leave pure solvent in the interlayer region. This manifests itself as a repulsive force and acts to thermodynamically stabilise the dispersion, thus preventing further flocculation.

2.7.7.5. Charge Neutralisation

The adsorption of positively charged polymer onto a negatively charged colloid particle (for example when highly charged cationic polymers are mixed in a clay suspension) bridging flocculation may occur but also simple charge neutralisation is observed. It has been suggested [83] that if the adsorption of polymers in these circumstances have no chains and loops, i.e. lie flat to the surface, there exists patches of positive and negative charge on particle surfaces. A patch of positive charge on one particle may then interact with a patch of negative charge on another particle during Brownian collisions causing flocculation.

3.   ADSORPTION OF WATER SOLUBLE POLYMERS FROM AQUEOUS SOLUTION ONTO CLAY MINERAL SURFACES

Before it is possible to discuss the behaviour of water soluble polymers at the clay-water interface it is imperative to understand the general behaviour of such polymers in solution since this will govern, to a certain extent, the adsorption behaviour. Indeed, Burchill et al [85] explained the differences between the adsorption of PVA and PEO (similar molecular weights) on smectite surfaces. In solution, both polymers exist as random coils but PVA, being more hydrophilic, is more expanded than PEO. Consequently the more expanded PVA polymer makes contact and covers a wider surface, trying to collapse onto the surface in the lowest energy conformation possible. Adsorption sites will still remain but are inhibited by previously adsorbed molecules and so the ensuing polymer molecules will adopt various conformations to adsorb at unoccupied sites. In contrast, the less expanded PEO molecule will adsorb and make as many contacts with the surface as possible, but will uncoil and spread over the surface less. Thus, fewer adsorption sites will remain in the proximity of the adsorbed molecule but larger areas of surface will remain unoccupied.

3.1   Behaviour of polymers in solution

It is possible to dissolve linear or branched amorphous polymers in a suitable solvent such that the polymer too behaves like a liquid. It should be noted that cross-linked polymers swell in suitable solvents but are not able to solubilise. A suitable solvent is one which is defined as thermodynamically 'good', i.e. one with which the polymer is highly compatible and in which the polymer-solvent interactions govern the extent to which the polymer chain is expanded. Expansion occurs because solvent allows remote segments of the polymer chain to come into close proximity, since two segments cannot occupy the same space

50

they experience a repulsive force between them, causing the chains to extend. The polymer is said to have an 'excluded volume' into which segments cannot move.

In solution, the polymer adopts a configuration in which segments are located from the centre of the molecule in a Gaussian distribution of arrangements which corresponds to a random coil configuration. Hence, the typical shape of a polymer in solution (provided there is relative ease of rotation about main chain bonds) is a random coil with a large number of conformations. Hindered rotation by bulky substituents and chemical groups will reduce the number of conformations a polymer may adopt and thus it may not adopt a random coil until higher temperatures.

It should be noted that 'like dissolves like'. Consequently, polar polymers and polyelectrolytes such as those used in these studies (e.g. polyethylene glycol, polyacrylamide and partially hydrolysed polyacrylamide) dissolve easily in polar solvents, particularly water

A solvent which is defined as thermodynamically 'poor', is one which is not suitable for dissolving the polymer. Very few solvent-polymer interactions exist and as a result coil expansion is restricted. In fact, the coil is compressed and often precipitates out of solution. The quality of a solvent is dependent upon temperature and an ideal solvent (or θ solvent) is one in which the polymer is neither compressed nor extended, i.e. in which equal numbers of compatible and non compatible interactions exist. This phenomenon occurs at the θ temperature.

3.1.1. Thermodynamics of polymer solutions

In dilute solution, due to its large size and inter-connectivity, polymer molecules are able to explore all possible configurations and as a result exists as random coils. Hence, there exists a Gaussian distribution of polymer configurations which has a most probable value such that if a molecule expands or contracts on interaction with solvent, it will adopt a less probable configuration (reduce entropy). Consequently, the dissolution of a polymer molecule in solution has a significantly lower entropy of mixing compared with the dissolution of much smaller, conventional solutes.

3.1.1.1. Flory-Huggins theory

The change in entropy involved, the enthalpy of solvation (hydration) and hence, the free energy of mixing of polymer and solvent have received considerable theoretical and experimental consideration [86]. Probably the most widely used theory to calculate the free energy of mixing of pure amorphous polymer with pure solvent is that of Flory-Huggins [87]. They consider the process to occur in two stages:

1. Initially, isolated polymer molecules are fixed in a rigid conformation in the solid state.
2. Finally, the polymer exists as a relatively flexible chain rapidly changing conformation subject to the constraints imposed by its own flexibility and solvent interactions.

As a result, the mixing process can be broken down into the transfer of solid from a perfectly ordered solid to a disordered flexible state (entropy change)

with conformational freedom, and the mixing of flexible polymer chains with solvent molecules (enthalpy change).

Using Flory-Huggins theory, the entropy of mixing can be separately calculated by modelling the solvent as a randomly occupied lattice. Each segment of the polymer is placed on any one lattice site and connected to the next segment. It is possible to model the number of ways in which a polymer molecule can be arranged on the partly filled lattice. The number of arrangements is then related to the entropy of mixing.

The enthalpy of mixing is also calculated separately, by determining the formation of polymer-solvent interactions which replace solvent-solvent and polymer-polymer interactions on dissolution. The probability of solvent If χ_{12} polymer interaction is determined from the lattice model and an interaction If χ_{12} rameter per molecule of solvent, χ_{12}, is introduced.

If χ_{12} >0 solvent-polymer interactions are not favoured (poor solvent)

If χ_{12} <0 solvent-polymer interactions are favoured (good solvent)

3.1.1.2. Flory-Krigbaum theory

Flory-Huggins theory is not perfect and many experimental observations have indicated that it has limitations and is not a good model of real polymer solutions, particularly at low concentrations. Flory and Krigbaum [88] devised a more realistic model based on regions of pure solvent interspersed with concentrated areas of solvated polymer.

3.1.2. Effects of physical properties on the behaviour of polymers in solution

3.1.2.1. Effect of molecular weight

The molecular weight of a polymer significantly affects the extent of polymer solvent interactions such that in a particular solvent at a particular temperature, the solubility will decrease as molecular weight increases. This is a purely thermodynamic phenomenon explained in terms of ΔH, ΔS and ΔG. However, the rate of polymer dissolution also decreases with increasing molecular weight. This is governed by the polymer diffusion, a purely kinetic phenomenon.

3.1.2.2. Effect of solvent

Obviously, the thermodynamic quality of the solvent is extremely important. However, a polymer such as polyethylene glycol (PEG) in good quality solvent such as water can experience many other physical effects. It is possible for PEG to self associate by forming intramolecular and intermolecular H-bonds between hydroxyl end groups and ether oxygen atoms in the main chain. The presence of an electron acceptor in the mixture for example $H^{\delta+}$ in water can allow solvation complexes to occur between water and the ether or hydroxyl oxygen atoms. The intra and intermolecular H-bonding of PEG in a dilute solution of carbon tetrachloride was investigated by Philippova et al [89] using IR spectroscopy. Figure 3.1.2.3 shows possible arrangements of PEG.

The effect of water as a solvent for PEG has received quite some attention. Some NMR studies have shown [90] that at high water contents, one molecule of water binds per repeat PEG unit. Other studies however [91], have shown that between 2 and 4 water molecules bind per repeat unit. Indeed, Liu and Parsons [91] observed linear increases in chemical shift of both OH and internal

ethylene protons on dilution up to 50% volume water, then very gradual increases on further increases in water content. They relate this to the formation of a stoichiometric hydrate with 3 water molecules. Infrared studies showed that PEG behaves the same in the melt as in benzene solution. However, on hydration, increases in band intensity of the ethylene rocking vibration (at 886 cm^{-1}) were interpreted as enhanced PEG order in aqueous solution. PEG is thought to adopt the TGT conformation for the COCCOC sequence.

Figure 3.1.2.3 The possible inter and intramolecular interactions of PEG in aqueous solution.

Intramolecular H-bonding

Intermolecular H-bonding
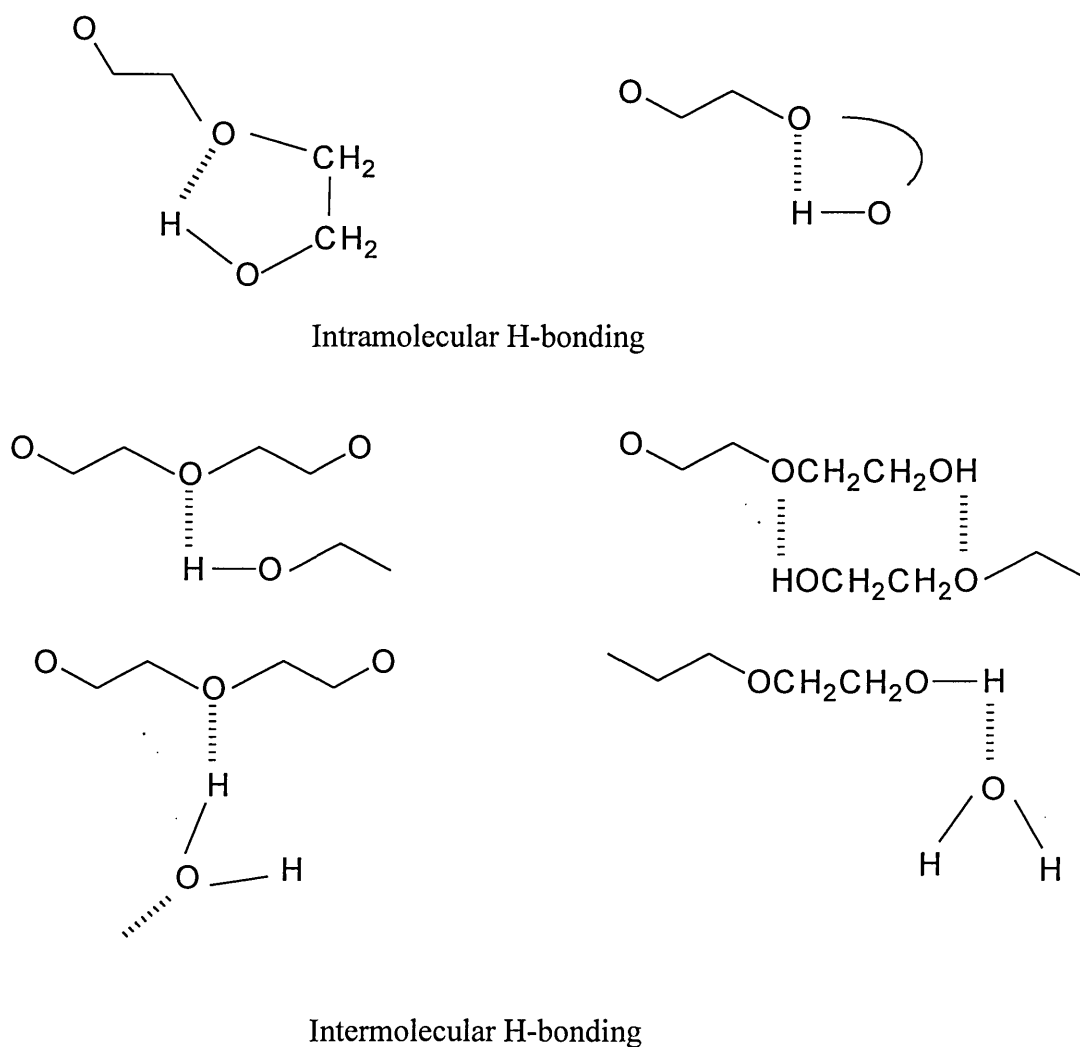
The behaviour of polyethylene oxide (PEO) in water is a balance between hydrophobic and hydrophilic interactions and has been studied extensively [92]. Water forms highly ordered cage structures around PEO molecule, which is an entropically unfavourable process. As temperature is increased, and provided the cage structure remains intact, the entropy becomes less favourable and the system will phase separate. Hence, polymers of this nature are said to exhibit cloud point behaviour [92] such that as the temperature is raised, the solubility of the polymer is reduced and the polymer 'clouds out'. The cloud point behaviour depends on the molecular weight and composition of glycol and the presence of electrolyte [93]. Small angle neutron scattering experiments [94] have shown that polymer self assembly is important in the phase separation in aqueous solution with inorganic salts. Polyacrylamide does not exhibit cloud point behaviour because the water does not form highly ordered structures around the polymer molecule.

It is important to note that in solutions containing PEO and polyacrylamide (PAM) there is no interaction between the two polymers [95]. Indeed, Maltesh et al [96] showed that, although H-bonding interactions between polyacrylic acid (PAA) (essentially 100% hydrolysed PAM) and PEO are known, partially hydrolysed polyacrylamide (HPAM), between 8% and 42.8% hydrolysis, showed no interactions with PEO. This may be due to the weak NH proton donating ability of PAM or to the random distribution of carboxylate groups which ensures that only a few, widely spaced interactions between ether oxygen and carboxylic acid will be formed; thus rendering the complex unstable. Although the fluorescence technique used by Maltesh et al [96] was able to identify interactions between HPAM and polyvinylpyrrolidone, it may not be able to detect the very weak interactions between hydrolysed polyacrylamide and PEO.

3.1.2.3. Effect of temperature

Temperature significantly affects the quality of the solvent, hence, above the θ temperature, the solvent will be thermodynamically 'good' and the polymer will expand and exist as random coils. As the temperature is lowered to the θ temperature, the solvent will behave ideally and the polymer will neither expand nor compress. However, subsequent lowering of the temperature will change the solvent quality to 'poor' and the polymer chains will contract and adopt a more compact configuration.

3.1.2.4. Effect of electrolyte

As mentioned previously, addition of electrolyte will significantly reduce the phase separation temperature of PEO-water systems. The cloud point being reduced by 40°C in a 2 $molkg^{-1}$ KCl solution [93]. Otherwise, the behaviour of glycol polymers in the presence of dissociated metal cations in solution can be considered to be similar to that of multidentate ligands such as crown ethers and cryptands. These molecules are known to co-ordinate around metal cations in solution which suggests that the complexation is due to ion-dipole interaction. Polyethers such as glycols are double action oxygen donor ligands [97], which are able to stabilise the cation and anion at the same time. Glycols with molecular weights between 150 and 300 $gmol^{-1}$ have been seen to undergo complexation with Na^+ and K^+ cations [97]. The complexation of Li^+ has been studied by Cobranchi et al [98] using infrared spectroscopy. Terminal OH groups interact with the cation but replacing these with methyl groups does not alter the kinetics of complexation. The terminal functional groups of larger molecules do not co-ordinate to metal cations probably due to being involved in intramolecular bonding. PEO molecules interact with group 1 and 2 metal ions and have been found to exist in a helical state [97]. Within the helix, each turn is

composed of approximately 7 units and the donor oxygen atoms occupy similar positions as in a crown ether.

Bauer and Rogers [99] have used Cl⁻ as the counter ion and found that the solid state structure of complexes between group 1 and 2 metal cations and small PEG molecules, reveal two PEG ligands co-ordinate to the metal cation, displacing all the anions and water molecules. For longer PEG chains, only one ligand co-ordinates, the remaining co-ordination sites being filled with water. No directly co-ordinated Cl⁻ is observed.

3.2.   Behaviour of anionic polyelectrolytes in aqueous solution

In aqueous solution, polyelectrolytes are dissociated. The effect of electrostatic repulsion between charged groups on the chain preventing the polymer from adopting a coiled configuration, causing it to expand and exist in a stretched configuration which renders their solutions highly viscous.

3.2.1.   Effect of physical properties on the behaviour of anionic polyelectrolytes in solution

The effect of molecular weight and temperature on the dissolution of polyelectrolytes in solution are very similar to their effect on neutral polymers as outlined above. However, due to their charged nature, the presence of salt or acid can change their behaviour considerably.

3.2.1.1   Electrolyte concentration

Around an area of charge on the polyelectrolyte a diffuse double layer develops in the same way as it does around a clay mineral surface. This causes the

electrostatic repulsion between different segments on the polymer and results in a stretched configuration. Consequently, increasing the ionic strength of the solution will cause the double layer to collapse and allow charged areas on the chain to approach each other more closely. The polyelectrolyte will then behave more like an uncharged polymer and as a result it may adopt a coiled configuration, reducing the solution viscosity.

3.2.1.2   Effect of pH

The presence of protons in solution forces the dissociation equilibrium towards the undissociated form of an acid species. This will make the polyelectrolyte behave more like a neutral polymer with polar segments and as result adopt a random coil configuration in solution.

3.3.   Adsorption of polymers at the solid-liquid interface

The adsorption of polymers from solution at the water-solid interface has received considerable attention [100, 101]. Some similarities exist with the adsorption of smaller, simpler organic molecules at the same interface particularly with respect to the nature of the interactions and the orientation of the adsorbed polymer. Consequently, the adsorption behaviour of polymers can often be predicted by the behaviour of smaller molecules which have the same functional groups and adopt similar orientations. However, a simple molecule can not behave in exactly the same way, the main differences between polymer adsorption and the adsorption of smaller molecules are [102]:

1   A polymer molecule is able to adopt a very large number of configurations in the bulk solution and also adsorbed at the interface. The number of these configurations will increase as the molecular weight increases (i.e. as the

number of segments increase). It is improbable that the adsorbing polymer will adopt a minimum energy configuration and is likely to adsorb in a metastable conformation.

2   A very large number of surface contacts (interactions with the surface) are possible and give rise to a large net energy of adsorption compared to smaller molecules. This multi-point attachment of polymer on the solid surface renders the adsorption process irreversible. Although the adsorption of each individual segment is considered to be reversible it is highly unlikely that all points of attachment will be severed simultaneously and allow the polymer to be totally desorbed from the surface.

3   Polymer adsorption is a much slower process than adsorption of smaller organic molecules. The kinetic factors affecting polymer adsorption are outlined by Elaissari et al [103] but in general the rate controlling step is governed by the slower rate of diffusion of larger molecules to the interface relative to smaller molecules (due to mass transport effects). Hence, equilibration adsorption times for polymers will be much longer than for smaller molecules. This is particularly important for polydisperse polymers where smaller molecules will be adsorbed first, only to be replaced by the preferentially adsorbed larger molecules. Surface coverage is also important since reducing the accessible surface area will force adsorbed polymers to change configuration to accommodate further adsorption. This is obviously a more difficult process and therefore takes a longer time and continues until maximum adsorption is obtained. The maximum adsorption is considered to be the equilibrium position or plateau on the adsorption isotherm.

Due to the complex nature of the adsorption process a classical picture of polymer adsorption has been devised [104] (figure 3.3) in which segments of polymer chain are able to behave in one of three ways:

1.	A series of consecutive polymer segments can all be in contact with the surface, known as TRAINS

2.	A series of segments which are only in contact with the solution and are bound at each end by a train are known as LOOPS. Loops are the bridges which separate trains.

3.	TAILS are the free end of the polymer chain which extend into the solution and which are bound at one end to a train.

Figure 3.3. Classical picture of polymer adsorption at the solid-liquid interface.

TAIL

LOOP

polymer

TRAIN

interface

Substrate
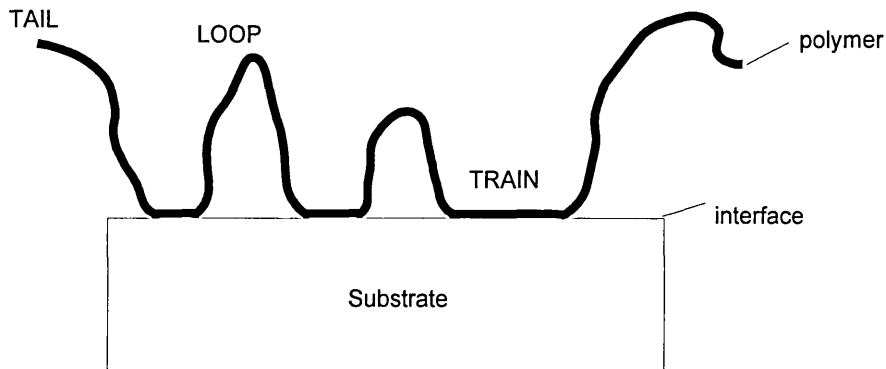
3.3.1.	Statistical mechanical approach

It is impossible to describe each individual configuration of adsorbed polymer and consequently statistical methods are employed to define the adsorption. An equilibrium adsorption configuration is defined which describes the average or most probable configuration. This is an energetic balance between the net energy change on adsorption; the decrease in entropy on constraining the flexible chain and the increase in entropy on release of solvent either associated with the surface or the polymer in solution.

3.3.2. Experimental parameters

Three important experimental parameters are used to describe polymer adsorption [104]:

1. The amount of polymer adsorbed per unit area of surface, Γ.

Adsorption isotherms may be calculated by determining the adsorbed amount, i.e. the difference in polymer concentration in solution before and after equilibration with a solid surface of known surface area. Adsorption isotherms for polymers are generally sharp with the amount adsorbed rising steeply at low polymer concentrations then reaching a plateau of maximum adsorption at higher concentrations.

2. The fraction of bound polymer

It is extremely important to know the nature of the interaction between polymer and solid surface, and the number of segments in contact with the surface. This is obtained directly using infra red spectroscopy (by measuring the absorption band shift for a species adsorbed from solution). Microcalorimetry techniques can also be used to obtain the number of segments in contact with the surface [105].

3. Adsorbed layer thickness

Small angle neutron scattering [106] gives information on the distribution of segments near the interface which enables the determination of the conformation of adsorbed polymer at the solid interface. In addition, Tadros [104] discusses the estimation of hydrodynamic thickness using hydrodynamic methods and their usefulness in predicting the adsorbed layer thickness and hence the conformation of polymer at the interface.

3.3.3. Effect of physical properties on the adsorption of polymers from solution.

3.3.3.1. Effect of temperature

The adsorption of polymers at the solid-liquid interface is affected very little by changes in temperature [100]. However, the change in solvent quality on changing the temperature will have an affect on the adsorption behaviour as outlined below.

3.3.3.2. Effect of solvent

It has been shown that the amount of polymer adsorbed from solution increases as the quality of the solvent decreases. Fleer and Lyklema [100] discuss the gain in free energy on adsorption of polymer segments which leads the surface to act as a nucleus to promote phase separation of polymer from solution. Since phase separation is promoted in poor quality solvents, then adsorption of polymer at the solid interface will be enhanced in a poor quality solvent.

3.3.3.3. Effect of molecular weight

The amount of polymer adsorbed increases with chain length, i.e. as molecular weight increases. This is particularly noticeable in poor quality solvents. There is considerable experimental and theoretical evidence reviewed by Fleer and Lyklema [100] that longer molecules adsorb in preference to shorter molecules. This is particularly important in polydisperse systems which must be treated as a mixture. Usually the smaller molecules will diffuse to the surface more quickly and adsorb first. These are then replaced by the preferentially adsorbed longer

chain molecules and at equilibrium there exists a solution enriched with short chain molecules.

3.3.3.4. Effect of particle size

The adsorption of polymers onto small particles does not correspond to the theoretical description of polymer adsorption onto an infinitely flat surface [107]. Cosgrove et al [108] studied the adsorption of PEO onto colloidal silica and noted the importance of particle concentration in reducing the gap between particles. Hence, at high particle to polymer number ratios and when polymer molecules were larger than the silica particles bridging flocculation occurred. Furusawa et al [109] observed an increase in polyacrylamide adsorption with decreasing hematite particle radius. They also point out the influence of particle concentration

3.4   Adsorption of anionic polyelectrolytes at the solid-liquid interface

This is a very special case of polymer adsorption which is made more complicated due to the electrostatic interactions which are possible. Polyelectrolytes may be adsorbed on opposite or similarly charged surfaces but adsorption on like charged surfaces becomes impossible when the electrostatic repulsion becomes too large.

Due to the behaviour of polyelectrolytes in solution, at high ionic strength and low pH, or at low polymer charge density, the adsorption behaviour resembles that of non-ionic polymer adsorption, having very similar adsorption isotherms. In this respect the adsorption of polyelectrolytes is 'irreversible', i.e., multi-point attachment to the surface described by the classical train, loop, tail model.

However, the desorption of polyelectrolyte can easily be achieved by significantly changing the electrolyte concentration or pH [110].

3.4.1 Effect of physical properties on the adsorption of anionic polyelectrolytes at the solid/liquid interface.

3.4.1.1. Effect of polyelectrolyte charge density

In general, the adsorption of polyelectrolyte decreases as the charge density of the chain increases. This is due to the potential which is created at the surface which prevents further adsorption. If an anionic polyelectrolyte is adsorbed on a positively charged surface however, it is found that adsorption increases with increasing charge density.

3.4.1.2 Effect of electrolyte and pH

At high salt concentrations or low pH, the charge density of the polyelectrolyte is reduced and so the amount adsorbed increases. Under these conditions, the polyelectrolyte exists as a random coil and will adsorb as such. This allows more surface area for further adsorption which would not be available if adsorption occurred in the extended conformations adopted by polyelectrolyte in high pH and low ionic strength solutions. Somasundaran and co-workers [111] have discussed the effect of pH on the adsorption of polyacrylic acid on alumina. At low pH the polymer exists as a random coil in solution and will adsorb as coils, subsequent raising of the pH partially expands the adsorbed coiled chains. At high pH the polymer exists as a stretched chain and will strongly adsorb in this extended conformation, lowering of the pH will have no effect on the chain conformation.

3.5 Adsorption of polymers and polyelectrolytes on clay minerals

The adsorption of polymers onto mineral surfaces is of great technological importance. In particular, the ability of polymer to both flocculate and stabilise colloidal particles (as outlined in previous chapter) has been used extensively in processes such as selective separation of mineral ores from impurities [112], in the manufacture of paper [113] and in oil well drilling fluid technology [5].

Due to the quantity and diversity of published literature in this area, only the most relevant work has been reviewed. This includes, the adsorption onto clay minerals (in particular montmorillonite) of neutral polymers such as polyalkyl glycol, polyethylene oxide, polyacrylamide and smaller analogous units such as ethylene glycol and acetamide; and the adsorption of anionic polymers such as partially hydrolysed polyacrylamide.

3.5.1 Bonding mechanisms between clays and organic species.

Mortland [114] and MacEwan and Wilson [46] expanded on the ideas identified by Parfitt and Rochester [115] (that the general bonding mechanisms between a surface and adsorbed species were Chemical adsorption; Hydrogen bonding; Hydrophobic bonding and van der Waals bonding) when specifically identifying the characteristics of clay-organic interactions. Mortland describes the dependence of the interaction on the properties of the organic molecule, the water content of the system, the nature of the exchangeable counter cation and the properties of the clay mineral.

3.6 Adsorption of cationic polymers on clay minerals

Positively charged organic molecules adsorb via electrostatic interaction between themselves and a negatively charged clay mineral surface. Mortland [114] identified the possible mechanisms as ion exchange of inorganic exchangeable cations by organic cations and protonation of adsorbed organic species.

3.7 Adsorption of neutral polymers on clay minerals

3.7.1. Ion-dipole interactions

Originally, the adsorption of polar, neutral organic molecules was attributed to a hydrogen bonding mechanism between molecule functional groups and the silicate surface. However, it has since been shown that the interaction of molecules with the silicate surface are weaker than ion-dipole interactions and that the nature of the exchangeable cation and its associated water molecules are extremely important to the adsorption process [114].

3.7.2 Entropy

The adsorption of linear, flexible, non-ionic polymers onto clay minerals is generally entropy driven [85, 116, 117, 118]. Although the adsorption of such polymers would be expected to reduce the entropy of the system, by confining a polymer to the clay surface, the adsorption is accompanied by the desorption of water molecules which are associated with the clay surface (figure 3.7.1). It is the increase in the translational degrees of freedom of these water molecules which provides the driving force (positive entropy contribution) for the adsorption.

Figure 3.7.1. Schematic showing the desorption of water molecules from clay mineral surface on adsorption of uncharged polymer. Also note the change from a random coil in solution to an extended chain conformation (After Theng [116]).
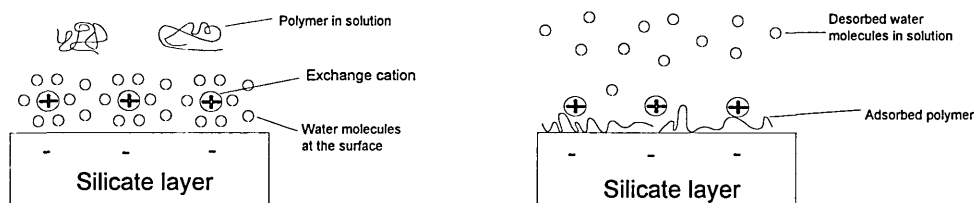
3.7.3. Hydrogen bonding interactions

The most common type of hydrogen bonding seen in clay-polymer interactions is the formation of the water bridge. This involves the linking of a polar molecule to an exchangeable cation through a hydrogen bond with a water molecule in the primary hydration shell.

3.7.4. Clay mineral oxygen and hydroxyls

A hydrogen bonding mechanism of interaction between clay minerals and molecules capable of hydrogen bonding is probable [119]. There is however, little experimental evidence supporting this theory and as such the most important mechanisms of bonding in such circumstances are that of ion-dipole or water bridge formation.

3.7.5. Effect of electrolyte/exchangeable cations

In dilute Na montmorillonite suspension, where the mineral surface is not restricted, the amount of polymer adsorbed increases with molecular weight as expected. The subsequent arrangement of clay platelets and the change in d-

spacing on cation exchange or increasing ionic strength, can significantly affect the adsorption of polymer. In fact, polymer adsorption decreases with increasing molecular weight in such circumstances [116]. This is significant when the dimension of the interlamellar space becomes so small that accessibility for large polymer molecules is reduced. Hence, increasing the solid loading in suspension or replacing the exchange cation with one which restricts swelling (i.e. Ca^{2+}/Cs^+) reduces the amount of adsorbed polymer. Theng [119] identifies surface accessibility as one of the most important effects to be considered in the adsorption of neutral polymers by montmorillonite. This has important implications in a practical sense when one must consider not only the type of exchangeable ion and electrolyte concentration chosen but also the order in which electrolyte and polymer are added (figure 3.7.5.).

Figure 3.7.5. Order of polymer/electrolyte addition: Effect on clay-polymer complexation.

Dispersed clay platelets

↓ *Polymer*   ↓ *NaCl*

Flocculated clay platelets

↓ *NaCl*   ↓ *Polymer*

↓ *Wash*   ↓ *Wash*

Adding polymer then NaCl   Adding NaCl then polymer

69
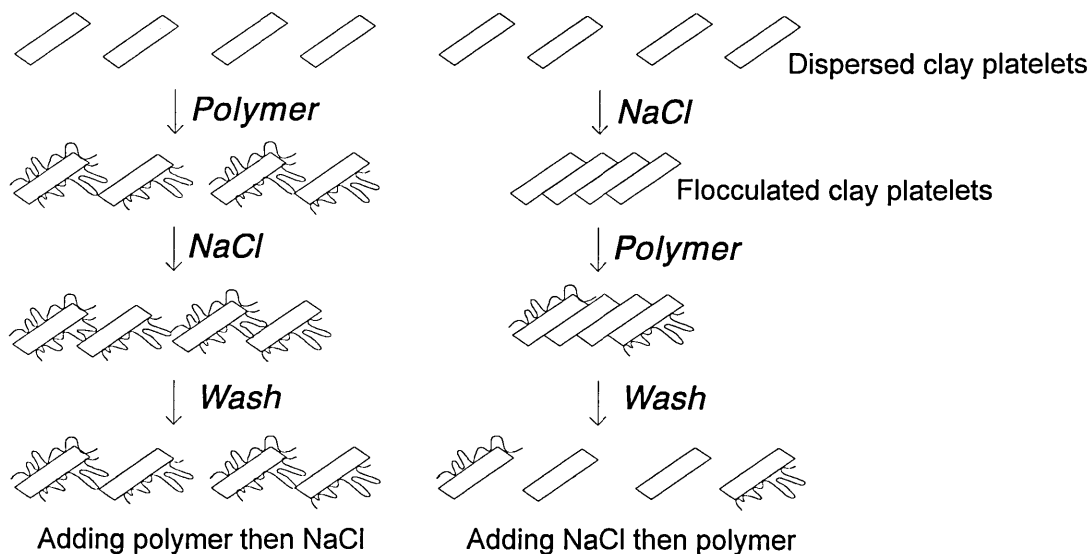
3.8.   Glycolic molecules

The study of glycol adsorption has received considerable attention. Indeed,
Brindley [120] reviewed the literature published upto 1966 and commented that
the formation of complexes between ethylene glycol and smectites had 'received
more attention than any other group of organo-silicate complexes'.
Other literature reviews by Grim [13], Theng [121] and MacEwan and Wilson
[46] have also covered this widely researched area. It is instructive however, in
the wider context of the adsorption of polyglycols on clay minerals, to consider
the main features of ethylene glycol adsorption.

The first studies in this area were by Bradley [122] and MacEwan [123].
Interlamellar water was expelled on adsorption of glycols, polyglycols and
polyglycol ethers [122] and a C-H---O(mineral surface) bond suggested, with
which MacEwan [123] agreed. It was concluded [123] that the molecules enter
the interlayer region of montmorillonite and arrange themselves in parallel
layers lying as flat as possible. Dowdy and Mortland [124] however, found no
evidence to support the hypothesis that C-H---O(silicate surface) bonds were
important to the adsorption process. This finding was supported by Tettenhorst
et al [125]. The possibility of hydrogen bonding between the glycolic hydroxyls
and the silicate surface was not excluded although it was concluded that this was
an additional mechanism which occurred after all the co-ordination sites on the
exchangeable cations are filled, or when a cation of low solvation energy was
present in the interlayer space.

The formation of multiple layer sheets between the mineral platelets was
ascribed [122, 123] to the adsorption of glycol on each basal face such that
between two platelets, two layers may form. The thickness and therefore
number of the organic layers could be calculated from the d-spacing obtained.

Thus basal spacings of 17.0±0.1Å (representing an organic layer thickness of 7.6Å) and 13.7±0.2 Å (representing an organic layer thickness of 4.3Å) correspond to double and single layers respectively.

Mackenzie [126] showed that the basal spacing of Ca-montmorillonite remained constant (17.1Å) over a wide range of glycol-water ratios thus emphasising that such a spacing was no guarantee that there was full glycol solvation. Studies by Reynolds [127] suggested that ethylene glycol forms staggered two layered complexes with montmorillonite in which water and exchangeable cations are situated between the two ethylene glycol layers just above and below a plane which separates the glycol layers. The glycol molecules lie with their zigzag plane normal to the silicate surface (figure 3.8.1). This points to the keying of methylene groups into the di-trigonal cavities in the silicate layer of the clay platelet surface.

Figure 3.8.1. Orientation of ethylene glycol in montmorillonite interlayer space according to Reynolds [127].
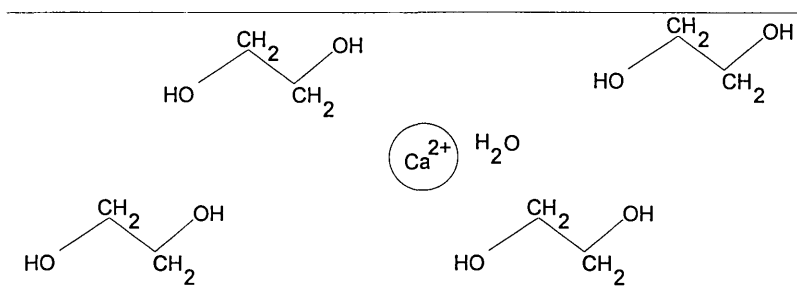
The basal spacing of montmorillonite-glycol complexes are not affected by their initial water content [125] in fact the minimum amounts of water and glycol required to maintain the 17.1Å were interdependent. Brindley [120] noted that total removal of water eliminates the opportunity of expansion and commented that water, even in trace amounts, plays an important function in the formation

of clay-organo complexes. Tettenhorst et al [125] stated that water molecules were an "essential component of montmorillonite-polyalcohol complexes". Tettenhorst et al [125] described the difficulty ethylene glycol may have in replacing water molecules which are associated with exchange cations. However, other authors [124, 128] have described the relative competition between water and ethylene glycol for co-ordination sites around the cations.

The desorption of ethylene glycol has been shown to be diffusion controlled [124] depending on the nature of the interlayer cation. If interlayer water cannot diffuse from the system, then glycol adsorption and retention will be reduced. Glycol retention on homoionic montmorillonites has been shown to depend upon the nature of the interlayer cation [129], following the order

Ca > Al > Na > K
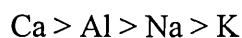
This data confirmed the conclusions [120, 130] that complexation between glycol and interlayer cation (ion-dipole interaction) was extremely important in ethylene glycol retention and disproved the theory that hydrogen bonding between surface and glycol was responsible for glycol adsorption.

Dowdy and Mortland [124] found infrared OH stretching bands at 2750 and 2650 cm^{-1} in Cu-montmorillonite-glycol complexes. These were assigned to glycol directly bound to Cu^{2+} cations through the oxygen atom and general inter and intramolecular hydrogen bonding, respectively. They also claim that IR data indicates that complete dehydration of the clay is obtained when equilibrated with glycol at a vapour pressure of 35 torr. It is difficult to tell from the spectra but this may not be the case and, as a result, the adsorption may be due to hydrogen bonding between glycol and the inner solvation shell of the exchangeable cation (a water bridge). This too would be a function of the solvation energy of the exchangeable cation.

Jonas and Thomas [131] have shown that the uptake of ethylene glycol molecules is affected by the proportion of K^+ cations. Indeed, at a given proportion, ethylene glycol is more effective than water at causing swelling. It has been shown, however, [132] that high charge montmorillonites are unable to swell to their full extent if they have been previously been K^+ exchanged. However, Hsieh [128] noted that the relative humidity had a significant and rapid effect on the basal expansion of Mg-smectites previously treated with low ethylene glycol vapour pressure, i.e. partially solvated samples. It has also been found [128] that the basal spacings of pure Mg-smectites vary with relative humidity between 13.6 and 16.0Å. Saturated ethylene glycol solvation of Mg-smectites have been found to give basal spacings of 17.1Å, corresponding to complete monolayer coverage of interlayer surfaces (a two layer complex) regardless of relative humidity. Basal spacings of 17.1 and 14.0Å were obtained at high and low relative humidities, respectively. At relative humidities between 0.4 and 0.7, random, interstratified one/two-layer complexes are formed, having d-spacings of 14.0 and 17.1Å. This is attributed to the adsorption of water molecules, present at high humidity, providing energy for a fast and reversible rearrangement to a two layer ethylene glycol configuration. This explains why a minimum amount of ethylene glycol 20-30 mg/g is required to form the two layer complex.

A change in b-dimension has been observed for glycolated Na and K-bentonites compared to homoionic bentonites at 60°C [133] but not Ca-bentonites. This has been interpreted as a rotation of the silica tetrahedra in the silicate layer when K^+, which is partially occluded by the di-trigonal cavity at low water contents [40], is solvated (glycolated) and moves into the interlayer space. For this reason, Ca^{2+} which exists near the silicate surface or in the interlayer space (being too large to fit in the di-trigonal cavities) does not exhibit a change in b-dimension.

The stability of homoionic montmorillonite-short chain polyglycol (upto 1, 5 pentanediol) complexes has received much attention by Tettonhorst, Brunton and Beck [125, 134]. One layer complexes had d-spacings of 13.6-13.7Å if it had terminal OH groups and 13.9-14.0Å if internal OH groups were present, a difference attributed to steric effect of interior OH groups. Two layer complexes had d-spacings of 17.0Å. The temperatures at which optimum formation of a single layer, from a heated double layer complex occurred, generally followed the cation series:

Mg > Ca > Ba >Li > Na > K
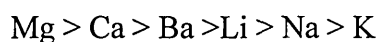
This does not directly follow the recognised patterns for ionic size or field strength, but may be function of both. The mean temperature of single layer collapse has been shown [134] to be proportional to the valence of the interlayer cation and inversely proportional to the ionic radii.

Eltantaway and Arnold [135] concluded that the amount of ethylene glycol adsorbed by the low pressure solvation technique of Ca-montmorillonite, is controlled by the nature of the cation, not the surface and gives incomplete surface coverage. However, saturated solvation techniques give unimolecular surface coverage of the interlayer sheets (2 layers between adjacent sheets) which is independent of the interlayer cation. Consequently, ethylene glycol is commonly used to estimate the surface area of swelling clays [136] another analogous molecule, ethylene glycol monoethyl ether (EGME) is also used for the same purpose. In work that provided the basis for their studies on ethylene glycol [135], Eltantaway and Arnold [137] suggested that incomplete EGME unimolecular surface coverage of Ca-montmorillonite was governed by the interaction between Ca and EGME and not the extent of the clay surface. NMR studies [138] have also shown that the interaction of poly(ethylene glycol) monoalkyl ethers with low charge synthetic saponites in aqueous suspensions is via the exchange cation.

Nguyen et al [139] used DRIFT and ATR FTIR techniques to show that the orientation of EGME in the interlayer region allows both surfaces to share a common, single layer of EGME and that the interaction between EGME and Ca^{2+} is thought to be the adsorption mechanism. However, it is impossible to interpret EGME hydroxyl band shifts due to OH interaction with Ca^{2+} in the presence of a clay containing significant quantities of water. Hence, these results are difficult to believe, particularly in the light of results obtained for ethylene glycol.

Parfitt and Greenland [117, 118] noted that a series of polyethylene glycols adsorbed strongly from aqueous solution onto clay minerals via water bridges (i.e., hydrogen bond formation between water molecules in the primary hydration shell of the exchange cation and the oxygen atom in the polyether). This is supported by the evidence that increasing adsorption of PEG followed the order [117]:

$$Al^{3+} < Ca^{2+} < Na^{+}$$
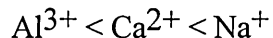
And that direct ion-dipole interaction was not the adsorption mechanism.

The enthalpy of adsorption was found to be negative for the smaller molecules and became more favourable as the polarisation of the cation increased. The entropy of adsorption was positive due to the desorption of water from the clay surface and, like ΔG, became more negative as the molecular weight increased.

The shape of the adsorption isotherms were correlated with the different conformations of PEG, Mw<400 (linear conformation) and PEG, >400 (random coil) in solution. And the equilibrium adsorbed amount of polymer on Ca-montmorillonite was found to increase with the molecular weight of polymer.

Washing a sample of Ca-montmorillonite complexed with PEG (Mw 300) with distilled water, removed more than 80% of the polymer but PEG (Mw 20,000) could not be removed from a similar complex [117] in the same way. This was attributed to the irreversible nature of adsorption of large polymers which form multi-point attachments which cannot all be simultaneously removed.

It was assumed that a regular organised structure is not obtained on PEG adsorption since no differences in PEG vibrations were seen between the infrared spectra of liquid PEG and PEG adsorbed on montmorillonite [118]. Infrared data indicates that subsequent adsorption of water to a montmorillonite-PEG complex occurs initially on the exchange cations. This is supported by XRD data which showed that adsorbed polymer does not prevent clays swelling and confirmed the influence of cations on this process. As with non complexed montmorillonites, Ca^{2+} limits the swelling whereas extensive swelling is observed with Na^+ counter cations.

Complexes formed between PEG, molecular weight 300 and 20,000 and Na-montmorillonite had d-spacings of 13.3 and 17.4Å, respectively [118]. This was interpreted as the formation of one polymer layer between the clay platelets of thickness 3.7Å or two polymer layers of total thickness 7.8Å. Theng [119] explains that these thicknesses are less than are predicted by the van der Waals radii of the molecules and thus indicate a certain amount of 'keying' or recession into the di-trigonal cavity of the silicate surface [140].

Zhao et al [141] have studied the adsorption rates and capacities of a range of PEG molecules on montmorillonites. The amount of PEG adsorbed, increased with increasing molecular weight up to Mw 2000 (corresponding to 100 mg g^{-1} of clay adsorbed) above which, increases in molecular weight gave no significant increases in the amount adsorbed. Burchill et al [85] also noted the

increase in adsorbed amount on increasing molecular weight. However, they observed no maximum in the amount adsorbed of PEG (Mw$\geq$ 2000) on Na-montmorillonite. In fact, the maximum adsorption of 1500 and 4000 molecular weight samples was reported as 154 (51 % surface coverage) and 202 mg g^{-1} of clay (61% surface coverage) respectively.

It was shown [141] pH has very little effect on the adsorbed amount of PEG. However, interlayer cations have a significant effect on the adsorption capacities of montmorillonites, the adsorption capacity of PEG on Ca montmorillonite being greater than on Na montmorillonite. A significant amount of research has been performed using microcalorimetry to calculate the number of bound polymer segments and thus determine the conformation of adsorbed PEG on mineral surfaces. Burchill et al [85] established that the PEG molecules adopt fully extended conformations on the surface of Na-montmorillonite and that for low molecular weight polymers, their size prevents significant loop development. Calorimetric measurements have also been performed on other surfaces. Killmann [105] determined the adsorption of PEG on aerosil from non-aqueous solutions and found that the adsorption is slightly exothermic due to the contribution of end groups to the thermodynamics of polymer in solution. This is not the case for high molecular weight PEO where microcalorimetry measurements have shown that PEG adsorption on dolomite and silica [153] is an endothermic process, the driving force being the increase in entropy. The release of three water molecules associated with each ether oxygen of PEO provides the increase in entropy required to overcome the unfavourable enthalpy term. Moudgil et al [142] have shown that increasing temperature displaces more water from the PEO molecule and allows more contacts with the surface thus increasing the enthalpy of adsorption. Trens and Denoyl [143] have used this technique to study PEG (Mw between 400 and 400,000) adsorption at the silica/water interface. Terminal hydroxyl groups are found to be only effective

at high concentrations. However, they have a higher affinity for the silica surface than the ethoxy oxygen and it is suggested that they are fixed at both ends (no tails) for dihydroxyl polymers and partly standing up (long tail) for the monohydroxyl polymer. Low surface coverage allows the molecules to adsorb in flat conformation giving a high fraction of bound segments. However, as surface coverage increases the polymer molecules stand up, so the number of bound segments decreases. The increase in polymer adsorption with increasing molecular weight is hence accompanied by increasing lengths of loops and tails.

Burchill et al [85] discussed the adsorption of PEG polymers from aqueous solution in terms of water bridges, suggesting that although direct co-ordination to the cations is possible, it is unlikely in water. The possibility of crown ether type structure formation between PEG and the hydrated cations was muted. It has been shown [144] that crown ethers and cryptands intercalate in the interlayer space of clay minerals, maintaining the layered structure. Casal et al [145] have proposed models for interlayer complex arrangements based on interlayer spacings and adsorbed amounts. This reveals one and two layer complexes with platelet separations of 4.2±0.3 and 8.1±0.1Å respectively. These values are governed by the charge and size of the exchangeable cation, the cavity size of the macrocycle and the steric hindrance of the ligands.

Intercalation complexes between PEO and montmorillonite has received some attention [146, 147] as a result of the ionic conductivity they have displayed. Ruiz-Hitzky and Aranda [146] found that the complexes formed by adsorption of PEO from acetonitrile onto Li-montmorillonite have d-spacings of 17.2Å and are stable in solvents such as acetonitrile, water and methanol, and are stable up to 500-600K (above which polymer is progressively eliminated giving a collapsed structure). They compare the polymer thickness of 9.5Å favourably with the diameter of helical crystalline $[P(EO)_n]X^-$ (~8Å). Thus they describe

the adsorbed polymer conformation as a helical chain whose axis is parallel to the silicate surface. They mention a splitting of the 1350 cm^{-1} (C-H deformation) into two bands in the infrared spectrum of adsorbed PEO but do not show the relevant spectra. This splitting is assigned to the ion-dipole interaction between ether oxygen atoms and interlayer cations, as in PEO/salt complexes. They do, however, mention the possibility of PEO interaction with silicate surface oxygen atoms. Wu and Lerner [147] disagree that PEO adopts a helical conformation in Na-montmorillonite-PEO complexes [146], believing instead that the polymer resembles an adsorbed layer. Two interlayer spacings 13.6 and 17.7Å are obtained corresponding to polymer layer thicknesses of 4.0 and 8.1Å respectively and polymer-clay stoichiometries of 0.15 and 0.30 g g^{-1} respectively.

Rubio and Kitchener [148] determined H-bonding of silanol and siloxane groups and hydrophobic interactions with methylated sites on the silica surface to be the adsorption mechanisms of lower molecular weight PEO onto silica surfaces. Behl and Moudgil [149] also mention the possibilities of electrostatic interactions between slightly anionic PEO and positively charged particles or the complexation of PEO with cations adsorbed on the solid surface as adsorption mechanisms. The adsorption of high molecular weight PEO on dolomite and apatite [149] revealed the principle adsorption sites to be isolated OH groups and physisorbed water on the mineral surface.

Recent studies [1, 8 150, 151] have been concerned with the adsorption of a range of polyalkylglycols from aqueous solution onto clay minerals in order to understand their mechanism of shale inhibition as a component of water based oil well drilling fluids. It had been proposed [151] that the cloud point behaviour of PEG was a feature of their shale inhibition mechanism by plugging clay pores with insoluble droplets of pure glycol. Indeed, clay particle retention has

been observed to increase above the cloud point of aqueous suspensions with PEO as a retention aid [93]. This was attributed to the phase separation and the fact that one of the resulting phases was rich in PEO. However, this argument was dismissed [1, 8, 150] as it did not address the stability of shales treated with glycol which did not exhibit cloud point behaviour. A more acceptable theory of shale stabilisation is that polyglycol molecules compete with water molecules for adsorption sites on the clay and thus interfere with the hydrogen bonding network [8, 150]. This might then prevent the adsorption of water molecules or hold clay platelets together and hence impart stability by restricting their swelling and dispersion.

Aston et al [150] showed shale recovery increased from zero in freshwater to 80% in a KCl/partially hydrolysed polyacrylamide/polyglycol solution. This solution also produced much harder shales which was thought to be due to direct interaction between the glycol and clay. They describe the displacement of water by glycol indicating the stronger affinity of clay for glycol than water. In particular, Aston et al [150] explained the increased performance of polyols in the presence of salt was not due to variations in adsorbed amount (these were approximately identical) but the cation type, determining an order of effectiveness:

$$KCl \sim CsCl > CaCl_2 > NaCl > \text{no salt} > LiCl$$
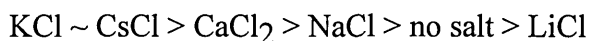
The interactions between cation and polyol are extremely important, and it is suggested the that hydration sphere around the cation is replaced (at least to some extent) by the glycol. Cliffe et al [1] performed quantitative IR and XRD measurements on the strong adsorption of polyols from KCl solutions onto montmorillonite. The adsorption was thought to be due to the specific interaction between non terminal portions of the polyol molecule and potassium cations and not general salinity effects. Therefore it is controlled by the concentration of polymer in solution and the presence of K^+ cations. In the

presence of K^+, stable complexes with an interlayer spacing of 14Å corresponding to one flat polyol layer were obtained whilst in the absence of K^+, less stable complexes containing two flat lying polyol layers were formed. A shift to lower wavenumber of the infrared band at ~ 1380 cm^{-1} attributed to a OC_2H_4 wagging vibration on adsorption of PAG from 0.2% PAG solution compared to that of 6% PAG/water solution was detected [1]. The shift increases as the polymer concentration in solution increases (as the amount of polymer on the clay increases) and approaches the value obtained for a pure polyol solution. This is attributed to the increasing significance of weak polyol-polyol interactions as they concentrate and orientate in the clay interlayer.

Rawson [3] determined the adsorption of the polyalkylglycol DCP101 on Mn-montmorillonite. These NMR results have shown that the polyol does not displace the exchangeable cation and, contrary to the findings of Cliffe et al [1] and Aston et al [150], indicated that the polyol does not cause a significant quantity of the Mn^{2+} hydration shell to be disturbed.

3.9.   Amide molecules

For amide molecules of the type $R\!\!-\!\!\overset{\displaystyle O}{\overset{\|}{C}}\!\!-\!\!NH_2$, both the oxygen and nitrogen atoms may act as suitable sites for interaction with the interlayer cation of the clay mineral [114, 140]. These can be distinguished using infrared spectroscopy since, if binding is via the oxygen atom, then the C=O stretching frequency will decrease and the C-N stretching frequency will increase. Conversely, if the nitrogen atom binds then the C=O stretching frequency will increase and C-N stretching frequency will decrease.

Most amide molecules have been found to co-ordinate through the carbonyl group [114]. However, Mortland [152] used infrared spectroscopy to show that

the adsorption of urea on montmorillonite was due to ion-dipole interactions and that the type of amide interaction depended upon the nature of the exchangeable cation. Hence, adsorption onto montmorillonite exchanged with alkali and alkaline earth metal cations caused the stretching frequency of the C=O band to increase, implying interaction between nitrogen atom and cation. However, adsorption onto montmorillonite exchanged with transition metal cations caused the C=O stretching band to shift to lower frequency and the band due to C-N vibration, to shift to higher frequency, thus indicating interaction between carbonyl and exchange cation. It should be noted that the author did point out the difficulty in interpreting the results without uncertainty.

Amide molecules do not normally adsorb from aqueous solution [114] onto clay minerals. However, if the amount of water is reduced, then amide molecules are able to compete with water for co-ordination sites around the cation; first by water bridges and then by direct co-ordination.

Stutzmann and Siffert [153] showed that adsorption of acetamide onto montmorillonite is irreversible and constant in solvent medium, however, on drying several orders of fixation are revealed:

- Weakly retained excess acetamide, removed by washing the complex twice.
- Reversible physisorbed acetamide; a partial fixation which has an unstable adsorption equilibrium of 18 mg g^{-1} clay. This is removed by heating to 60°C.
- Irreversible chemisorbed acetamide; an intense fixation having a maximum adsorption equilibrium of 3 mg g^{-1} clay. This is revealed on removal of the physisorbed acetamide.

The adsorbed amount increased as the polarising power of the monovalent interlayer cation increases.

i.e. $Li^+ > Na^+ > Cs^+$

However, Espinasse and Siffert [154] showed that the amount of acetamide
adsorbed on montmorillonite increased as the polarisation of di- and tri- valent
exchangeable cation decreases:

$$Na^+ > Ca^{2+} > Al^{3+}$$
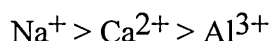
This was attributed to the partial flocculation of di- and trivalent cation
exchanged montmorillonite and a subsequent decrease in accessible surface.
Evidence that adsorption on Na-montmorillonite was much greater than
adsorption on Na-montmorillonite in the presence of NaCl which causes
flocculation supports this theory.

Two adsorption mechanisms for the adsorption of acetamide on Na
montmorillonite were postulated by Stutzmann and Siffert [153] who used
infrared spectroscopy to analyse acetamide-Na montmorillonite complexes.

1.   Chemisorption mechanism

The appearance of two new bands at 1720 and 1345 cm^{-1} in the infrared
spectrum of the complex were attributed to C=N stretching and O-H
deformation modes respectively. These are assumed to be due to protonation of
the acetamide (a) by polarised water molecules around the exchange cation,

i.e.

$$CH_3-C\underset{NH_2^+}{\overset{OH}{<}} \quad (a)$$
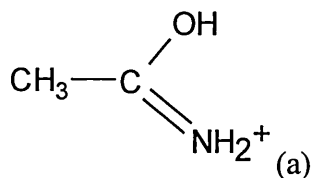
The protonated acetamide is then thought to form an ionic interaction
(chemisorption) between cationic acetamide and the negatively charged mineral
surface.

2.   Physisorption mechanism

Stutzmann and Siffert [153] observed large shifts (135 and 225 cm^{-1}) to high
frequency of the antisymmetric and symmetric NH_2 stretching bands,

respectively. Implausibly, this was attributed to the formation of acetamide-acetamide (b) and acetamide-water (c) intermolecular hydrogen bridges. The corresponding decrease in the C=O stretching frequency and increase in the C-N stretching frequency observed was used to support this postulation.

(b)　　　(c)
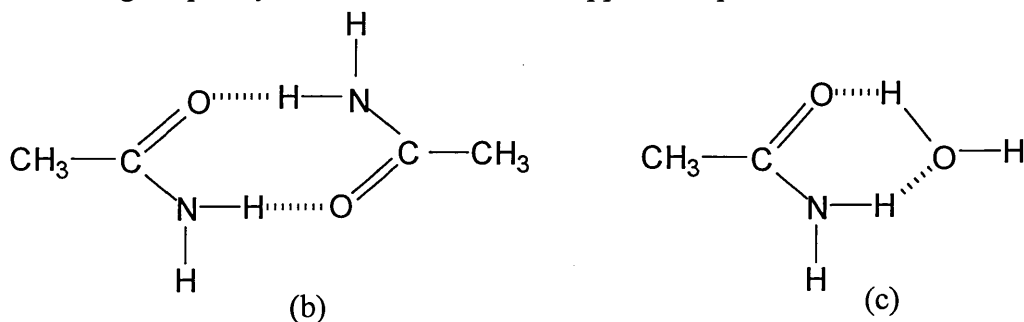
This hydrogen bonding network was thought to aid adsorption but was found to break on heating, resulting in elimination of acetamide from the mineral (chemisorbed acetamide did remain however). Hence, an additional hydrogen bonding (physisorption) mechanism, weaker than the chemisorption mechanism, was thought to exist between acetamide molecules only, or acetamide and water molecules (which exist on the clay surface or in the hydration sphere of the exchange cation).

In addition, X-ray diffraction data reveals d-spacing of 12.7Å at normal water contents [153], indicating that acetamide does not adsorb in the interlayer space but is irreversibly adsorbed on the external surfaces of montmorillonite.

Isobutyramide (IBA) has also been used to represent the monomeric unit of polyacrylamide and it has been shown to adsorb in 3 stages [155]:

Stage 1. adsorption of IBA on the more energetic edge surfaces,

Stage 2. adsorption on external faces,

Stage 3. IBA intercalation in the interlayer space (accompanied by an increase in d-spacing form 12.8 to 14.9Å). At this saturation adsorption (0.235 mg g^{-1} clay) one IBA molecule occupies two di-trigonal silicate cavities on two

different sheets. It should be noted that IBA adsorption does not increase the tactoid sizes nor their number.

Schamp and Huylebroeck [156] found that polyacrylamide adsorption was completely irreversible since none could be desorbed from the clay mineral. The effect of molecular weight on adsorption depended on the exchange cation and the arrangement of clay particles in suspension. Hence, adsorption increased with increasing molecular weight for a Na-montmorillonite (deflocculated clay) but decreased with increasing molecular weight for a flocculated clay such as H-montmorillonite. Hence, two types of adsorption site were identified:

1. External surface adsorption-fast adsorption, increasing with increasing molecular weight found for deflocculated clays where all the flat surfaces are accessible.

2. Pore adsorption-slow adsorption, decreasing with increasing molecular weight, found for flocculated clay where polymer has difficulty entering between the plates but can adsorb in pores which have similar dimensions to the polymer coil.

Bailey et al [2] have shown that increasing the K-montmorillonite loading in solution or increasing the ionic strength of the solution decreased the amount of polyacrylamide adsorbed to a plateau value of 300 mg g^{-1} clay. This was attributed to the collapse of the layers, reducing the interlamellar spacing and thus reducing the polymer adsorption. Further work by Argillier et al [157] has shown that increasing the KCl concentration to 20 gdm^{-3} and thus reducing the specific surface area reduced the adsorption of polyacrylamide on K montmorillonite from 550 to 125 mg g^{-1}. Further increases in the KCl concentration had no effect on the adsorbed amount.

Similarly, increasing the solid/liquid ratio has been shown to reduce the adsorbed amount [157, 158]. This was attributed to aggregation of the clay particles induced by polymer adsorption and the subsequent decrease in accessible surface.

Unlike isobutyramide, Bottero et al [155] showed that increasing the amount or molecular weight of polyacrylamide adsorbed, increases the number and size of Na-montmorillonite tactoids by destruction of the regular stacking arrangement of clay platelets. ^{13}C-NMR data indicated that at an adsorbed amount of 0.2 g g^{-1} clay, the polymer adopted a flat conformation. However, increasing the adsorbed amount or increasing molecular weight created more loops and tails, the polymer behaving less like a constrained molecule and more like it would in solution. Calorimetric and X-ray diffraction data confirmed this finding [155], showing that increasing molecular weight reduced the number of bound segments and increased d-spacings respectively.

Recently, considerable attention has been paid to the adsorption of hydrophobically associating waterborne polyacrylamides on K montmorillonite clays [157, 158]. The adsorption of such polymers does not follow that of unmodified polyacrylamide as they are able to form multilayers by hydrophobic polymer interactions.

A significant amount of research has been performed on polyacrylamide adsorption on the clay mineral kaolinite. Kaolinite is a 1:1 clay mineral [13] and as such exhibits significantly different properties to montmorillonite; in particular it has exposed SiO and AlOH faces and only a very low cation exchange capacity.

Lee et al [159] revealed that the adsorption of PAM on Na-kaolinite was independent of ionic strength and pH (3< pH <9) although they did report decreased adsorption at higher solid/liquid ratios due to a reduction in the number of accessible faces. It was shown that adsorption occurred at two sites:

1. High density adsorption on the edge surfaces due to hydrogen bonding interactions between C=O and Al-OH.

2. Low density adsorption on aluminium hydroxide basal surfaces due to non-specific dipole interactions or the entropic release of water. Adsorption onto the silica surface is not expected in keeping with the results of Griot and Kitchener [160] who failed to find evidence of polyacrylamide adsorbed on aged (hydrated) silica.

Although Pefferkorn et al [161] also indicated that the adsorption of polyacrylamide on Na-kaolinite is controlled by hydrogen bonding interactions between carbonyl and the hydroxyl on the edge faces, they were in contradiction with Lee et al [159] reporting that the two different basal surfaces were non-adsorbing. Pefferkorn et al [161] did show that pH controls the adsorption of polyacrylamide. Hence at pH <5, edge charges are protonated to give Al-OH and hence increase adsorption. Conversely, adsorption decreases at pH >10 due to the reduction of isolated Al-OH adsorption sites.

Atesok et al [162] also showed that adsorption of polyacrylamide on Na-kaolinite at natural pH is governed by hydrogen bonding interactions and solvent interactions. Atesok et al [163] noted that the flocculation of kaolinite was enhanced by a PAM/Ca^{2+} system compared to PAM alone. They explained that Ca^{2+} had no effect on polymer adsorption and suggested that calcium increased flocculation by bridging between particles. Lee et al [164] however contradict these findings revealing that the adsorption of polyacrylamide on

siliceous material is increased in the presence of Ca^{2+} due to a specific interaction between calcium and the polymer.

Lee and Somasundaran [165] studied the adsorption of PAM on various oxide minerals and also concluded that adsorption was due to favourable hydrogen bonding between the carbonyl group and proton donating surface hydroxyl groups (M-OH and $M-OH_2^+$) on the mineral surface.

The adsorption of polyacrylamide on SiC and sand was independent of ionic strength [166]. Page et al [167] confirmed this finding for polyacrylamide adsorption onto kaolinite sand and SiC at 30 or 90°C. They showed however, that adsorption was reduced at the higher temperature due to the rupture of hydrogen bonding networks.

Broseta and Medjahed [168] discovered that the adsorption of polyacrylamide increased as the hydrophobicity of the surface increased. Adsorption was lower on sand (400 mgm^{-2}) than on the same substrate rendered hydrophobic by treatment with short chain (C-6) silane (470mgm^{-2}) or long chain (C-18) silane (720mgm^{-2}). This was attributed to the decreased affinity for the surface of hydrophilic molecules such as water and the short range interactions of non-ionic PAM with the hydrophobic C-18 apolar backbone. However, adsorption of PEG onto the hydrophobic surface almost totally prevented PAM adsorption [168]. This is not what would be expected for PEG which has moderately balanced hydrophilic/hydrophobic behaviour. The competition between solvent molecules and polymer segments for surface sites does not explain this 'protective' effect of PEG. This effect is explained [168] in terms of the distribution of ether oxygen atoms along the main chain and the low overall dipole moment a PEG molecule will have. This will significantly reduce the ability of PEG to form strong dipole interactions.

3.10.   Adsorption of anionic polymers on clay minerals

Anionic polymers tend to be repelled from the negatively charged clay surface [114, 116] and unlike nonionic and cationic polymers tend not to enter the interlayer region of expanding minerals. However, at high electrolyte concentration or low pH, when the polyelectrolyte behaves considerably more like an uncharged polymer, adsorption may take place between the platelets. Polyvalent cations also promote the adsorption of anionic polymers by a bridging mechanism between negatively charged groups on polymer and clay surface [169]. In addition, at low pH, negatively charged polymers are able to adsorb onto the edges of the clay particles since, under such conditions, the clay edges adopt a positive charge.

The adsorption of partially hydrolysed polyacrylamide (HPAM) has received considerable attention, particularly with respect to its use in oil well drilling fluids [2, 170]. The driving forces for adsorption such as van der Waals (dispersion) interactions, H-bonding and entropy, compete with electrostatic repulsion between the negatively charged polymer and mineral surface during the process of HPAM adsorption [170]. The reduction of interlayer space and the subsequent reduction in available internal surfaces is also a factor which will reduce the polymer adsorption density.

HPAM does not adsorb at low ionic strength or high pH due to strong electrostatic repulsions between negatively charged polymer and mineral surface. Adsorption occurs at high ionic strength although reduced adsorption is obtained in KCl since it is more flocculating than NaCl. At high ionic strength, adsorption is independent of ionic strength [2, 170] reaching a plateau value of $200\text{-}300mg\ g^{-1}$ clay this was the same plateau value obtained by Bailey et al [2] for neutral and cationic polyacrylamide adsorption at high ionic strength. These

results indicate that under such conditions, adsorption is due to van der Waals (dispersion) interactions.

Lee et al [159] noted increased adsorption of HPAM on edge and basal surfaces of kaolinite at high ionic strength and low pH and that it occurred in a stepwise manner; Firstly, the screening of electrostatic repulsions between polymer and mineral surface ans secondly, neutralisation of polymer (and possibly mineral) charge by cation condensation. As a result, adsorption densities comparable to neutral polyacrylamide are obtained. Page et al [165] also revealed that adsorption of hydrolysed polyacrylamide is increased in increasing ionic strength solution. However, it was shown that the adsorption of polymer is reduced on increasing the temperature by interfering with both the electrostatic and non-electrostatic interactions.

Diffraction measurements [170] show that mineral-polymer interactions are also enhanced at low pH. At 0% relative humidity a d-spacing of 17Å is obtained at pH 4 whilst at pH 12.3, a d-spacing of 11.6Å is obtained. This clearly indicates the interlayer adsorption and disruption of platelet stacking at lower pH. The pH dependence of HPAM adsorption on kaolinite has also been considered by Lee et al [159] and in keeping with the findings of Lecourtier et al [166] on other siliceous material found that adsorption decreased as pH increased. The authors describe two distinct processes which are pH dependent:

4< pH <7 the acid groups on the polymer become fully dissociated which increases the electrostatic repulsion between polymer and mineral thus reducing HPAM adsorption.

pH >10 there is a reduction in the number of isolated Al-OH adsorption sites and an increase in the number of Al-O$^-$ groups obviously leading to greater electrostatic repulsion between polymer and mineral.

The presence of Ca^{2+} allowed adsorption of HPAM onto montmorillonite [170] even at low ionic strength. This was attributed to both charge screening by the cation and also the possibility that Ca^{2+} on the surface may act a bridge, inducing adsorption. Bocquenet and Siffert [171] showed that HPAM uptake increased for Ca-kaolinite and Ca-illite compared to Na-kaolinite and Na-illite respectively. They too explain that Ca^{2+} may act either as an adsorption site on Ca-clay or that it may affect the dimensions of polymer in solution. Both mechanisms are thought to work at the same time although it is difficult to determine which mechanism predominates. Chaveteau et al [172] also attribute the increased adsorption of HPAM on sand and SiC in the presence of Ca^{2+} to the fixation of Ca^{2+} on dissociated surface silanol groups, and thus the creation of a new adsorption site and also the decrease in HPAM solubility on interaction with Ca^{2+}. Lee et al [164] explained that the increased adsorption of HPAM on sand, SiC and kaolinite in the presence of Ca^{2+} was threefold:

- reduction of electrostatic repulsion by charge screening.
- specific interaction with polymer in solution reducing its affinity for the solvent
- fixation on negative surface, reducing mineral charge and creating new adsorption site where it might act as a bridge.

An increase in ionic strength (monovalent Na^+) was found to reduce the effectiveness of the Ca^{2+} cation [164] by decreasing the electrostatic interactions possible between Ca^{2+} and polymer or mineral surface.

Espinasse and Siffert [154] discovered that the adsorption of HPAM on homoionic montmorillonites increases with increasing polarising power of the exchange cation [153]. This is attributed to the higher polarising power of the polyvalent cations and hence their ability to protonate the amide group. This is the reverse of the result obtained for acetamide where the polyvalent cations were blamed for reducing the adsorption by flocculating the clay. It was

91

postulated [154] that, in contrast to acetamide, flocculation of the clay by polymer bridging between particles reduces the flocculating effect of exchange cations which cause flocculation.

Increasing molecular weight was found to have little effect on adsorption of HPAM from solution onto montmorillonite, in fact, the effect of ionic strength proved to be the most important parameter considered by Espinasse and Siffert [154]. Increasing the ionic strength of the solution increased the adsorption by a factor of between 2 and 5. This was explained in terms of a reduction in the molecule size by charge screening of the carboxylate groups and hence the greater accessibility of the polymer to the mineral surface.

Stutzmann and Siffert [153] have revealed that adsorption increases with increasing degree of hydrolysis. They reasoned that since HPAM bonds to several platelets causing aggregation it is thus the size of the gap between the platelets which controls the adsorption of more polymer in the interlayer space. Hence, increasing the degree of hydrolysis extends the chain length and thus in turn increasing the volume between flocculated platelets. This allows the amount of polymer adsorbed to increase with increasing hydrolysis. Espinasse and Siffert [154] also showed that increasing the degree of hydrolysis of the anionic polyacrylamide, increases the amount adsorbed from NaCl solution. These authors postulate that the effect of salt on the $COO^-:COOH$ ratio will be greater for the polymers with higher degrees of hydrolysis. Consequently, these polymers will form lower dimension coils which will adsorb preferentially. These seem rather unlikely explanations and it has been shown [173] that HPAM uptake onto Na-kaolinite is inversely proportional to polymer hydrolysis. Increasing the polymer hydrolysis extends the chain and, hence, reduces the adsorption of polymer. The decrease in polymer size in saline solution accounts for the observed increases in adsorption in the presence of

NaCl. In addition, increasing HPAM ionicity (increased hydrolysis) reduces the adsorption density on SiC, sand and kaolinite [164, 172]. However, in the presence of Ca^{2+} above 30% hydrolysis, the adsorption increases as the Ca^{2+} interactions with the polymer decrease its solubility and enhance its adsorption.

The adsorption of hydrolysed polyacrylamide onto kaolinite is limited solely by the number of available adsorption sites and not competition with intramolecular bonding as is the case for sodium polyacrylate [174] Three possible adsorption mechanisms were postulated:

1. Anionic exchange between surface OH and carboxylate ions on the polymer.
2. Establishment of bridges involving divalent cations.
3. H-bonding between surface oxygen atoms ad unionised carbonyl and amide groups on the polymer.

In addition to these mechanisms Stutzmann and Siffert [153] also suggest that the polarisation of water co-ordinated to the exchange cation can protonate the amide group which can then be held to the mineral surface by a chemisorption process (i.e. an ionic bond). This is the mechanism previously suggested in the same paper for acetamide in which the polarising power of the cation is the most significant factor in the adsorption.

Broseta and Medjahed [168] studied the adsorption of hydrolysed polyacrylamide on sand and silane (C-18) treated sand. At high ionic strength and low pH the adsorption resembled neutral polyacrylamide adsorption, increasing with increasing hydrophobicity of the surface. However, when significant electrostatic interactions were present, the reverse is true. Indeed, the adsorption of HPAM on C-18 treated sand is less than on sand itself. The authors attribute this to the increased electrostatic repulsion between the anionic polymer and effective negative charge carried by hydrophobic surfaces due to the preferential solubility of anions close to the hydrophobic substrate.

4. **TECHNIQUES**

The two principal techniques used for the quantitative and qualitative
determination of water soluble polymer adsorption on montmorillonite clays, as
presented in this thesis, were Fourier transform infrared (FTIR) spectroscopy
and X-ray diffraction (XRD). A brief outline of the theory and principles
underpinning these techniques and their relevance to this project are outlined
below. In addition, a brief description of the other techniques used will also
appear.

4.1 Infrared spectroscopy

Infra-red radiation occurs in the region of the electromagnetic spectrum with
wavelength between approximately 10^{-3} and 10^{-6} m. Any polyatomic molecule
will absorb particular frequencies of infrared radiation and will be excited from
a low energy to a higher energy stationary state, i.e. will undergo a vibrational
(or rotational) excitation. Many detailed explanations of this theory can be
found [175, 176, 177, 178], but a brief description of the absorption of infrared
radiation by a molecule which gives rise to the characteristic infrared spectra
will be given.

4.1.1. The harmonic oscillator (semi-classical approach)

For a diatomic molecule of reduced mass, μ $\left(= \dfrac{m_1 m_2}{m_1 + m_2} \right)$, and spring

constant, k, (figure 4.1.1.) and which obeys Hookes law, the system will
oscillate with frequency, ν, given by:

$$\nu = \frac{1}{2\pi} \sqrt{\frac{k}{\mu}} \qquad\qquad \text{eqn 4.1.1a}$$

Figure 4.1.1. model of a diatomic molecule at equilibrium and under extension

equilibrium separation   under extension
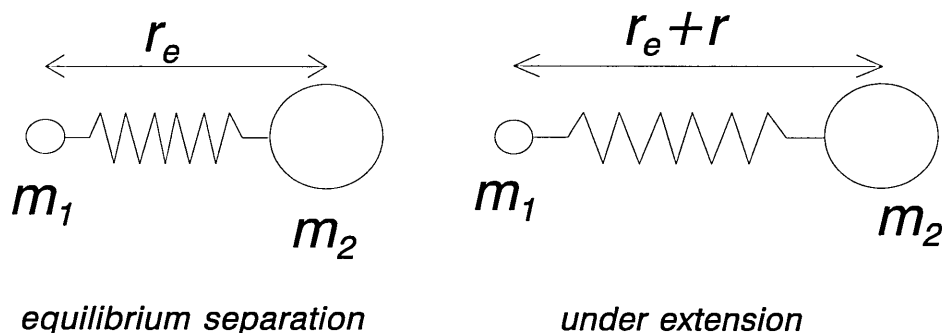
Quantum mechanics has shown [179] that the harmonic oscillator can only take discrete, quantised energy values which are characteristic of a particular molecule, given by:

$$E = h\nu\left(v + \frac{1}{2}\right)$$ eqn 4.1.1b

where v is the vibrational quantum number which may take all positive integer values and h is the Planck constant.

The frequency of the radiation must be exactly equal to the frequency of molecular vibration, which produces the oscillating dipole moment, in order for a quantum of radiation to be absorbed. Since radiation with frequencies which are not exactly equal to the frequency of molecular vibration are not absorbed, then a collection of normal modes with particular frequencies will give rise to a characteristic absorption spectrum. This forms the basis of identification by infrared spectroscopy.

For the harmonic oscillator, quantum mechanics has shown that for a transition between lower and upper vibrational states v" and v', with vibrational wavefunctions, ψ_v'' and ψ_v' respectively, the transition moment is given by

$$R_v = \int {\psi_v'}^* \, \hat{\mu} \, \psi_v'' \, dx$$

eqn 4.1.1c

95

Where, x is the internuclear separation $(r-r_e)$ and μ, is the oscillating dipole moment.

It is found that if:

$R_v=0$ then the transition is forbidden

$R_v \neq 0$ then the transition is allowed

If v' and v" differ by integer values other than 1, then the transition moment will be zero and transition will be forbidden. This gives the selection rule $\Delta v = \pm 1$

The potential energy for a harmonic oscillator is a parabolic function (figure 4.1.2a.) on which evenly separated vibrational energy levels (hv apart) exist, as dictated by quantum mechanics.

4.1.2. Anharmonicity

Unfortunately the harmonic model suggests that the molecule will never be able to escape the potential well and dissociate. This is not the case for real molecules and hence an anharmonic potential is used (figure 4.1.2b) to account for the restoring force in real molecules becoming weaker as the displacement increases. Consequently, when the amplitude of vibration becomes sufficiently large the molecule may dissociate. The potential energy is no longer a parabola but is usually modelled by a Morse potential:

$$V(x) = D_e \left[1 - \exp\{-a(r_e - r)\} \right]^2 \qquad \text{eqn 4.1.2a}$$

Where D_e is the dissociation constant (the energy a molecule requires to extend from the equilibrium separation to infinite separation) and a is a constant.

At low potential energies, the anharmonic oscillator behaves similarly to the harmonic oscillator and consequently its potential follows the a parabolic function. However, as the atoms which compose the molecule become more and more separated, so the potential energy tends towards the energy of dissociation.

The vibrational energy levels are approximated by:

$$E = h\nu\left[\left(v + \frac{1}{2}\right) - x_e\left(v + \frac{1}{2}\right)^2\right] \qquad \text{eqn 4.1.2b}$$

For the transition $v' \leftarrow v''$ the energy difference is $h\nu(1 - 2vx_e)$, hence, the difference in energy between successive energy levels becomes less as the vibrational quantum number, v, increases.

The selection rule for the anharmonic oscillator becomes $\Delta v = \pm 1, \pm 2, \pm 3...$

The probability of an overtone transition such as $\Delta v = 2$, is however, much lower than the fundamental transition, $\Delta v = 1$. Consequently, the overtone transitions are usually much weaker than the fundamental transitions.

Figure 4.1.2 Potential energy curves for the a) harmonic and b) anharmonic oscillators

a) Harmonic   b) Anharmonic
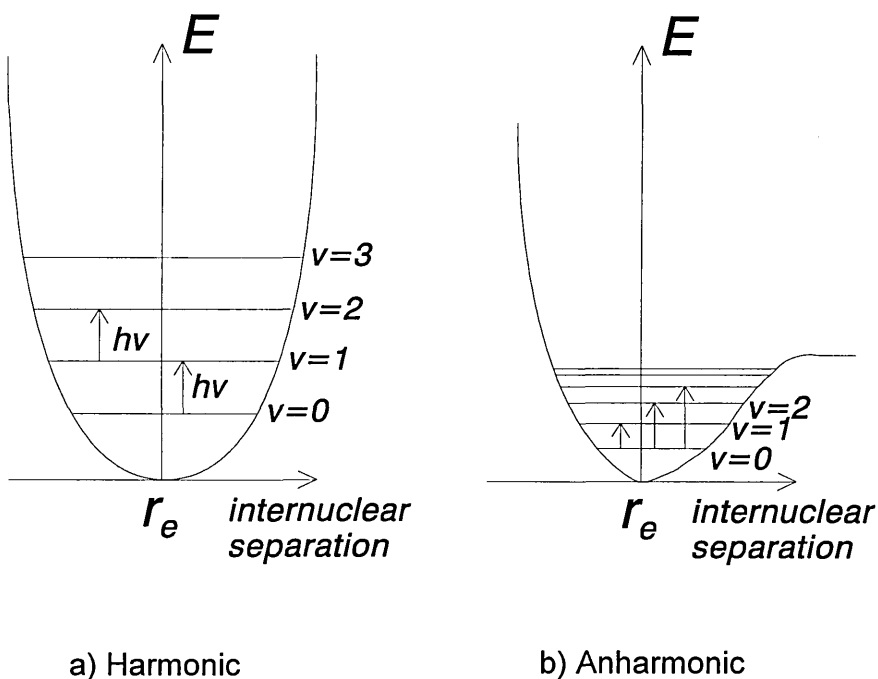
4.1.3.   Intensity of infrared transitions

The intensity of a vibrational transition is governed by three factors:

1. The infrared intensity is proportional to $R_V{}^2$, the square of the transition moment obtained from equation 4.1.1c

i.e. $$R_V{}^2 = \left[\int \psi_V'{}^* \, \hat{\mu} \, \psi_V'' \, dx \right]^2 \qquad \text{eqn 4.1.3a}$$

For a simple harmonic oscillator, it has been seen previously that R_V is non-zero when $\Delta v = \pm 1$. Hence for a SHO, only one term is obtained from equation 4.1.3a, and the infrared intensity is shown to be proportional to $\left(\dfrac{\partial \mu}{\partial x} \right)^2_{x=0}$.

For an anharmonic oscillator, however, R_V is non-zero when $\Delta v = \pm n$ (where n is an integer). Hence, non-linear solutions to equation 4.1.3a are obtained. These are overtone bands and their intensity is obtained from terms such as $\dfrac{\partial^2 \mu}{\partial x^2}$.

Although the intensity of these bands is usually small, they are often observed in the infrared spectrum of clay minerals.

2. The population of initial states

Transitions allowed by selection rules, i.e. $\Delta v = \pm 1$, may be observed. However, the absorption probability of transitions other than $1 \leftarrow 0$ are very low and at thermal equilibrium are predicted by:

$$\frac{N_1}{N_0} = \frac{g_1}{g_0} \exp \left(-\frac{\Delta E}{kT} \right) \qquad \text{eqn 4.1.3b}$$

where N_1 and N_0 are the numbers of molecules in, and g_1 and g_0 the degeneracies of, the upper and lower energy states, respectively. The Boltzmann distribution is given by $\exp \left(-\dfrac{\Delta E}{kT} \right)$, where ΔE is the energy difference between the upper and lower energy levels.

At room temperature, $\frac{N_1}{N_0} \langle\langle 1$ for most vibrational states, so the most likely

transition is the $1 \leftarrow 0$, fundamental transition.

3. The number of molecules present

The Beer-Lambert law states that for a single component of concentration, c, in

a cell of path length, l, the transmittance (intensity ratio of transmitted radiation,

I, to incident radiation) I/I_0, is given by:

$$I/I_0 = \exp(-\varepsilon cl) \qquad \text{eqn 4.1.3c}$$

where ε is the extinction coefficient.

Then absorbance, $A = \log\left(I/I_0\right) = \varepsilon cl$ eqn 4.1.3d

It should be noted that for multiple components, $A = l(\varepsilon_1 c_1 + \varepsilon_2 c_2 ...)$.

4.2.   Fourier transform infrared (FTIR) spectroscopy

FTIR spectroscopy is very similar to dispersive infrared techniques but there

exist some fundamental differences. The spectrometers are similar: both have an

infrared source which emits infrared radiation over a broad range of frequencies,

(a globar heated by an electric current); both have a detector which measures the

intensity of radiation from the source which has passed through the spectrometer

(a mercury cadmium telluride (MCT) detector); and both use the 'delay

principle' to separate the frequencies or infrared radiation from one another. In a

dispersive instrument a prism or grating is used to resolve the radiation into

separate components by an amount which varies with wavelength. In a Fourier

transform instrument however, a Michelson interferometer arranges the

wavelengths and intensities as a function of mirror path difference and a Fourier

transform is used [181, 181] to separate the Fourier components of the radiation.

4.2.1.   Michelson Interferometer

In the interferometer (figure 4.2.1a) the source emits light which is collimated onto a KBr beamsplitter. One part of the radiation is reflected onto a mirror (m_1) which is moved parallel to the beam at constant rate. The other part of the light is transmitted onto a stationary mirror (m_2). Both mirrors reflect the radiation so that each part recombines to cause constructive and/or destructive interference.

<u>Figure 4.2.1a Schematic of the Michelson interferometer</u>

Fixed mirror m

Movable
mirror m

Source

Direction
of motion

Beamsplitter

Sample

Detector
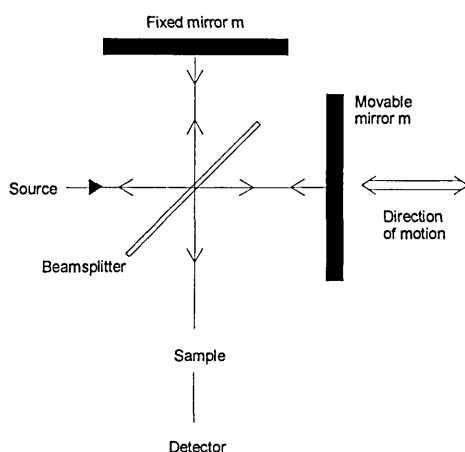
The interference is caused by the difference in path-length each part of the beam has travelled on recombination. Obviously this changes as mirror (m_1) is moved. The recombined radiation is passed through the sample and so only frequencies of radiation that are not selectively absorbed reach the detector and are displayed as an interferogram.

The interferogram has a very distinctive shape (figure 4.2.1b) due to the interference of many different frequencies and amplitudes of infrared radiation.

When the path difference (x) is zero, all frequencies are in-phase and constructive interference occurs (all the infrared energy from the source is detected, except of course for that absorbed or lost in reflections). However, at all other values of difference in path length there are as many frequencies that destructively interfere as constructively interfere and the interferogram dies away.

Figure 4.2.1b A typical interferogram
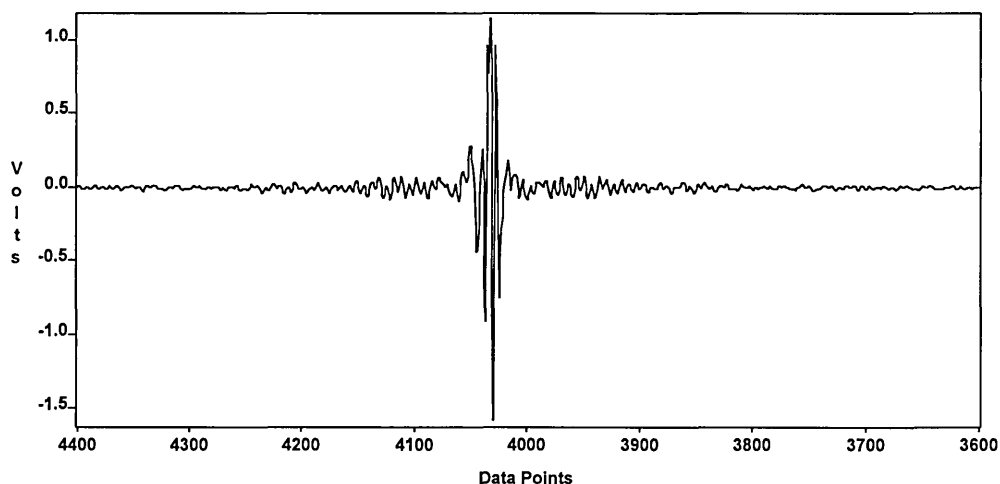
4.2.2   The Fourier transform

The intensity of infrared radiation must be measured as a function of frequency in order to obtain an infrared spectrum. The Fourier transform is a mathematical process for 'sorting' the component frequencies of a polychromatic source and enables the intensity to be recorded as a function of wavenumber. The interferogram can be resolved into the sum of many cosine waves of different frequency [181]:

$$I(x) = \int_{-\infty}^{\infty} S(\bar{\nu}) \cos(2\pi\bar{\nu}x) \, d\bar{\nu} \qquad \text{eqn 4.2.2a}$$

However, the spectral intensity, $S(\bar{\nu})$, (the intensity of the source at a given wavenumber as modified by the instrument and sample) is required and is obtained by computing the cosine Fourier transform of I(x) over all x

$$S(\bar{v}) = \int_{-\infty}^{\infty} I(x)\cos(2\pi\bar{v}x)dx \qquad \text{eqn 4.2.2b}$$

This is an even function, hence,

$$S(\bar{v}) = 2\int_{0}^{\infty} I(x)\cos(2\pi\bar{v}x)dx \qquad \text{eqn 4.2.2c}$$

4.2.3.   Instrumental parameters

There are several instrumental operation parameters which have a profound effect on the infrared spectrum obtained. The most important, and their effect on the spectrum are:

1. Resolution. The ability of FT instruments to achieve "higher resolution and undistorted spectra" compared with dispersive instruments [182] are some of the principal advantages of this method of infrared mineral analysis.

For the purposes of this thesis, the Rayleigh criterion for resolution is used [180], in which two adjacent spectral bands with $sinc^2$ lineshapes are said to be resolved when the centre of one band is at the same frequency as the first zero value of the other.

In an FT instrument, resolution, $\Delta\bar{v}$, is controlled by the maximum path length difference, x_{max}, of the interferometer by the relationship:

$$\Delta\bar{v} \propto \frac{1}{x_{max}} \propto \frac{1}{2d_{max}} \qquad \text{eqn 4.2.3a}$$

The mirror travel distance, d_{max} controls the maximum path difference and hence the resolution.

2. Apodisation. Mathematically the Fourier integral requires integration between zero and infinite path difference. This is obviously impossible, being constrained by the maximum mirror travel distance. Effectively the interferogram is truncated by multiplying by a boxcar function (multiplies the

interferogram by 1 for x < x_{max}, and by 0 for x > x_{max}). The Fourier transform of the interferogram truncated by a box-car function however, leads to distortion of the frequency spectrum (side-lobes on bands). In order to reduce this problem, a suitable apodisation function is employed. A common apodisation function, used exclusively in these studies, is the triangular apodisation function (multiplies the interferogram by 1-x/x_{max} for x < x_{max} and by 0 for x > x_{max}) which produces less distortion in the spectral band. Unfortunately, spectral truncation of this kind degrades the resolution.

3. The sampling interval Δx. A laser is used to discretely sample the interferogram giving a summation of discrete digitised points. For accurate digitisation the sampling interval $\Delta x \leq \frac{1}{2} \lambda_{min}$. Any wavelengths smaller than $2\Delta x$ will not be digitised correctly, which leads to spectral distortion, a phenomenon known as aliasing.

4. The number of points transformed. Using more points in the Fourier transform will increase the definition of bands in the frequency spectrum. Often the number of points transformed is artificially increased by zero filling; a method of enhancing spectral definition by increasing the number of points to be transformed, without reducing the signal:noise ratio. Zero filling results in much smoother frequency spectra.

4.2.4. Resolution enhancement and curve fitting

In many of the infrared spectra presented within this thesis, the features of many bands are obscured, the causes of this are:

1. The occurrence of infrared bands at frequencies very close to each other such that they will partially overlap, making the analysis of band parameters very difficult.

2. Band broadening due to vibrational motions of chemical groups in a distribution of environments (inhomogeneous broadening) enhances the overlap of adjacent bands, compounding the first problem.

In order to extract quantitative information regarding the number of peaks; the peak positions and the relative peak intensities, Fourier self deconvolution (FSD) and second derivative (SD) spectroscopy are used to artificially narrow spectral linewidths and have been used to help interpret the results presented in this thesis. It must be noted, that the term resolution enhancement is a misnomer since the two methods used to distinguish the features of overlapping absorption bands, do not improve instrument resolution, in fact, they actually reduce it [183].

4.2.4.1. Second derivative spectroscopy (SD)

Quite simply, this method involves determination of the second derivative, $\dfrac{d^2 S(\bar{v})}{d(\bar{v})^2}$, of an infrared absorption band. It is extremely useful in determining the wavenumber position of the band since the bands are narrowed to 40% of the original band width [180], revealing the turning points (band maxima).

Figure 4.2.4.1. Second derivative of an infrared absorption band

Lorentzian profile   First derivative   Second derivative
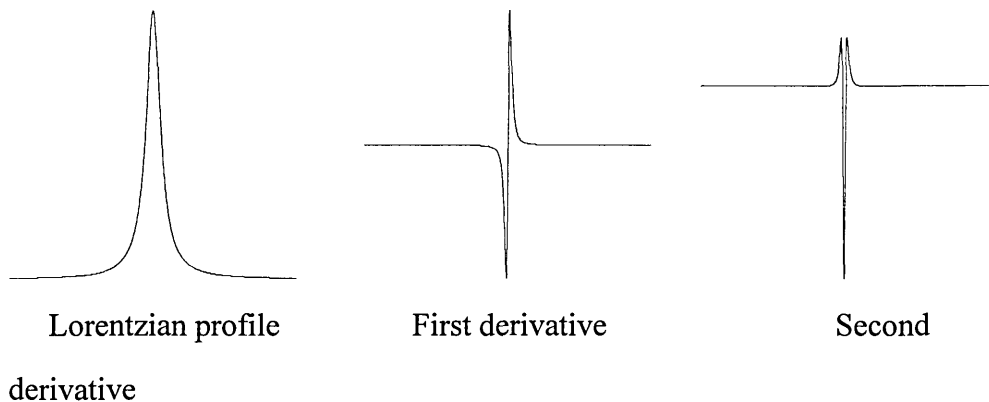
One of the major problems with calculating derivative spectra is the amplification of noise. To reduce this problem, the original spectrum (in the spectral domain) is smoothed by truncating the interferogram (in the Fourier domain) by multiplication by a boxcar function. Care must be taken to ensure the spectrum is not distorted by the smoothing process but this can be checked by comparing the spectral features of the smoothed and original data.

4.2.4.2. Fourier self deconvolution (FSD)

FSD is based on the principle that for an infrared absorption band with Lorentzian profile, the greater its full with at half maximum, (FWHM), the more rapidly the interferogram decays. Hence, the inverse Fourier transform of an infinitely narrow band (Dirac delta function), is a cosine wave [183] (figure 4.2.4.2.a). As the band becomes broader, so the rate of decay of the interferogram increases (figure 4.2.4.2.b and c). Consequently, the method of narrowing a wide band in the spectral domain involves reducing the rate at which its interferogram decays in the Fourier domain. Mathematically, this is achieved by multiplying the interferogram by an exponentially increasing function. This enhances all spatial frequency components including noise, so an

apodisation function is employed to allow the interferogram to decay, but at a much slower rate than for the original band (figure 4.2.4.2.d)

Figure 4.2.4.2 The effect of band width on rate of interferogram decay
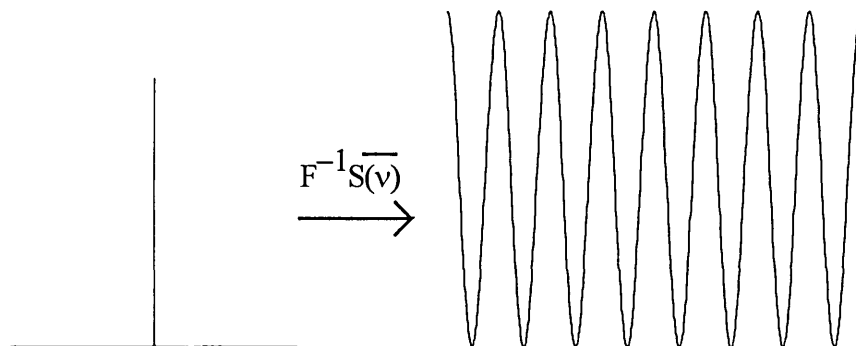
a) Infinitely narrow function
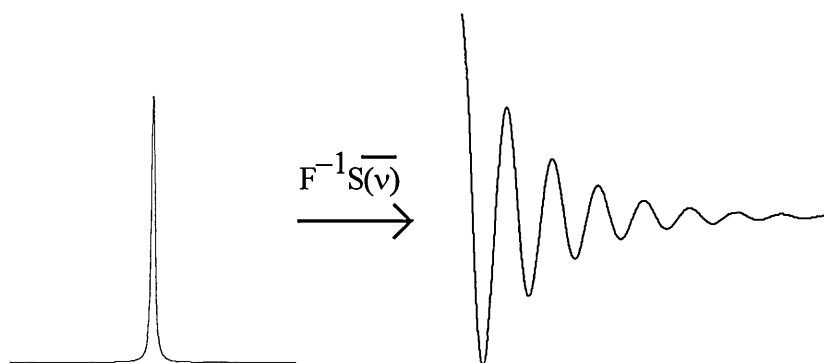
b) Narrow Lorentzian band
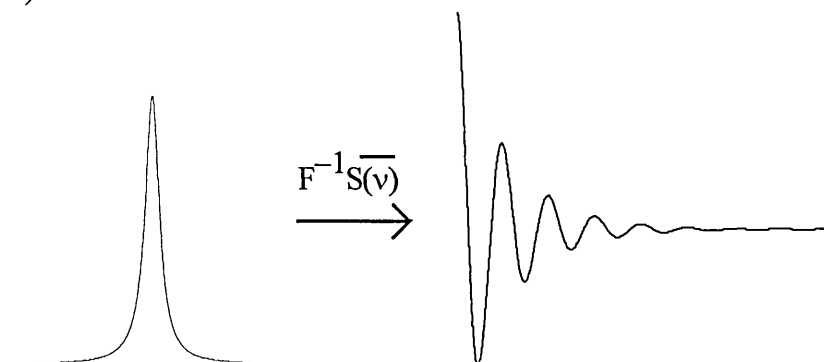
c) Broader Lorentzian band

Figure 4.2.4.2d. Band narrowing using Fourier self deconvolution
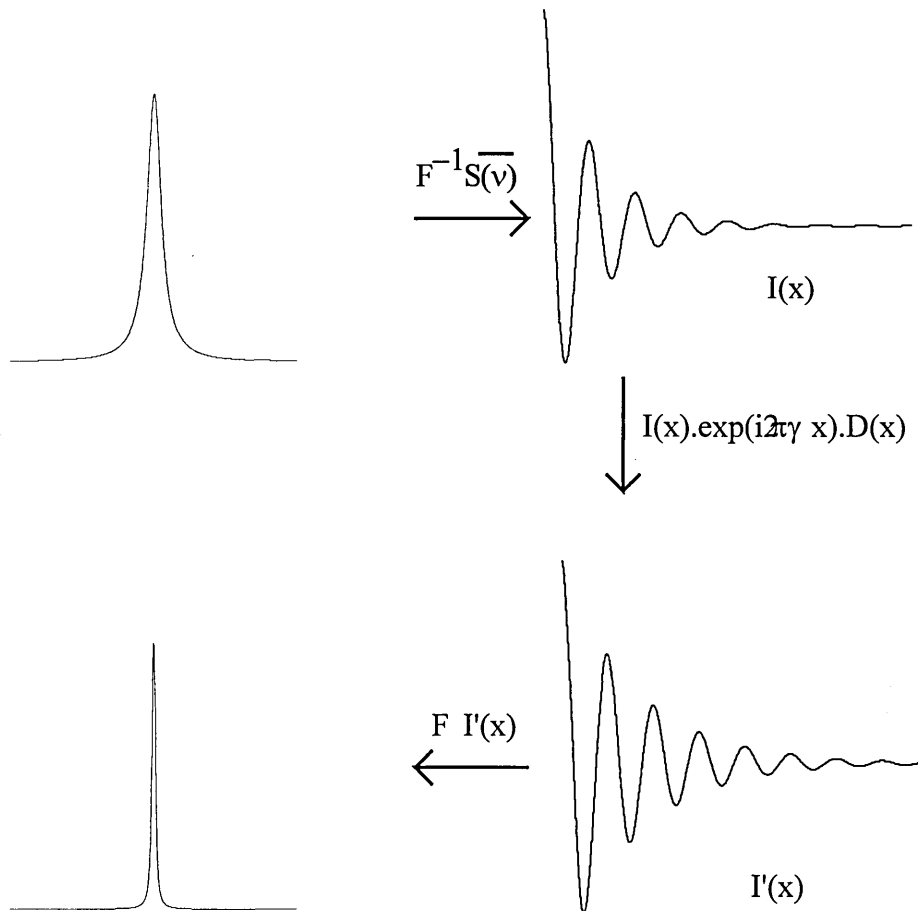
From equation 4.2.2c, the original spectral density is given by

$$S(\bar{\nu}) = 2\int_0^\infty I(x)\exp(i2\pi\bar{\nu}x)dx = F\{I(x)\} \qquad \text{eqn 4.2.4.2a}$$

And, from equation 4.2.2a, the original interferogram by

$$I(x) = \int_{-\infty}^\infty S(\bar{\nu})\exp(i2\pi\bar{\nu}x)d\bar{\nu} = F^{-1}\{S(\bar{\nu})\} \qquad \text{eqn 4.2.4.2b}$$

Now, the new interferogram is given by,

$$I'(x) = I(x).\exp(i2\pi\gamma x).D(x) \qquad 4.2.4.2c$$

Where, $D(x)$ is the apodisation function and $\exp(i2\pi\gamma x)$ is the exponentially increasing function which depends on γ, the HWHM.

Therefore, the new spectral density, $S'(\bar{\nu})$, is obtained by

$$S'(\bar{\nu}) = F\{I'(x)\} \qquad 4.2.4.2d$$

The FSD depends critically upon three carefully chosen parameters:

1. The apodisation function $D(x)$. This function determines the shape of the deconvoluted band, $S(\bar{v})$. The apodisation functions used in FSD are the same as in general interferogram truncation in FTIR spectroscopy and as such must place emphasis on the centreburst region of the interferogram and decay to zero with increasing path difference. The choice of apodisation function is a compromise between S/N and the output lineshape [184]. However, the Bessel function is generally regarded as a good choice [185]; triangular, cos and sinc^2 are other acceptable functions.

2. Enhancement factor, κ. This value is related to the ratio of original spectral linewidth, γ, to the narrow spectral linewidth, γ' [184]:

$$\kappa = \gamma / \gamma'$$

Kauppinen et al [185] state that the S/N ratio of the deconvoluted spectrum is highly dependent upon κ, and note that the maximum practical κ value is given by:

$$\kappa = \log_{10}\left(S/N\right)$$

At high κ values, the final S/N is also dependent upon the apodisation function.

3. The band width of the original band, γ. This must be chosen very carefully since underestimating γ prevents complete band separation due to poor linewidth narrowing, whereas, overestimation gives side lobes which may mask other, real bands [186].

Artefacts such as the spurious side lobes (due to over deconvoluting) or uncontrolled increases in noise, may be minimised using the interactive procedure outlined by Smeller et al [187] for extracting information from

Fourier self deconvolution. Some of the problems regarding noise and its distribution in absorbance profiles; water vapour; and flattened spectral maxima due to inhomogeneous sample preparation and ways of overcoming them have been discussed by Mantsch and Moffatt [184].

From Fourier self deconvolution, the spectroscopist is able to gain information regarding the number of component bands, the band positions and the relative integrated intensities (Mantsch and Moffatt [184] describe the preservation of integrated intensities. However in practice this is not achieved) in a poorly resolved infrared spectrum. It must be noted however, that information regarding linewidth cannot be derived since the band widths are not retained in the FSD calculation.

4.2.4.3. Curve fitting

On its own, curve fitting provides unreliable information on spectral features. However, when performed with the hindsight of information gained from second derivative spectroscopy and Fourier self deconvolution [188], it is possible to fit real bands to a real spectrum with some degree of certainty to provide quantitative information.

One of the major problems with most curve fitting procedures is that most infrared bands have Lorentzian or predominantly Lorentzian profiles [189]. Unfortunately, infinite baselines are required to fit Lorentzian band profiles, but theses are not found in most infrared spectra due to the presence of other absorption bands. As a result, less collapsed Gaussian bands often appear to fit the spectral lineshapes better than Lorentzian bands. Although the curve fitting procedure is able to fit bands with Gaussian or part Gaussian profiles, it is impossible to determine whether the band actually contains some Gaussian

component or whether it is an artefact of the spectrum. Consequently, in order to extract quantitative information, all fitted bands presented in this thesis will have Lorentzian profiles.

In the advanced FIRST curve fitting package, which is part of the Mattson FIRST software used to obtain and manipulate the spectra presented in this thesis, the fit criterion $\chi^2\left[=\sum_i \frac{(N_i-n_i)^2}{n_i}\right]$, is used to compare the parameters (peak position, peak height and FWHM) of a set of fitted bands n_i, with the parameters of the experimental band N_i, in an iterative process. The fit criterion is optimised when it reaches a minimum value (by default the value of $\chi^2=0$, i.e. when $N_i=n_i$) or the number of iterations is complete. The peak position, peak height, FWHM and integrated intensity may then be determined. It must be noted that the fitting of synthetic bands to a real spectrum is never perfect and is always a non-unique solution.

4.2.5.   Advantages of using FTIR spectroscopy

FTIR spectroscopy is a very powerful tool and has many advantages compared to dispersive infrared techniques, the most important perhaps being:

- Multiplex (Fellgett) advantage-All spectral elements are observed simultaneously, not individually as in a dispersive instrument, which enables many spectra to be obtained at rapid speeds. These spectra may be co-added to improve the signal:noise ratio of a spectrum in the time taken to record a single dispersive spectrum.
- Throughput (Jacquinot) advantage-At a given resolution, the energy throughput is much greater in an interferometer than in a dispersive instrument since there are no slits to restrict throughput. Consequently, the amount of signal

reaching the detector is much greater. This is particularly important in the far infrared analysis (> 700 cm^{-1}) of minerals where significant information may be obtained, but where infrared energies are very low.

• Connes Advantage-Absolute control of the spectral wavelength is achieved by sampling with a laser whose wavelength is fixed. This ensures that no frequency drift is observed which is particularly important in subtracting the individual spectrum of a particular phase to remove unwanted absorptions due to this phase. This is particularly important for clay minerals where some infrared absorption bands (particularly the silicate stretching modes) are extremely intense and may mask other important features of the spectrum due to impurities, or adsorbed species. It is also important in the interactive spectral subtraction of unwanted water vapour from sample spectra.

The Fourier transform spectrometer does have disadvantages however, particularly if the source is noisy. In such cases, the detector will observe all the noise all the time as it integrates over all frequencies thus reducing the signal:noise ratio. In addition, unlike dispersive instruments which acquire dual beam spectra (sample and reference spectra at the same time) and immediately eliminate unwanted water vapour absorption bands, FT spectra are obtained as single beam experiments. As a result, it is necessary to ratio the sample spectrum against a reference spectrum taken previously to obtain the actual absorption spectrum. Due to variations in humidity, the water vapour spectrum will differ slightly between the reference and sample spectra and consequently the absorption spectrum will contain unwanted absorption bands due to water vapour. These can be eliminated by purging with a dry infrared inactive gas such as nitrogen or interactive spectral subtraction of the individually acquired water vapour spectrum.

4.2.6. Experimental

Infrared spectroscopy is used extensively in clay mineralogy particularly in the characterisation of mineral structure, composition and reactions. One of the principle advantages of infrared spectroscopy particularly compared to X-ray diffraction, is its sensitivity. Because each layer absorbs infrared radiation independently, it is possible to recognise structures without depending upon the packets of layers which are required to give coherent X-ray diffraction. Farmer [182] and Russell and Farmer [190] have extensively studied layer silicates using transmission infrared spectroscopy. Sample preparation is extremely important, the two most popular methods of analysis being:

1. Pressed pellet or disk

The commonest disks prepared are those using high purity potassium bromide, KBr, which has a wide infrared window (down to ~450 cm^{-1}) and forms an amorphous matrix at high pressures. Generally, two concentrations of pressed pellet are prepared [26] (~3 mg in 170 mg of KBr and ~0.5 mg in 170 mg of KBr) to enable studies to be made of the weaker (OH stretching and bending modes) and strongest (Si-O bands) spectral features, respectively. Mineral particles are randomly oriented within the KBr matrix and thus no orientation dependency of the bands is observed. It must be remembered that some interactions may occur between the exchangeable counter cation in the clay and the potassium ion in the matrix at room temperature. Polyethylene is used in the preparation of pressed disks to enable analysis of the far infrared spectra of minerals. Particle size is extremely important in the preparation of minerals for infrared spectroscopic examination [26, 191]. Conventionally, the <2μm fraction of the mineral is obtained by centrifugation or sedimentation. It is important, however, that all samples (particularly those of mineral-polymer complexes) are ground using a mortar and pestle to ensure that the particle size

is <2μm. This helps to reduce the distortion and broadening of infrared bands [182, 190] and minimise λ^{-4} scattering of infrared radiation which leads to a sloping baseline. KBr crystals commonly used in disk preparation enhance the grinding of mineral-polymer particles to <2μm particle size.

2.   Sedimented films

An aqueous mineral dispersion can be sedimented onto an infrared transparent window such as CaF_2, Si, or ZnSe to give a uniform deposit on evaporation of water. Due to the strong cohesion of plates, deposition may be made onto a plastic sheet and, after drying the deposit, it may be peeled to give a self-supporting mineral film. Brown and Brindley [192] have commented that films produced by this method have a preferred orientation in which the c-axis of the mineral lies normal to the surface. It has been stated that preparations of layer silicates of this nature behave like quasi-two-dimensional crystals [190].

A Mattson Polaris FTIR spectrometer using FIRST software has been used to record the infrared spectra of clay-polymer complexes prepared from aqueous solution by two methods:

1. The adsorption of polymer from solution onto dispersed montmorillonite was studied by mixing clay suspension and polymer solution. The solids were centrifuged and dried, then prepared into a pressed KBr pellet. This is then clamped in a transmission cell in the sample compartment of the infrared spectrometer, with the infrared beam perpendicular to the face of the pellet.
2. Free standing montmorillonite films may be dipped into polymer solution, removed after the desired equilibration time, then clamped in a transmission cell and dried, perpendicular to the direction of the infrared radiation, in the nitrogen purge of the infrared spectrometer.

4.2.7. Transmission spectroscopy in clay mineralogy

As mentioned in the previous chapters, infrared spectroscopy is used extensively in determining the behaviour of water and other polar molecules in the interlayer of montmorillonite.

Infrared spectroscopy has also been used to determine the composition of the natural clay to aid in classification. Bukka et al [25] were able to differentiate between Cheto and Wyoming montmorillonites using FTIR spectroscopy. Some studies have shown that the structural OH stretching and bending modes of montmorillonite are sensitive only to the nature of the metal ion in the octahedral lattice [193, 194, 195] and the nature of the exchangeable cation [25, 40] not vibrations of the silicate lattice.

The orientation of particular bonds in the smectite structure have also been studied. Wyoming bentonite 'paper' shows very little angular dependence of the structural OH stretching mode [196], i.e. tilting the film at 45° to the incident infrared radiation did not change the intensity of the band assigned to structural OH stretching. However, Farmer and Russell [197] have shown that Wyoming montmorillonite has four Si-O stretching bands at 1120, 1080, 1048 and 1025 cm^{-1} of which the band at 1080 cm^{-1} was found to show some angular dependence. This band has been assigned [43] to the vibration, perpendicular to the clay surface, of apical oxygen atoms that are shared between the tetrahedral and octahedral layers, i.e. parallel to the incident radiation. The other well-defined bands are assigned to in-plane Si-O stretching modes [197]. It has been suggested [197] that the position and appearance of the silicate stretching bands are dependent on the degree of order (regularity) of the structure.

4.3. Infrared Microscopy

A full description of the details of infrared microscopy and its application in polymer and mineral analysis can be found by Roush [198] and Messerschmidt and Harthcock [199]. However, it is important to discuss some of the most important features of the Nic-plan infrared microscope used in the studies presented in chapter 5 of this thesis.

The microscope is a basic conventional microscope fitted with 32x and 15x Cassegrain objective lens which may be used either in transmission or reflectance mode and is attached to a Nicolet 800 infrared spectrometer fitted with an MCT detector. A cover which encloses the sample stage enables the whole system to be purged with dry air which helps to remove water vapour and carbon dioxide from the infrared spectra.

Two apertures are fitted above and below the sample in order to select the appropriate area around a particle for analysis. These are also used to align the microscope in the optical mode (alignment of the optical and infrared images is imperative to ensure the correct area is sampled) and ensure that stray light from other sources is minimised.

The minimum sample size suitable for infrared microspectroscopic analysis is between 10 and 20 μm, this being controlled by the wavelength of the infrared radiation. Samples of size less than the wavelength of the radiation ($\sim$10 μm) can cause spectral distortions. This is due to the diffraction of the radiation which causes the beam to spread out and allows light to fall outside the predetermined sample area, a source of stray light which causes spectral distortion. In addition, aberrations in the optics or the sample (particularly the

sample thickness) are corrected using a refocussing lens located below the sample.

4.3.1. Experimental

Pressed KBr pellets containing bentonite were prepared (as explained previously) and dehydrating aqueous bentonite suspensions were studied using the Nic-plan infrared microscope mentioned previously. In each case a suitable area, usually ~ 50x50 or 100x100 μm (depending upon the size of the feature) is located and studied in the transmission mode. The infrared spectrum of a dehydrating montmorillonite suspension was commonly taken close to the edge of the droplet. This is done to ensure that the sample path length was sufficiently thin to enable the very intense Si-O stretching vibrations (between 1200 and 950 cm^{-1}) to be recorded without completely absorbing and causing cut-off.

4.4. Attenuated total reflection (ATR) spectroscopy

Multiple internal reflection spectroscopy was first reported by Harrick [200] and he and co-workers expanded the theory and experimental possibilities. Since then with the increasing usage of the technique many review articles [201, 202]] have been published which outline the various areas in which ATR, or internal reflection spectroscopy (IRS) as it is often referred, is used.

4.4.1. ATR theory

Total internal reflection (the theoretical basis for IRS) occurs when the angle of incidence θ_{inc} , of radiation propagating through a medium, having a high refractive index, n_1, exceeds the critical angle, θ_c , at the direct interface with

an optically less dense medium, having lower refractive index n_2 (figure 4.4.1a). The critical angle is related to the refractive indices of the two media by:

$$\sin\theta_c = \frac{n_2}{n_1} = n_{21} \qquad \text{eqn 4.4.1a}$$

The interference between incident and reflected radiation in the optically more dense medium, causes a standing wave perpendicular to the totally reflecting interface to develop. The electric field amplitude of the standing wave is non zero at the interface and consequently there is an instantaneous non-zero energy flow into the rarer medium (the energy flow is zero time averaged to ensure no loss of energy and total internal reflection). In the rarer medium, the electric field component of the standing wave decays exponentially, and is known as the evanescent wave (figure 4.4.1b)

Figure 4.4.1

a) Total internal reflection
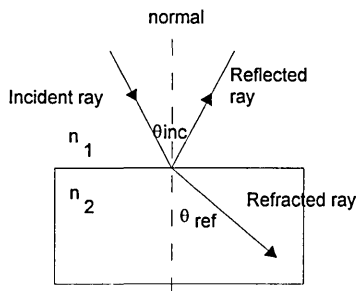
b) Electromagnetic field near a totally reflecting interface
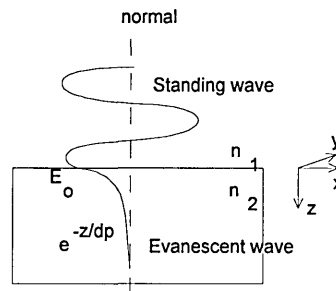
4.4.2.   The evanescent field

The evanescent field is a non-transverse wave with components in all directions (x, y, z). It is confined to the surface region and decays exponentially with distance normal to the surface, into the less dense medium, represented by:

$$E = E_o \exp\left(-\frac{z}{d_p}\right) \qquad \text{eqn 4.4.2a}$$

Where E_0 is the electric field amplitude at the surface and E is the electric field amplitude at distance z from the interface. The depth of penetration d_p is defined as the distance from the interface where the electric field amplitude decays to $\frac{1}{e}$ of its value of the interface and is calculated from:

$$ d_p = \frac{\lambda_1}{2\pi \left(\sin^2 \theta_{inc} - n_{21}^2 \right)^{\frac{1}{2}}} \qquad \text{eqn 4.4.2b} $$

Where, λ_1, is the wavelength of the radiation in the denser medium.

It must be remembered that d_p is not the actual depth measurement since the electric field amplitude at d_p is only 37% of its value at the surface. The actual depth sampled d_s is approximately $3d_p$.

Another parameter, the effective thickness, d_e, which is defined as the thickness of sample which gives the same absorbance as a transmission spectrum at normal incidence, allows direct comparison between spectra obtained in transmission or by ATR.

From eqn 4.4.2b, one can see that it is relatively easy to change the depth of penetration simply by changing the angle of incidence or the reflection element. In addition, it can be seen that the depth of penetration increases with increasing wavelength hence a sample spectrum obtained by the ATR method will be more intense at higher wavenumber than absorption bands in a normal transmission spectrum of the same sample. When comparing ATR with transmission spectra it must also be noted that ATR spectroscopy is a surface sensitive technique. It is not surface selective in the way that some other surface analytical techniques are, however, in terms of infrared spectroscopy a sample thickness of the order of microns is very thin. Transmission spectroscopy is, in contrast, a bulk analysis technique.

4.4.3. Approximations in ATR

The ATR theory outlined above represents an idealised model of the real situation. Several assumptions are made to keep the model simple including approximating the absorbing medium to be homogeneous (i.e. that its refractive index does not change with distance from the reflecting interface); that there are no diffraction effects; and that beams are narrow and well collimated so that the time average of the evanescent field is zero.

One of the most confusing assumptions on which ATR theory relies is that the absorption coefficient of the rarer medium being zero, i.e. it is non-absorbing. This is not the case and as a result, the decay of the evanescent field is controlled by both its natural exponential decay and absorbance. However, it has been shown [203] that the evanescent field is significantly modified only by very strong absorbers and so the equations used for a non-absorber are usually valid. Since radiation penetrates to a total depth, of the order, of a few microns, energy will be lost in the excitation of molecules. Consequently the electric field intensity of the reflected radiation is lower than the electric field intensity of the incident radiation and the reflection will be attenuated. The attenuated radiation contains important vibrational information regarding the adsorbing medium.

4.4.4. Experimental

In the research reported in this thesis zinc selenide (ZnSe) and silicon (Si) multiple internal reflection elements (IRE), commonly referred to as the ATR prism, have been used exclusively due to their high refractive index, wide infrared transmission window, chemical inertness, and the ability to obtain precise dimensions and angles. The advantage of using a multiple reflection

crystal is its multiple sampling of the rarer medium (the sample) which improves the sensitivity.

Two ATR accessories have been used to perform these experiments. A Spectra Tech horizontal cell fitted with a 70° ZnSe prism was used to study the dehydration of clay mineral films but more commonly used was the Specac Squarecol cell (figure 4.4.4), particularly to investigate the orientation of clay platelets in dehydrated films or the adsorption of polymer onto such clay films.

The Squarecol ATR prism (ZnSe or Si), is square in cross-section and has dimensions similar to those of the infrared radiation, is sealed into a stainless steel trough by means of two viton O-rings which are each compressed and secured by a stainless steel plate to ensure the arrangement is liquid-tight. The cell is oriented in the sample compartment of the spectrometer such that the angle of incidence is 45°. The trough of the Squarecol cell can readily be filled with aqueous solution and indeed, experiments on aqueous bentonite suspensions were performed by adding the pre-prepared dispersion in this way.

Studies to determine the adsorption of polymer from aqueous solution *in-situ* however, require thin layers of bentonite to be deposited on the internal reflection element (IRE) by sedimentation and evaporation of aqueous bentonite suspensions prior to inclusion in the cell as outlined by Billingham et al [204, 205]. This is a very similar procedure to the preparation of thin self supporting bentonite films for analysis by transmission spectroscopy. A common disadvantage of ATR spectroscopy is the difficulty in obtaining good optical contact between a solid sample and the reflection element. This is not considered to be a problem in these experiments since thin sedimented bentonite films deposit directly onto the surface. The trough can then be filled with

solutions containing polymer and ionic salts and the adsorption/diffusion process observed.

Figure 4.4.4. Schematic of the Squarecol ATR unit
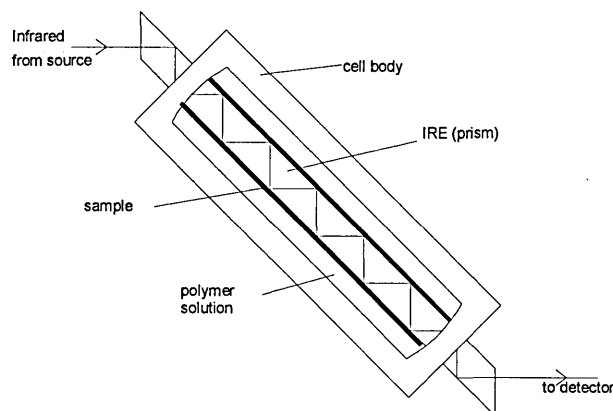
It is extremely difficult to determine the actual thickness of the bentonite layer on the crystal surface. Attempts using surface profile measurements have destroyed the film, and reflected laser measurements have been impossible due to the limited reflectivity of bentonite. As a result, quantitative ATR analysis is extremely difficult.

4.4.5.   ATR spectroscopy in clay mineralogy

Other than the method used in this study (outlined by Billingham et al [204, 205]), many workers have used FTIR-ATR spectroscopy to study the adsorption of organic species on mineral surfaces. This has been predominantly to study the behaviour of collector molecules (the organic species used in the separation and purification of natural rocks).Three, *in-situ*, methods have been highlighted in the literature [206]:

1.   Pressing of dried mineral-organic complex or particulate suspension against an inert internal reflection element.

The settling of mineral-organic complex from aqueous suspension has been used by Mielczarski [207] and Mielczarski et al [208], and Hunter and Bertsch [209] studied the degradation of tetraphenylboron in aqueous clay pastes in this way. The pressing of dry clay-organic complexes against an ATR prism has been used predominantly to study the behaviour of clay minerals in the presence of organic species [139, 210, 211]. Although orientation information was elucidated from the spectra [139, 210], Guzonas et al [211] identified one of the major problems regarding this method, that being poor optical contact between prism and clay mineral. Guzonas et al [211] were unable to obtain good optical contact between thin mica sheets and the IRE and in addition were unable to attain uniform thickness of large mica sheets over the entire ATR prism. The micro-ATR unit which is available at SHU [212] and which uses much smaller ATR crystals (~1 cm^2 sampling surface area, compared with ~6 cm^2 of a conventional parallelepiped prism available from Graseby Specac Ltd) was used in the hope of covering the IRE with one small, thin mica sheet. Unfortunately, however, experiments performed both at Schlumberger Cambridge Research and SHU were unable to achieve this.

2. IRE coated with a vacuum deposited layer of inorganic material.

Kuys and Roberts [213] identified the reaction products, determined the kinetics and postulated the mechanism of styrene phosphonic acid on cassiterite (SnO$_2$ which was vacuum deposited on a Ge IRE) *in-situ*. Other studies have determined the adsorption characteristics of sodium dodecyl sulphate [214] and sodium laurate [215] on ATR optics sputter coated with alumina. This method has obvious advantages compared to method 1, since intimate contact between the IRE and mineral is achieved and reproducible film thicknesses may be obtained. Similar work [216, 217] has used the oxidised surface of a Si ATR prism to study the adsorption behaviour onto SiO$_2$ of amines and silanes respectively.

3. Reactive IRE

It is possible to fabricate single mineral crystals such as fluorite (CaF_2) and Sapphire (Al_2O_3) into an internal reflection element such that it may internally reflect infrared radiation and act as the substrate for adsorption of organic material [206]. As a result, it is possible to study, *in-situ*, the direct adsorption of organic material at the mineral solvent interface without the complications of an additional component. Consequently, there has been significant research into the adsorption of sodium dodecyl sulphate onto an alumina IRE [112, 206, 218] and adsorption of sodium oleate onto a fluorite IRE [112, 206]. In addition to these studies, Yalamanchili et al [219] have grown and machined KCl crystals into ATR prisms and studied the adsorption of collector molecules on these soluble salt crystals. This is probably the easiest method of obtaining ATR spectra of mineral-organic interactions as there are no problems with optical contact. However, it is limited by the infrared window of the particular mineral and the ability to fabricate an ATR crystal from the mineral. This is obviously impossible for montmorillonite which exists as small plates and mica where reflection and refraction at each platelet boundary in the mica sheet would interfere with the attenuated signal from the clay-organic interface.

4.4.6. Quantitative information

In principle, a significant amount of quantitative information can be obtained from IRS, including:

• Adsorption state. The nature of interaction may be determined by measuring the wavenumber shift of characteristic vibrational modes of the organic or mineral material.

• Adsorption density. Sperline et al [220] derived a relationship for the Gibbs surface excess which enables the adsorption density to be calculated.

Consequently, using rapid scan FTIR spectroscopy, adsorption kinetics at the reflecting element can be studied *in-situ* in real time.

• Sample Orientation. The angle at which the adsorbed molecule is oriented to the surface may be calculated by establishing the two limiting cases of molecule orientation (either perpendicular or parallel to the surface) and determining the proportion of each using polarised radiation. This is known as the method of dichroic ratios [221] (section 4.5.2).

4.5.   Polarisation measurements

Polyatomic molecules contain oscillating dipole moments which are positioned in a particular way on a set of Cartesian co-ordinates (x, y, z). Consequently, polarised light is extremely useful for the determination of molecular orientation, since only radiation polarised in a particular plane will interact with the components of the electric dipole in that plane. Indeed, the probability of an infrared transition is proportional to the square of the cosine of the angle between the dipole moment and the direction of the field [175].

Several clay mineralogists [43, 197] have commented upon the absorbance band at 1086 cm^{-1} in the infrared spectrum of montmorillonite and attributed it to a Si-O vibration perpendicular to the surface of the clay platelet. Consequently, polarised measurements have been used in this thesis to determine the orientation of the clay platelet in the dehydration of an aqueous montmorillonite suspension.

4.5.1.   Polarised radiation

For unpolarised light, the electric field vector oscillates in all directions. In transmission however, radiation may be polarised, by means of a wire grid

polariser, either perpendicular to (TE), or parallel to (TM) the plane of incidence of the radiation (figure 4.5.1). In such circumstances, the electric vectors are restricted to one angle (either perpendicular or parallel to the direction of propagation).

Figure 4.5.1. Plane polarisation of propagating radiation
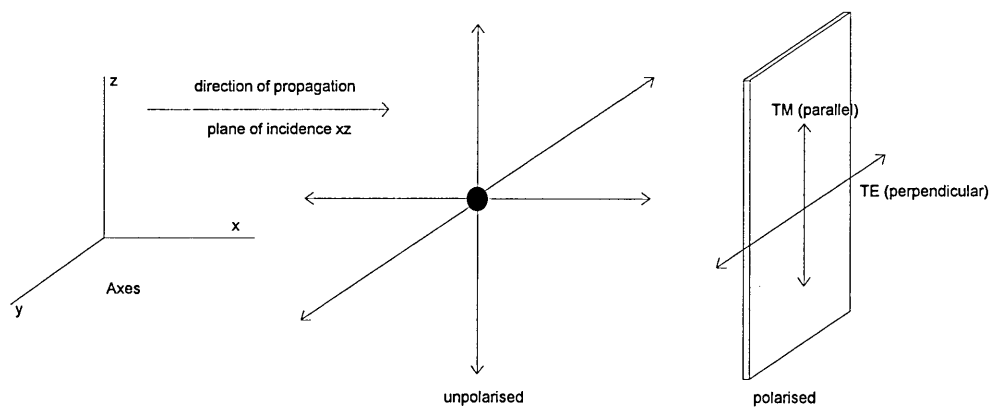
Similarly, in ATR, when the radiation is unpolarised, the evanescent field has components in all directions (x, y, z) and may interact with all dipole moments (figure 4.4.1b).

It should be noted that in ATR, the plane of incidence is defined as the plane perpendicular to the interface between the dense and rarer media (the xz plane).The radiation may be polarised:

1. Perpendicular (TE) to the plane of incidence. Only the E_y electric field vector is associated with the evanescent field. E_y is perpendicular to the plane of incidence, but parallel to the surface.

2. Parallel (TM) to the plane of incidence. Both the E_x and E_z electric vectors are associated with the evanescent field. E_x and E_z are parallel to the plane of incidence, but E_x is parallel to the surface and E_z is perpendicular to the surface.

4.5.2. Dichroic ratio

It is possible to define the ratio of absorbance with TE polarised light to the absorbance with TM polarised light as the dichroic ratio

$$\text{Dichroic ratio} = \frac{A_{TE}}{A_{TM}} \qquad \text{eqn 4.5.2a}$$

where A_{TE} and A_{TM} are the integrated areas of a particular absorbance band in TE and TM polarised radiation respectively.

Since absorbance, $A \propto E^2$, the square of the electric field [175] then,

$$\frac{A_{TE}}{A_{TM}} = \frac{E_y^2}{E_x^2 + E_z^2} \qquad \text{eqn 4.5.2b}$$

The effective thickness in TM polarised light is known to be greater than in TE polarised light [202]. Consequently, absorbance bands obtained in TM polarisation will be more intense than those obtained in TE polarisation and only relative intensities are comparable.

4.6. X-ray diffraction

X-ray radiation occurs in the region of the electromagnetic spectrum with wavelength between approximately 10^{-9} and 10^{-11} m. Many detailed explanations of the production of X-rays and X-ray diffraction theory can be found [192, 222, 223], but a brief description of the fundamental principles which gives rise to the characteristic X-ray spectrum and diffraction trace will be given here.

4.6.1. Production of X-rays

X-rays are produced when a beam of electrons, accelerated by a high voltage, are rapidly decelerated by striking a metal target due to collisions with the metal

atoms. The resultant spectrum of radiation is known as continuous or white radiation (figure 4.6.1a). If the electron is stopped in one impact (i.e. all the energy is converted into an X-ray) then a minimum wavelength of X-ray is attainable which depends upon the accelerating voltage. The intensity of X-rays in the continuous spectrum is defined as the rate of flow of energy through unit area, perpendicular to the direction of motion of the wave and is dependent on the accelerating voltage and current of the electrons and the atomic number of the target. Although X-ray intensity has S.I. units (joules $m^{-2} s^{-1}$), X-ray intensity measurements are made on a relative basis in arbitrary units.

When the energy of the electron striking the metal target exceeds a critical value (characteristic of that particular metal target), sharp intensity maxima appear superimposed on the white radiation at certain wavelengths (figure 4.6.1a). The target atoms are ionised by the accelerated electron beam and as a result, one of the electrons in a higher energy orbital reduces its energy to fill the vacancy created, and emits the energy difference as an X-ray photon. The energy of the photon depends on the energy difference between the two energy states and will be characteristic of the target metal. The intensity of the characteristic lines above the continuous spectrum is dependent on both the tube current and the difference between the tube voltage and critical excitation voltage.

The characteristic lines in the X-ray spectrum are referred to as K, L and M corresponding to transitions from higher energy levels to the K, L and M shells which have quantum numbers 1, 2 and 3 respectively (figure 4.6.1b). The line in the spectrum also has a subscript depending upon whether the orbitals are adjacent, α, or separated by another orbital, β. It is only the K lines which are useful in X-ray diffraction, the longer wavelength radiation being too easily absorbed.

Figure 4.6.1

a) Characteristic X-ray spectrum
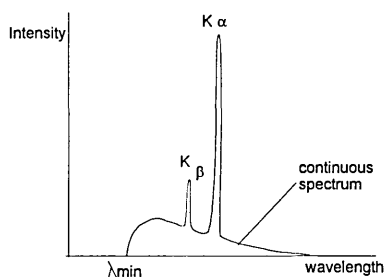
b) Electron transitions between orbitals
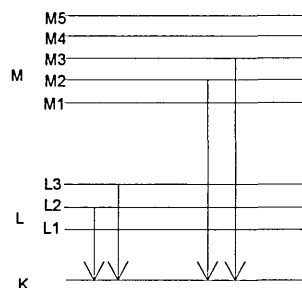
4.6.2. Absorption of X-rays

When an X-ray passes through a sample its intensity is attenuated which is dependent upon the thickness and density of the sample and the nature of the radiation [222]. Two types of absorption occur:

1. Scattering in all directions such that the X-rays do not reach the detector and so are apparently adsorbed.

2. Absorption of X-ray photons to facilitate electronic transitions in the atom. This phenomenon is utilised in techniques such as X-ray Photoelectron Spectroscopy (XPS) and X-ray Fluorescence Spectroscopy (XRF).

4.6.3. Diffraction

It is the scattered radiation which is of importance in X-ray diffraction. Each atom acts as a scattering centre for the X-rays and scattering may be in:

1. Most directions which do not satisfy the Bragg equation, i.e. no scattering because all rays destructively interfere and cancel

2. A few directions which satisfy the Bragg equation. Scattering is found to be strong because rays constructively interfere to give a diffraction pattern.

4.6.3.1. The Bragg equation

If the X-radiation falls on a plane of atoms in a sample (each atom acts as a scattering centre) a distance d apart, at an angle θ, then diffraction occurs if the Bragg equation is satisfied:

$$n\lambda = 2d \sin\theta \qquad \text{eqn 4.6.3.1}$$

Where λ is the wavelength of the radiation and n is an integer representing the order of diffraction. Hence, diffraction is produced when the path lengths of diffracted rays differ by an exact multiple of the wavelength and the scattered radiation is all in-phase and constructively interferes.

4.6.4. Diffractometer components

Important features of the Phillips 1050 diffractometer used to obtain the diffraction traces presented in this thesis, are:

• Source of radiation-Co K_α was used for most analyses since it has a longer wavelength than Cu K_α. This is very useful in clay mineral analysis as it shifts low angle peaks (those of most interest) to slightly higher 2θ positions, aiding their identification. However, Cu K_α was used in some experiments. The accelerating voltage and current used in each experiment was 40 kV and 20 mA respectively.

• Filters and monochromators-The methods of X-ray analysis require monochromatic radiation. The high intensity, high energy K_α energy is used for X-ray diffraction and as a result it is important to remove all other radiation (i.e. K_β and the continuous spectrum). This is performed by using the absorption characteristics of a filter (commonly Ni) which removes all unwanted wavelengths.

• Detector-A diffractometer counter converts the X-ray into an electric current which can be interpreted simply.

• Angular Scanning rate-The detector and sample were rotated by means of a goniometer within an angle range between 4 and 20° and with an angular increment of 0.05° every 2 seconds.

4.6.5. Experimental methods

Two commonly encountered preparative techniques [192, 223] and used exclusively in the diffraction traces recorded and presented in this thesis are:

1.   Deposited film

In exactly the same way that thin oriented films may be prepared for transmission and ATR infrared analysis, they can be prepared for X-ray diffraction determination. In these experiments, the clay or clay-organic complex is deposited on a glass slide and the film allowed to dry at 60°C. The d-spacing in clay minerals may be calculated from the wavelength and incident angle of X-radiation in the diffraction experiment. Orienting the sample in this way significantly affects the relative intensities of the basal and non-basal reflections. In fact, the diffraction pattern may only show the 00l basal reflections, with very little evidence of any hkl reflections. The basal spacing obtained for montmorillonite comprises the thickness of the clay platelet (calculated to be 9.6Å, depending on the interlayer cation [14]) and the interlayer separation which varies depending upon the adsorption of polar molecules between the platelets (figure 2.6.1.1). Consequently, for quantitative work, only the peak positions can be used with any degree of accuracy.

2.   Powder diffraction

The clay or clay-organic complex was dried at 60°C and finely ground using a mortar and pestle (care must be taken to prevent deformation of the layer silicate structure). The solid is than packed into an aluminium sample holder and compacted using a roughened glass slide. Extreme care must be taken with

plate-like minerals whilst pressing or smoothing the solid into the cavity of the sample holder to ensure orientation is not imparted to the platelets. Samples which have random orientation do not have any preferential reflections and consequently the relative intensities of diffraction peaks are preserved and can be used with peak positions in quantitative analysis.

4.6.6.   X-ray diffraction in clay mineralogy

1. X-ray identification of clay minerals

Every clay mineral has a particular characteristic layer structure which is determined from the basal reflections. The basal reflections of montmorillonite vary with the level of hydration, as discussed previously in chapter 2. In addition, MacEwen [224] described the adsorption of glycerol onto montmorillonite to give a sharp, intense basal spacing of 17.7 Å as a suitable method for the identification of montmorillonite minerals.

2. Determination of adsorbed species

The use of X-ray diffraction to determine whether polymer adsorbs in the interlayer space or if it adsorbs on the external clay surface has been mentioned previously in chapter 3. X-ray diffraction data provides information regarding the orientation and packing density of organic molecules (polymers) in the interlayer space and give a measure of the van der Waals dimensions of the adsorbed molecule. It must be noted, however, that this method may not be entirely accurate since the basal planes are not flat on a molecular scale and because the organic molecule is capable of keying into the di-trigonal cavity of the silicate tetrahedral sheet of the clay platelet [140].

4.7. Kjeldahl total nitrogen analysis

To determine the amount of nitrogen containing polymer (polyacrylamide) adsorbed onto the clay mineral in an aqueous dispersion, the Kjeldahl technique for total nitrogen analysis was employed. The clay-polymer complex was mixed and centrifuged (the exact details can be found in the relevant experimental section) and allowed to dry at 60°C then finely ground using a mortar and pestle. Weighed quantities of the clay-polymer complex were prepared for digestion by mixing with 25 ml conc. H_2SO_4 (low nitrogen content) and two catalyst tablets, which contain 94% K_2SO_4, 5.5% $CuSO_4.5H_2O$ and 0.5% Se, in a digestion tube. The Cu and Se act as catalysts for the digestion whilst the K_2SO_4 aids digestion by raising the boiling point of the conc. sulphuric acid. The digestion mixtures containing the samples are then heated to 380°C for four hours which converts the nitrogen containing compounds into $(NH_4)_2SO_4$, H_2O and CO_2.

After digestion, the digestion tubes are cooled and the contents analysed in the Kjeldahl Autoanalyser. The digestion solution is made basic by adding 30 ml of 40% NaOH which converts NH_4^+ to NH_3 which is then steam distilled and adsorbed into 4% boric acid solution. The ammonia complexes with the boric acid to form a strong base which is titrated with 0.1 mol dm^{-3} HCl to determine the percentage nitrogen by weight in the sample.

4.8. X-ray Fluorescence (XRF)

XRF spectrometry utilises the absorption of X-rays by a sample as mentioned previously. The bombardment of the elements in the sample with X-rays produces characteristic X-ray fluorescence radiation at a number of specific wavelengths in the same way that X-rays are produced by electron bombardment of a metal target. In the spectrometer, individual wavelengths of

fluorescence radiation may be diffracted (separated) and detected individually. The intensity of any wavelength of the characteristic radiation is proportional to the concentration of the element in the sample which produces that radiation. Thus, chemical analysis on the clay samples may be performed.

A Phillips PW2400 spectrometer was used to determine the elemental composition of natural and homoionic Na and K exchanged SWy-1 montmorillonite. Each sample of clay mineral was finely ground and dried at 120°C. In order to reduce particle size and mineralogical effects [225], 1 g of sample was evenly mixed with 10g of powdered lithium tetraborate and this mixture was heated at 1250°C until the powders fused and formed a melt. The melt was then cooled to form a fused bead which may then be placed in the XRF spectrometer to quantitatively determine its chemical composition.

4.9. Chemicals

4.9.1. Clay minerals

The experiments described within this thesis were performed using, SWy-1 Wyoming bentonite, supplied by Schlumberger Cambridge Research. The chief component being the clay mineral, montmorillonite and impurities such as quartz and mica. Hence, before being used in any experimental procedure, the raw bentonite was purified by centrifugation sedimentation procedures [223].

The bentonite was evenly dispersed in a 5% w/w aqueous suspension and allowed to settle under the influence of gravity or the increased influence of gravity in a centrifuge. The <2μm fraction of bentonite was obtained by sedimentation for the times outlined by Moore and Reynolds [223] since this fraction is left in suspension and larger fractions settle out, as predicted by

Stokes law. The purified bentonite was then dried and used without further treatment, referred to as natural bentonite. In addition, Na and K exchanged bentonite were prepared by treating an aqueous solution of the natural clay, which contained mostly Na^+ and Ca^{2+} counter cations (table 4.7.1), with 1M solution of the chloride salt of the univalent cation. This was allowed to equilibrate for ~4 hours then the suspension was centrifuged, the supernatant discarded, and the solids re-suspended in fresh metal chloride solution. This process was repeated 3 times to saturate the clay with the desired cation. The bentonite was then resuspended in deionised water and centrifuged, a process repeated several times in order to wash away excess ions which might be trapped between the platelets.

As described previously, chemical analysis of the bentonite was performed by XRF spectrometry The results of which are shown in Table 4.7.1. The values in table 4.9.1 compare very favourably with the chemical composition of SWy-1 Wyoming montmorillonite presented by van Olphen and Fripiat [26].

Table 4.9.1. Chemical analysis of bentonite by XRF spectrometry.

| Clay	percentage weight of oxide							
	Na_2O	MgO	Al_2O_3	SiO_2	K_2O	CaO	TiO_2	Fe_2O_3
Natural	1.48	2.54	19.22	62.86	0.55	1.73	0.11	3.85
K+	0.15	2.27	20.61	68.28	3.39	0.75	0.14	4.27
Na+	3.06	2.46	20.84	68.75	0.36	0.05	0.13	4.23

4.9.2.   Polymer additives

Polyalkyl glycol (PAG)

The two polyalkyl glycols used in the studies presented within this thesis were supplied by Schlumberger Cambridge Research and had the trade names

DCP101 and BREOX 50 A 140. These were assumed to be random co-polymers (unknown sequencing) of ethylene and propylene oxide (figure 4.9.2a) in a 50:50 ratio, DCP101 having a molecular weight of ~ 600 gmol^{-1} and BREOX 50 A 140, a molecular weight 1700 gmol^{-1}.

Figure 4.9.2a Structural units of PAG

HO $\mathrm{-\!\!\!+\!\!CH_2-\!\!CH_2-\!\!O\!\!+\!\!\!}_n$ HO $\mathrm{-\!\!\!+\!\!CH(CH_3)-\!\!CH_2-\!\!O\!\!+\!\!\!}_n$
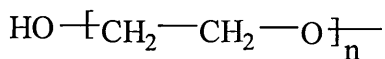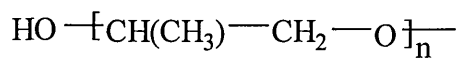
Polyethylene oxide   Polypropylene oxide

Polyacrylamide (PAM)

Polyacrylamide samples were supplied by Allied Colloids with a range of molecular weights between 1×10^5 and 15×10^6 gmol^{-1}. The structure of PAM is shown in figure 4.9.2b.

Figure 4.9.2b Structural units of PAM and HPAM (PAM and PAA)

$\mathrm{-\!\!\!+\!\!CH_2-\!\!CH\!\!+\!\!\!}_n$ $\mathrm{-\!\!\!+\!\!CH_2-\!\!CH\!\!+\!\!\!}_n$

C   C
O   NH$_2$ O   OH
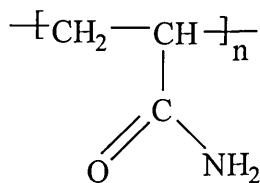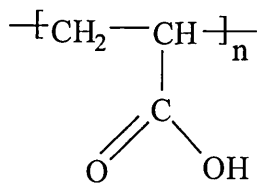
Polyacrylamide   Polyacrylic acid

Partially hydrolysed polyacrylamide (HPAM)

This too, was supplied by Allied Colloids with a molecular weight of 1×10^6 gmol^{-1} and an anionic content of 10.64 mmolg^{-1}. The structural components of HPAM are shown in figure 4.9.2c, the degree of hydrolysis being determined by the proportion of polyacrylic acid in the polymer molecule.

5.   BENTONITE HYDRATION PROCESSES

5.1.   Introduction

One of the principal aims of this PhD project was the *in-situ* determination of polymer adsorption from aqueous solution onto montmorillonite, using the FTIR-ATR spectroscopic technique. As a result, it was necessary to deposit thin layers of bentonite onto the sampling surface of an ATR prism, i.e. onto silicon and zinc selenide substrates, by the evaporation of water from an aqueous mineral suspension. These clay mineral dehydration processes have been monitored using several infrared techniques.

5.2.   Experimental

5.2.1.   Materials

SWy-1 bentonite was purified by sedimentation to obtain the $<2\mu m$ fraction and used in its natural state, i.e. without cation exchange. Aqueous bentonite suspensions were prepared by dispersing the bentonite in deionised water and allowing to 'age' by stirring for 12 hours.

In addition, homoionic Li-, Na-, K- and Ca-Greenbond bentonites were used in the preparation of aqueous homoionic bentonite suspensions. Deuterated bentonite was prepared by dispersing 3g of SWy-1 bentonite in 50 cm^3 of D$_2$O (Aldrich Chemical Co., 99.9% purity) and stirring under a sealed atmosphere of dry nitrogen for 7 days.

5.2.2. Spectroscopy

5.2.2.1. Transmission-KBr disks

KBr pellets containing bentonite were prepared as outlined in chapter 4.2.6 and their infrared spectra obtained in one of two ways:

1. In a normal transmission experiment, clamped in a 13 mm transmission cell holder and placed in a Mattson Polaris FTIR spectrometer.

2. Using an infrared microscope, by locating a mineral aggregate in a suitable area (50x50 μm) using a 16x or 32x microscope objective lens and obtaining transmission spectra on a Nicolet 800 FTIR spectrometer.

KBr disks containing montmorillonite were heated in a Graseby Specac heated transmission cell. The cell was allowed to reach thermal equilibrium at the appropriate temperature for 15 minutes prior to spectral acquisition on a Mattson Polaris FTIR spectrometer.

5.2.2.2. Transmission-dehydrating films

Bentonite films were deposited by pipetting a small drop of 20 gdm^{-3} SWy-1 aqueous bentonite suspension on the substrate (either Si or ZnSe) and allowing it to dry naturally in the dry air purge of the spectrometer. Film dehydration was monitored using an infrared microscope, by locating a suitable area (100x100 μm) using a 16x microscope objective lens. Transmission spectra were then obtained on a Nicolet 800 FTIR spectrometer at 5 minute intervals.

5.2.2.3. ATR spectroscopy

ATR spectra were obtained in one of two accessories:

1. Using a Spectra Tech horizontal ATR accessory fitted with a 70° zinc selenide ATR crystal. A 60 gdm^{-3} SWy-1 aqueous bentonite suspension was deposited on the ATR crystal then spectra collected, every 7.2 minutes, on a Nicolet 800 FTIR spectrometer.

2. ATR spectra of a dehydrating 20 gdm^{-3} bentonite suspension were obtained using the Graseby Specac Squarecol cell fitted with the 45° zinc selenide ATR prism as described in chapter 4.3.4. Spectra were collected every 5 minutes on a Mattson Polaris FTIR spectrometer.

TE and TM polarised ATR spectra were obtained by means of placing a Spectra tech wire grid polariser in front of the Graseby Specac Squarecol cell fitted with the zinc selenide ATR prism. The unpolarised spectrum was obtained first then the TM and TE spectra obtained successively. Each individual spectrum required 256 scans so, took 130 seconds to acquire. Hence, the TM polarised spectrum was acquired 140 seconds after the unpolarised spectrum and the TE polarised spectrum was acquired 300 seconds after the unpolarised spectrum (allowing for insertion of the polariser). To ensure significant water loss was not incurred during acquisition of the spectra the cell was fitted with the lid provided.

5.2.2.4 Instrumentation

Table 5.2.2.4a lists the instrumental parameters used for recording the spectra in transmission and ATR on the Mattson Polaris infrared spectrometer. Approximately the same parameters were set for recording the transmission

spectra or the ATR spectra on the Mattson Polaris and Nicolet 800 spectrometers. Where a different parameter was used on the Nicolet 800 this appears in brackets in table 5.2.2.4a.

Table 5.2.2.4a Instrumental parameters

Parameters	Transmission	ATR
Resolution	4 cm^{-1}	4 cm^{-1}
Number of scans	100 (126)	256 or 512
Apodisation	triangular	triangular
Detector	MCT	MCT
Beamsplitter	KBr	KBr

5.3.   Results and Discussion

5.3.1.   Transmission spectra of dried bentonite powder

Figure 5.3.1a shows a typical spectrum of dry powdered bentonite dispersed in a thin potassium bromide disk, obtained in a normal (macroscopic) transmission experiment, and ratioed against an air background.

Table 5.3.1 gives the band assignments of the principal bands in the infrared spectrum, based on the assignments by Farmer [182], Farmer and Russell [197], Bukka et al [25] and van Olphen and Fripiat [26].

## Figure 5.3.1a Transmission spectrum of dry bentonite powder in KBr disk
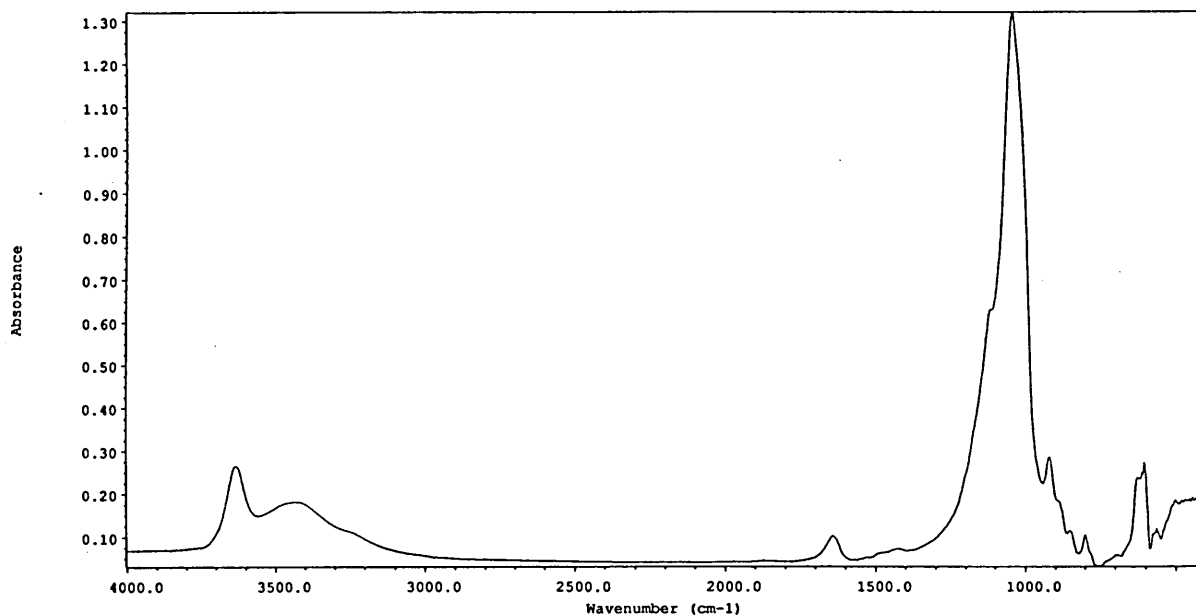
Table 5.3.1. Band assignments for bentonite powder

Band position (cm^{-1})	Assignment
3634	structural O-H stretch
3433	H-bonded O-H stretch
3250	overtone of H-O-H bending mode
1635	H-O-H bending mode
1122	Si-O stretch
1048	Si-O stretch
918	OH deformation (linked to $2Al^{3+}$)
889	OH deformation (linked to Al^{3+}, Fe^{3+})
853	OH deformation (linked to Al^{3+}, Mg^{2+})
795	OH deformation (linked to Mg^{2+}, Fe^{3+})

In addition, small bands are noticeable at 1987 and 1861 cm^{-1}. These bands may be due to quartz impurities in the clay mineral sample, since overtone/combination bands of silicate minerals such as quartz are commonly observed in this region [226]. However, these two bands are also particularly well developed in the diffuse reflectance spectra of montmorillonite [226] and hence may be attributed to overtone/combination bands of the main silicate stretching band.

The intensity of the O-H stretching bands in three transmission spectra obtained from a single KBr disk by infrared microscopy show little variation. Indeed, the absorbance ratio A(3630)/A(3436) varies between only between 1.56 and 1.47. Commonly, the bentonite powder was dispersed in the KBr disk as small aggregates, ranging in size between 150x200 μm and 10x15 μm. Generally, the aggregates appeared as flattened features on the surface of the disk and consequently could be focused easily. However, by focusing on the surface of the pellet above an aggregate which was completely enveloped in the KBr matrix, then raising the sample stage towards the objective lens, it was possible to examine aggregates dispersed inside the volume of the disk. No difference was observed in the infrared spectrum of the surface and bulk bentonite aggregates dispersed in the KBr disks (figure 5.3.1b).

In contrast, however, there are large variations (between 1.8 and 0.84) in the absorbance ratio A(3630)/A(3436) in three normal (macroscopic) infrared transmission spectra obtained from three different KBr disks containing varying concentrations of bentonite powder (figure 5.3.1c). This suggests some variation in either the bentonite water content of different KBr disks prepared from the same stock powder, or variations in the water content of the dried KBr powder used to prepare the disks.

Figure 5.3.1b Comparison of transmission (microscopic) spectra of dry bentonite aggregates of varying size dispersed in the same KBr disk.
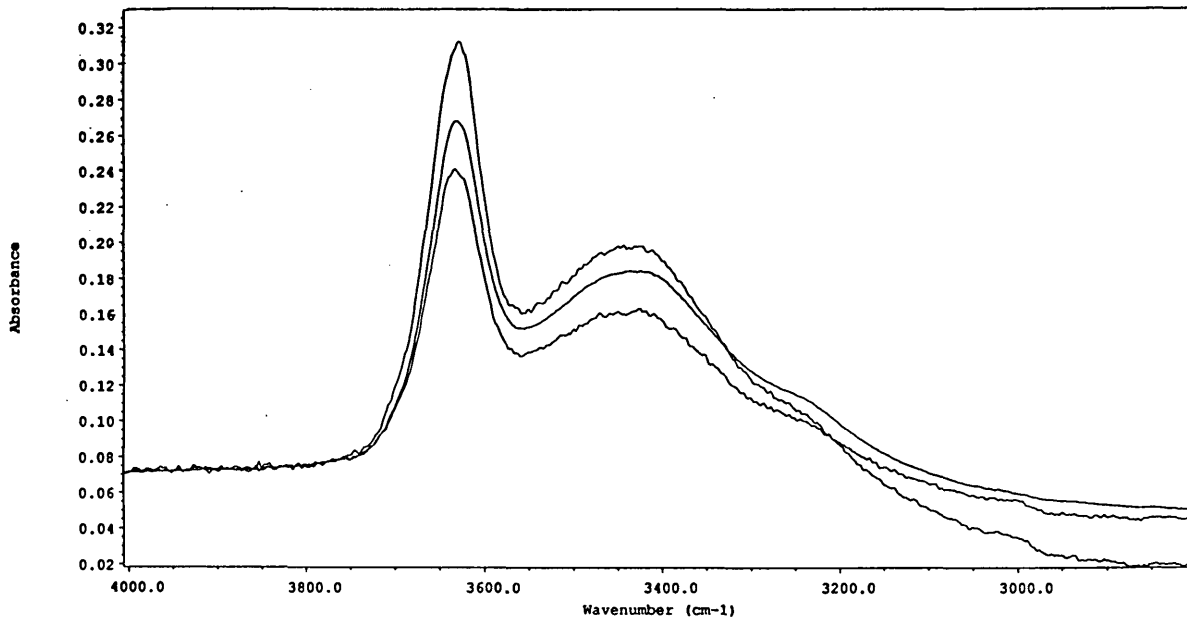

Figure 5.3.1c Comparison of transmission (macroscopic) spectra of dry bentonite powder dispersed in three KBr disks of varying concentrations.
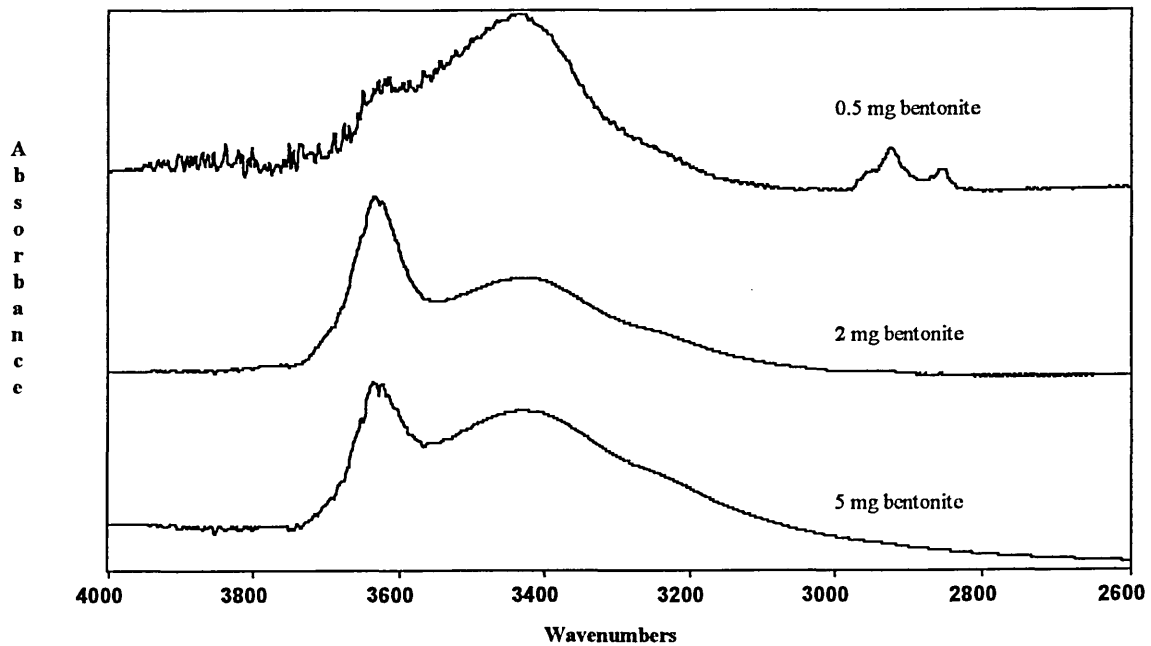
5.3.2. Transmission spectra of heated bentonite powder

Figure 5.3.2a shows the infrared spectrum of dry bentonite powder dispersed in a KBr disk in the region between 1300 and 850 cm^{-1} (the Si-O stretching region) at room temperature.

Figure 5.3.2a Transmission spectrum of dry bentonite powder in KBr disk at room temperature.
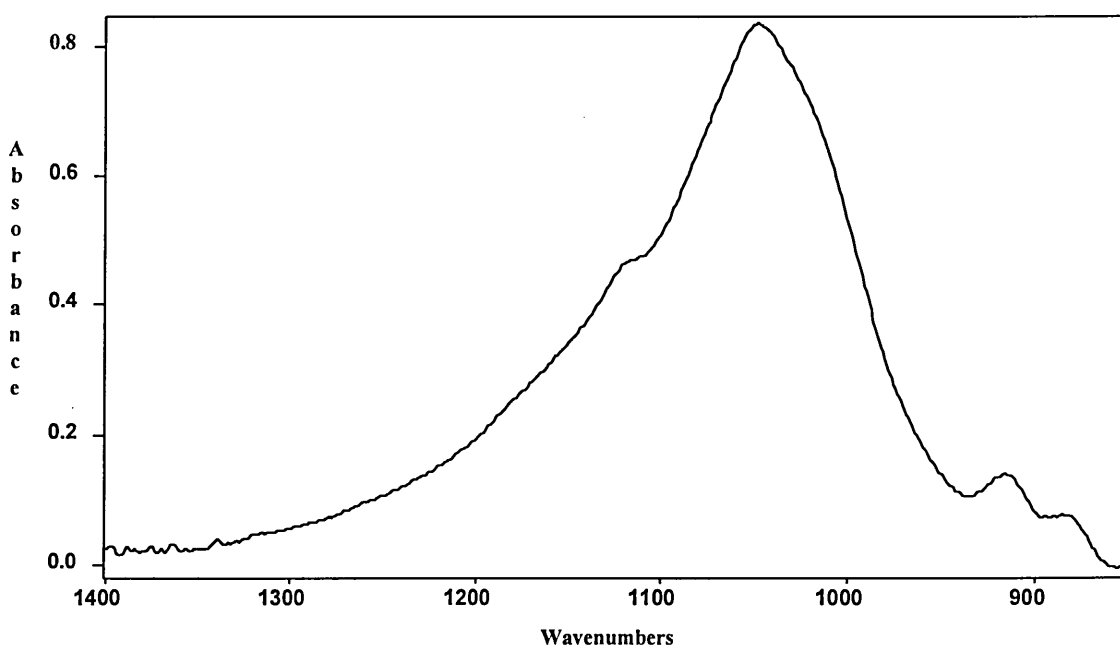
There are several overlapping absorption bands in the silicate stretching ν(Si-O) region between 1400 and 850 cm^{-1} [43, 45, 197]. These may be resolved into their individual lineshapes in order to determine individual peak positions, bandwidths and integrated intensities.

Fourier self deconvolution of the spectrum of bentonite powder in the region between 1400 and 850 cm^{-1} (figure 5.3.2a) was performed using the parameters outlined in table 5.3.2a. The results of the Fourier self deconvolution are shown

in figure 5.3.2b. In addition, the second derivative spectrum of bentonite powder in figure 5.3.2a is shown in figure 5.3.2c.

Table 5.3.2a Parameters used for Fourier self deconvolution of figure 5.3.2a

Spectrum	Enhancement factor, κ	Linewidth, γ (cm^{-1})	Apodisation function D(x)
Figure 5.3.2a	1.76	40	Bessel

With the information from Fourier self deconvolution and second derivative spectroscopy it is possible to fit curves to this region of the spectrum to give a synthetic spectrum (figure 5.3.2d).

Figure 5.3.2b Fourier self deconvoluted spectrum of dry bentonite powder in KBr disk in the region 1400-850 cm^{-1}, at room temperature.
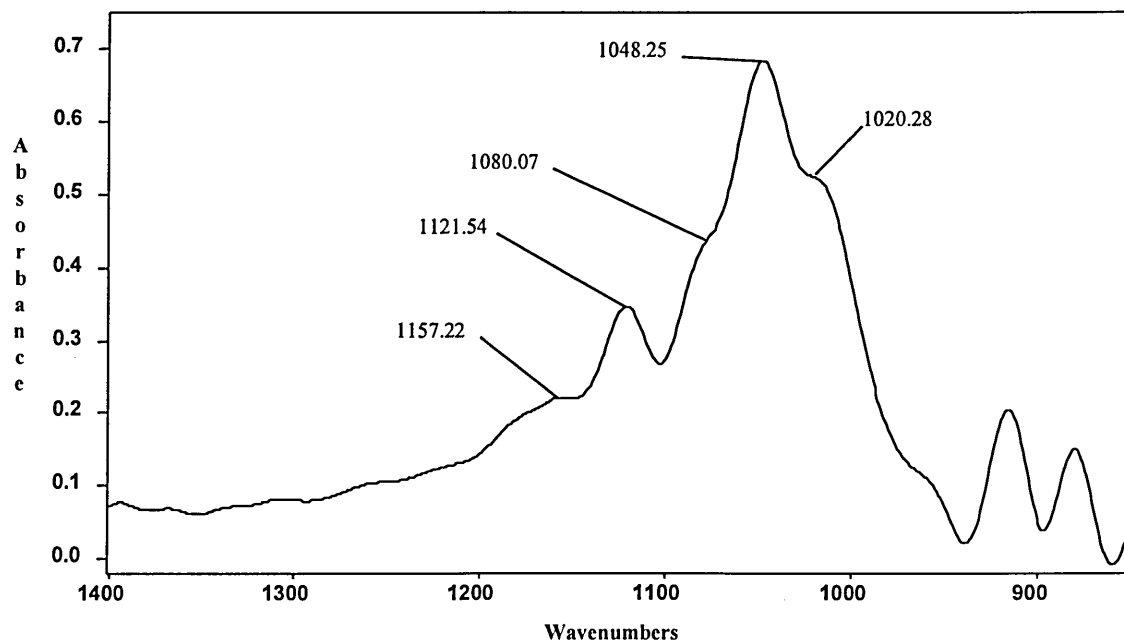
Figure 5.3.2c Second derivative spectrum of dry bentonite powder in KBr disk, at room temperature.

Figure 5.3.2c Second derivative spectrum of dry bentonite powder in KBr disk, at room temperature.

## Figure 5.3.2d Synthetic spectrum and component bands of dry bentonite powder in KBr, at room temperature.
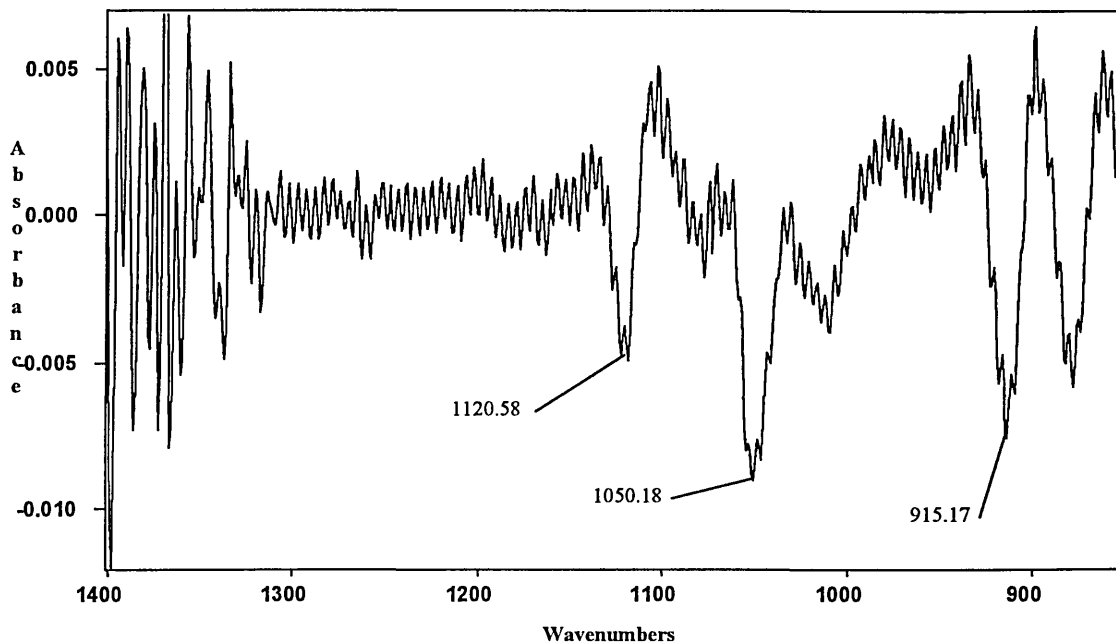
Figure 5.3.2d Synthetic spectrum and component bands of dry bentonite powder in KBr, at room temperature.
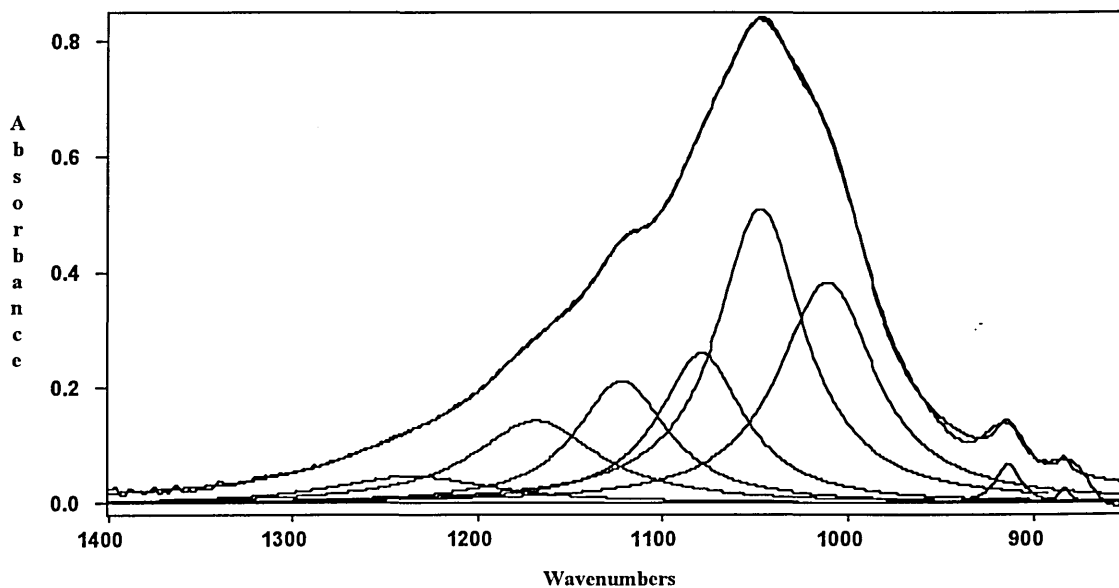
Table 5.3.2b summarises the main Si-O band positions in the spectrum of bentonite at room temperature, observed by Fourier self deconvolution, second derivative spectroscopy and curve fitting procedures

Table 5.3.2b Summary of the main Si-O band positions in the spectrum of bentonite at room temperature.

	Main Si-O band positions (cm^{-1})			
Figure 5.3.2b (FSD)	1121	1080	1048	1020
Figure 5.3.2c (SD)	1120	1078*	1050	1017*
Figure 5.3.2d (CF)	1122	1079	1047	1011

* These bands are very broad and heavily masked by noise in the second derivative spectrum, consequently, their position my not be entirely accurate.

Figure 5.3.2d and table 5.3.2b display all the component Si-O stretching bands of the broad, intense band (in the region between 1400 and 850 cm^{-1}) in the infrared spectrum of montmorillonite at room temperature. The position of these bands is in good agreement with the peak positions observed in oriented films by Farmer and Russell [197] and Lerot and Low [43]. They are also in good agreement with the band positions observed by Yan et al [45] over a range of water contents of montmorillonite gels, who described them in order of increasing wavenumber position as Peak I, Peak II, Peak III and Peak IV.

The remaining bands at 914 and 884 cm^{-1} are OH deformation bands and are incorporated to complete the curve fit. In addition, fitted bands at 1235 and 1168 cm^{-1} can be clearly seen in the Fourier self deconvoluted spectrum and are necessary to satisfy the fit criterion. However, their origin is unknown since no reference to such bands in this region has been made in the published literature. A further unassigned band at ~960 cm^{-1} can be observed in the FSD and SD spectra of montmorillonite in this region but does not improve the fit criterion, so was not included in the fitted spectrum. This may account for the discrepancy between the position of the curve fitted band at 1010 cm^{-1} and the position of

the band as determined by Fourier self deconvolution and second derivative

spectroscopy.

Figure 5.3.2e shows the infrared spectrum of dry bentonite powder dispersed in

a KBr disk in the region between 1400 and 850 cm^{-1} (the Si-O stretching

region) at 200°C.

Figure 5.3.2e Transmission spectrum of dry bentonite powder in KBr disk

at 200°C.
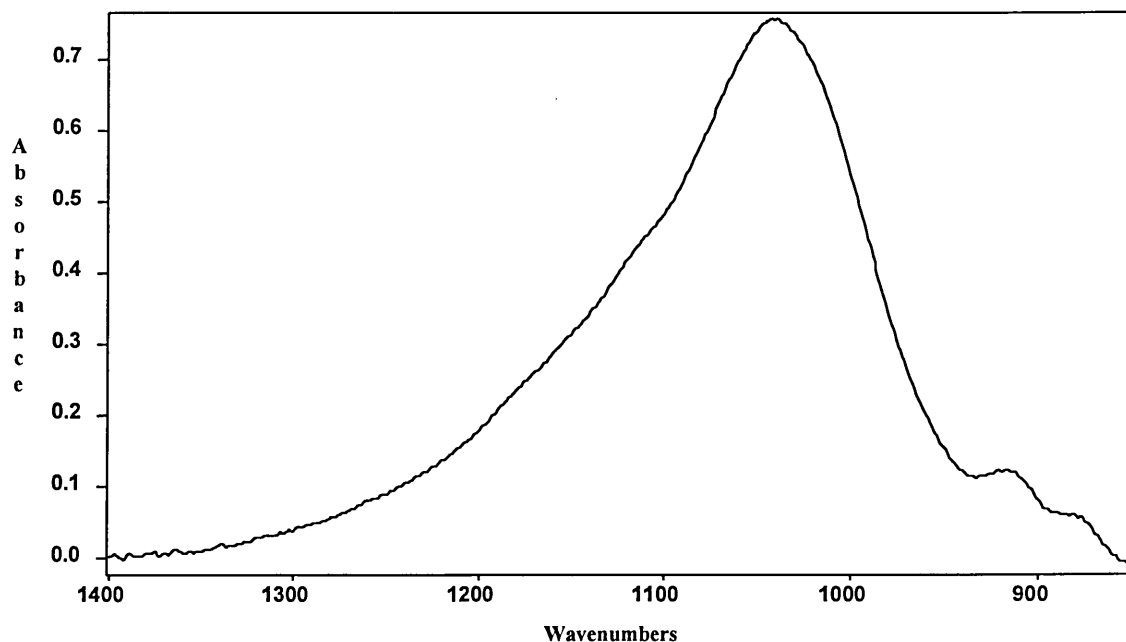
Fourier self deconvolution (performed using the same parameters outlined in

table 5.3.2a) and second derivative spectra of figure 5.3.2e are shown in figures

5.3.2f and 5.3.2g respectively. With the information from Fourier self

deconvolution and second derivative spectroscopy it is possible to fit curves to

this region of the spectrum to give a synthetic spectrum (figure 5.3.2h).

Figure 5.3.2f Fourier self deconvoluted spectrum of dry bentonite powder in KBr disk, at 200°C.
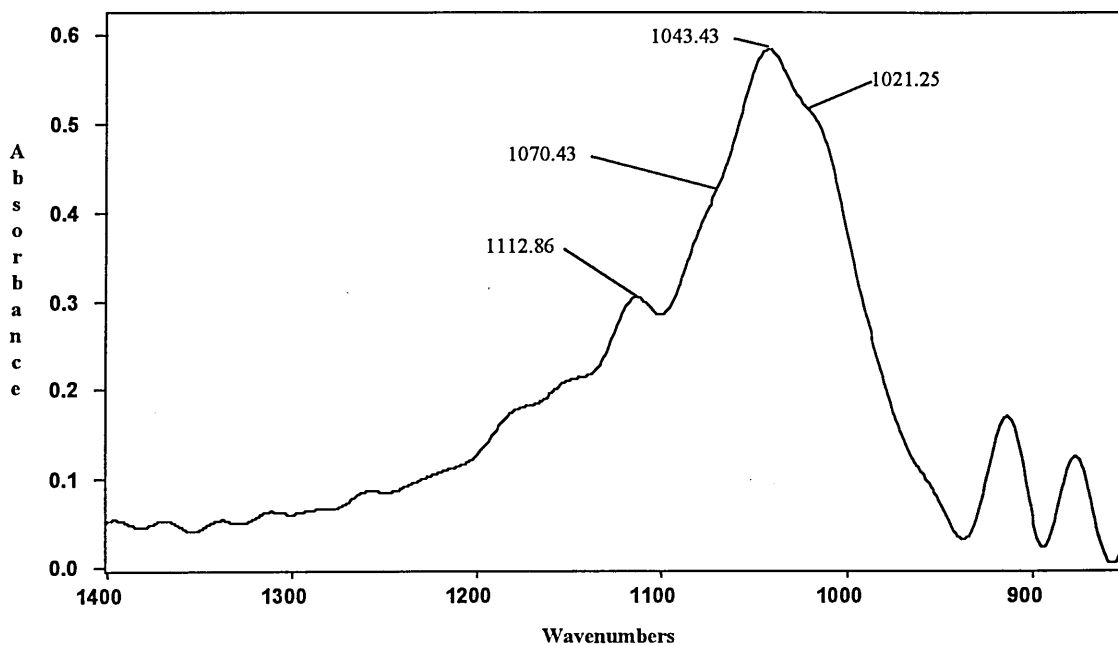

Figure 5.3.2g Second derivative spectrum of dry bentonite powder in KBr disk, at 200°C.
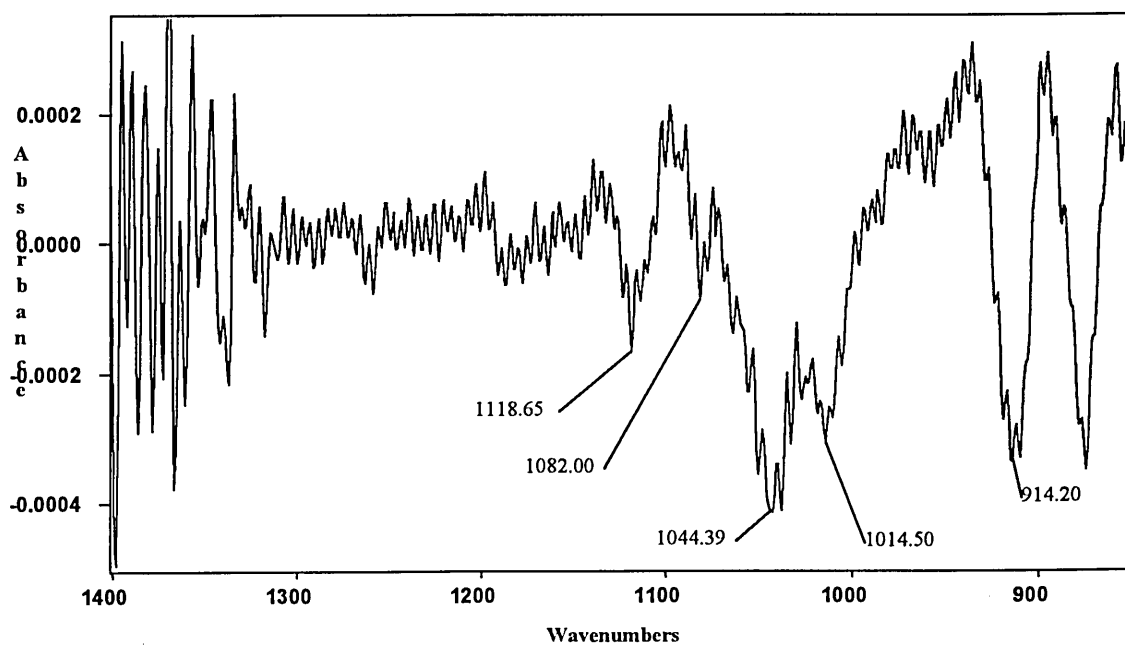
Figure 5.3.2h Synthetic spectrum and component bands of dry bentonite powder in KBr disk, at 200°C.
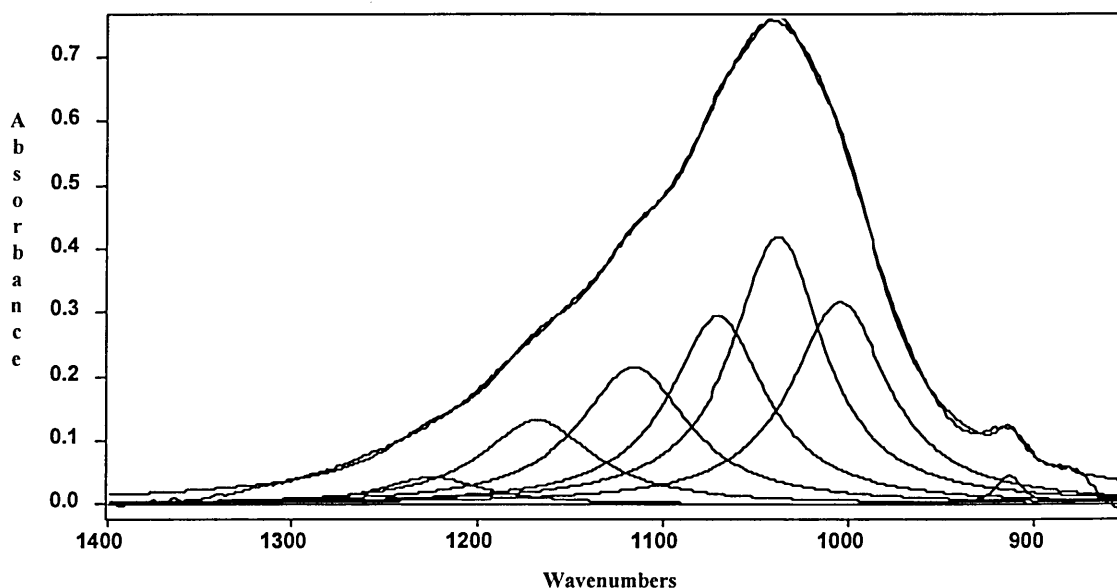
Table 5.3.2c summarises the main Si-O band positions in the spectrum of bentonite at 200°C, observed by Fourier self deconvolution, second derivative spectroscopy and curve fitting procedures

Table 5.3.2c Summary of the main Si-O band positions in the spectrum of bentonite at 200 °C, observed by Fourier self deconvolution, second derivative spectroscopy and curve fitting procedures.

	Main Si-O band positions (cm^{-1})			
Figure 5.3.2f (FSD)	1112	1070	1043	1021
Figure 5.3.2g (SD)	1118	1082*	1044	1014*
Figure 5.3.2h (CF)	1115	1070	1038	1004

* These bands are very broad and heavily masked by noise in the second derivative spectrum, consequently, their position my not be entirely accurate. Again, the bands at 1235, 1167, 913 and 882 cm^{-1} minimise the fit criterion, but the band visible at 960 cm^{-1} does not and hence is not incorporated in the curve

fit. The omission of this band from the curve fit may account for the discrepancy between the peak positions of the fitted peaks and those extracted by FSD and SD.

The effect of heat on the main intense band in the silicate stretching region is shown in figure 5.3.2i. It can be seen that the peak of the main band appears to shift to lower frequency. Evidently, many of the bands in this region experience a shift in wavenumber position; this has been quantitatively established using the results of second derivative spectroscopy, Fourier self deconvolution and curve fitting. This is in good agreement with the findings of Yan et al [45] who observed a shift to low frequency of $v(Si-O)$ on decreasing the water content (M_W/M_C) of montmorillonite gels.

Figure 5.3.2i Transmission spectra of bentonite powder with increasing temperature. Spectra are offset to zero and overlaid.
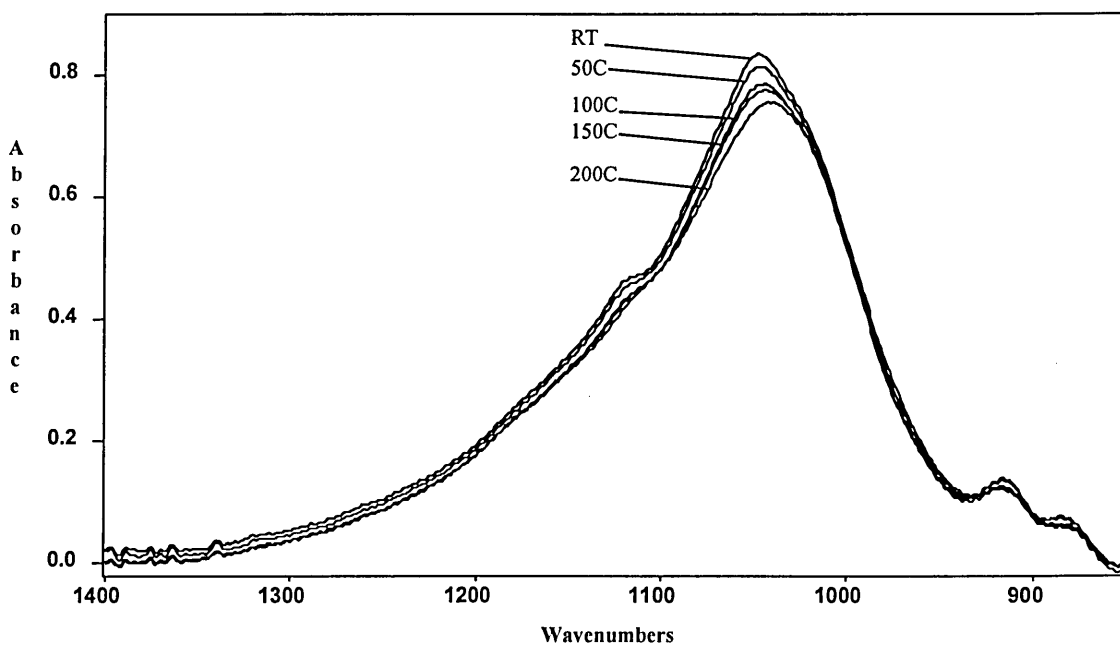
The most significant band shift observed is the 11 cm^{-1} shift of the band at 1081 cm^{-1} at room temperature, to 1070 cm^{-1} at 200°C. This is clearly shown in

Graph 5.3.2a where a constant gradual shift to lower frequency is observed with 10°C increases in temperature.

In addition, the Si-O stretching bands at 1047 cm^{-1} and 1011 cm^{-1}, in the spectrum of bentonite at room temperature, are both observed to shift (by ~6 or 7 cm^{-1}) to lower frequency in the spectrum of bentonite heated to 200°C. Like the band shift from 1081 cm^{-1} to 1070 cm^{-1}, the shift from 1047 and 1011 cm^{-1} to lower frequency is constant and gradual. However, it should be noted that the absorbance ratio A(1047)/A(1011) remains at an approximately constant value of 1.20 (±0.1) over the entire temperature range (Graph 5.3.2b).

Graph 5.3.2a Wavenumber position variation of Si-O stretching band at 1080 cm^{-1}, with increasing temperature.
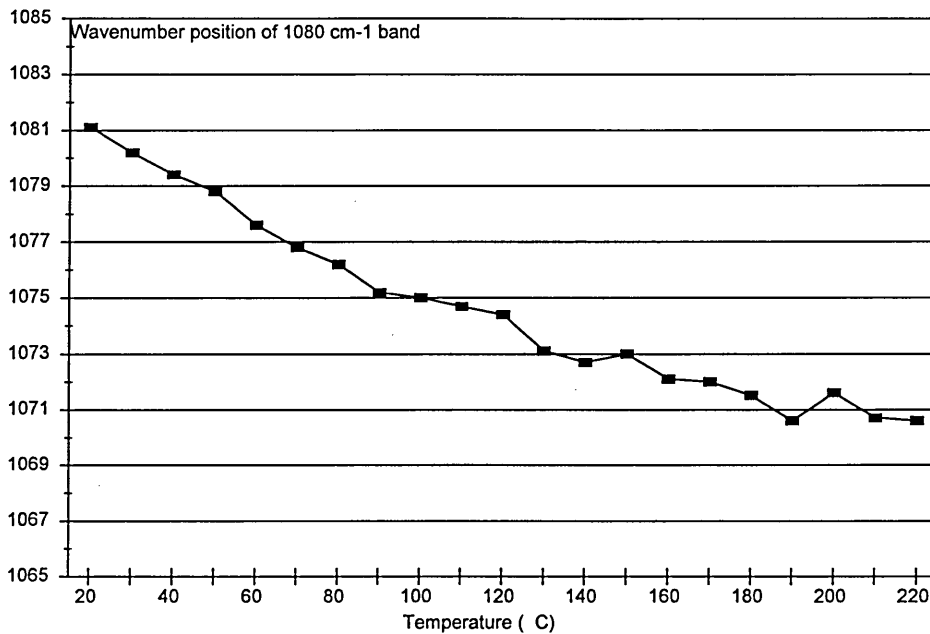
Graph 5.3.2b Variation of the absorbance ratio A(1047)/A(1011) with increasing temperature.
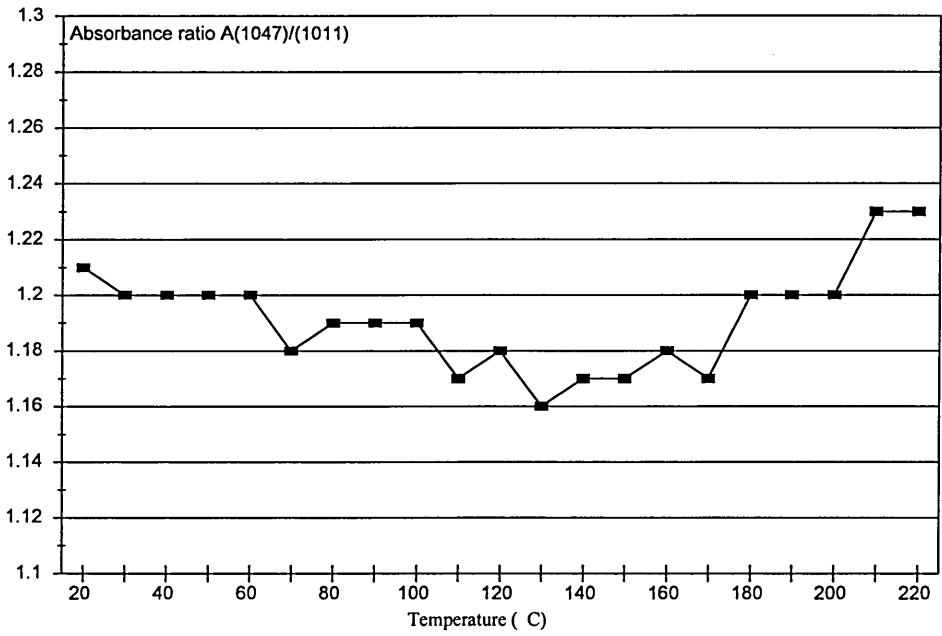
In contrast however, the absorbance ratio A(1047)/A(1080) decreases from 2.00 to 1.34 over the temperature range (Graph 5.3.2c).

Graph 5.3.2c Variation of the absorbance ratio A(1047)/A(1080) with increasing temperature.
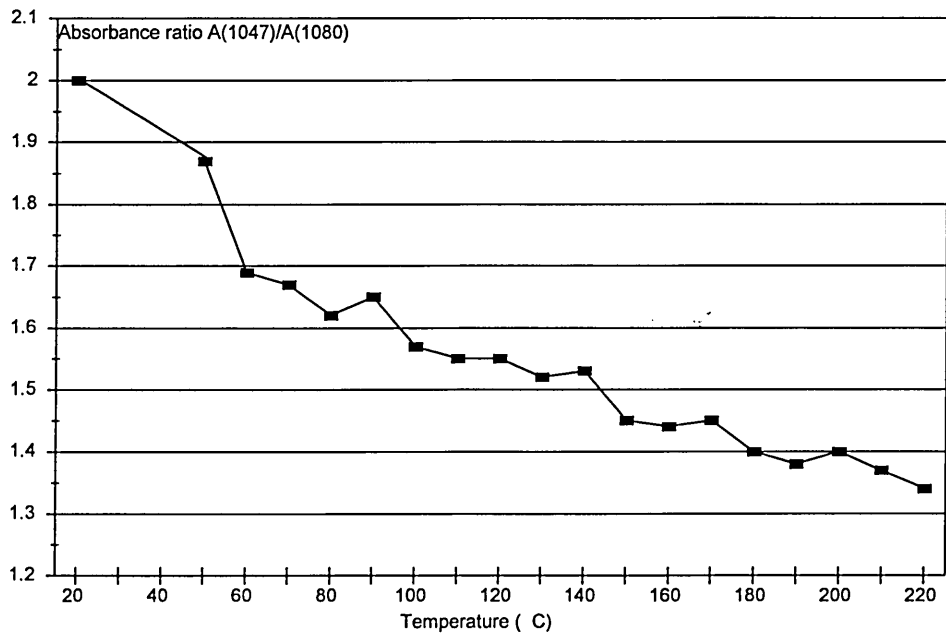
The major variation in the absorbance ratio A(1047)/A(1080) is at low temperature (below 100°C). This may then be related to the removal of physisorbed water from the clay mineral (and from the hygroscopic KBr). The 1080 cm^{-1} band which has been found to shift to lower wavenumber with increasing temperature has been attributed to a vibration perpendicular to the platelet surface.

Variations in the relative intensity of this band have been attributed to changes in the clay platelet orientation, relative to the infrared radiation [43, 227]. In the experiment presented here however, the bentonite platelets within the KBr disk exist as randomly oriented aggregates. As a result, it seems highly unlikely that the reduction in intensity of the band at 1080 cm^{-1} relative to the bands at 1047 and 1011 cm^{-1} is due to a change in orientation of the clay platelets; a more plausible explanation would be the removal of physisorbed water from the montmorillonite as it is heated.

Obviously, the heating of dry bentonite samples to high temperatures in this way will remove water which exists on external faces and in the interlayer region of the montmorillonite platelets. Evidence of water removal is apparent in figure 5.3.2j, in which the spectrum of bentonite in the region between 4000 and 2800 cm^{-1} is shown at room temperature, 50°C, 100°C, 150°C and 200°C.

Figure 5.3.2j Transmission spectra of bentonite powder with increasing temperature.
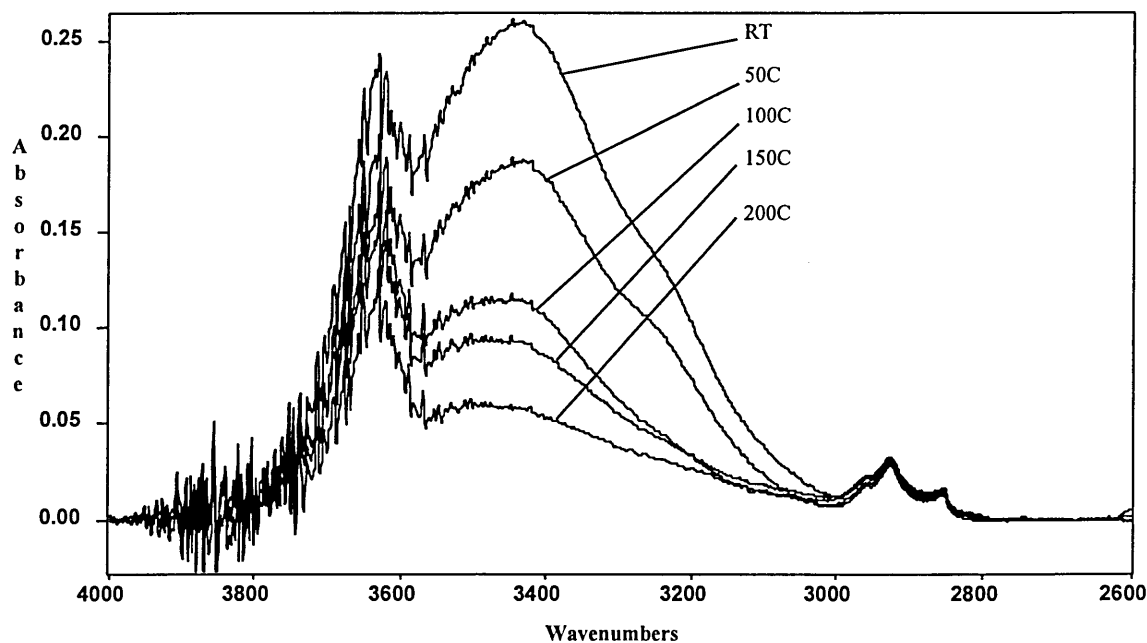
Clearly, there is a reduction in the intensity of the bands at 3434 and 3250 cm^{-1}, signifying a reduction in the H-bonded water with increasing temperature. It should be noted though, that not all the water associated with the montmorillonite is removed.

In addition, the band at 3634 cm^{-1} (assigned to structural OH) also appears to decrease in intensity as temperature increases. Partial decomposition of the structural OH group is highly unlikely since this should not occur until the temperature approaches 800°C. More plausible explanations are:

1. The interaction of structural OH groups with species in the di-trigonal cavity, namely the exchangeable cations. As physisorbed and chemisorbed water is removed from the interlayer so the cations become less solvated and the platelets are able to approach each other more closely. As a result, interlayer cations of the correct dimensions are able to settle into the di-trigonal cavities of

the silicate layer of the clay platelet surface [40, 133]. The electric field of the exchange cation would then exert a repulsive force on the proton of the M-OH bond at the base of the di-trigonal cavity (figure 2.6.1.1). Consequently, the infrared intensity at 3630 cm^{-1} (attributed to the structural OH stretching mode) might be reduced when the exchange cation sits in the di-trigonal cavity. Our result is consistent with those of Sposito et al [40] who noted the increase in the intensity of the bands due to M-OH bending modes (at 916 and 883 cm^{-1}), on increasing water content. This was attributed to the solvation of the exchange cation, and hence, its removal from the di-trigonal cavity into the interlayer space, thus removing the repulsive force on the proton of the structural M-OH at the base of the di-trigonal cavity. Indeed, decreases in the band intensity at 916 and 883 cm^{-1} (due to AlAl- and AlFe-OH vibrations respectively) relative to the main, intense Si-O band have been observed on heating to 200°C in these experiments. This is also consistent with the findings of Malek et al [42] who showed that the dehydration of exchange cations in montmorillonite terminates at 200°C. It was determined that at this temperature, exchange cations migrate into hexagonal holes in the silicate layer surface and the clay collapses, denoted by the reduction in the basal spacing.

2. The reduction in intensity of the band at 3634 cm^{-1} may also be an artefact in the spectrum. This could arise from the intensity reduction of the bands associated with various H-bonded water species [34] which also contributed to the intensity of the band at 3630 cm^{-1}. Unfortunately, due to the highly complex pattern of absorption bands in this region (reflecting the highly complex arrangement of water molecules in the interlayer space) it is impossible to perform accurate Fourier self deconvolution, second derivative spectroscopy and curve fitting. Hence, it is impossible to extract quantitative information from this region and interpret changes of intensity with any degree of accuracy.

5.3.3. Transmission spectra of deposited bentonite films

Figure 5.3.3a shows the spectral region between 1400 and 850 cm^{-1} (in the region of the silicate stretching bands) during the evaporation of water from a 20 gdm^{-3} aqueous bentonite suspension, to form a thin bentonite film on a silicon wafer.

Figure 5.3.3a Evolution of transmission spectra of bentonite film formation on a silicon substrate, by the evaporation of water.
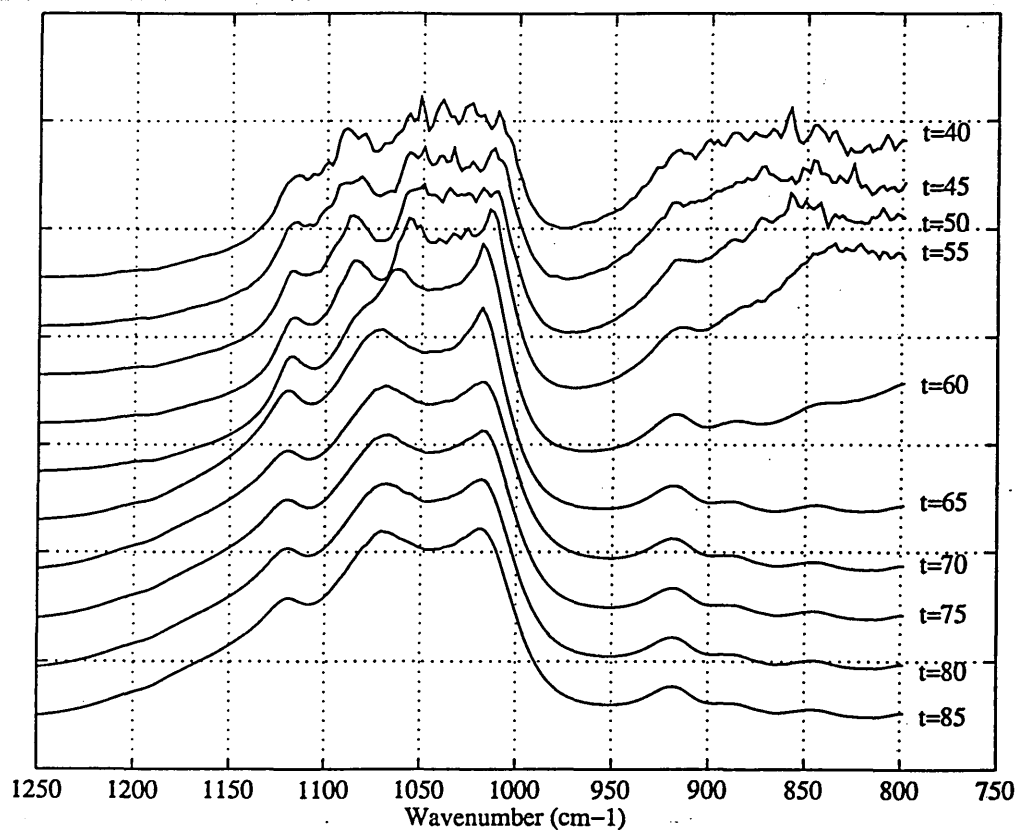
The initial spectra, acquired between t=0 min and t=50 mins, exhibit very large values of absorbance due to the high water content which raises the local baseline below 1000 cm^{-1}. The main silicate stretching band, centred at 1050 cm^{-1} in dry bentonite (figure 5.3.2a), is obscured in figure 5.3.3a due to the high absorbance of the band (>2 absorbance units) and its subsequent cut off which gives the appearance that it is split into two bands. The band at ~1115 cm^{-1} is observed in all of the spectra and is not shifted during the evaporation process

156

although it has been seen to shift very slightly (~2 cm^{-1}) to lower frequency when bentonite is heated to 200°C. This band is considered to be a characteristic of the spectrum of bentonite both in aqueous suspension and in dry powder. As the bentonite suspension is slowly dehydrated in the dry air purge of the spectrometer, the OH deformation band at 919 cm^{-1} becomes visible after 50 mins. By t=60 mins, as the water content of the film is further reduced, the OH deformation band at 853 cm^{-1} also becomes visible. In addition, between t=50 and t=60 mins, as the overall intensity of the main silicate band is reduced by water evaporation, a transient band at 1086 cm^{-1} becomes visible.

By t=55 mins this band has reduced in intensity and shifted to 1080 cm^{-1} where, by t=60 mins it has merged with the main, intense silicate stretching band. The final position of the band at 1080 cm^{-1} corresponds to the band at 1081 cm^{-1} which may be observed by means of Fourier self deconvolution, second derivative spectroscopy and curve fitting in the transmission spectrum of dry bentonite powder dispersed in a KBr disk at room temperature. This band has been seen to shift to much lower frequency (1070 cm^{-1}) as the montmorillonite is heated to 200°C to remove further water of hydration.

The observed reduction in intensity of the transient band relative to the main Si-O peak may be due to the removal of physisorbed water, as postulated previously for a similar change in relative intensity in the transmission spectrum of a heated KBr disk containing montmorillonite. However, in this case, orientation effects cannot be discounted and the reduction in intensity of the band at 1080 cm^{-1} relative to the main Si-O peak may be due to the formation of an oriented film.

Figure 5.3.3b shows the evolution of silicate stretching bands (in the region between 1250 and 850 cm^{-1}) for the dehydration of a bentonite suspension to form a mineral film on a zinc selenide substrate.

Figure 5.3.3b Evolution of transmission spectra of bentonite film formation on a zinc selenide substrate, by the evaporation of water.
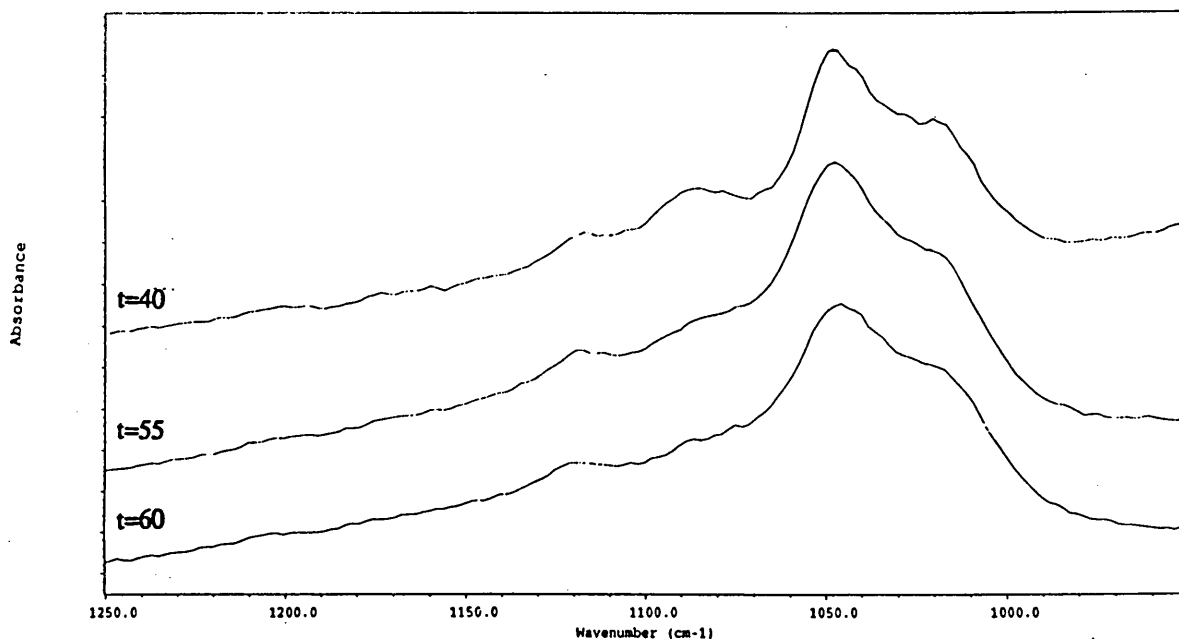
These spectra are almost identical to those seen previously for bentonite film formation on a silicon substrate. They clearly show the transient band at 1086 cm^{-1} and its subsequent reduction in intensity and shift to lower frequency on reducing the water content of the film. The only difference being, that the film thickness which produced spectrum 5.3.3b was less than that which produced figure 5.3.3a. Consequently, the main silicate band in figure 5.3.3b is not cut off as it is in figure 5.3.3a. The difference in film thickness also accounts for the more rapid disappearance of the band at 1086 cm^{-1} in the dehydrating aqueous suspension on the ZnSe substrate. The thicker film (on the Si substrate) required

158

longer to fully dehydrate. This effect is expected due to the arbitrary positioning of the microscope objective lens.

Figure 5.3.3c shows the evolution of the broad OH band (in the spectral region between 4000 and 2600 cm^{-1}) during the drying of the montmorillonite film on a silicon substrate. The early time spectra show the very large absorbance of the bulk water, although the intensity of the band decreases rapidly during the drying. The spectrum after t=60 minutes shows the first appearance of the non-bonded OH band at 3634 cm^{-1}. This corresponds to the time at which the transient band at 1080 cm^{-1} has disappeared into the main, intense silicate band. Further drying of the film reduces the water content until the absorbance ratio A(3634)/A(3434) becomes 1.49, the value obtained for dry bentonite powder.

Figure 5.3.3c Evolution of transmission spectra of bentonite film formation on a silicon substrate, by the evaporation of water.
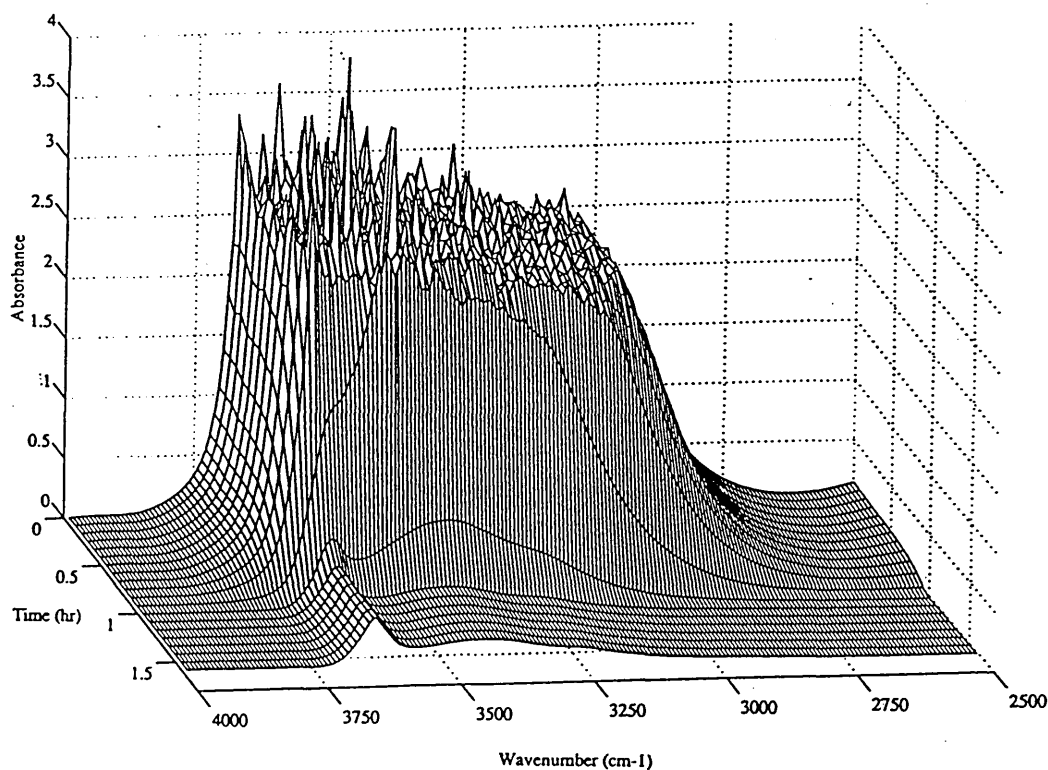
## 5.3.4.   ATR spectra of bentonite suspensions

The ATR spectrum of a bentonite suspension in the silicate stretching region is shown in figure 5.3.4a with the spectrum of water subtracted. In this spectrum, the band which was seen previously at 1086 cm^{-1} in the early time transmission spectra of a dehydrating montmorillonite film is clearly visible. Consequently, the small band at 1086 cm^{-1} appears to be characteristic of bentonite dispersed in water when the water/bentonite ratio is above a certain value. In addition small bands at 1202 and 1150 cm^{-1} can be observed. These may well correspond to the bands at 1234 and 1168 cm^{-1} observed in the curve fitted spectrum of dry bentonite dispersed in a KBr disk (figure 5.3.2d) and whose origin is unknown.

Figure 5.3.4a The ATR spectrum of aqueous bentonite with the spectrum of water subtracted.
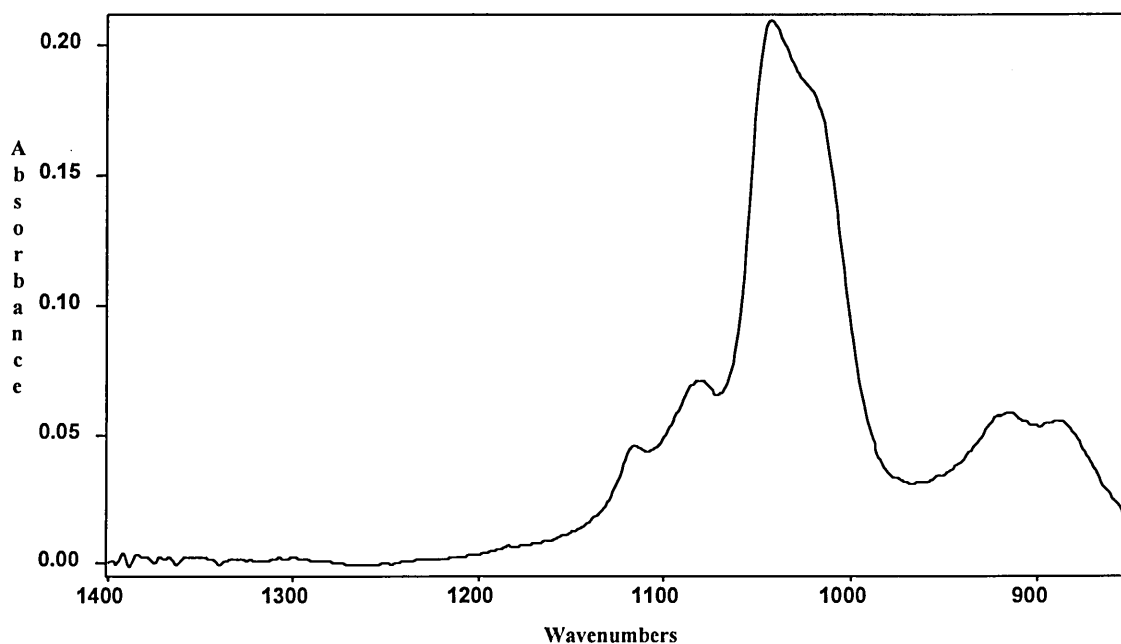
Although Jones et al [228] have discussed the ATR spectrum of bentonite suspensions, the subtle differences between the dry powdered bentonite and

bentonite dispersed in excess water were not observed. Jones et al [228] did, however, discover a time dependence of the intensity of the main Si-O stretching band of a circulating bentonite suspension. The increase in intensity of the band at 1040 cm^{-1} was tentatively ascribed to a decrease in the effective particle size of the bentonite particles caused by the hydration and dispersion forces.

5.3.5. ATR spectra of deposited bentonite films

In the same way that the formation of a deposited montmorillonite film on Si or ZnSe by evaporation of water can be monitored using FTIR microscopy, film formation from an identical suspension can be monitored using FTIR ATR spectroscopy. The advantage of this method is the very small pathlength of sample as determined by the depth of penetration of the evanescent wave. Consequently, the ATR spectrum of an evaporating film shows no cut-off of the Si-O band since only a small amount is sampled in the region of the evanescent field close to the crystal. The intensities of all the bentonite absorption bands increase during the dehydration as bentonite deposits onto the zinc selenide prism within the characteristic penetration depth of the evanescent field.

The depth of penetration of the evanescent field into a bentonite layer of refractive index 1.5, deposited on a 70° zinc selenide horizontal ATR prism with refractive index 2.43, at 1040 cm^{-1}, has been calculated using equation 4.4.2b to be 0.90 μm. The total depth sampled is hence, ~2.7 μm. In contrast, the depth of penetration of the field into a bentonite layer formed adjacent to a ZnSe ATR prism with 45° optics (ZnSe Squarecol prism), at the same wavelength, has been calculated to be 1.87 μm, a total depth sampled of ~5.6 μm.

bentonite increase in intensity whilst the bands due to water disappear as the water content of the film decreases, thus revealing the bands at 916 and 889 cm^{-1} due to M-OH deformation modes.

Figure 5.3.5a Evolution of ATR spectra of bentonite film formation. Early time spectra.
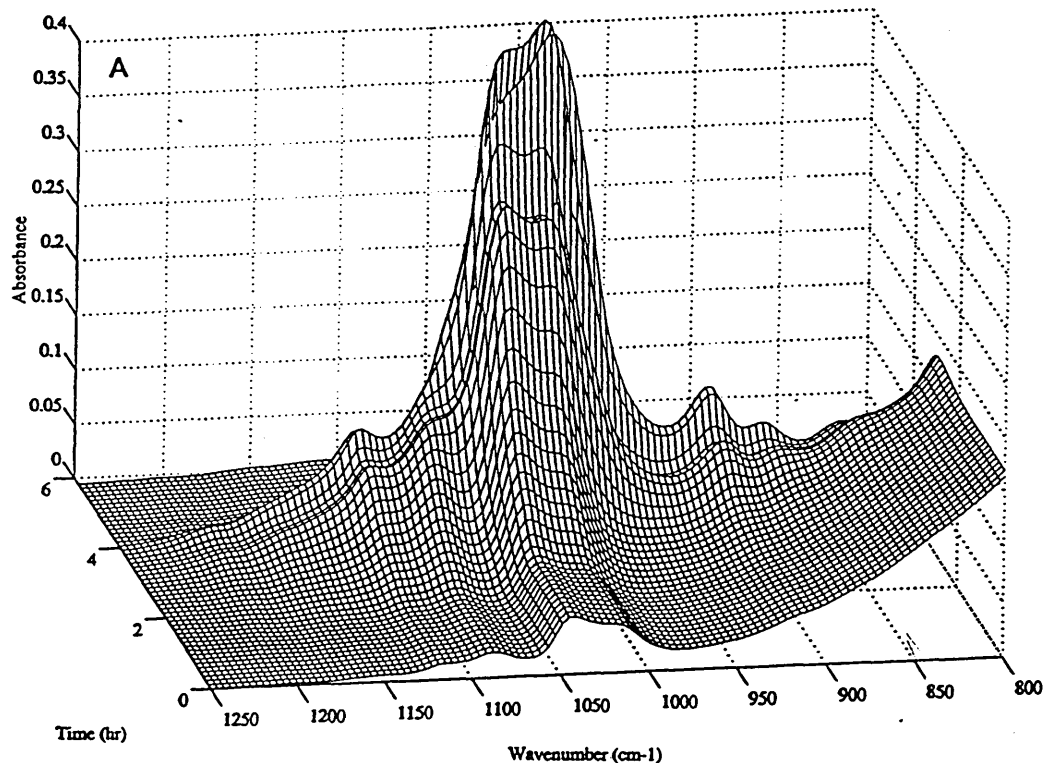
The first significant change in the structure of the silicate bands, is a small shift in the band at 1086 cm^{-1} to lower frequency after 2.26 hours. Over a period of ~35 minutes, the band at 1086 cm^{-1} shifts to 1080 cm^{-1} accompanied by a decrease in intensity. This band completely disappears by t=3.82 hours. It should be noted here that small apparent frequency shifts might result from changes of relative intensity. Concurrently, the band at 1018 cm^{-1} becomes more pronounced and surpasses the intensity of the main Si-O peak at 1044 cm^{-1}. The band at 1044 cm^{-1} in turn becomes a shoulder band to the band at 1018 cm^{-1}. This change in relative intensity of the bands at 1044 and 1018 cm^{-1} is very difficult to explain especially since this band ratio in the transmission spectrum of a KBr disk

containing randomly oriented montmorillonite, remained constant when heated

from room temperature to 200°C. This may be indicative of the formation of an

oriented film or may be an artefact in the spectrum due to detachment of the film

from the ATR crystal.

Figure 5.3.5b shows the later stages of film formation. Above 3.93 hours, the

intensity of all absorption bands can be seen to decrease with time, presumably

due to poor contact between the film and ATR crystal as the film becomes

detached.

Figure 5.3.5b Evolution of ATR spectra of bentonite film formation. Later
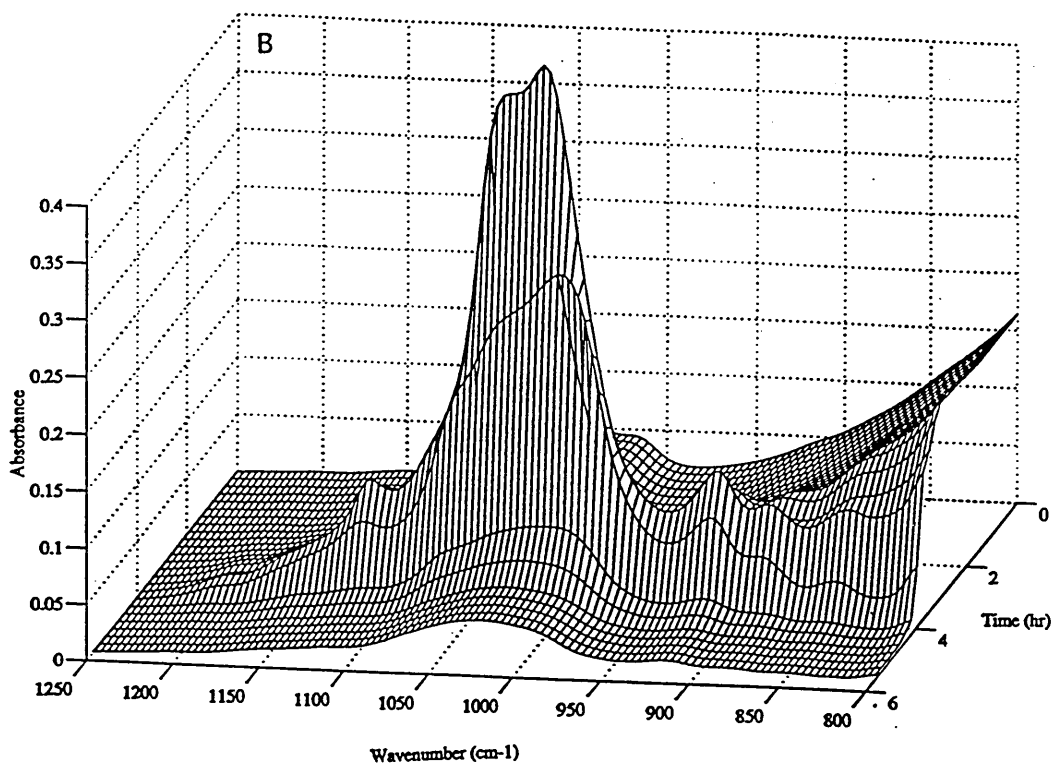
time spectra.

The detachment of the bentonite film from the ATR prism above 3.93 hours can

also be observed in figure 5.3.5c which shows the corresponding evolution of the

OH band in the spectral region 4000 to 2600 cm^{-1} during the formation of the

bentonite film. The film detachment appears to be somewhat more abrupt in this

region than in the silicate stretching region, perhaps because the depth of

penetration at 3630 cm^{-1} is only one third its value at 1040 cm^{-1}. As a result, a

detached film may still be sampled to some extent in the lower frequency range

but not in the higher frequency range. The presence of an air gap between the

prism and the film may account for many artefacts seen in the ATR spectra of

bentonite dried for t>3.93 hours.

It is noteworthy that the appearance of the band at 3634 cm^{-1} due to free

hydroxyl groups in figure 5.3.5c, is gradual, however the appearance of a distinct

peak after t=3.92 hours corresponds approximately to the disappearance of the

transient silicate band at 1086 cm^{-1}. This may indicate that the band at 1086

cm^{-1} is attributed to the reduction of the water/clay ratio below a critical value.

Figure 5.3.5c Evolution of ATR spectra of bentonite film formation. Later
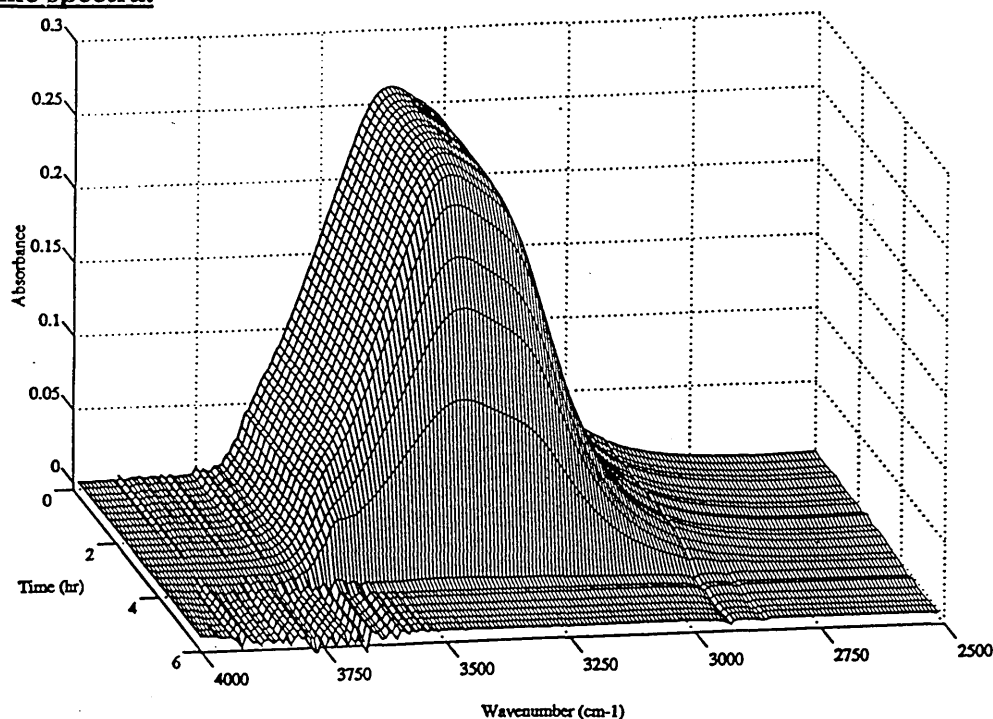
time spectra.

5.3.6.   Polarised ATR measurements of dehydrating bentonite

The results presented in sections 5.3.3 and 5.3.5 were obtained for aqueous

montmorillonite suspensions, dehydrated to form dried films on horizontal

5.3.6. Polarised ATR measurements of dehydrating bentonite

The results presented in sections 5.3.3 and 5.3.5 were obtained for aqueous montmorillonite suspensions, dehydrated to form dried films on horizontal substrates. The reduction in water content of the bentonite suspension is accompanied by a gravitational sedimentation of the platelets onto the substrate. It has been explained previously, that this sedimentation method is known to produce highly ordered films [192].

The band shift from 1086 cm^{-1} to 1080 cm^{-1}, on dehydration of an aqueous bentonite suspension ties in well with the observed band shift from 1081 cm^{-1} to 1070 cm^{-1} on heating (further dehydrating) a randomly oriented sample of dry powdered bentonite. However, it is necessary to perform polarised ATR measurements to ensure that the disappearance of the transient band at 1086 cm^{-1} is associated with the reduction of the water/bentonite ratio of the suspension below a critical value and not the formation of an oriented bentonite film from a disordered suspension. These experiments were performed in the Graseby Specac Squarecol cell in which the sample face is vertical and the suspension will deposit in the trough of the cell.

Figure 5.3.6a shows the comparison between unpolarised, TE and TM polarised ATR spectra of an aqueous bentonite suspension in the region between 1400 and 850 cm^{-1}. In figure 5.3.6a, the silicate bands in TM polarised light appear more intense than those in TE polarised light. This result is not unexpected since the depth sampled by TM polarised radiation is greater than that sampled in TE polarisation [202]. As one would expect, the bentonite platelets are randomly oriented in the suspension and so the absorbance ratio A(1044)/A(1086) is approximately the same in the unpolarised and TE and TM polarised spectra (graph 5.3.6a).

Figure 5.3.6a Unpolarised, TE and TM polarised ATR spectra of a bentonite suspension. Spectrum of water not subtracted.
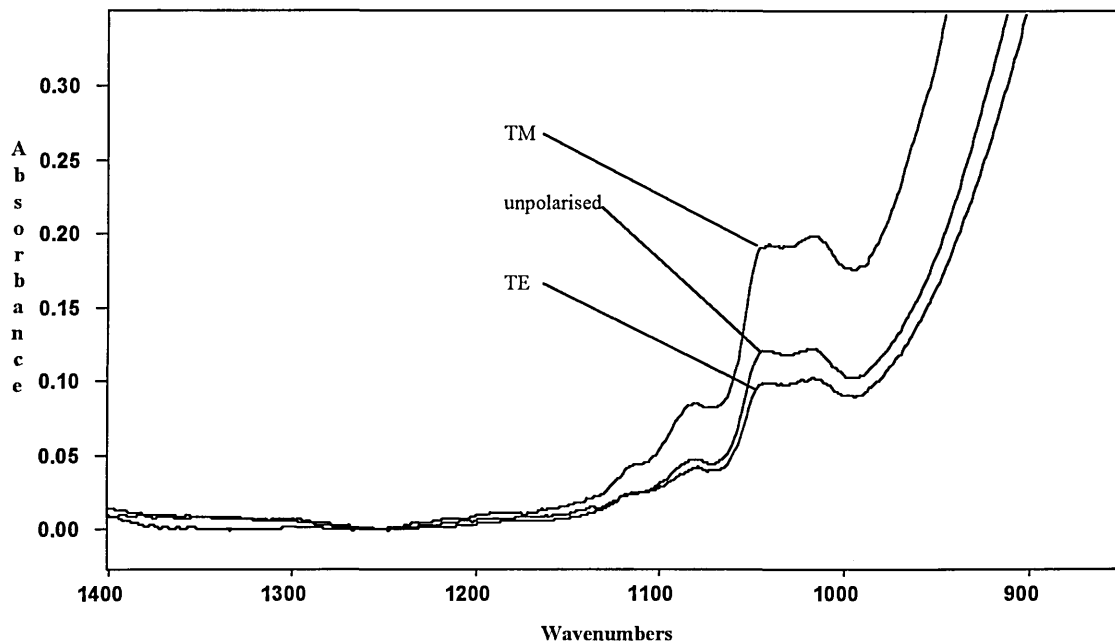
As the bentonite suspension is dehydrated, then the band at 1086 cm^{-1}, visible in both the TE and TM polarised spectra and the unpolarised spectrum observed in figure 5.3.6a, is shifted to 1080 cm^{-1} (figure 5.3.6b). The band shift to lower wavenumber is observed in all three spectra (unpolarised and TE and TM polarised). Hence, it can be inferred that the shift is independent of orientation and is due to the change in the water/bentonite ratio on dehydration. Figure 5.3.6b shows the unpolarised and TE and TM polarised ATR spectra of the dry bentonite film.

The position of the band at 1086 cm^{-1} appears to be controlled only by the clay/water ratio since this is unaltered by the polarisation of the radiation regardless of the orientation of the platelet. Despite earlier findings that heating (dehydrating) bentonite randomly oriented in a KBr disk caused the absorbance ratio A(1047)/A(1080) to decrease, there is also evidence that the intensity of this transient band is dependent upon the polarisation of the infrared radiation.

166

Hence, the intensity of the band appears to be determined by the orientation of bentonite platelets.

It should also be noted that the band at 1047 cm^{-1} will also show some orientation dependence since it has been assigned, by Farmer and Russell [197], to an in-plane Si-O stretching mode, i.e. a vibration parallel to the platelet surface (at right angles to the perpendicular stretching mode).

Figure 5.3.6b Unpolarised, TE and TM polarised ATR spectra of a dried bentonite suspension.
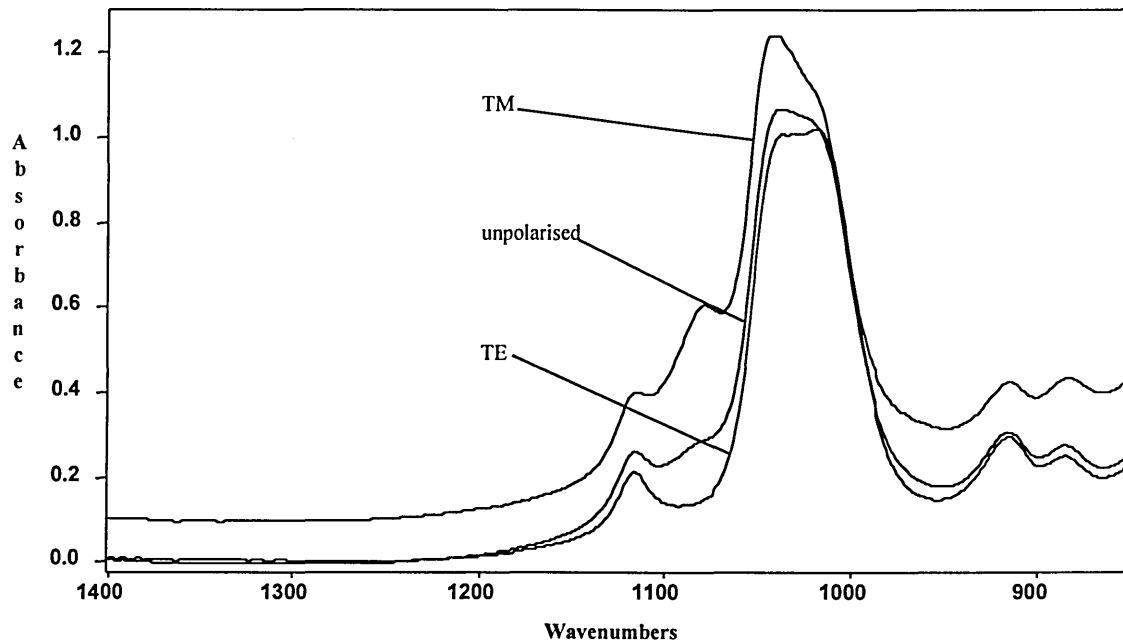
Graph 5.3.6a shows the variation in the absorbance ratio A(1047)/(1086) with drying time.

Graph 5.3.6a Variation of the absorbance ratio A(1047)/A(1080) for unpolarised and TE and TM polarised light with drying time.

Absorbance ratio A(1040)/A(1086)

▼ TE polarised   ● Unpolarised   ■ TM polarised
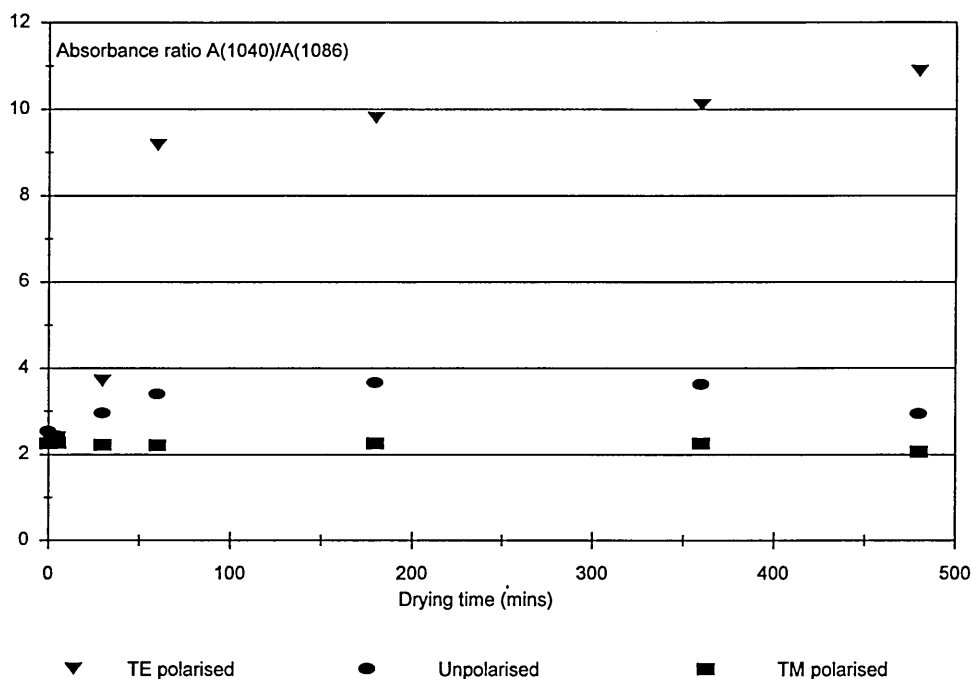
One would intuitively expect that, as the suspension dries, the platelets would deposit to form an oriented film in the trough of the Squarecol cell. The platelets which comprise the dried film would be expected to be oriented such that their c-axis was perpendicular to the bottom of the trough, and parallel to the vertical sampling face of the ATR prism. If this were the case, then the Si-O vibration at 1086 cm^{-1}, assigned to a stretching mode perpendicular to the platelet surface would be in the same plane as the c-axis. A schematic of this system is shown in figure 5.3.6c.

Assuming that this is the orientation of the platelets, then the Si-O vibration perpendicular to the platelet surface would be expected to interact with the E_y electric field component of the evanescent field.

Figure 5.3.6c. Expected orientation of clay platelet in deposited film
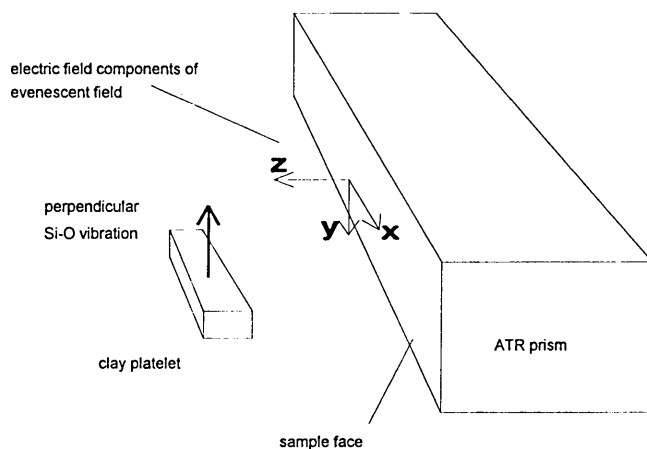
Similarly, if the platelets deposited in the orientation outlined above and shown in figure 5.3.6c, the Si-O vibration at 1047 cm^{-1}, parallel to the platelet surface, would be directed parallel to the bottom of the trough, and perpendicular to the sampling face of the ATR prism. If this were the case then the Si-O vibration parallel to the platelet surface would be expected to interact with both the E_X and E_Z electric field components of the evanescent field.

Hence, in TE polarised radiation (contains only the Ey electric field vector), the intensity of the band at 1086 cm^{-1} would be expected to increase relative to the band at 1047 cm^{-1}. Conversely, in TM radiation (contains both the E_X and E_Z electric field vectors), the intensity of the band at 1047 cm^{-1} would be expected to increase relative to the band at 1086 cm^{-1}.

Consequently, if the platelets deposited to form an ordered film with their c-axis parallel to the surface of the ATR prism and perpendicular to the bottom of the trough, in TE polarised light the absorbance ratio A(1040)/A(1080) would be expected to be small, and in TM polarised light the ratio of the same bands would be expected to be large.

However, graph 5.3.6a shows that the reverse is in fact the case: in TE radiation the absorbance ratio A(1040)/A(1080) is large, and in TM polarised light the ratio of the same bands is small.

Clearly, this result is unexpected and implies that in the region close to the vertical ATR prism (within the depth sampled by the evanescent field), the bentonite platelets are oriented with their c-axis perpendicular to the sampling face of the ATR prism (parallel to the bottom of the trough) rather than their expected orientation. In these circumstances the Si-O stretching mode perpendicular to the clay surface interacts with the E_x and E_z components of the evanescent field and the Si-O stretching mode parallel to the clay surface interacts with the E_y component of the electric field (figure 5.3.6d) .

Figure 5.3.6c. Actual orientation of clay platelets close to the ATR prism in a bentonite film deposited by gravitational sedimentation
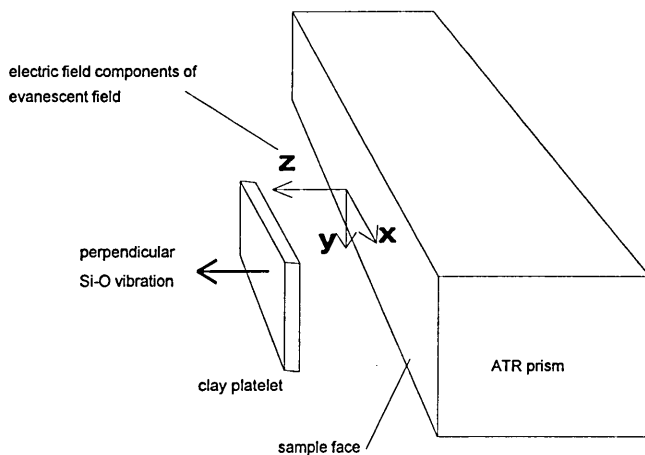
It can be concluded that the orientation of bentonite platelets may be influenced by the vertical sample surface of the ATR prism as they sediment under the influence of gravity. This effect would be particularly important for the larger size fractions of the clay mineral (~2 μm) which are sampled by the evanescent field which has been calculated to sample to a total depth of ~5.6 μm. This has

clear implications for the formation of a filter cake deposit of bentonite from the oil well drilling fluid on the borehole wall, and the likely way in which this filter cake is constructed.

Although gravitational sedimentation has been described by Brown and Brindley [192] as a suitable technique for oriented montmorillonite film preparation for X-ray diffraction analysis, it is unlikely that the film deposited in the trough of the Squarecol cell will be perfectly ordered. Firstly, due to the influence of the vertical prism face on platelet orientation and secondly, due to the high concentration (2% suspension) and short evaporation time (~8 hours) allowed for film formation. Indeed, Marguiles et al [227] produced very highly oriented montmorillonite films from extremely dilute (0.01%) aqueous suspensions which were allowed to evaporate very slowly (for 48 hours) in air. It was shown [227] that a much less oriented film was obtained if a 0.1% aqueous suspension was evaporated rapidly at 60°C.

The disordered nature of the films produced does not seem too unlikely when one considers the various faults including voids, edge to face stacking, regions of gross folding, ordered domains and regions of disordered stacking which typically exist in a clay-water system [229].

5.3.7.   ATR spectra of bentonite in D_2O

The modification of the silicate absorption band in dilute aqueous suspension suggests an interaction between the SiO_4 tetrahedra and water, such as hydrogen bonding. If there is a specific interaction between bentonite and water, then dispersing in D_2O should modify the structure of the silicate absorption bands relative to that in the spectrum of an aqueous suspension.

The transmission spectrum of the deuterated bentonite in the region between 4000 and 2000 cm^{-1} is shown in figure 5.3.7a.

5.3.7a Transmission spectrum of bentonite exchanged with deuterium for one week.
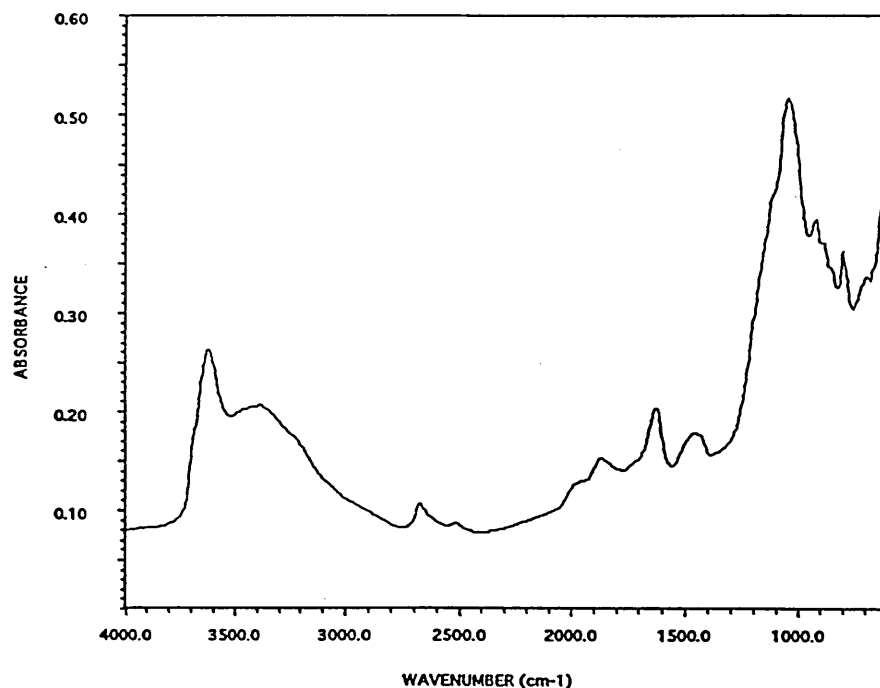
In figure 5.3.7a, characteristic bentonite OH stretching bands can be clearly observed at 3630, 3440 and 3250 cm^{-1} indicating that complete D$\leftrightarrow$H exchange does not occur in the exchange process. However, some D$\leftrightarrow$H exchange can be observed at lower frequency where the deuterium analogues of these characteristic bands can be seen, displaced by a factor of $\sim\sqrt{2}$ (Table 5.3.7a).

Full D$\leftrightarrow$H exchange may not have occurred for several reasons, the most likely being that the deuterium exchange procedure was not sufficiently 'energetic' when compared to the method outlined by Bukka et al [25]. In addition, some re-exchange of H for D may occur in the preparation and analysis of the deuterated clay, reducing the amount of the deuterium exchanged product.

Table 5.3.7 Deuterium analogues of characteristic OH band positions.

OH band position (cm^{-1})	Deuterium analogue (cm^{-1})	Ratio of H/D wavenumber position
3634	2677	1.36
3434	2515	1.37
3250	2390	1.36
1635	1204	1.36

The ATR spectra in the region between 1400 and 850 cm^{-1} of bentonite dispersed in H_2O and in D_2O are shown in figure 5.3.7b.

Figure 5.3.7b Comparison of ATR spectrum of bentonite dispersed in H_2O and in D_2O. The solvent spectrum is subtracted in each case.
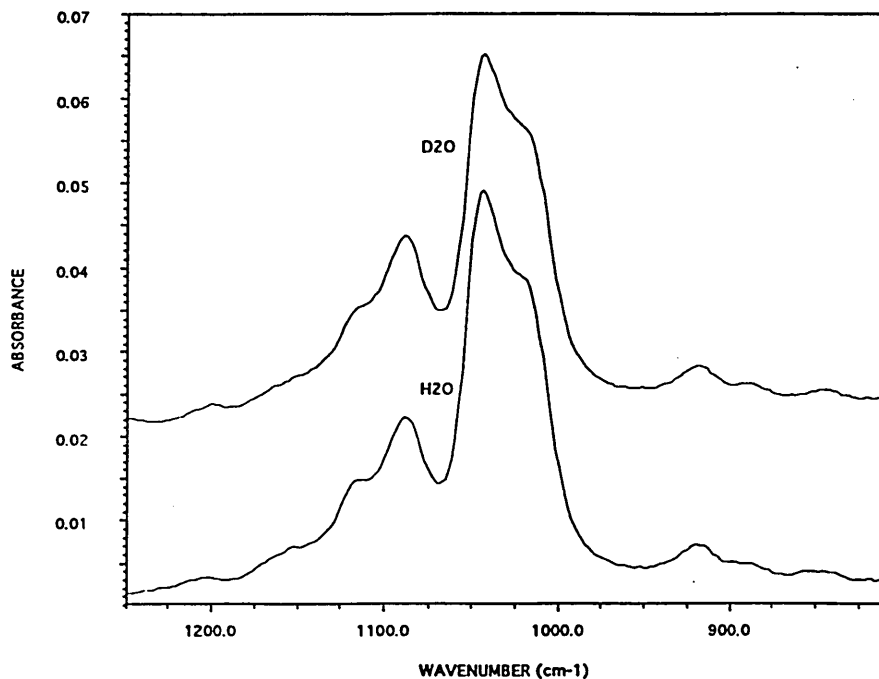
The two spectra are almost identical and show that there is no effect on the shape or position of the silicate stretching vibrations on replacing H_2O with D_2O. In particular, the band found at 1086 cm^{-1} associated with the spectrum of highly dispersed bentonite is clearly visible in the bentonite-D_2O spectrum. The bands at 1202 and 1156 cm^{-1} which have been observed previously in the transmission spectrum of dry bentonite (figure 5.3.2d) and the transmission and ATR spectra of aqueous bentonite suspensions and have as yet been unassigned, are also clearly visible.

Figure 5.3.7c shows the evolution of ATR spectra (in the region between 1400 and 850 cm^{-1}) of a dehydrating bentonite-D_2O suspension to form a bentonite film on a zinc selenide substrate at early times.

<u>Figure 5.3.7c Evolution of the silicate stretching bands of a dehydrating bentonite-D₂O suspension.</u>
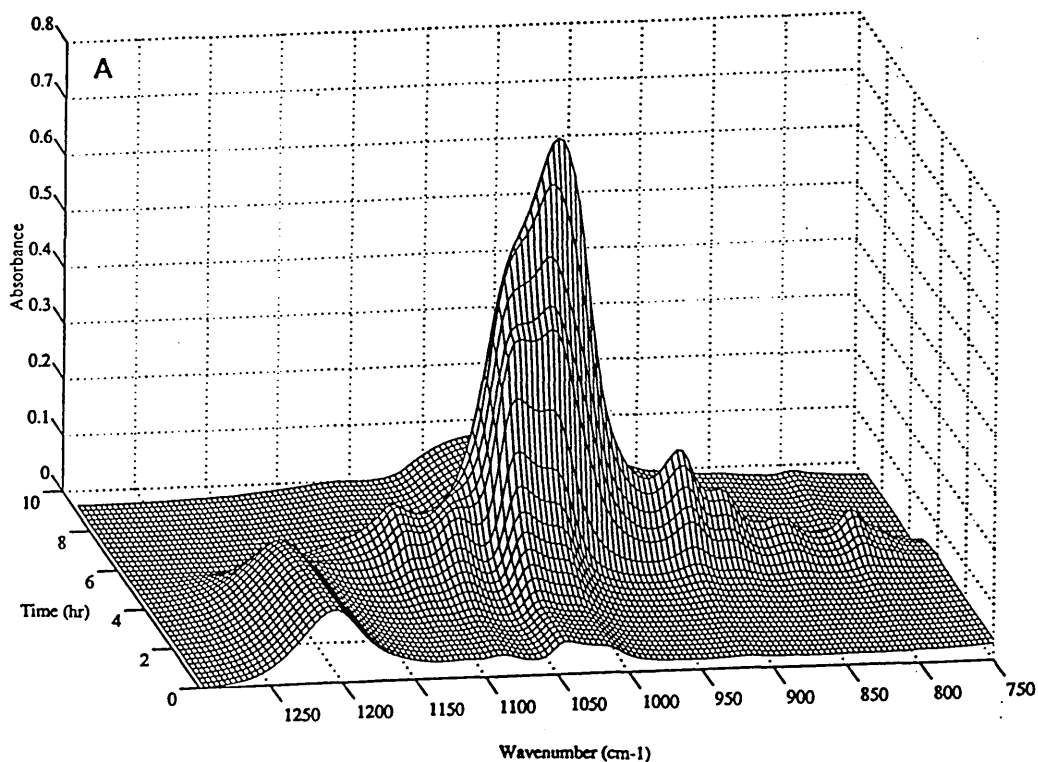
The evolution of the silicate bands during the evaporation of D_2O is broadly similar to that observed during the evaporation of water from an aqueous bentonite suspension. At t=3.46 hours the band at 1086 cm^{-1} begins to shift to lower frequency and it reaches 1080 cm^{-1}, by t=4.06 hours. Concurrently the shoulder at 1018 cm^{-1} becomes more pronounced and by t=4.30 hours has surpassed the intensity of the band at 1042 cm^{-1}. The band which has shifted to 1080 cm^{-1} has disappeared by t=4.90 mins, by which time the band at 1042 cm^{-1} becomes a shoulder to the band at 1018 cm^{-1}.

Figure 5.3.7d shows the evolution of the OD and OH bands in the spectral region between 4000 and 2000 cm^{-1} during drying. The decrease in intensity of the OD peak at 2485 cm^{-1} is accompanied by an increase in OH band intensity at 3628 and 3420 cm^{-1}.

Figure 5.3.7d Evolution of the OD and OH bands during drying of a bentonite-D_2O suspension.

Wavenumber (cm-1)

175
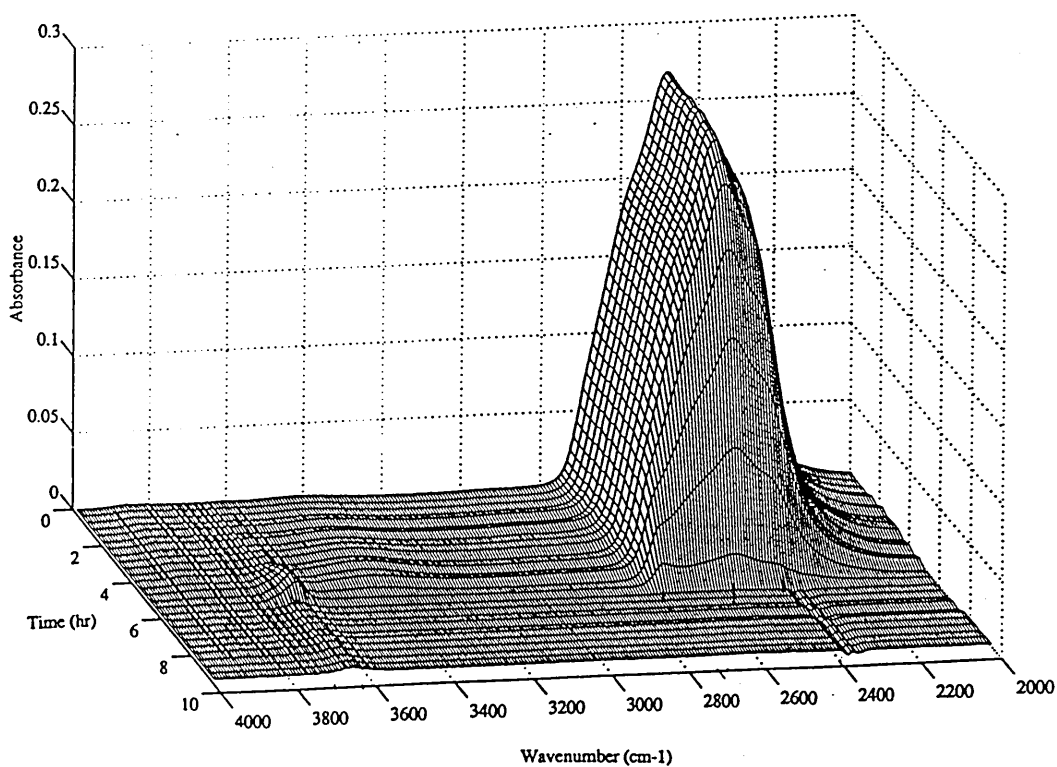
A small shoulder band at 2680 cm^{-1} (the deuterium analogue of the characteristic band at 3628 cm^{-1}) appears at t=5.14 hours. At t=5.26 hours, a shoulder band is visible at 2390 cm^{-1} (the deuterium equivalent of the shoulder band at 3250 cm^{-1} in the spectrum of bentonite). As with the spectra of film formation on an ATR prism by evaporation of H_2O from a bentonite-H_2O suspension, at long dehydrating times (figures 5.3.5b and 5.3.5c), the intensity of all Si-O, OH and OD stretching bands are reduced, probably due to film detachment from the IRE.

5.3.8.   ATR spectra of various homoionic bentonites

Clearly, the results of section 5.3.7 indicate that changing the solvent from H_2O to D_2O has very little effect on the ATR spectra of bentonite and bentonite films. In order to determine which clay and/or solvent properties determine the differences between the powder and suspension spectra of bentonite, a selection of homoionic bentonites were investigated. Figure 5.3.8a shows the ATR spectra of aqueous homoionic Li-, Na-, K- and Ca-bentonites suspensions.

The wavenumber position of the transient band at 1086 cm^{-1} shows small variations between the three alkali metal-exchanged clays; Li^+ at 1087 cm^{-1}, Na^+ at 1084 cm^{-1} and K^+ at 1086 cm^{-1}. The relative intensity of the band at 1018 cm^{-1} also appears to be dependent upon the nature of the exchange alkali metal cation. The shoulder is more pronounced in the lithium form and is progressively less pronounced in the sodium and potassium bentonites. The position of the main Si-O band at 1044 cm^{-1} is not affected by the nature of the alkali metal cation.

Figure 5.3.8a Comparison of the ATR spectra of homoionic Li-, Na- K- and Ca-bentonites suspended in water.
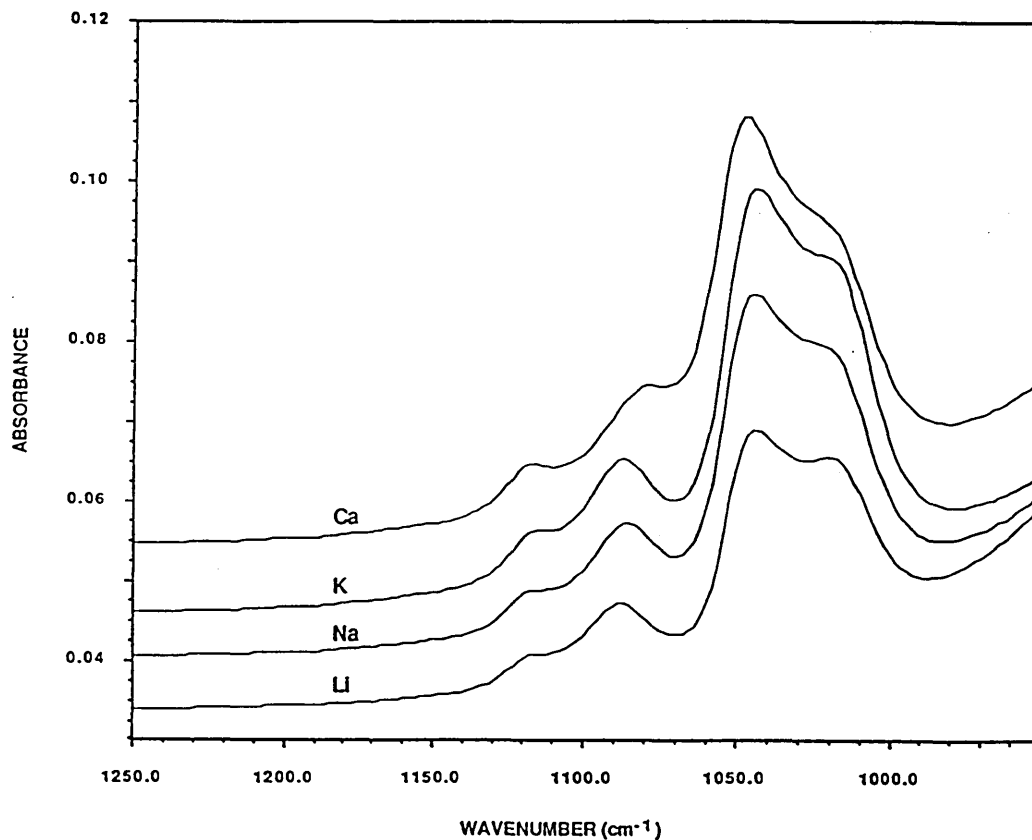
The ATR spectrum of homoionic calcium bentonite is quite different from the spectra obtained for the homoionic alkali metal bentonites. The band at about 1086 cm^{-1} has been replaced by a weak shoulder at 1077 cm^{-1} which is similar to the band seen previously at 1080 cm^{-1} in dehydrating bentonite suspensions. In addition, the main Si-O band has been shifted to a higher frequency value of 1047 cm^{-1} and the shoulder band at 1018 cm^{-1} is less well developed than the corresponding bands in the alkali metal homoionic clays.

Further work at SCR [41], has established the effect of increasing the NaCl concentration on the ATR spectrum of an aqueous bentonite suspension. As the electrolyte concentration is increased to 0.01 M, a small shoulder at 1080 cm^{-1} grows and, with increasing concentration, replaces the band at 1086 cm^{-1}. This is similar to the shift from 1086 to 1080 cm^{-1} observed on drying a bentonite suspension. In addition, the main Si-O stretching band is shifted to higher

frequency with increasing electrolyte concentration, until its spectrum resembles that of Ca-bentonite.

Variations in the Si-O band intensity at ~1040 cm^{-1} in the transmission spectra of Li-, Na- and K- exchanged homoionic aqueous bentonite suspensions have been observed by Gan and Low [44]. However, they made no reference to the clearly observable band at 1086 cm^{-1} or any shift in its position on increasing the electrolyte concentration. It was found [44] that the intensity of the band at 1040 cm^{-1} was in the order Li > Na > K for suspensions of equal clay content and that the intensity of the band gradually decreased with increasing electrolyte concentration in the range 0.0001 to 0.01 M; the absorbance did not depend upon the nature of the halide anion (Cl$^-$, Br$^-$, I$^-$). The band intensity decreased more rapidly with increasing electrolyte concentration for concentrations above 0.01 M, particularly for the potassium clay. The authors were unable to offer an explanation for this observation. More recently, Yan et al [45] have discussed the shift to higher frequency in the position of all Si-O stretching modes with increasing water content (M_w/M_c) but concentrated on the two more prominent Si-O absorption bands (Peaks II and III). Similar shifts to high frequency of the H-O-H bending mode of water were also seen under similar conditions. The authors attributed this to the change in the structure of water (becomes more like bulk water) with increasing M_w/M_c. They tentatively ascribed this to coupling between the Si-O stretching vibrations of the silicate layer surface and the H-O-H bending mode of water at various water contents.

Generally, the absorption bands at 1086 and 1018 cm^{-1} do not normally feature in the published infrared spectra of bentonite nor in their band assignments. Several reasons exist for these bands to be so infrequently commented upon. Firstly, and perhaps most importantly, is that the silicate bands in clay minerals are extremely intense and consequently only a small amount of material may be

analysed. Commonly, experiments are performed on clay minerals in the form of a free standing film [33, 40] which contain very large quantities of clay mineral. The second most important reason is that these spectral features appear to require high values of the water/clay ratio which makes sample preparation very difficult. The bentonite films used by Johnston et al [33] would have had a maximum water content which corresponds to an aqueous suspension of 1000 gdm^{-3}. Another reason for the bands at 1086 and 1018 cm^{-1} being so poorly documented is their poor definition in the infrared spectrum. The band at ~1020 cm^{-1} can just be observed as a shoulder in some published infrared spectra of bentonite.

In the experiments presented here, the absorption band at 1086 cm^{-1}, observed in the spectrum of an aqueous bentonite dispersion, has been found to shift to 1080 cm^{-1} and disappear into the main silicate stretching band on drying or increasing the electrolyte concentration. In addition, the band at ~1080 cm^{-1} has been found, using Fourier self deconvolution, second derivative spectroscopy and curve fitting techniques, to shift to lower wavenumber (1070 cm^{-1}) on heating to 200°C. The nature of the solvent (D_2O replacing H_2O) has been shown to have no effect on the spectrum of solvated bentonite. However, the nature of the exchangeable cation has been shown to have some influence on the spectrum of the hydrated mineral.

A band at ~1086 cm^{-1} has been reported previously by several authors [43, 45, 191, 197, 230]. Farmer and Russell [197] observed a band at ~1080 cm^{-1} which they attributed to an Si-O stretching mode, perpendicular to the plane of the clay platelets. This band is thought to be due to the vibration between silicon and the oxygen atom shared between the tetrahedral and octahedral layers of the clay platelet. The authors point out that the frequency of this band is not, as one would expect, influenced by partial isomorphous substitution in the octahedral

layer. Farmer [230] observed a band of variable intensity at 1086 cm^{-1} in the transmission spectrum of bentonite and also attributed it to an Si-O stretching mode perpendicular to the surface of the clay surface.

In addition, Lerot and Low [43] observed a band at ~1086 cm^{-1} in a Bell Fourche montmorillonite film and attributed it to a vibration perpendicular to the clay surface (parallel to the incident radiation). This band increased in intensity as the angle of the film to the incident radiation increased. Lerot and Low also noted an increase in intensity of the 1086 cm^{-1} band as the water/Bell Fourche montmorillonite ratio was increased from that in an air dried film (where the 1086 cm^{-1} band is invisible). It was suggested that the increase in water content in the film causes the platelets to separate and disorder, this enables more of the perpendicular vibrations to intercept the infrared beam. These findings indicate that the intensity of the band due to the Si-O vibration perpendicular to the platelet surface may be orientation dependent.

The polarised ATR measurements presented in this thesis indicate that despite the platelets being deposited in an oriented arrangement (albeit not the expected orientation) by gravitational sedimentation, the band position changes only with water content, not ,with the polarisation of the radiation. However, the band intensity has been shown to be determined by the orientation of the clay platelet in a dehydrating suspension and hence the polarisation of the radiation. Since Lerot and Low [43] observed only changes in band intensity, not shifts in band position, their findings do not address the shifts in band position observed in the ATR and transmission experiments presented in this thesis.

Farmer and Russell [197] stated that the physical state of the mineral can significantly affect the position and sharpness of silicate stretching bands in the infrared spectrum of a clay mineral. They report small shifts in frequency,

sharpening and increasing intensity of the band due to the Si-O vibration perpendicular to the clay surface as particle size decreases. This may well explain the observations presented in the previous section since the 1086 cm^{-1} band is most intense when the bentonite is fully dispersed, and decreases in intensity when flocculation occurs and aggregates form, either on drying or increasing the electrolyte concentration. In addition, the ability of a Ca^{2+} exchangeable cation to cause flocculation of a clay suspension is much greater than that of alkali metal cations such as Na^+ or Li^+. This is in good agreement with the observations of the homoionic clay mineral suspensions, in which the position of the transient band is at high frequency and well defined in the spectrum of Li^+, Na^+, and K^+ montmorillonite, but is shifted to much lower frequency, and less well-defined in the spectrum of Ca^{2+} montmorillonite.

Although, the increase in particle size does explain some of the observed data, it does not explain the band shift from 1080 to 1070 cm^{-1} on heating a randomly oriented bentonite powder dispersed in a KBr disk to 200°C.

Closely associated with increasing particle size, the decrease in interlayer separation on drying or addition of electrolyte may be another explanation for the observed shift in band position presented in previous sections. It is possible that as the two mineral platelets approach one another, vibrational coupling between them may occur. Farmer and Russell [191] established however, that the infrared spectrum of a 2:1 layer silicate such as bentonite does not depend upon the interlayer spacing. Only very small frequency shifts, attributed to the polarising effect of the interlayer cation, were observed even at a d-spacing of 9.5Å [191]. This implies that there is very little coupling between the adjacent clay mineral platelets regardless of whether the dipoles are oriented parallel or perpendicular to the platelet surface.

Whilst coupling between the Si-O stretching vibrations and H-O-H bending vibrations [45], may be a plausible explanation for modification of the structure of the Si-O absorption bands on hydration, the most likely explanation is the dissociation of the exchange cation from the surface of the tetrahedral silicate sheet. It would be expected that highly solvated cations such as Na^+ and Li^+ would exist in the interlayer space and less solvated cation such as Ca^{2+} would exist much closer to the silicate surface of the clay platelet.

In the case of homoionic sodium bentonite in water or dilute sodium chloride solutions, the dissociation of the exchange cation gives rise to the formation of an electrical double layer and electrostatic repulsion between the platelets [13]. In the homoionic calcium bentonite however, the calcium ion does not fully dissociate and extended electrical double layer formation does not take place. The relative changes between the spectra of dry and hydrated bentonite should follow the lyotropic series ($Li^+ > Na^+ > K^+ > Rb^+ > Cs^+$). The low hydration energy of the cesium ion, for example, should result in little hydration of homoionic caesium bentonite and thus little difference between the spectra of dry and wet bentonite would be expected.

The ATR spectra of bentonite suspensions are sensitive to the ionic strength, c, of the suspending solution (at least down to c=0.01 molar) and the clay/water ratio above the value at which the band at 1086 cm^{-1} begins to shift to lower frequency. The similarity of the changes in the ATR spectra during drying and an increase in ionic strength is not surprising. Both drying and increasing ionic strength have the effect of reducing the spacing between the clay platelets. Norrish [54] has shown that below a certain value of ionic strength of about 0.3 molar, the mean interlayer spacing of bentonite in a suspension varied linearly with $1/\sqrt{c}$, while Glaser and Méring [50] have shown step-like increases in the

interlayer spacing of bentonite as the relative humidity of the equilibrating atmosphere (and thus water content of the clay) was increased.

The presence of a well-developed band at 1086 cm^{-1} appears to be indicative of electrical double layer formation and the osmotic swelling of bentonite. The shifting of this band to 1080 cm^{-1} appears to be associated with the compression of the electrical double layer and the onset of crystalline swelling or hydration of bentonite. The crystalline swelling of bentonite is observed in sodium bentonites at high ionic strength (up to c=5 molar) and calcium bentonites in water. Further decrease in the interlayer spacing and the complete disappearance of the band at 1080 cm^{-1} is achieved only by drying. The disappearance of the band at 1080 cm^{-1} indicates that the bentonite is no longer solvated.

It is possible that the shift of the band at 1086 cm^{-1} to 1080 cm^{-1} and its subsequent shift to 1070 cm^{-1} on heating to 200°C is related to a fully solvated counter ion which, on drying or increasing salt concentration, reduces its hydration sphere until a dried film is obtained in which the counter cation settles into a di-trigonal cavity in the silicate sheet in much the same way as explained by Sposito et al [40]. Further heating of the clay to 200°C causes removal of more interlayer water and allows the exchangeable cation to settle further into the di-trigonal cavity [42].

The observed frequency shift of the band associated with the Si-O vibration perpendicular to the clay platelet on dehydration is probably due to the change in the b-dimension (rotation of the SiO_4 tetrahedra) observed by Ravina and Low [59] and Odom and Low [60]. This contradicts the findings of Lerot and Low [43] who concluded that in the range of water contents studied (between 2 and 22 g g^{-1} Bell Fourche montmorillonite), no shift in the wavenumber

position of the band at 1086 cm^{-1} was observed and explained that swelling produced no change in b-dimension.

In these present observations, the band at 1086 cm^{-1} in aqueous bentonite suspensions with water contents of 50 and 16 g g^{-1} of SWy-1 bentonite, is seen to shift to lower frequency as the water content of the suspension is reduced.

These findings are corroborated by the findings of Volzone et al [133], who observed changes in b-dimension for glycolated Na and K-bentonites (relative to the dry homoionic bentonite) but observed no such change for Ca-bentonite. They explain that the Na$^+$ and K$^+$ cations are partially occluded by the di-trigonal cavity of the silicate layer but became glycolated into the interlayer space. This causes a rotation of the silica tetrahedra. However, Ca^{2+} is a much larger cation so does not settle into the di-trigonal cavity. It also does not form an extended double layer in the interlayer space. Hence, Ca^{2+} does not cause a relaxation of the silicate lattice on glycolation (solvation) but, in addition, does not move significantly away from the layer platelet surface.

It should be noted that the b-dimension increases from the natural water content up to a water content of 3.0 g g^{-1} clay [59] at which point it remains constant. This fits in well with the finding that the 1086 cm^{-1} band is associated with a suspension in which the water/bentonite content is above a certain value. It is not known however, if the b-dimension diminishes further when air-dried bentonite with a natural water content is heated to 200°C to remove more water.

The applicability of this theory has not been tested fully for two main reasons:
1. The equilibrium water content at which the band shifts from 1086 cm^{-1} to 1080 cm^{-1} is not known in the studies presented here. It must be remembered, of course, that the formation of bentonite films by evaporating water in a stream

of dry air (the purge of the FTIR spectrometer) was not a well-controlled process and the water content of the film was not known and was not constant during spectral collection. An improved method of film formation, enabling ATR or transmission spectra to be collected under conditions of known equilibrium water content, will be required to further interpret the evolution of the spectra. One possibility would be to monitor the compaction of a bentonite suspension in a high temperature/high pressure ATR cell developed at Schlumberger Cambridge Research for monitoring cement hydration [229]. It has been found that hydrostatic pressure has no influence on the ATR spectrum of an aqueous bentonite suspension [232]. However, rather than simply pressurising an aqueous montmorillonite suspension, by using a porous frit, it might be possible to filter (squeeze water from) the suspension in a controlled manner in order to evaluate the rate of band shift with applied pressure.

2. In the studies presented here it was impossible to perform concurrent FTIR and XRD measurements in order to correlate the band shift in infrared with changes in the 001 reflection (d-spacing) and the 060 reflection (b-dimension). Correlation between the FTIR and XRD experiments performed independently is also difficult due to the differing drying rates imposed by the two different techniques.

5.4.   Conclusions

Differences between the infrared spectrum of an aqueous bentonite suspension, dry bentonite powder and a heated bentonite powder, have been monitored using transmission, microscopy, and ATR FTIR spectroscopy.

A band at 1086 cm^{-1} in the infrared spectrum of 'wet' bentonite has been observed to shift to lower wavenumber and disappear on drying to a bentonite film of natural water content. This band can be picked out using second

derivative, Fourier self deconvolution and curve fitting techniques and has been observed to shift further to lower wavenumber on heating.

The band at 1086 cm^{-1} appears to be a characteristic of interlayer cation hydration and the formation of an extended double layer in the interlayer space. It is much more developed in the spectrum of bentonite exchanged with easily hydrated cations (e.g. Na$^+$). The band is much less well developed in the spectrum of bentonite exchanged with cations which are less easily hydrated (e.g. Ca^{2+}) and in which extended double layer formation does not occur. On dehydration, the exchange cations lose their hydration shells, and move closer to the surface bentonite platelets. The smaller cations, e.g. Na$^+$ and K$^+$, are able to settle into the di-trigonal cavity of the silicate layer surface, however, the larger cations, e.g. Ca^{2+}, are unable to settle into the cavity and exist close to the platelet surface. The settling of the smaller cations into the di-trigonal cavity causes a rotation of the silica tetrahedra thus changing the b-dimension, and reducing the Si-O frequency of vibration.

In addition, increasing the electrolyte concentration causes the band at 1086 cm^{-1} to shift to lower frequency and diminish in intensity. This is due to collapse of the electrical double layer on increasing the ionic strength and the subsequent close approach of clay platelets, thus enabling the exchange cations to approach and enter the di-trigonal cavity and cause rotation of the silica tetrahedra.

No evidence of hydrogen bonding of water to the bentonite Si-O surface was observed using D$_2$O as solvent, although some D$\leftrightarrow$H exchange was observed.

Unexpectedly, the dehydration of an aqueous bentonite suspension appears to cause some of the bentonite platelets to deposit on the wall which constrains the

suspension. These platelets are oriented such that their c-axis is directed perpendicular to the plane of the vertical constraining wall, a direction perpendicular to that expected of a clay platelet deposited to form an oriented film by gravitational deposition from aqueous suspension. This is thought to be important an important mechanism in the formation of a filter cake on the wall of the borehole by deposition of clay mineral from a circulating oil well drilling fluid.

6. ADSORPTION OF POLYACRYLAMIDE ON BENTONITE

6.1. Introduction

It was pointed out in chapter 1 that certain polymers are commonly added to water based oil well drilling fluids in order to prevent degradation of the wellbore wall and to minimise degradation of cuttings, aiding their removal from the borehole to the surface. Polyacrylamide (figure 4.9.2b) is one such polymer commonly used for this purpose.

In order to fully understand and explain the behaviour of polyacrylamide in the drilling fluid it is necessary to fully understand its interaction with clay mineral both dispersed in aqueous suspension (as in the drilling fluid) and clay mineral in the form of a free standing film, which represents the major portion of underground shale deposits.

6.2. Experimental

Two methods have been employed to investigate the behaviour of polyacrylamide in the two physical forms as outlined above. Firstly, bentonite films both free standing (self supporting) films and films supported on an internal reflection element were allowed to soak in aqueous polyacrylamide solution or aqueous polyacrylamide/KCl solution. Secondly, fully dispersed bentonite in aqueous suspension was contacted with aqueous polyacrylamide or aqueous polyacrylamide/KCl solution.

6.2.1. Materials

SWy-1 bentonite was purified by sedimentation to obtain the $<2\mu m$ fraction and used in its natural state, i.e. without cation exchange (containing predominantly Na^+, and small amounts of Ca^{2+} and K^+ exchange cations, as outlined in table 4.9.1). Aqueous bentonite suspensions were prepared by dispersing the bentonite in deionised water and allowing to 'age' by stirring for 12 hours. Polyacrylamide (PAM) of zero or negligible ionic content and molecular weight 100k, 500k and 7000k were used as obtained from Allied Colloids. Hydrolysed polyacrylamide (HPAM) containing 30% anionic (COO^-) functionality and molecular weight 7000k was also used as obtained from Allied Colloids. In all experiments in which polyacrylamide was contacted with bentonite, the polymer was dissolved in aqueous solution overnight using a rotary sample mixer operating at 300 rpm prior to mixing. In all experiments deionised water was used whose pH was 7 and whose conductivity was $<20 \mu Scm^{-1}$.

6.2.2. Spectroscopy

6.2.2.1. Transmission - Free standing films

Free standing films were prepared by thinly smearing highly concentrated bentonite paste ($\sim2000 \ gdm^{-3}$) across a clean polyethylene sheet. This was covered with a polyethylene bag and allowed to dry for 16 hours at ambient temperature. The free standing film could then be easily peeled from the polyethylene sheet and stored in polyethylene sample bags at ambient temperature. The bentonite film thicknesses were measured using an electronic micrometer gauge and were found to vary between 7 and 20 μm.

In each experiment, a small square (greater than the 13 mm diameter aperture of the transmission cell holder) weighing between 5 and 7 mg, was immersed in aqueous polyacrylamide solutions with concentration of 5 gdm^{-3}, 3.3 gdm^{-3}and 1 gdm^{-3} for the required time. This obviously represents a very small amount of clay in a large excess of polymer solution. The bentonite-polyacrylamide films could then be placed on the transmission cell holder and dried in the dry nitrogen purge of the Mattson Polaris FTIR spectrometer. These experiments were repeated dissolving KCl in the aqueous polyacrylamide solution prior to soaking of the bentonite film in order to obtain a final KCl concentration of 100 gdm^{-3}.

6.2.2.2. Transmission - Aqueous dispersions

SWy-1 Bentonite-polyacrylamide dispersions were prepared by adding aqueous solution of polyacrylamide (Mw 100k, 500k and 7000k) to 20 gdm^{-3} bentonite suspension in order to obtain polyacrylamide concentrations in mixed suspension of 5 gdm^{-3}, 3.3 gdm^{-3}and 1 gdm^{-3}.

These clay-polymer dispersions were mixed overnight at room temperature, using a rotary sample mixer operating at 300 rpm, to allow equilibration. The dispersions were centrifuged at 20000 rpm and dried overnight at 40°C. The dried solids were dispersed in KBr disks and their transmission infrared spectrum acquired on a Mattson Polaris FTIR spectrometer with 4 cm^{-1} resolution, a triangular apodisation function and 100 co-added scans. These experiments were repeated dissolving KCl in the aqueous polyacrylamide solution prior to mixing with the bentonite dispersion, in order to obtain a final KCl concentration of 100 gdm^{-3}. This enables the bentonite to be fully dispersed on polyacrylamide addition.

6.2.2.2. ATR spectroscopy - bentonite film

Bentonite films were prepared on the sampling faces of the silicon Squarecol ATR prism as outlined in section 4.4.4. The cell was then sealed containing the bentonite coated ATR prism and the infrared spectrum of the supported air dried bentonite film acquired at room temperature. Each spectrum was acquired with a resolution of 4 cm^{-1}, a triangular apodisation function and a total of 512 co-added scans on a Mattson Polaris FTIR spectrometer fitted with a dry nitrogen purge. Without removing or repositioning the Squarecol cell from its original position in the sample compartment of the infrared spectrometer, the trough (maximum capacity 2 cm^3) was filled with 2 cm^3 of aqueous polyacrylamide solution of molecular weight 100k, 500k and 7000k and concentrations 5 gdm^{-3}, 3.3 gdm^{-3} and 1 gdm^{-3}. Infrared spectra of the bentonite film (in contact with polyacrylamide solution) were obtained at 10 minute intervals on a Mattson Polaris FTIR spectrometer. These spectra were also acquired at room temperature and under a dry nitrogen purge; the same instrumental parameters were employed as were employed for spectral acquisition of the bentonite film alone. These experiments were repeated dissolving KCl in the aqueous polyacrylamide solution prior to addition to the Squarecol cell in order to obtain a final KCl concentration of 100 gdm^{-3}.

6.2.2.3. ATR spectroscopy - polyacrylamide film

Polyacrylamide films were prepared by separately depositing 1 cm^3 aqueous polyacrylamide solution of concentration 5 gdm^{-3}, 3.3 gdm^{-3}, and 1 gdm^{-3}, onto one sampling face of the ZnSe Squarecol ATR prism and drying flat for two hours at 65°C. The cell was sealed containing polymer coated ATR optics and the infrared spectrum obtained at room temperature, under a dry nitrogen atmosphere, on a Mattson Polaris FTIR spectrometer. The instrumental

parameters being the same as outlined for spectral acquisition of bentonite coated ATR optics above.

6.2.2.4. X-ray Diffraction

All basal spacings were measured between 4 and 20° 2θ using a Phillips 1050 diffractometer operating at 40 kV and 40 mA with Co K_α radiation.

The d-spacing of SWy-1 bentonite free standing films and free standing films immersed in aqueous polyacrylamide or polyacrylamide/KCl solution were obtained by placing the dried film from the infrared spectrometer on a glass slide and placing in the diffractometer.

The d-spacing of mixed dispersions of aqueous SWy-1 bentonite suspension and aqueous polyacrylamide or polyacrylamide/KCl (Mw 100k and 500k) solution were obtained by removing the moist centrifuged solids and then thinly deposited on a glass slide. The film was then dried at 40°C overnight and stored under ambient conditions before being placed in the diffractometer. Mixed dispersions of aqueous SWy-1 bentonite suspension and aqueous polyacrylamide or polyacrylamide/KCl (Mw 7000k) solution formed extremely viscous gel structures which could not be thinly deposited to form a film on a glass slide. As a result, these mixed complexes were dried at 40°C for several days before being finely ground using a mortar and pestle. The powder was then packed into a holder and placed in the diffractometer.

6.2.2.5. Kjeldahl total nitrogen analysis

The total nitrogen content of mixed dispersions of aqueous SWy-1 bentonite suspension and aqueous polyacrylamide or polyacrylamide/KCl solution were

obtained by drying the centrifuged solids at 40°C overnight. A weighed amount was added to a digestion tube for nitrogen analysis as outlined in section 4.7. This was process was repeated in order to assess the reproducibility of the technique.

6.3. Results and Discussion

6.3.1. Adsorption isotherms

In order to characterise the adsorption behaviour of polyacrylamide from aqueous solution onto dispersed bentonite it is extremely important to establish the amount of polymer adsorbed (section 3.3.2). Although adsorption isotherms provide little information regarding the state of the adsorbed layer, they can provide essential information regarding the adsorption process, particularly the adsorption mechanism (from the isotherm profile).

6.3.1.1 Without electrolyte (zero KCl loading)

Figure 6.3.1.1a shows the adsorption isotherms for the addition of aqueous polyacrylamide solution to an aqueous SWy-1 bentonite suspension at zero KCl loading. The amount of nitrogen present naturally on the bentonite (not associated with the polyacrylamide) was determined to be 0.016%. Hence, by subtracting the amount of nitrogen present naturally on the clay, the quantity of adsorbed polyacrylamide may then be calculated.

Figure 6.3.1.1a Adsorption isotherms for polyacrylamide onto SWy-1 bentonite in aqueous suspension (zero KCl loading).
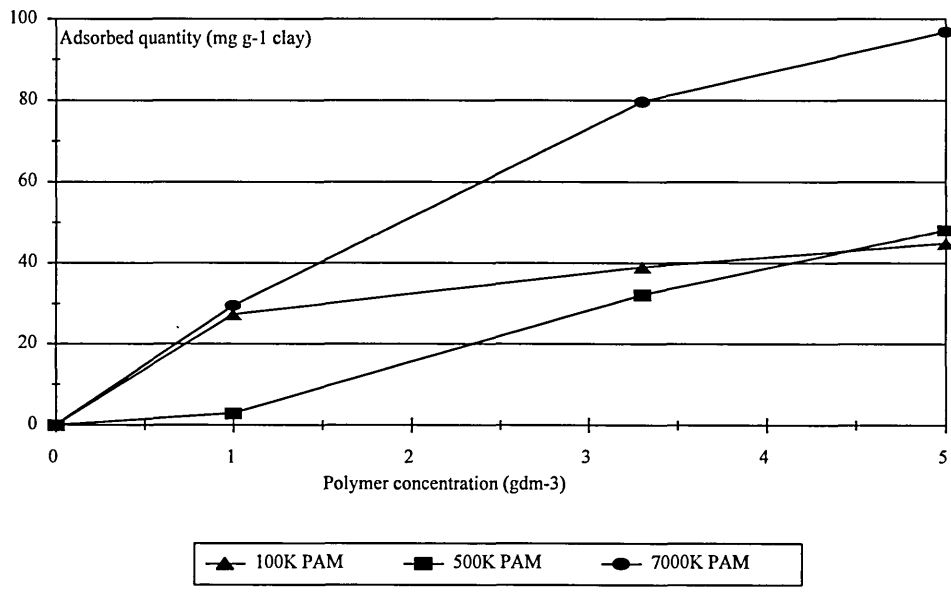
Polyacrylamide is commonly added to drilling muds at a concentration of 4 gdm^{-3}, although the effective dose plateau for the polymer has been found to be approximately 1 gdm^{-3}. The polymer is added in excess (~4 gdm^{-3}) to prevent shale deposits, which contain clay material, stripping polyacrylamide from the mud so quickly that polymer would have to be replaced continually rather than periodically.

Consequently, the concentration range of polyacrylamide in solution of interest is between 1 and 5 gdm^{-3} and so it is in this range that the adsorption isotherms have been calculated. In fact, the adsorption isotherms have been calculated at only three polyacrylamide concentrations (namely 1.0, 3.3, and 5.0 gdm^{-3}) in order to determine the amount of adsorbed polymer when it is present in excess, when there is a deficiency and at an intermediate concentration in the oil well drilling fluid.

Although very few points have been calculated to define the adsorption isotherms, the amount of adsorbed polyacrylamide (Mw 100k and 7000k) appears to increase with increasing concentration at low solution concentrations. As the solution concentration of polyacrylamide increases, then the amount adsorbed reaches a maximum value and remains approximately constant with increasing polyacrylamide concentration. This 'plateau' corresponds to an adsorbed quantity of 42 mg PAM(100k) g^{-1} clay. The adsorption of polyacrylamide (7000k) does not appear to have reached its plateau value by a polymer solution concentration of 5 gdm^{-3}, although it does appear to be approaching its maximum adsorbed quantity (96 mg g^{-1}).

The adsorption of polyacrylamide of molecular weight 100k and 7000k visible in figure 6.3.1.1a, appears to be almost an order of magnitude lower than the maximum adsorbed amounts quoted by Bottero et al [155] and Schamp and Huylebroeck [156]. In fact, Bottero et al [155] quote maximum adsorption values of 250 mg g^{-1} clay and 680 mg g^{-1} clay for the adsorption of polyacrylamide, molecular weight 120k and 3000k respectively, on sodium montmorillonite.

Although our result appears to be very low, many explanations may exist for this large disparity. The most significant contribution to the discrepancy in adsorbed quantities is likely to be due the clay loading of the aqueous dispersion, or more accurately, the solid to liquid ratio (S/L), defined by Bailey et al [2] as the ratio of clay to total liquid volume. The effect of increasing the solid/liquid ratio on the adsorbed quantity here seems quite plausible, since increasing the solid loading will increase the flocculation of the bentonite platelets in the dispersion [157]. This flocculation will reduce the available surface area, restricting polyacrylamide access to the interlayer region. Bottero et al [155] obtained adsorbed quantities of an order of magnitude greater than

those found here at a solid to liquid ratio of about 2×10^{-3}. Interestingly, this is an order of magnitude less than the S/L ratio used to obtain the result presented here (20 gdm^{-3} aqueous bentonite suspension represents a S/L ratio of 2×10^{-2}). In addition, Bailey et al [2] showed that the adsorbed amount of neutral polyacrylamide, molecular weight $\sim 10^7$, decreased with increasing S/L ratio from 10^{-4} and 10^{-3}. Extrapolation of adsorbed quantities back to a S/L ratio of zero, revealed an adsorption maximum of 650 mg g^{-1} clay [2]. Similarly, Schamp and Huylebroeck [156] observed maximum adsorbed quantities of polyacrylamide (Mw 250k) of 757 and 787 mg g^{-1} clay at Na montmorillonite suspension concentrations of 0.05 and 0.025% w/v. These clay concentrations correspond to S/L ratios of 5×10^{-4} and 2.5×10^{-4} which are two orders of magnitude lower than those used in the studies presented here. Significantly, Stutzmann and Siffert [153] and Espinasse and Siffert [154] observed maximum adsorbed quantities for hydrolysed polyacrylamide (molecular weight of the order 10^6) on sodium montmorillonite between 3 and 15 mg g^{-1} clay. These low adsorption values are not unsurprising considering 1 g of clay was contacted with 20 ml of aqueous amide solution which represents a S/L ratio of 0.05 (greater than that used in our findings).

In addition to the S/L ratio, there are several other factors which might contribute to reduced polyacrylamide adsorption. The first, and most relevant factor to the results presented by Stutzmann and Siffert [153] and Espinasse and Siffert [154] is the anionicity of the polyacrylamide molecule. Polyacrylamide adsorption has been shown to be sensitive to the anionic content of the polyacrylamide, being significantly reduced at a 10% anionic content in low salinity conditions [2]. This is due to electrostatic repulsion between the negatively charged polymer segments and negatively charged mineral surface. This effect is probably small here since the polyacrylamide used is less than 3% anionic.

Another important feature which will restrict polyacrylamide adsorption on bentonite is the nature of the exchange cations in the interlayer region. The presence of exchange cations other than Na^+; for example K^+ and Ca^{2+}, in the interlayer will significantly reduce the ability of the bentonite platelets to disperse, reducing the accessible surface area and preventing polyacrylamide from penetrating between the platelets. Indeed, reduced polyacrylamide adsorption on H^+/Al^{3+} [156] and K^+ [2, 157] exchanged montmorillonite has been attributed to the reduced dispersion of the clay platelets in aqueous suspension.

Factors such as ionic strength and pH are also known to have a significant bearing on the adsorption of polyacrylamide onto bentonite [2]. However, at the pH and ionic strength used in these experiments, 7 and $<20 \ \mu Scm^{-1}$, respectively, no impact on the adsorbed quantity is expected. The effect of electrolyte ($100 \ gdm^{-3}$ KCl) can be observed in section 6.3.1.2.

Although significantly lower than the findings presented by other workers in this field, the findings presented in figure 6.3.1.1a for polyacrylamide, of molecular weight 100k and 7000k, tie in with the theory of polymer adsorption [100] that increased polymer adsorption is observed on increasing polymer molecular weight. Indeed, in the results presented here, the adsorption plateau increases from $42 \ mg \ g^{-1}$ clay to $96 \ mg \ g^{-1}$ clay on increasing the polyacrylamide molecular weight from 100k and 7000k. This follows a similar pattern to that observed by Bottero et al [155] and Schamp and Huylebroeck [156] (albeit at lower adsorbed amounts) who observed increased adsorption with increased molecular weight.

In contrast, however, the adsorption isotherm obtained for polyacrylamide (Mw 500k) on bentonite differs significantly from those obtained for polyacrylamide

of molecular weight 100k and 7000k shown in figure 6.3.1.1a. For polyacrylamide (Mw 500k), the amount adsorbed does not increase significantly at low polymer concentrations, in fact, at a polymer concentration of 1 gdm^{-3}, the adsorbed quantity is only 2.9 mg g^{-1} clay compared with 27.4 mg g^{-1} clay for polyacrylamide (Mw 100k) at the same concentration. In addition, a plateau region of maximum adsorbed polyacrylamide (Mw 500k) is not observed and the adsorbed quantity simply increases as the polymer solution concentration increases. Thus for 1 gdm^{-3} solutions, the order of polyacrylamide adsorption follows the series Mw 500k < Mw 100k < Mw 7000k. It is only at a concentration of 5 gdm^{-3} polyacrylamide (Mw 500k) in solution that the adsorbed quantity becomes comparable with, and actually increases above, the maximum adsorbed amount observed for polyacrylamide (Mw 100k).

The reason for the anomalous behaviour of the polyacrylamide (500k) is not fully understood. The three polyacrylamide samples were all supplied by Allied Colloids and differed only in their molecular weight. Obviously, more data points at intermediate concentrations would enable better determination of the isotherm profiles. However, the adsorbed quantities are reproducible and as a result it seems that the adsorption mechanism of polyacrylamide, of molecular weight 500k, differs from that of the lower (Mw 100K) and higher (Mw 7000k) molecular weight polyacrylamide.

One factor which might critically affect the adsorbed quantity of polyacrylamide (Mw 500k) is the intercalation of the polymer between the platelets. Schamp and Huylebroeck [156] suggested two mechanisms of polyacrylamide adsorption; surface adsorption in the interlayer region between bentonite platelets and adsorption in the pores created between stacks of platelets. However, this does not appear to explain the anomalous behaviour of polyacrylamide (Mw 500k) for several reasons. Firstly, polyacrylamide

adsorption should increase with molecular weight and it clearly does not for polyacrylamide of molecular weight 500k. Secondly, the clay platelets are dispersed in aqueous suspension and the polymer molecules would be expected to penetrate between them. Although penetration of polyacrylamide between the bentonite platelets has been shown to be reduced by the high S/L ratio used in these experiments, on drying, the polyacrylamide molecules would be trapped between bentonite platelets in the aqueous suspension to allow polymer intercalation. Finally, X-ray diffraction data presented later in this chapter (section 6.3.2) indicates that all molecular weights of polyacrylamide are adsorbed between the clay platelets and that increasing the solution concentration and molecular weight of polyacrylamide increases the interlayer spacing. Consequently, a transition from intercalated to non-intercalated bentonite-polyacrylamide complexes showing a molecular weight dependence does not appear to offer an explanation for the findings presented here.

A more plausible explanation is that the conformation of adsorbed polymer which is trapped between the platelets, or, of polymer in solution prior to adsorption between the platelets, is critical to the adsorption mechanism and subsequently to the quantity of adsorbed polymer. Schamp and Huylebroeck [156] observed a minimum in the adsorbed amount of polyacrylamide (Mw 250k) on Na montmorillonite. Similar minima were observed in the adsorption isotherms of polyacrylamide (Mw 140k) on H kaolinite and H illite (flocculated clays) and it was concluded that the observed minimum for a particular molecular weight is independent of the type and concentration of clay. The position of the minimum for adsorption of polyacrylamide (Mw 250k) on Na montmorillonite occurred at an initial polymer concentration between 0.5 and 1.0 gdm^{-3} [156]. It was postulated [156] that this polymer concentration corresponds to a phase transition of polyacrylamide in solution at which separate polyacrylamide molecules in solution interact. As a result, at this

concentration the polymer requires a larger surface area than is available and, accordingly, the adsorption decreases. The reduced adsorption of polyacrylamide (Mw 500k) in these studies, is most noticeable at a polyacrylamide concentration of 1 gdm^{-3}. This invites the question, what is the conformation of polyacrylamide both in solution and adsorbed between the platelets at these concentrations?

Bottero et al [155] did not report any similar reduction in the adsorption of polyacrylamide of molecular weight between 44k and 3000k onto sodium montmorillonite. However, this may be because these workers did not use equilibrium concentrations above 2 gdm^{-3} or that the large error (± 50 mg g^{-1} clay) in the adsorbed amount of polyacrylamide (Mw 44k) from solutions of concentration between 1 and 2 gdm^{-3} was not considered significant. This error may be associated with a reduction in the adsorbed amount at a characteristic solution concentration due to a particular conformation of polyacrylamide in solution prior to adsorption.

Although the X-ray diffraction and infrared experiments presented in sections 6.3.2 and 6.3.3 can provide no information regarding the conformation of polyacrylamide in solution, they can provide information regarding the interactions and conformation of the adsorbed polymer layer.

6.3.1.2   Effect of electrolyte (100 gdm^{-3} KCl loading)

The presence of electrolyte in solution can have a profound effect on the adsorption of polyacrylamide onto bentonite dispersed in aqueous suspension. Figure 6.3.1.2a displays the adsorption isotherms for the addition of polyacrylamide to SWy-1 bentonite in solution containing 100 gdm^{-3} KCl

Figure 6.3.1.2a Adsorption isotherms for the adsorption of polyacrylamide to SWy-1 bentonite in aqueous suspension containing 100 gdm^{-3} KCl.
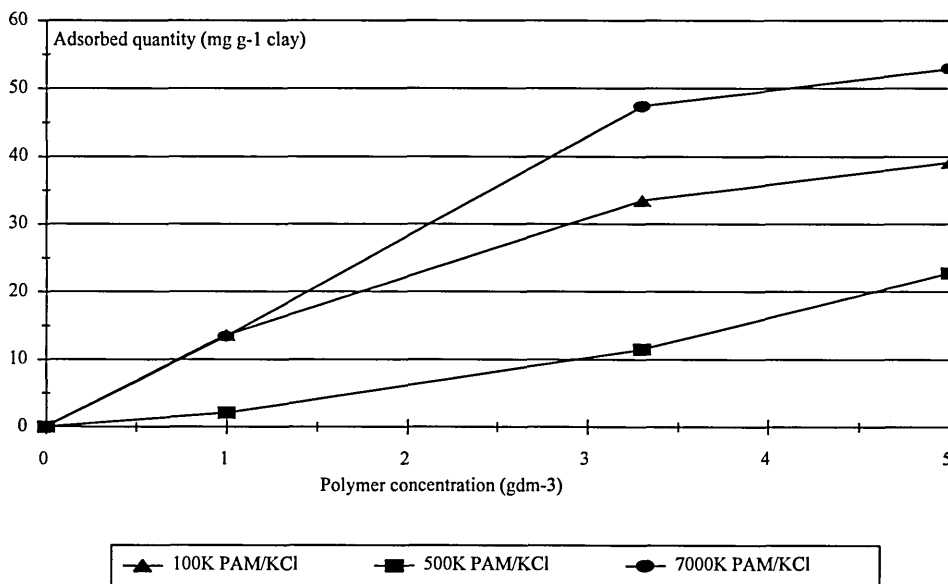
The effect of KCl on polyacrylamide adsorption can be most clearly observed for the adsorption of polyacrylamide (Mw 7000k) in figure 6.3.1.2a. As with adsorption of polyacrylamide (7000k) without the presence of KCl, the adsorbed amount increases at low polymer concentrations in solution. However, the adsorption isotherm in the presence of electrolyte, appears to reach a plateau corresponding to a maximum adsorption of 52.9 mg g^{-1} of clay. The quantity of adsorbed polyacrylamide in KCl solution is reduced by 50% of the maximum adsorbed amount of polyacrylamide (7000k) when KCl is not present.

The reasons for reduced adsorption in the presence of KCl have been discussed extensively by Bailey et al [2, 157, 170]. The adsorption of polyacrylamide (Mw ~10^7) has been shown to decrease significantly from a maximum adsorption of 650 mg g^{-1} clay to between 200 and 300 mg g^{-1} clay in the presence of 0.15 mole dm^{-3} KCl [2, 170]. This has been attributed to the collapse of the electrical double layer on increasing electrolyte concentration, causing flocculation and a reduction in adsorption.

The adsorption isotherm obtained for the adsorption of polyacrylamide (Mw 100k) from solution on aqueous bentonite suspension in the presence of 100 gdm^{-3} KCl also follows a similar adsorption isotherm profile as the corresponding adsorption process in the absence of KCl (figure 6.3.1.1a). The plateau value observed for polyacrylamide (Mw 100k) in KCl solution is still lower than that obtained for polyacrylamide (Mw 7000k) in KCl solution, however, the reduction in the maximum adsorbed amount is considerably less (only reduced by10%). The reduction in polyacrylamide (Mw 100k) adsorption is less in KCl solution than the reduction of polyacrylamide (Mw 7000k) in similar solution. Although the electrical double layer of the clay platelet will be collapsed to the same extent in both cases, the smaller molecule (lower molecular weight) will not be inhibited from penetrating between the platelets as at the higher molecular weight

The anomalous adsorption of polyacrylamide (Mw 500k) from solution not containing KCl is also observed in 100 gdm^{-3} KCl solution. Indeed, the adsorption isotherm follows an almost identical profile to that seen in the absence of KCl (figure 6.3.1.1a), having low adsorption at low polymer solution concentration, which increases with increasing polymer concentration without reaching a plateau value of maximum polymer adsorption. The adsorbed quantity of polyacrylamide (Mw 500k) is significantly reduced in the presence of KCl, indeed the adsorbed quantities at polymer solution concentrations of 3.3 and 5.0 gdm^{-3} are reduced by 60%.

It appears that access of polyacrylamide, of molecular weight 500k, to the interlayer region of the clay platelets is also reduced in the presence of electrolyte as it is for polyacrylamide of higher and lower molecular weight. However, the adsorption mechanism which determines such low adsorption quantities of polyacrylamide (Mw 500k) does not appear to be affected by the

presence of electrolyte in solution. In fact, it is notable that the reduction in the maximum adsorbed amount is greater for polyacrylamide of molecular weight 500k (~60%), than for the larger polyacrylamide of molecular weight 7000k (~50%). This finding supports the postulation that the adsorption of polyacrylamide (Mw 500k) is reduced due to the formation of large intermolecular polyacrylamide complexes at a critical concentration in solution. These large complexes would have a much larger surface area requirement and so adsorption decreases.

6.3.2.   X-ray diffraction

It is extremely important, with clay material, to understand where the polymer, in this case polyacrylamide, adsorbs. At the various molecular weights and concentrations in solution, polyacrylamide may adsorb exclusively on the external surfaces of the clay mineral or it may penetrate between the bentonite platelets and adsorb in the interlayer space. X-ray diffraction was performed on the dried centrifuged solids from the mixed dispersion in order to determine the change in clay d-spacing (if any) on addition of polyacrylamide.

The d-spacing of natural SWy-1 bentonite (without cation exchange) was determined to be 12.6Å, this corresponds to an interlayer separation of 3.0Å, due solely to the presence of water which surrounds the exchange cations in the interlayer space.

6.3.2.1   Without electrolyte (zero KCl loading)

The diffraction traces of the dried solid complex of mixed dispersions of aqueous polyacrylamide, molecular weight 100k, solution and aqueous bentonite suspension can be observed in figure 6.3.2.1a.

Figure 6.3.2.1a Diffraction traces of dried bentonite polyacrylamide (100k) complexes at various polyacrylamide solution concentrations.
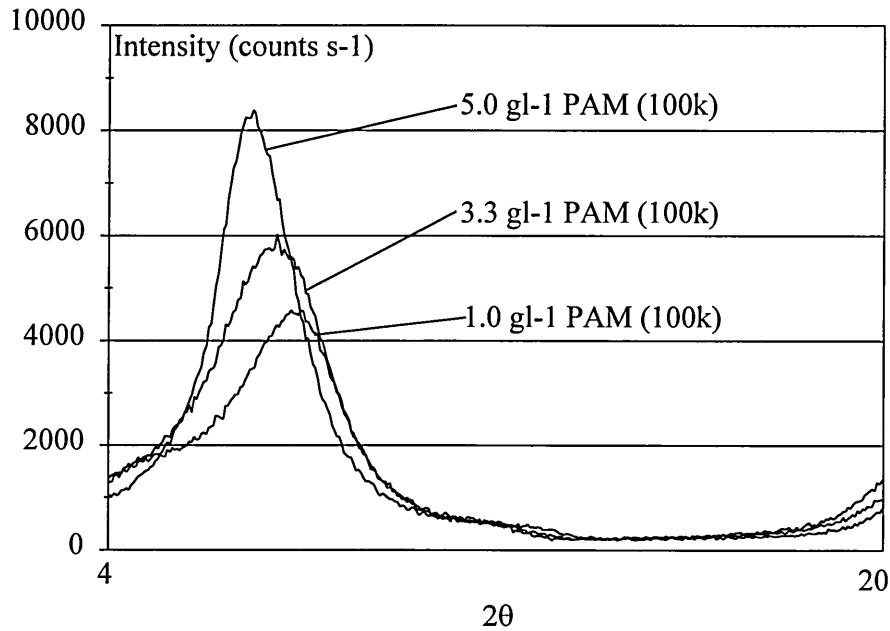
The intensity of the 001 diffracted X-ray is measured as a function of 2θ. Consequently, it should be remembered from the Bragg equation (eqn. 4.6.3.1) that for the first order reflection, at a given wavelength, the angle θ is inversely proportional to the distance separating the diffracting planes, d. Hence, in figure 6.3.2.1a, 2θ is observed to decrease with increasing polyacrylamide concentration which implies that the basal spacing increases with increasing concentration of polyacrylamide in solution.

Similarly, the X ray diffraction traces obtained from the dried solids of mixed dispersions of aqueous polyacrylamide, molecular weight 500k and 7000k, solutions and aqueous bentonite suspensions are shown in figures 6.3.2.1b and 6.3.2.1c, respectively.

Figure 6.3.2.1b Diffraction traces of dried bentonite polyacrylamide (500k)

complexes at various polyacrylamide solution concentrations.
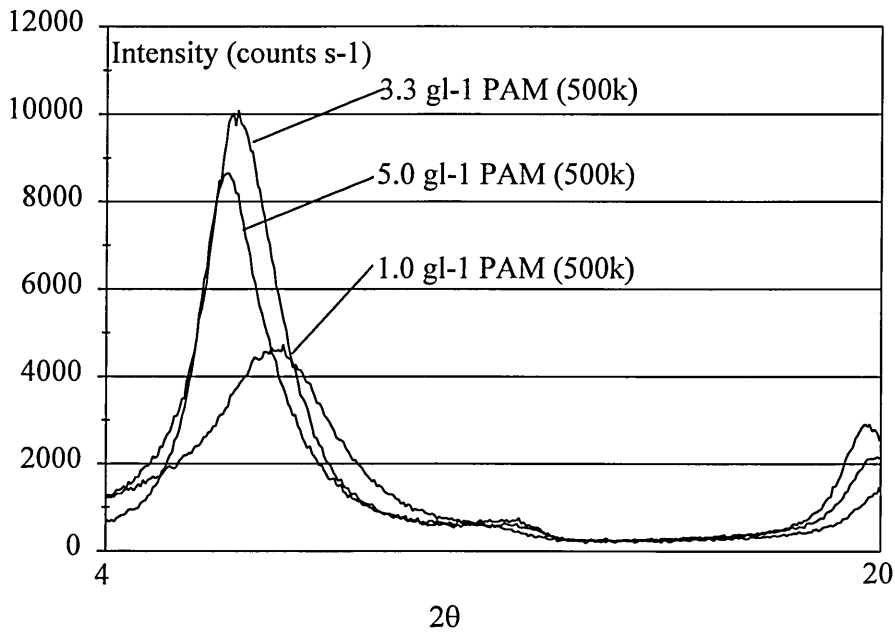
Figure 6.3.2.1c Diffraction traces of dried bentonite polyacrylamide (7000k)

complexes at various polyacrylamide solution concentrations.
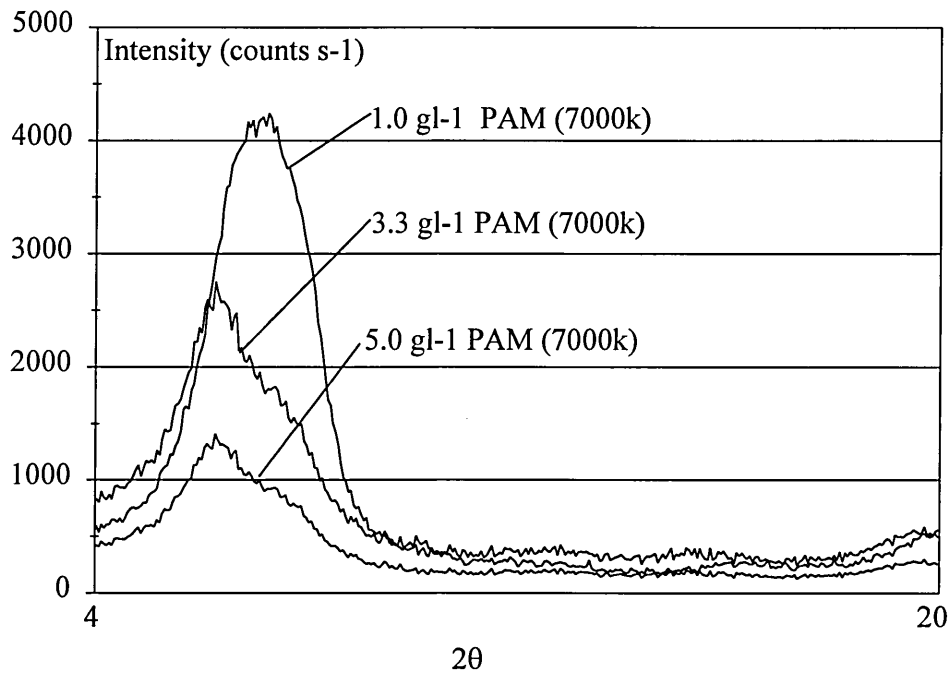
In figure 6.3.2.1b, the value of 2θ at which the intensity of the diffracted X-rays reach a maximum decreases with increasing concentration of polyacrylamide (Mw 500k) in solution. This corresponds to an increase in the basal spacing (the interlayer separation) with increasing polyacrylamide (Mw 500k) concentration. Similarly, in figure 6.3.2.1c, the d-spacing increases (value of 2θ corresponding to maximum intensity decreases) with increasing polyacrylamide (Mw 7000k) concentration.

Graph 6.3.2.1a shows the overall effect of polyacrylamide concentration on the d-spacing of dried complexes prepared by mixing aqueous bentonite suspension with polyacrylamide (molecular weight 100k, 500k and 7000k) in aqueous solution

Graph 6.3.2.1a Effect of polyacrylamide concentration on the d-spacing of dried, mixed bentonite-polyacrylamide complexes.
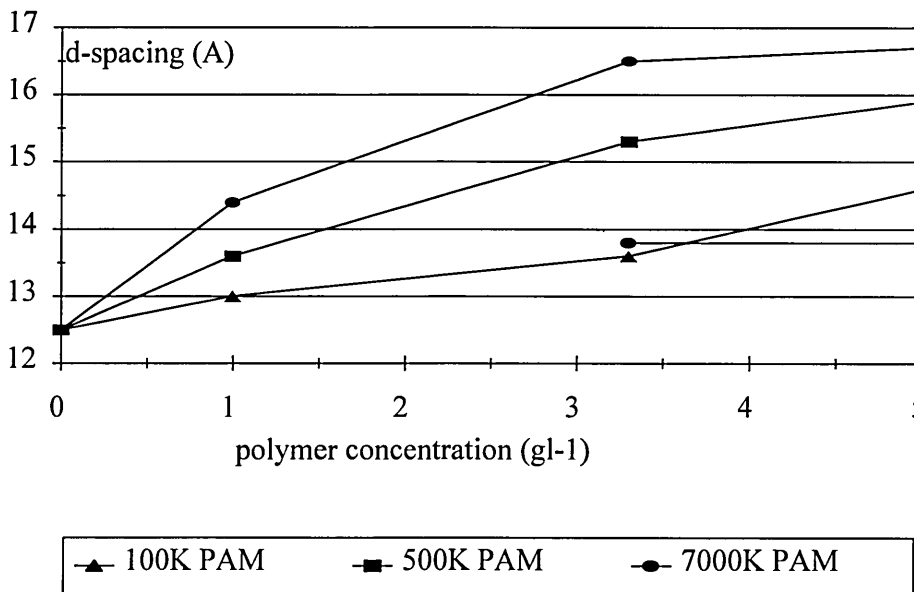
Increasing d-spacing with increased solution concentration of polyacrylamide have been observed previously by Bottero et al [155]. The observed d-spacings

for complexes prepared from 2 gdm^{-3} polyacrylamide (Mw 44k and Mw 3000k) solution ranged between 17Å and 20Å, respectively. The d-spacings observed here are much lower than those observed by Bottero et al [155]. This is not unlikely when one considers that the adsorbed quantities in our findings are also significantly lower than those observed by Bottero et al [155].

Whilst highlighting the increase in d-spacing on increasing concentration of polyacrylamide in solution, graph 6.3.2.1a also highlights another important feature; that the d-spacing also increases with increasing polyacrylamide molecular weight. Clearly, the d-spacing of the bentonite-polyacrylamide prepared at each polymer solution concentration follows the series, Mw 7000k > Mw 500k > Mw 100k.

It should be noted that the diffraction profiles observed in figures 6.3.2.1a and 6.3.2.1b for the adsorption of polyacrylamide of molecular weight 100k and 500k respectively are extremely broad and of low intensity. This is indicative of the diffraction trace of the complex having several maxima, relating to several 001 reflections. Individually, each maximum has quite a narrow profile but they are in such close proximity that they superimpose upon each other to give a broad peak. Several 001 reflections corresponds to several interlayer separations. Two maxima at 16.5 and 13.9 Å are clearly visible (figure 6.3.2.1c and graph 6.3.2.1a) in the diffraction trace of complexes prepared at the two higher polyacrylamide (Mw 7000k) concentrations, (3.3 gdm^{-3} and 5.0 gdm^{-3}). The presence of two interlayer spacings indicates that within the complex there are packets of platelets which have one spacing and which diffract radiation at a certain angle and other packets of platelets at another spacing.

The broad nature of the diffraction profiles makes it extremely difficult to determine the exact d-spacing of polyacrylamide complexes. However, it seems

likely that the interlayer separation corresponding to polyacrylamide intercalation corresponds to a d-spacing somewhere between 14.2 and 15.0Å. between the layers.

It is possible to calculate the expected interlayer separation by knowing the van der Waals radius of the polyacrylamide molecules. Although no reference to the van der Waals radius of the polyacrylamide molecule could be found, the van der Waals radius of isobutyramide (a monomer similar to polyacrylamide) is known to be 2.8Å [155]. Consequently, the theoretical d-spacing of the polyacrylamide complex may be calculated by adding the thickness of a bentonite platelet to the van der Waals diameter of the isobutyramide molecule. This implies that the d-spacing of a polyacrylamide-bentonite complex should be (9.6Å + 2x2.8Å)= 15.2Å when the polyacrylamide is adsorbed in a flat conformation [155]. This theoretical d-spacing is slightly greater than the upper end of the d-spacing range expected which may be due to approximating the van der Waals radius of polyacrylamide to that of isobutyramide in the d-spacing calculation. More likely however, is that the polyacrylamide molecule may key into di-trigonal cavities in the silicate surface of the clay platelet, reducing the d-spacing slightly.

It should be noted that lower d-spacings are observed at low adsorbed amounts which corresponds to polyacrylamide adsorbed in a flat conformation [155]. However, much larger d-spacings (>15.2Å) are observed in complexes prepared by the adsorption of polyacrylamide (500k and 7000k) from 3.3 and 5.0 gdm^{-3} solutions. This agrees with the findings of Bottero et al [155] who observed an increase in the loop size of adsorbed polyacrylamide chains on bentonite as the adsorbed amount of high molecular weight polymer increased.

It should be noted that the d-spacing of complexes prepared using polyacrylamide, of molecular weight 500k, do not show the same anomalous behaviour shown by adsorption isotherms of these particular complexes. In fact, the bentonite-polyacrylamide (Mw 500k) complex prepared from a 1 gdm^{-3} solution has an intercalated d-spacing in the region between 14.0 and 15.2Å. This corresponds to a low adsorbed amount in which the polyacrylamide is adsorbed in a flat conformation. This would be expected as the amount of polyacrylamide is significantly reduced, we believe, by the intermolecular interaction between polyacrylamide molecules at a critical solution concentration. It is possible that the very small amount of polyacrylamide adsorbed between the platelets has actually been trapped between the bentonite platelets as the complex is dried. Consequently, some differences may exist in the conformation of polyacrylamide (Mw 500k) which can not be detected using X-ray diffraction but have been detected using infrared spectroscopy.

These tentative interpretations assume one important factor; that the d (001) spacing obtained from the X-ray diffraction trace are due solely to polyacrylamide in the interlayer space. It does not allow for partial expansion of the platelets due to water in the interlayer region. In order to determine the extent to which water contributes to the interlayer separation, it would be extremely advantageous to perform heated experiments in order to drive water out of the interlayer space. Diffraction maxima from such an experiment would correspond to the platelet separation caused by polymer alone. As a result, it can not be unequivocally stated that the d-spacings observed are due solely to polyacrylamide in the interlayer space. Further experimentation to establish the influence of water on the behaviour of polyacrylamide in the interlayer space is still necessary to prove or disprove these postulations.

6.3.2.2 Effect of electrolyte (100 gdm^{-3} KCl loading)

The diffraction trace obtained from glass slides coated with the centrifuged solids from mixed bentonite-polyacrylamide complexes prepared in the presence of 100 gdm^{-3} KCl showed negligible or very broad maxima in the region between 4 and 20 2θ. Figure 6.3.2.2a shows typical diffraction traces, in this case for the dried centrifuged solids obtained from mixed aqueous polyacrylamide (100k) and aqueous bentonite suspension

Figure 6.3.4.3.3a Diffraction traces for the dried bentonite- polyacrylamide (100k) complexes prepared in 100 gdm^{-3} KCl solutions.
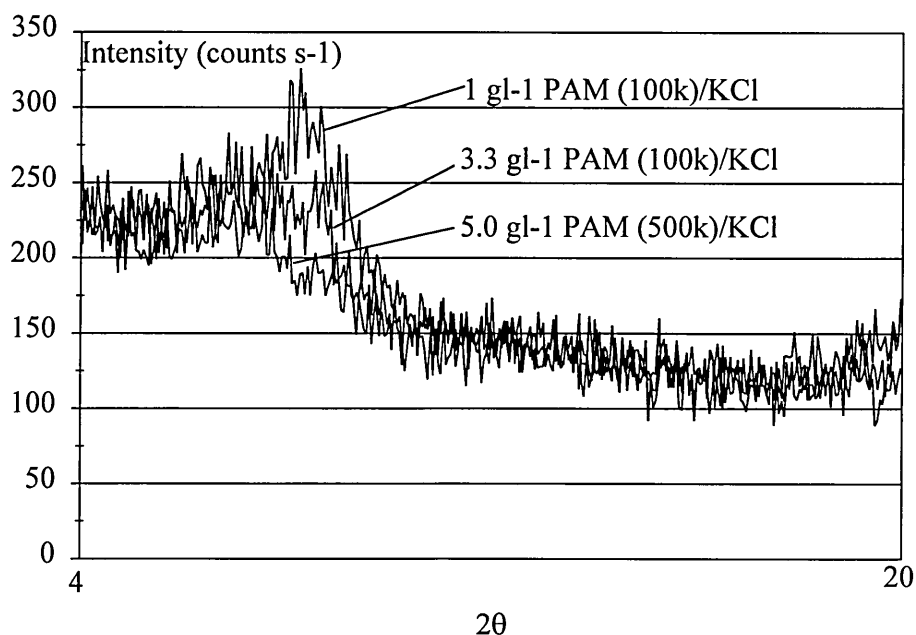
The maxima observed in the diffraction trace of a 1 gdm^{-3} polyacrylamide (100k) complex corresponds to a d-spacing of 12.7 Å, i.e. bentonite without adsorbed polyacrylamide. Although a maximum can be observed in the diffraction trace, its intensity is very low, between 100 and 200 counts s^{-1} compared to between 2000 and 10000 counts s^{-1} in the complexes prepared in the absence of KCl. This is attributed to insufficient numbers of platelets

210

stacking together in packets with the same d-spacing, to provide coherent basal (001) diffraction. Several reasons for this exist, the most important, being the sample preparation. If these samples had not been prepared as films on glass slides but instead, finely ground and studied, as a randomly oriented powder, then more coherent scattering might have been observed.

6.3.3.   Infrared studies

6.3.3.1. Transmission spectra of polyacrylamide

Figure 6.3.3.1a shows a typical transmission spectrum of negligible ionic strength polyacrylamide (Mw 7000k) dispersed in a thin potassium bromide disk and ratioed against an air background.

Table 6.3.3.1a gives the band assignments of the principal bands in the infrared spectrum, based on the assignments by Kulicke et al [233].

Figure 6.3.3.1a Infrared spectrum of polyacrylamide
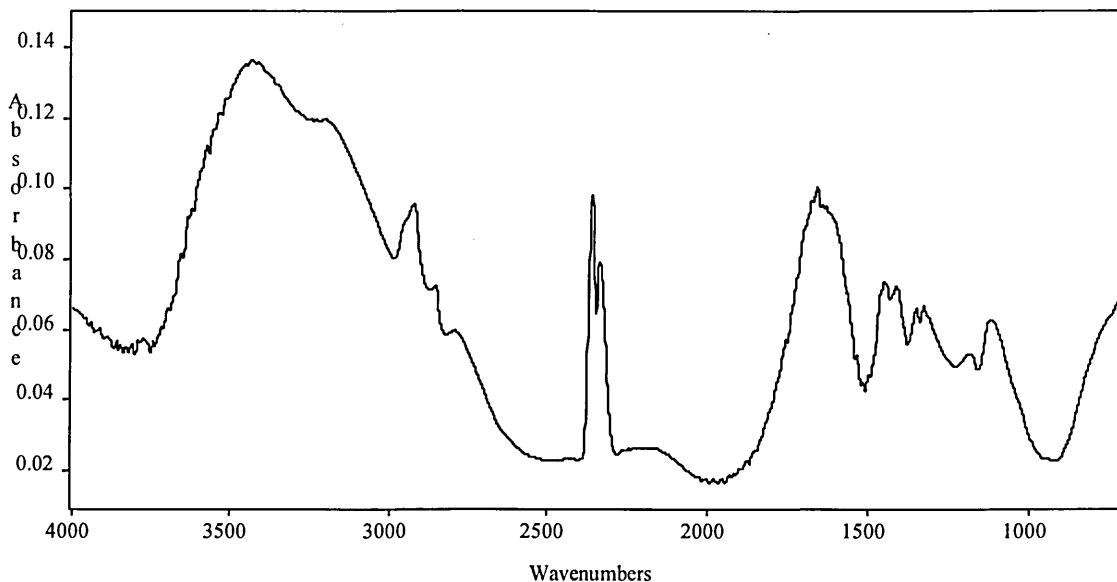
Table 6.3.3.1. Band assignments for polyacrylamide

Band position (cm^{-1})	Assignment
3440	H-bonded ν(OH) (water)
3330	antisymmetric ν(NH$_2$)
3190	symmetric ν(NH$_2$)
2960	antisymmetric ν(CH$_3$)
2930	antisymmetric ν(CH$_2$)
2870	symmetric ν(CH$_2$)
1660	ν(C=O) (amide I)
1615	δ(NH$_2$) (amide II)
1450	δ(CH$_2$)
1410	ν(C-N)
1351	w(CH$_2$)

It is important to note that polyacrylamide has only one infrared absorption band (at 1120 cm^{-1}) in the spectral region between 1250 and 850 cm^{-1}. This is extremely useful since no absorption bands overlap with the Si-O stretching bands which occur between 1100 and 1000 cm^{-1}. Consequently, adsorption of polyacrylamide onto the silicate surface of a bentonite clay platelet may be observed spectroscopically.

The absorption at 2960 cm^{-1} has been assigned to the antisymmetric ν(CH$_3$) vibration (due to terminal methyl groups). This band is lower in intensity than the bands attributed to CH$_2$ antisymmetric and symmetric stretching modes (at 2930 and 2870 cm^{-1}, respectively) since, there are relatively fewer terminal methyl groups on the polyacrylamide (Mw 7000k). However, the intensity of the band at 2960 cm^{-1} relative to the bands at 2930 and 2870 cm^{-1}

(approximately half that of the band at 2930 cm^{-1}) does not reflect the relative numbers of main chain CH$_2$ and CH$_3$ groups. This may be indicative of a polydisperse sample, in which there are significant numbers of polyacrylamide molecules with molecular weight less than 7000k. This would increase the number of terminal groups (CH$_3$) relative to the number of main chain CH$_2$ groups in a particular sample.

Figure 6.3.1b shows a comparison of the infrared spectrum of nonionic (negligible ionic) and 30% anionic polyacrylamide, evenly dispersed in a KBr disk, in the region between 4000 and 2600 cm^{-1} (both spectra have been ratioed against an air background).

<u>Figure 6.3.3.1b Comparison of infrared spectrum of nonionic and 30% anionic polyacrylamide.</u>
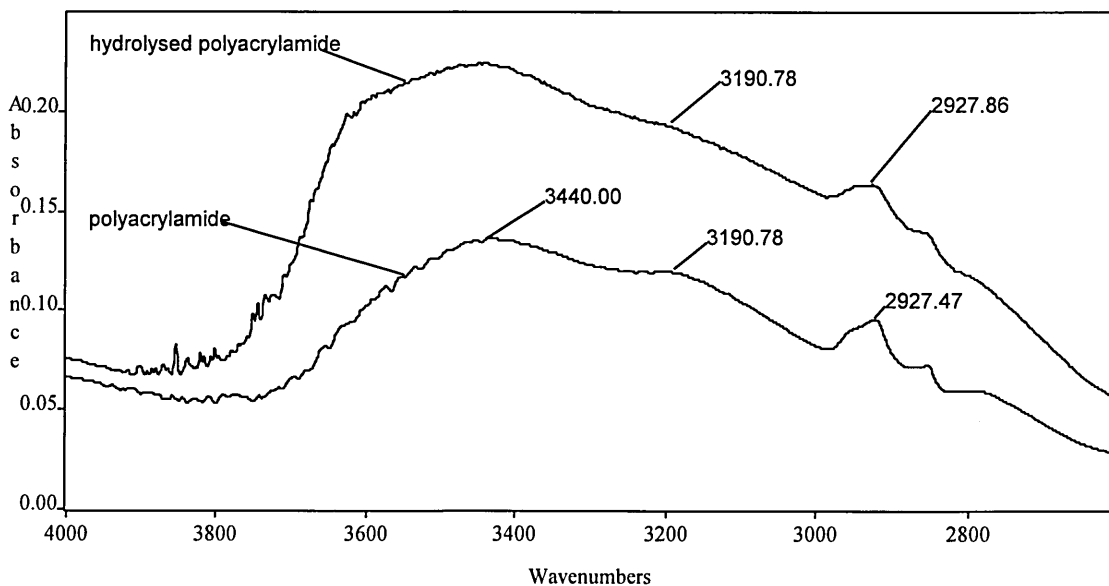
The most intense band in this region is the band at 3440 cm^{-1}. This band is attributed to an OH stretching mode which indicates that a significant amount of hydrogen bonded water is present in both the solid polyacrylamide and solid

hydrolysed polyacrylamide samples. The broad nature of both spectra in this region may also be indicative of a significant amount of hydrogen bonded water.

It must, of course, be borne in mind that the nominally neutral polyacrylamide used in these experiments, contains a small, albeit less than 3%, anionic functionality and that the hydrolysed polyacrylamide sample contains approximately 30% (COO^-) functionality. Both are therefore likely to contain small amounts of hydrogen bonded -COOH acid, which further complicates the spectral region between 4000 and 2600 cm^{-1}.

It seems likely then, that the broad nature of the infrared absorption bands in this region may also indicate that the bands are subject to inhomogeneous broadening due to each molecule (or functionality which gives rise to an absorption band in this region) existing in a heterogeneous environment. Bellamy [234] states that amide molecules strongly self associate unless they are in dilute solutions in polar solvents. As a result it can be inferred that in the solid, polymer molecules are involved in a large number of inter and intramolecular hydrogen bonds between units on separate polyacrylamide molecules and also between separate units on the same polymer chain. Indeed, the band visible at 3190 cm^{-1}, due to the symmetric NH_2 stretching mode, provides further evidence of H-bonding, since the position of this band corresponds to hydrogen bonded NH_2 [235]; the band due to a hydrogen bonded antisymmetric stretching mode would be visible at 3330 cm^{-1} if the intense band attributed to OH stretching mode were not present. It should be noted that infrared absorption bands due to non hydrogen bonded antisymmetric and symmetric NH_2 modes of a primary amide would be found at higher frequency, near 3520 and 3410 cm^{-1} respectively [235].

It should also be noted that the shoulder band at 3190 cm^{-1} (NH$_2$ symmetric stretching mode) appears to be more intense relative to the band at 2927 cm^{-1} (antisymmetric C-H stretch) in the spectrum of neutral polyacrylamide compared to that of anionic polyacrylamide. This is likely to be due to the hydrolysis of some NH$_2$ functional groups on the anionic polymer, reducing the NH$_2$ band intensity in the spectrum of the hydrolysed polymer. Further evidence of this should be found at lower frequency, i.e. in the amide I and II stretching regions (figure 6.3.3.1c).

Figure 6.3.3.1c Comparison of infrared spectrum of nonionic and 30% anionic polyacrylamide.
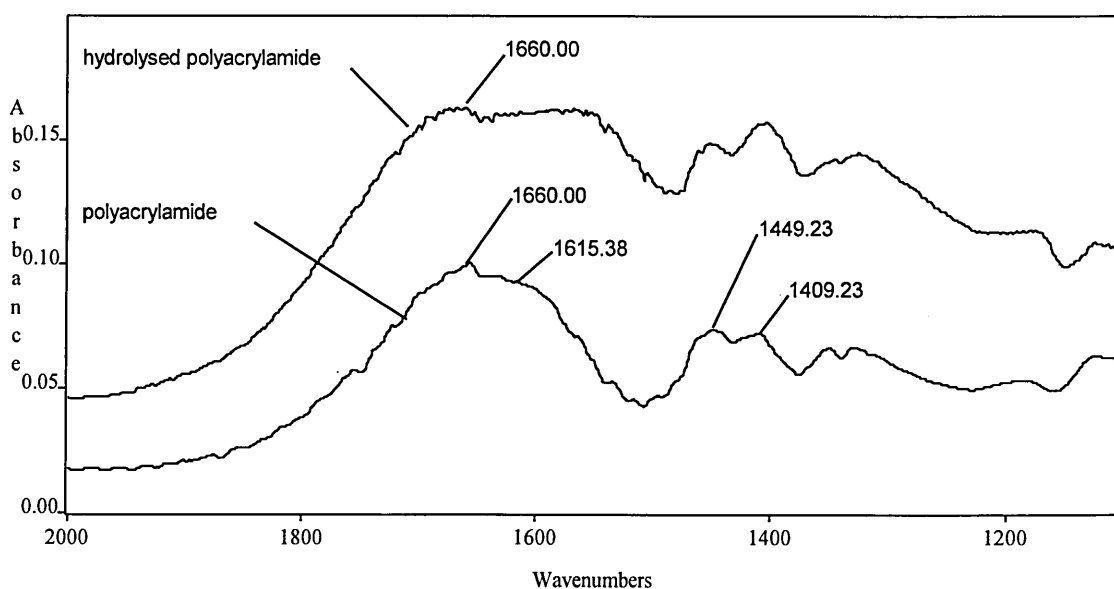
The bands observed at lower frequency in the spectra of polyacrylamide and hydrolysed polyacrylamide (figure 6.3.3.1c) are also very broad (as they are at higher frequency, between 4000 and 2600 cm^{-1}). The broad nature of the bands makes it extremely difficult to determine band positions and relative intensities with any certainty. Unfortunately, quantitative determination of the band positions and relative intensities using FSD, SD and CF is impossible due to the

presence of water vapour, spectral noise and high local baselines. However, the infrared absorption at 1660 cm^{-1} may be attributed to the amide I band (C=O stretching mode) since it agrees with the value stated by Kulicke [233] and is close to 1650 cm^{-1}, the wavenumber position predicted for the amide I band in solid primary amides by Bellamy [235]. This band would be expected to be shifted to higher frequency in solution where the polyacrylamide molecules are involved in less hydrogen bonding interactions than in the pure solid.

The position of the amide II band however, is somewhat more difficult to determine. In the solid neutral polymer, it appears to be situated at 1615 cm^{-1} which agrees with the wavenumber position cited in the literature [235]. However, an extra band, between 1700 and 1600 cm^{-1}, due to an H-O-H bending mode (of water) would also be expected in both spectra shown in figure 6.3.1c, since both polymers showed intense bands due to OH stretching modes in the region between 4000 and 2600 cm^{-1}. The H-O-H bending band would distort the spectra shown in figure 6.3.1c causing band positions and relative intensities to appear shifted and altered. As a result, it is extremely difficult to determine the exact position of the amide II band, particularly in the spectrum of hydrolysed polyacrylamide. This makes it impossible to determine the absorbance ratio A(amide I)/A(amide II) and hence the effect on the ratio of increasing the anionic content of the polymer from zero to 30%.

Again, the broad nature of the bands in the spectral region between 2000 and 1100 cm^{-1} may be indicative of inhomogeneous broadening. This has been attributed to the heterogeneous environment of polymer functional groups (C=O and NH$_2$), i.e. the large number of intra and intermolecular hydrogen bonds in the solid polymer.

As with any infrared analysis, sample preparation appears to make a significant contribution to the infrared spectrum obtained. Indeed, differences have been observed between the transmission infrared spectrum of polyacrylamide evenly dispersed in a KBr disk as shown in figure 6.3.3.1a and the infrared ATR spectrum of polyacrylamide deposited onto the sampling face of the ZnSe Squarecol ATR prism (figure 6.3.3.1d).

Figure 6.3.3.1d Comparison of the transmission and ATR infrared spectra of solid neutral polyacrylamide.
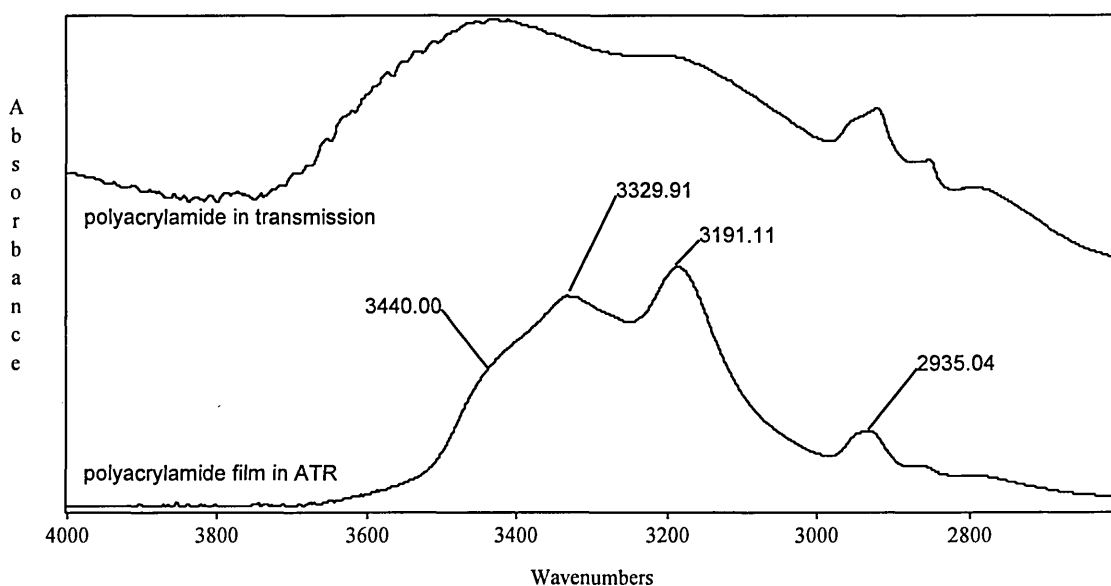
The first point to note is that the ATR spectrum of neutral polyacrylamide is significantly narrower in the spectral region between 4000 and 2600 cm^{-1} than in the transmission spectrum, probably due to the removal of water on drying the film at 65°C. Consequently, the OH stretching band at 3440 cm^{-1} now appears as a high frequency shoulder to the bands at 3330 and 3190 cm^{-1} (NH_2 antisymmetric and symmetric stretching bands). Additionally, it is interesting to note that the wavenumber position of the bands at 3330 and 3190 cm^{-1} are unchanged from their position in the transmission spectrum of neutral polyacrylamide. This indicates that despite containing considerably less water, NH_2 groups on the polyacrylamide molecules in the solid film are still involved

in extensive hydrogen bonding (probably intra and intermolecular hydrogen

bonds)

6.3.3.2. Adsorption of polyacrylamide onto free standing bentonite films

The infrared spectrum of an SWy-1 bentonite film is shown in figure 6.3.2a.

Figure 6.3.3.2a Infrared spectrum of a free standing SWy-1 bentonite film.

Wavenumbers
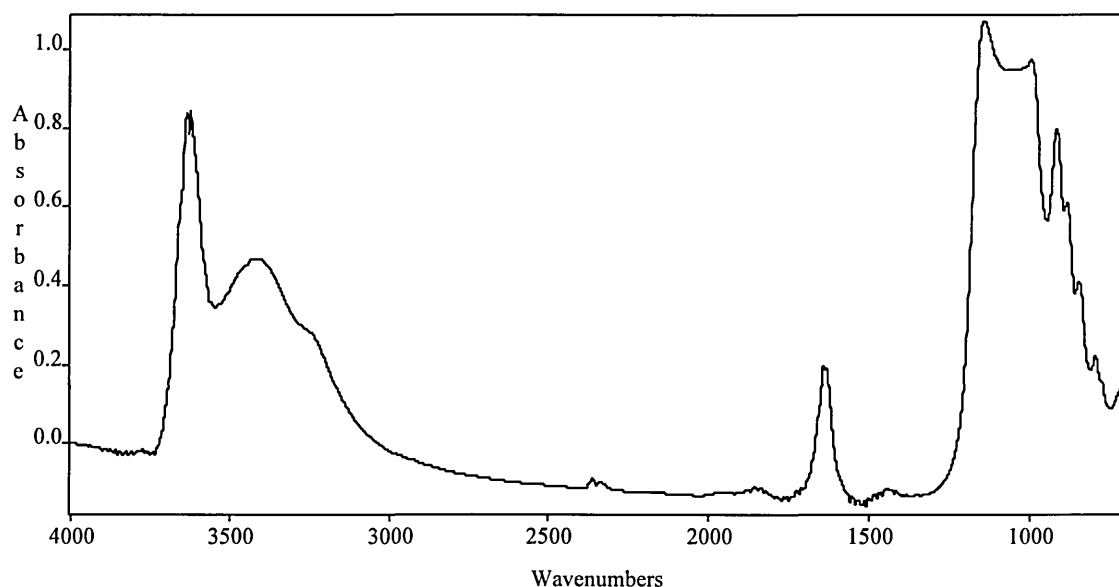
In the region between 4000 and 1100 cm^{-1}, the film has an identical spectrum to

that of pure bentonite dispersed in a KBr disk as shown in figure 5.3.1a.

However, due to the thickness of the film, the intense Si-O stretching bands

(between 1100 and 950 cm^{-1}) cause the spectrum to appear 'cut off'. Below 950

cm^{-1} the OH deformation bands become observable.

None of the free standing bentonite films remained intact when immersed in

aqueous polyacrylamide solution, regardless of the concentration or the

molecular weight of polyacrylamide present. Not even the presence of

100 gdm^{-3} KCl in solution (KCl is a flocculating agent expected to inhibit bentonite dispersion) could prevent the dispersion of the bentonite films. After immersion in solution, the films degraded and broke apart and the bentonite could be seen to form a flocculated gel. This could not be removed and analysed as a free standing film since it had essentially become a bentonite-polyacrylamide dispersion with a very low clay loading (between 5 and 7 mg in solution).

This result seems to indicate that polyacrylamide is not, by itself, a polymer which may rigidly stabilise clay containing shale in the wellbore. However, large excesses of polyacrylamide may help to form flocculated gel structures with dispersed bentonite which limit full bentonite dispersion. Consequently, polyacrylamide would be expected to contribute to the stabilisation of both the borehole and drilled cuttings dispersed in the drilling fluid.

6.3.3.3. Adsorption of polyacrylamide onto bentonite films supported on an ATR prism

Figure 6.3.3.3a shows the infrared spectrum of the silicon Squarecol ATR prism coated on each sampling face with an air dried bentonite film and ratioed against the ATR prism with clean sampling faces. The spectrum appears to be very similar to the infrared spectrum of the free standing bentonite film in figure 6.3.3.2a and, hence, has the typical features and assignments of the bentonite infrared spectrum described in table 5.3.1. However, this spectrum has a very strange absorption band profile below 1500 cm^{-1} due to intense Si-O vibrations of the silicon ATR prism. Figure 6.3.3.3b shows the spectrum of the clean silicon ATR prism ratioed against an air background which clearly shows 'cut off' due to the intense Si-O absorption bands of the silicon crystal below 1500 cm^{-1}.

Figure 6.3.3.3a Infrared spectrum of the silicon Squarecol ATR prism coated with an air dried bentonite film.
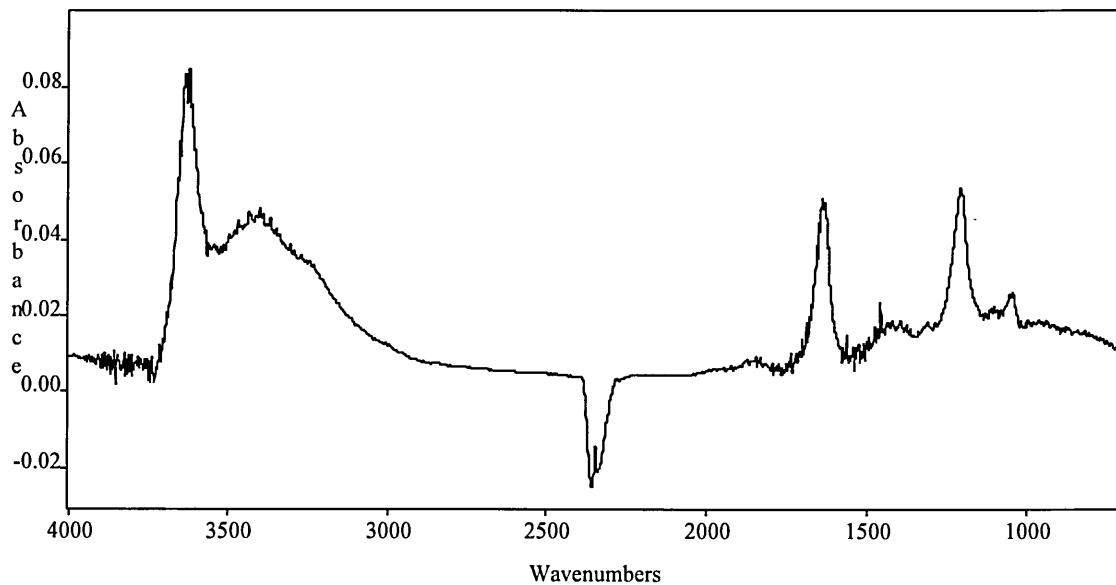
Figure 6.3.3.3b The infrared spectrum of a clean silicon ATR prism
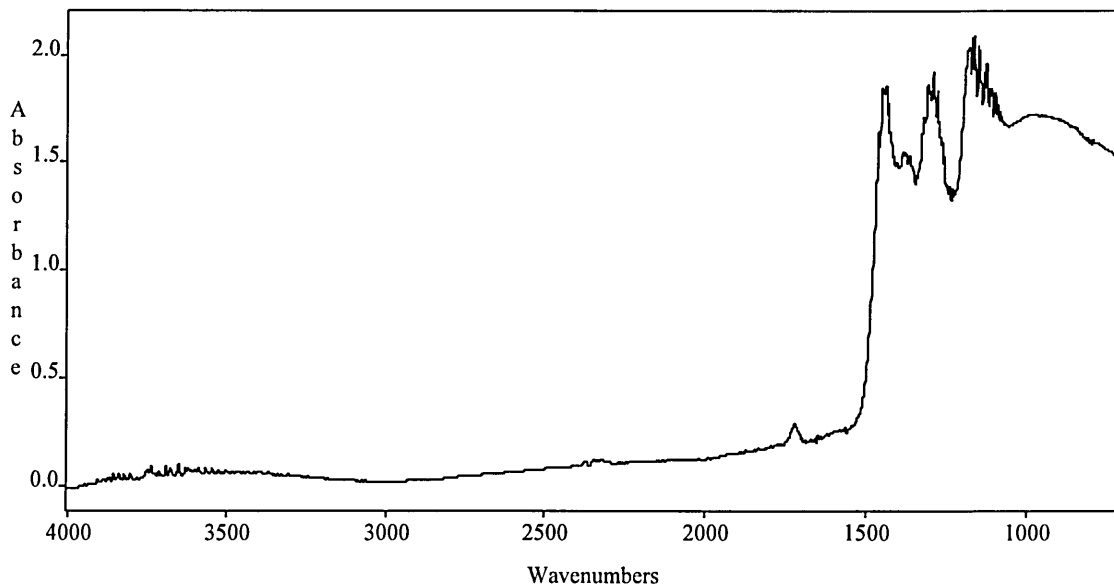
The intense Si-O vibrations of the ATR prism ensure that any sample vibrations below 1500 cm^{-1} (bentonite or polyacrylamide) cannot be studied using Si-ATR spectroscopy. This does not present a significant problem since the region between 1100 and 950 cm^{-1} could not be studied anyway due to cut off by the intense Si-O vibrations of the film.

The addition of 1 gdm^{-3} aqueous polyacrylamide (7000k) solution to the trough of the Squarecol cell containing bentonite coated optics has a profound effect on the infrared spectrum of the supported bentonite film. Figure 6.3.3.3c shows the evolution of the infrared spectra of the supported bentonite film in the region between 4000 and 2600 cm^{-1} on addition of 1 gdm^{-3} aqueous polyacrylamide (7000k) solution to the trough of the Squarecol cell.

Figure 6.3.3.3c The evolution of infrared spectra after addition of 1 gdm^{-3} aqueous polyacrylamide (7000k) solution to bentonite coated Si IRE. Spectra stacked for clarity.
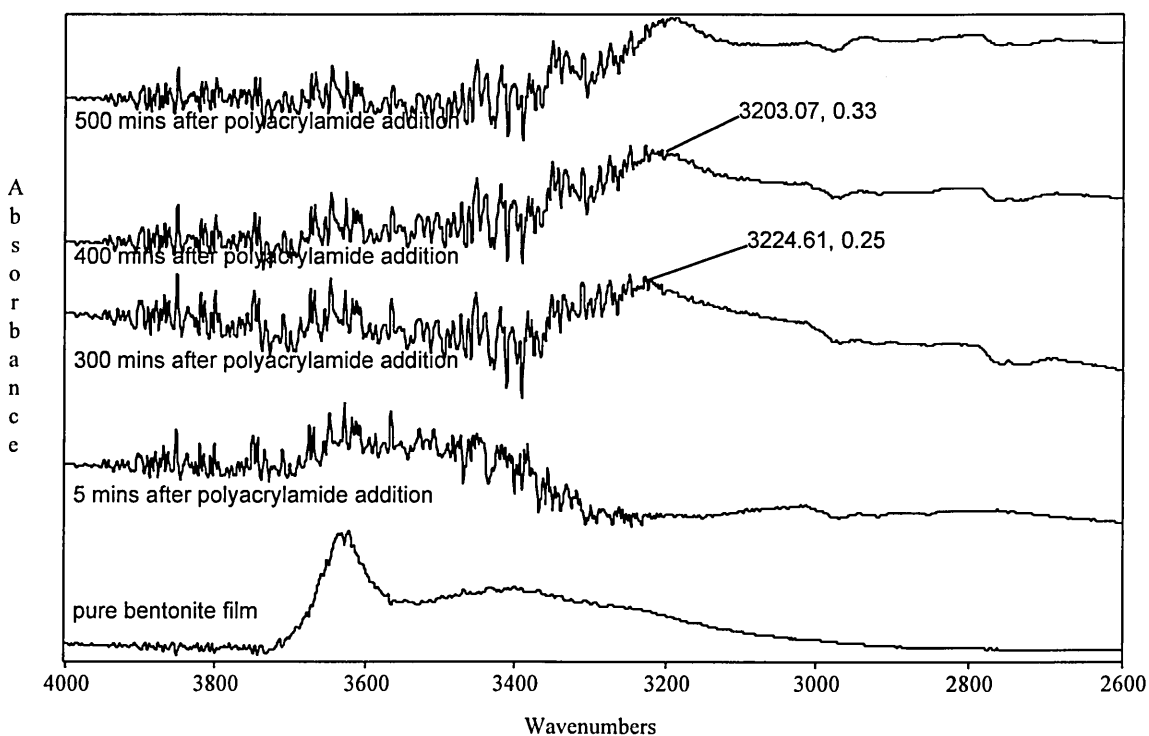
The spectrum of pure water has been dynamically subtracted from the spectra presented in figure 6.3.3.3c to allow the polyacrylamide bands in this region to be analysed. The spectra contain a considerable amount of water vapour and, at the low absorbance levels encountered (<0.1 absorbance units), noise also makes a significant contribution to the spectra causing the bands to appear distorted. Consequently, the spectra have been stacked for clarity.

From figure 6.3.3.3c, it can be seen that the characteristic bentonite band at 3630 cm^{-1}, which has an intensity of 0.08 absorbance units in the spectrum of the supported bentonite film, has completely disappeared (or been reduced in intensity to less than 0.02 absorbance units where it will be masked by water vapour) just 5 mins (the time taken to acquire the first spectrum) after addition of the 1 gdm^{-3} polyacrylamide solution.

There is no evidence of any absorption band in the 3200 cm^{-1} region of the spectrum after acquisition of the first spectrum (5 mins) following addition of polyacrylamide solution. However, after only a further 20 mins, a band appears at ~3225 cm^{-1} which is still present after 300 mins which has been assigned to the characteristic symmetric NH_2 stretch of polyacrylamide in aqueous solution [235]. This band is later seen to shift to lower frequency, being found at 3203 cm^{-1} after 400 mins and 3190 cm^{-1} after 500 mins. The position of this band is indicative of solid polyacrylamide and it may be concluded that after 500 mins the polyacrylamide molecules in the aqueous solution in the region close to the sampling face of the ATR prism are involved in extensive intra and intermolecular H-bonding. This seems to indicate that as the experiment progresses, polyacrylamide molecules assemble at the solid-liquid interface (in the region close to the prism sampled by the exponentially decaying evanescent field)

Figure 6.3.3.3d shows the region of the infrared spectrum between 2000 and 1500 cm^{-1} after addition of 1 gdm^{-3} aqueous polyacrylamide (7000k) solution to the trough of the Squarecol cell containing bentonite coated optics.

Figure 6.3.3.3d The evolution of infrared spectra after addition of 1 gdm^{-3} aqueous polyacrylamide (7000k) solution to bentonite coated Si IRE.
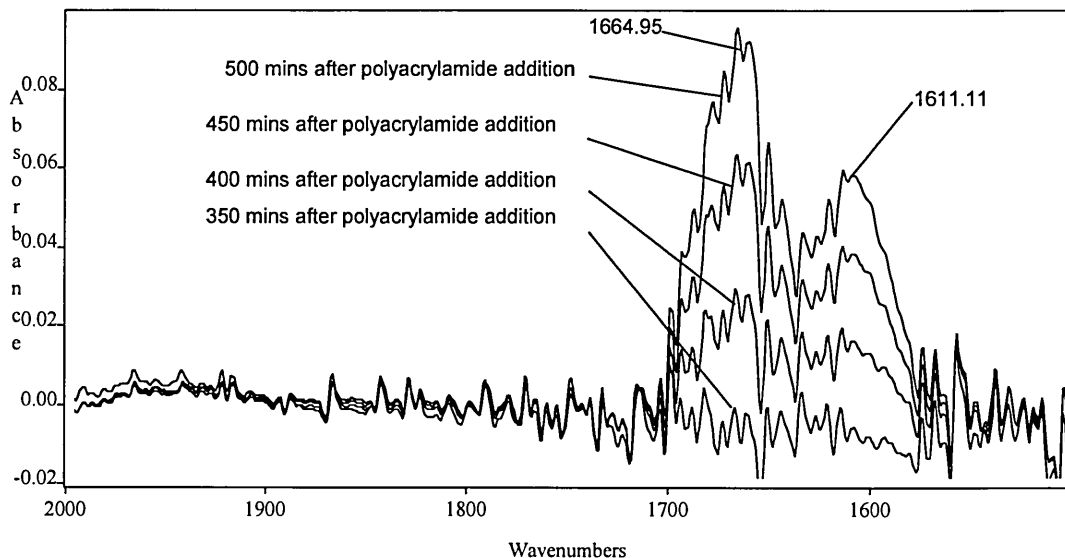

Again the spectra are distorted by water vapour and noise, however after 400 mins the first evidence of polyacrylamide can be observed by the appearance of the amide I and amide II bands at 1664 cm^{-1} and 1611 cm^{-1} respectively. The position of the amide I band is very close to its value in solid polyacrylamide and is indicative of polyacrylamide involved in extensive intra and inter molecular hydrogen bonding. These bands increase further in intensity as time progresses and as more polyacrylamide diffuses closer to the ATR prism and into the depth sampled by the evanescent field. This supports the earlier finding that the polyacrylamide concentration is increasing in the region sampled by the evanescent field, due to polymer assembly at the solid-liquid interface.

In addition, when the cell is dismantled at the termination of the experiment (after 500 mins), the bentonite film is not intact on the surface of the ATR prism but exists as a flocculated slurry in the trough of the Squarecol cell.

It seems likely that the evanescent field is unable to sample the interaction between bentonite and polyacrylamide because the bentonite platelets which comprise the film, are hydrated and dispersed before the polymer can interact with them. Consequently, bands observed in the infrared spectrum are likely to be due predominantly to polyacrylamide in solution and in particular polyacrylamide assembly at the water/Si ATR prism interface.

These findings are hardly surprising since they mirror the results obtained from experiments on self supporting bentonite films. The supported bentonite films in these experiments appear not to be rigidly stabilised by the presence of excess aqueous polyacrylamide solution. The water is likely to disperse the bentonite, indicated by the almost immediate disappearance of characteristic bentonite bands, before the polyacrylamide is able to interact with the bentonite. The polyacrylamide bands observed are likely to be due to diffusion of polyacrylamide into the region near the ATR prism sampled by the evanescent field or even adsorption of polyacrylamide at the solid-liquid interface. The diffusion or adsorption of polyacrylamide may be inhibited by adsorption onto dispersed bentonite in the solution or even adsorption of polyacrylamide onto the small amount of bentonite which may still reside on the ATR surface.

As in the analogous experiment using an unsupported bentonite film, it may be concluded that, although polyacrylamide does not rigidly stabilise the bentonite film, it does form flocculated gel structures with dispersed bentonite. These flocculated gel structures will aid the stabilisation of bentonite which comprises

a significant proportion of the shale in the borehole and in drilled cuttings contained in the oil well drilling fluid.

6.3.3.4. Adsorption of polyacrylamide onto dispersed bentonite

Although the measurement of adsorption isotherms provides information regarding the amount of adsorbed polyacrylamide and the adsorption mechanism, it does not provide information regarding the state of the adsorbed layer. Consequently, infrared spectroscopy has been used in order to understand the interaction between polyacrylamide and bentonite in aqueous dispersion and the conformation of adsorbed polymer. Figure 6.3.3.4.a shows the spectral region between 4000 and 2600 cm^{-1} of the infrared spectrum of the dried centrifuged solids from a mixed dispersion of aqueous bentonite suspension and polyacrylamide (Mw 100k) solution of concentrations 5, 3.3, and 1 gdm^{-3}.

Figure 6.3.3.4a The infrared transmission spectra of dried bentonite-polyacrylamide (Mw 100k) complexes at various polymer concentrations.
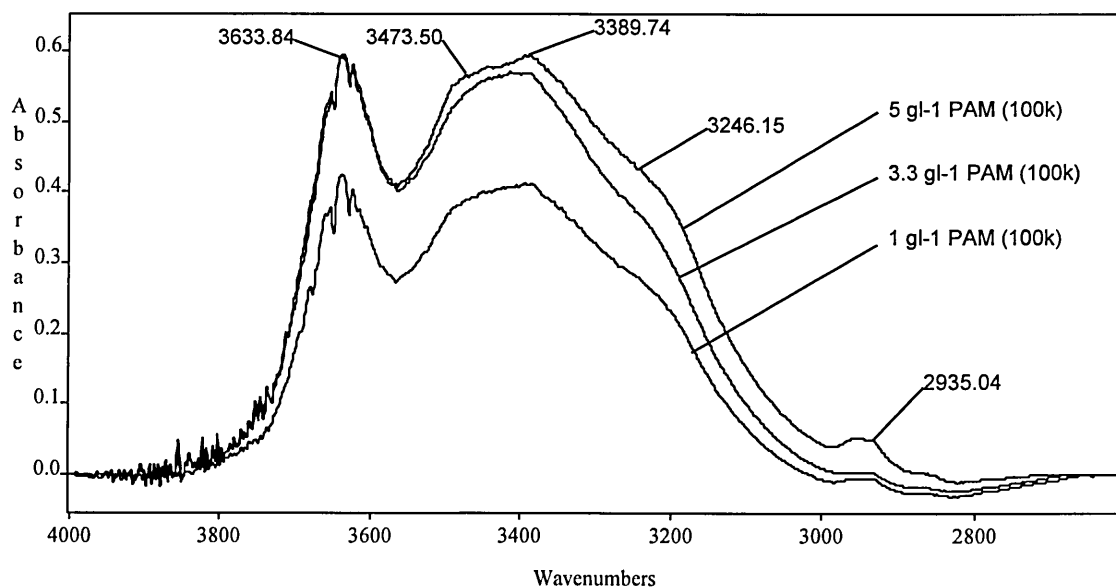
The spectra of the dried solids from aqueous bentonite suspensions mixed with aqueous polyacrylamide solutions of various molecular weight in this region is more complicated than that of pure bentonite between 4000 and 2600 cm^{-1} (figure 5.3.1b). The characteristic bentonite band at 3634 cm^{-1}, assigned to a structural OH stretching vibration can be clearly observed but, in addition, bands can also be observed at 3475 and 3393 cm^{-1}. These bands are most prominent in the spectrum of bentonite mixed with 5 gdm^{-3} polyacrylamide solution but they may also be observed as shoulders in the spectra of dried complexes of bentonite mixed with 1 and 3.3 gdm^{-3} aqueous polyacrylamide solution. A shoulder can also be observed at ~3250 cm^{-1} which has been attributed to the overtone of the H-O-H bending band of bentonite at 1640 cm^{-1} [34]. This band may also be observed in the spectrum of pure bentonite in the region between 4000 and 2600 cm^{-1} (figure 5.3.1b).

The bands at 3475 and 3393 cm^{-1} are superimposed upon spectral bands due to hydrogen bonded water in pure bentonite and have been attributed to the NH_2 antisymmetric and symmetric stretching modes, respectively. Their wavenumber position however, has been shifted considerably to higher frequency (the antisymmetric NH_2 stretching band by 145 cm^{-1} and the symmetric stretching band by 203 cm^{-1}). This observation supports the findings of other workers [153, 236] who observed similar shifts to higher frequency of the NH_2 antisymmetric and symmetric stretching bands (by approximately 135 and 225 cm^{-1} respectively) of acetamide adsorption on montmorillonite. Stutzmann and Siffert [153] attributed these large shifts to the formation of intermolecular hydrogen bonds and concluded that one of the adsorption mechanisms of acetamide on montmorillonite was the formation of acetamide-acetamide and acetamide-water hydrogen bonds.

The conclusions of Stutzmann and Siffert [153] seem only partially correct. The positions of the NH_2 stretching bands, in solid polyacrylamide, are shifted to low frequency (3330 and 3190 cm^{-1}) due to considerable intra and intermolecular hydrogen bonding as outlined in section 6.3.3.1. Bellamy [235] and Silverstein et al [237] both state that the NH_2 antisymmetric and symmetric stretching bands are shifted to higher frequency as the degree of hydrogen bonding is reduced, i.e. in progressively more dilute solution. Indeed, Bellamy [235], quotes 3520 and 3410 cm^{-1} as the wavenumber positions of 'free' NH_2 stretching bands for primary amides.

The wavenumber position of the NH_2 antisymmetric and symmetric stretching bands observed in the bentonite-polyacrylamide complex of 3475 and 3393 cm^{-1} are very close to the positions quoted for 'free' antisymmetric and symmetric NH_2 stretching. Hence, although evidence of hydrogen bonding is present in the polyacrylamide-bentonite complex, it appears that the hydrogen bonding is not that which is observed in the pure solid polyacrylamide. It can therefore be concluded that polyacrylamide adsorption is predominantly controlled by hydrogen bonding between polyacrylamide and water in the interlayer space, and that intramolecular interactions within polyacrylamide molecules and intermolecular interactions between separate polyacrylamide molecules are significantly reduced on adsorption onto bentonite.

Figures 6.3.3.4b and 6.3.3.4c show the corresponding spectral region, between 4000 and 2600 cm^{-1}, for the adsorption of polyacrylamide of molecular weight 500k and 7000k respectively.

Figure 6.3.3.4b The infrared transmission spectra of dried bentonite-polyacrylamide (Mw 500k) complexes at various polymer concentrations.
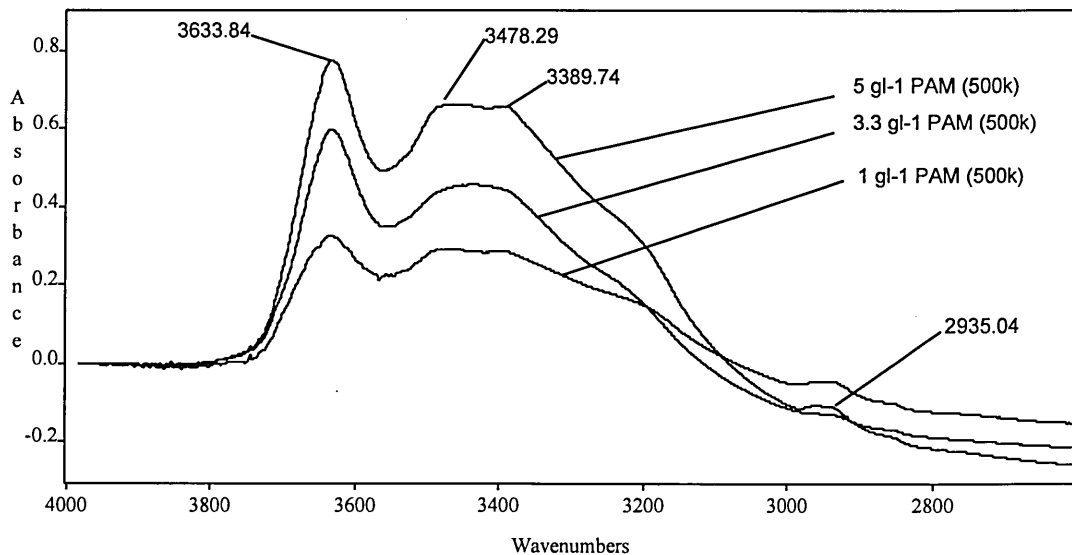
Figure 6.3.3.4c The infrared transmission spectra of dried bentonite-polyacrylamide (Mw 7000k) complexes at various polymer concentrations.
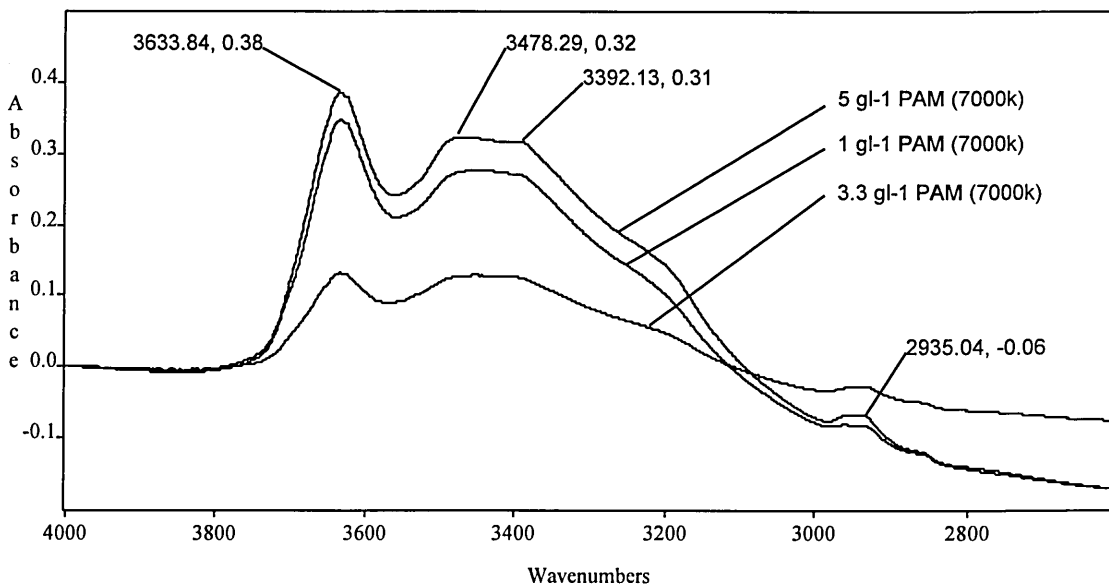
Comparison of figures 6.3.3.4a, 6.3.3.4b and 6.3.3.4c reveals strong similarities between the spectra obtained for complexes prepared from polyacrylamide of

different molecular weight. Indeed, the shift to higher frequency of the bands due to NH_2 antisymmetric and symmetric stretching modes shows no molecular weight dependence, the NH_2 band shifts to higher frequency being approximately the same for all molecular weights (145 ± 4 cm^{-1}, for the higher frequency band, and 203 ± 2 cm^{-1} for the lower frequency band).

Although the spectra presented in figures 6.3.2.1a, 6.3.2.1b and 6.3.2.1c appear very similar, one small, but significant, shift in the wavenumber position of the band attributed to the antisymmetric CH_2 stretching mode can be observed in the infrared spectrum (in the C-H stretching region between 3000 and 2800 cm^{-1}) of the dried complex prepared from aqueous dispersed bentonite and 1 gdm^{-3} polyacrylamide (Mw 500k) solution. This may provide evidence to support the anomalous adsorption behaviour of polyacrylamide (Mw 500k) onto bentonite.

One must first consider the adsorption of polyacrylamide (Mw 100k) onto bentonite from a 1 gdm^{-3} solution. This reveals a band due to the antisymmetric C-H stretching mode at 2936 cm^{-1} (figure 6.3.3.4d). Indeed, the adsorption of polyacrylamide from 3.3 and 5.0 gdm^{-3} polyacrylamide (Mw 100k) solutions also reveals bands at the same wavenumber position. Similarly, the adsorption of polyacrylamide (Mw 7000k) from solutions of all concentrations also reveals bands due to the antisymmetric C-H stretching at 2936 cm^{-1} (figure 6.3.3.4e).

It should be noted that figures 6.3.3.4d and 6.3.3.4e are merely expansions of figures 6.3.3.4a and 6.3.3.4c, respectively.

Figure 6.3.3.4d The infrared transmission spectra of dried bentonite-polyacrylamide (Mw 100k) complexes at various polymer concentrations.
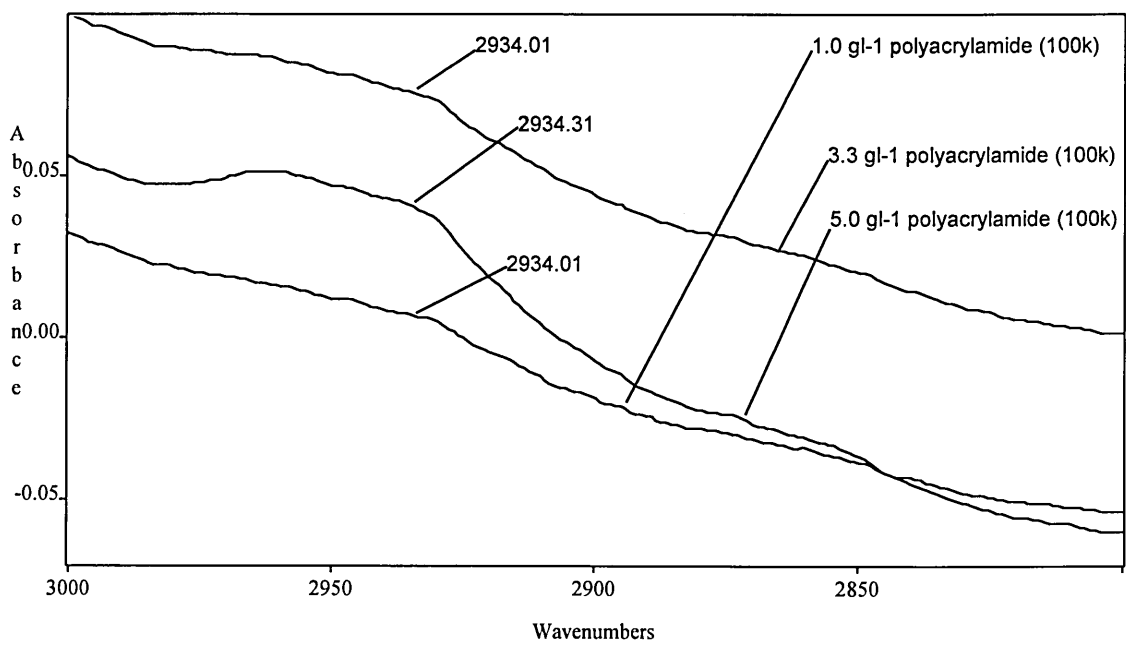

Figure 6.3.3.4e The infrared transmission spectra of dried bentonite-polyacrylamide (Mw 7000k) complexes at various polymer concentrations.
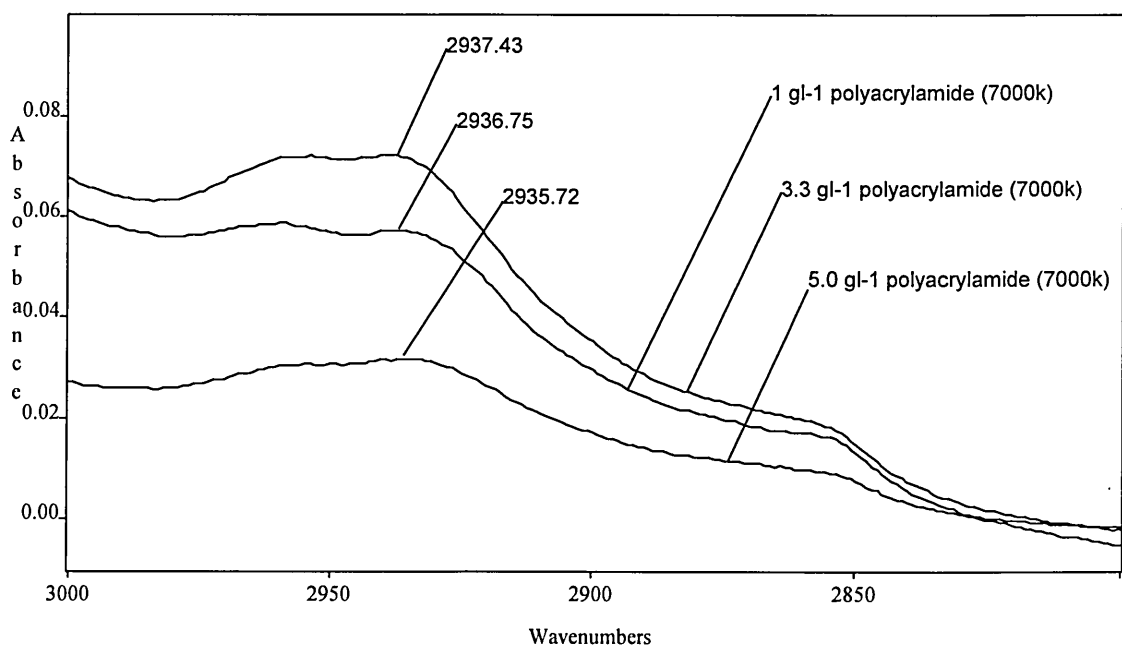
The wavenumber position of the band due to the CH_2 antisymmetric stretching mode at 2936 cm^{-1}, seen in the spectra of polyacrylamide (Mw 100k and 7000k) adsorbed on bentonite, is shifted to high frequency compared to its position at ~2927 cm^{-1} in solid polyacrylamide. This may be attributed to a change in polyacrylamide conformation on adsorption in the interlayer space corresponding to a conformation in which inter and intramolecular hydrogen bonding is reduced.

Figure 6.3.3.4f (an expansion of figure 6.3.3.4b) however, shows the C-H stretching region, between 3000 and 2700 cm^{-1} for dried bentonite-polyacrylamide (Mw 500k) complexes prepared in aqueous dispersion.

Figure 6.3.3.4f The infrared transmission spectra of dried bentonite-polyacrylamide (Mw 500k) complexes at various polymer concentrations.
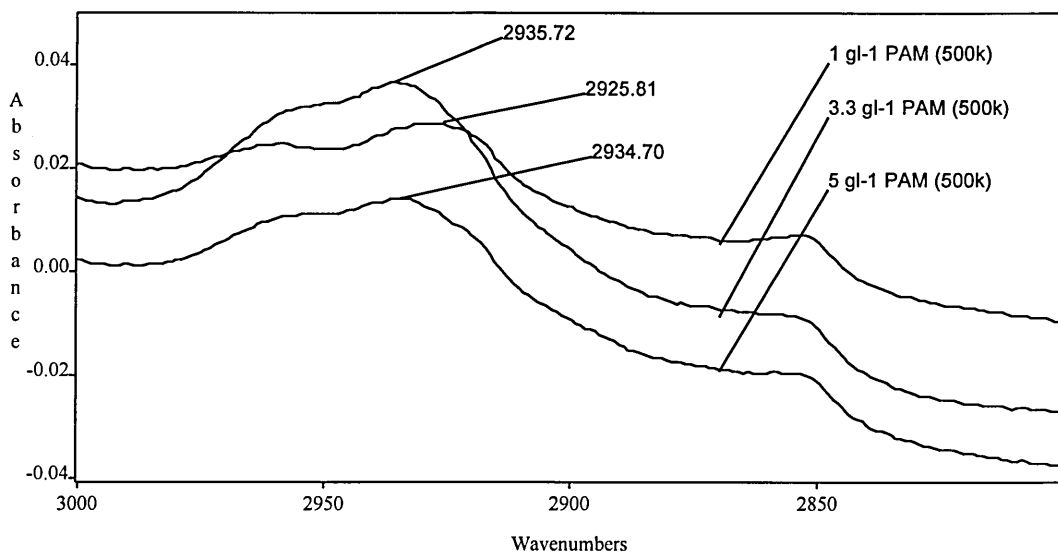

From figure 6.3.3.4f, it can be clearly seen that at polyacrylamide solution concentrations of 3.3 and 5.0 gdm^{-3}, the band attributed to the C-H antisymmetric stretching mode is located at 2935 cm^{-1} as it is in the complexes

prepared using polyacrylamide (Mw 100k and 7000k) and presumably adopts a similar conformation. However, the position of this band in the bentonite-polyacrylamide complex, prepared from 1 gdm^{-3} polyacrylamide (Mw 500k) solution, is found at lower frequency, at 2925 cm^{-1}. This may be indicative of polyacrylamide (Mw 500k) adsorbed from 1 gdm^{-3} solution, adopting a slightly different conformation on adsorption than polyacrylamide in any of the other complexes. The wavenumber position of this band is close to its observed position in solid polyacrylamide and consequently, may be related to a polyacrylamide conformation in which polymer chains interact. This subtle change in C-H stretching frequency may be indicative of subtle differences in adsorbed (or trapped) polymer conformation which reflect extensive polyacrylamide-polyacrylamide intramolecular hydrogen bonding in a 1 gdm^{-3} solution concentration, as mentioned previously.

It should be noted however, that other evidence to support this theory is difficult to find. Indeed, X-ray diffraction traces have shown that adsorbed polyacrylamide (Mw 500k) from 1 gdm^{-3} solution probably adopts a flat conformation (d-spacing corresponds to that of a flat polyacrylamide molecule) on adsorption, in the same way that polyacrylamide adsorbed at low levels in other bentonite-polyacrylamide complexes adopts a flat conformation. In addition, the position of the CH_2 bending mode is shifted by 12 cm^{-1} from its wavenumber position (1450 cm^{-1}) in the spectrum of pure solid polyacrylamide, to 1461 cm^{-1} on adsorption of polyacrylamide onto bentonite (figures 6.3.3.4g, 6.3.3.4h and 6.3.3.4i). This is indicative of a change in conformation of the polymer on adsorption between the clay platelets corresponding to a conformation in which the number of inter and intramolecular hydrogen bonds is reduced. The position of this band, it must be noted however, is unaffected by the concentration of polymer or polymer molecular weight.

In addition, the intensity of the band at 2960 cm^{-1} (assigned to the antisymmetric stretch of terminal methyl groups) appears to be strong, particularly compared to the intensity of bands assigned to main chain methylene stretching modes. This may indicate that a significant proportion of adsorbed polymer is composed of the low molecular weight impurities (from the polydisperse polyacrylamide sample). Although low molecular weight molecules are commonly observed to adsorb preferentially in the early stages of any adsorption process (due to kinetic effects such as mass transport), they are often displaced by higher molecular weight molecules at longer equilibration times, due to thermodynamic effects [100]. It appears in these experiments that, even at long equilibration times, the adsorption of low molecular weight impurities (due to polydispersity) between the bentonite platelets is significant for two reasons. Firstly, the adsorption of polyacrylamide has been found to be irreversible, and as a result, it is very difficult to displace the adsorbed low molecular weight fraction of the polydisperse polyacrylamide sample. Secondly, following the adsorption of low molecular weight polyacrylamide, the adsorption of subsequent larger molecules may be inhibited by flocculation; caused by adsorbed polymer, by the high S/L ratio and the presence of flocculating exchange cations.

Thus, the infrared spectra, and the adsorption isotherms may show adsorption of low molecular weight polyacrylamide impurities. As a result, the low adsorbed amount of polyacrylamide (Mw 500k) from 1 gdm^{-3} solution, may be that of impurities of low molecular weight polyacrylamide. Similarly, the shift in the position of the band assigned to the antisymmetric CH$_2$ stretching mode may be attributed to the adsorption of low molecular weight material from a polydisperse sample. The molecular weight distribution of these polyacrylamide samples have not been determined, consequently, without this knowledge, it is only possible to speculate as to the reasons behind these observed effects.

Other interesting features may also be observed at lower frequency in all polyacrylamide-bentonite complexes, in particular in the amide I and II stretching region.

Figure 6.3.3.4g shows the infrared spectrum in the region between 2000 and 1300 cm^{-1} for the adsorption of polyacrylamide of molecular weight 100k from aqueous solution onto dispersed bentonite.

Figure 6.3.3.4g The infrared transmission spectra of dried bentonite-polyacrylamide (Mw 100k) complexes at various polymer concentrations.
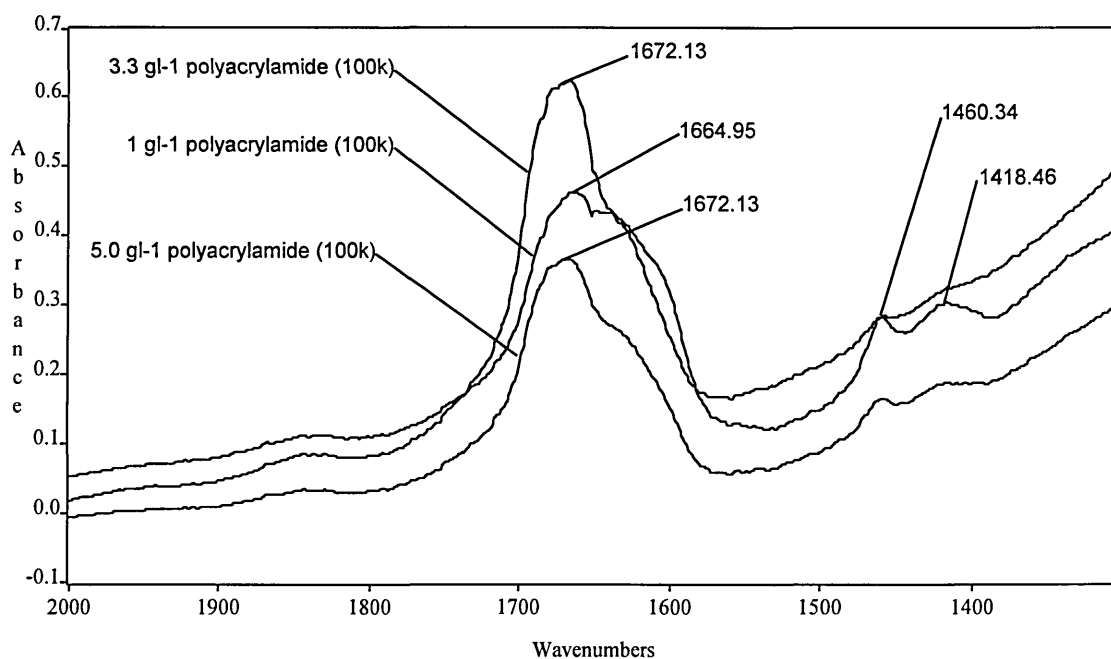
Figures 6.3.3.4h and 6.3.3.4i shows the infrared spectrum in the region between 2000 and 1300 cm^{-1} for the adsorption of polyacrylamide of molecular weights 500k and 7000k respectively from aqueous solution onto dispersed bentonite.

Figure 6.3.3.4h The infrared transmission spectra of dried bentonite-polyacrylamide (Mw 500k) complexes at various polymer concentrations.
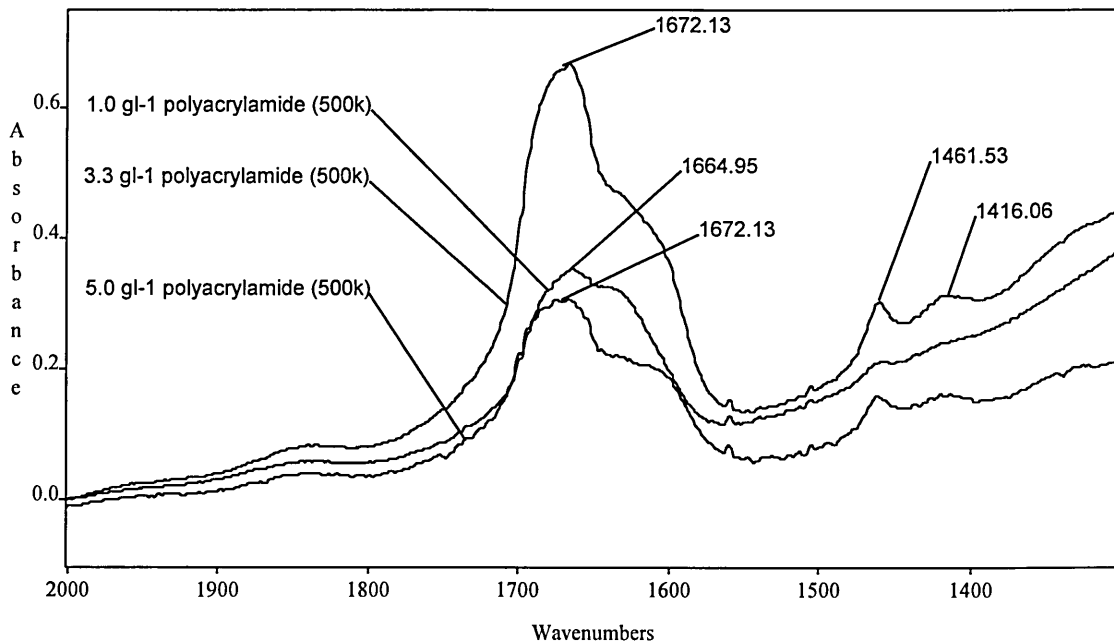
Figure 6.3.3.4i The infrared transmission spectra of dried bentonite-polyacrylamide (Mw 7000k) complexes at various polymer concentrations.
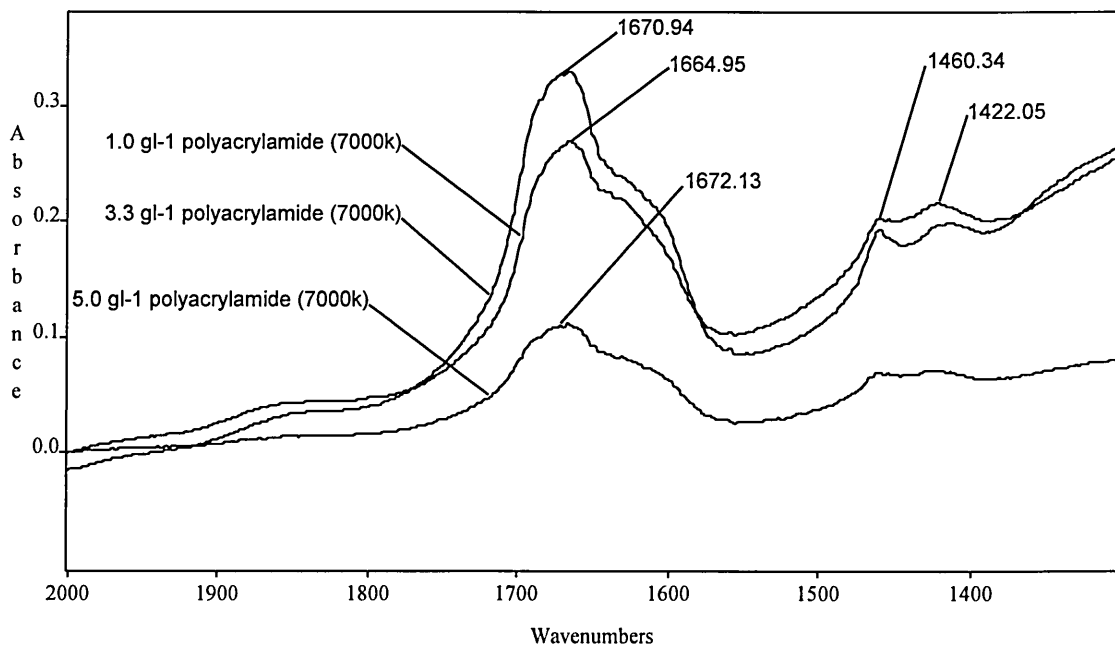
The first point to note from figure 6.3.3.4g is that the bands attributed to polyacrylamide in this spectral region are less broad and much better defined than they are in the spectrum of the pure solid polyacrylamide in figure 6.3.3.1c. The narrowing of the characteristic polyacrylamide bands in this spectral region is indicative of polyacrylamide molecules existing in a more homogeneous environment. This implies a reduction in the inter and intramolecular hydrogen bonding between molecules which is observed in the solid polyacrylamide. It is possible to conclude that polyacrylamide is separated from itself and other polyacrylamide molecules in the interlayer space. This is probably due to adsorbed polyacrylamide adopting an uncoiled (flat) conformation on adsorption [11, 155]. There is no suggestion that hydrogen bonding does not occur in the interlayer region, however, it is likely that the predominant hydrogen bonding interactions would be with water molecules which exist in this region.

In addition, the amide I band at 1660 cm^{-1} in the spectrum of pure solid polyacrylamide is shifted to 1664 cm^{-1} in the spectrum of complex prepared from polyacrylamide solution 1 gdm^{-3} then to 1672 cm^{-1} in the spectra of complexes prepared from 3.3 and 5.0 gdm^{-3} aqueous polyacrylamide (Mw 100k) solution. Bellamy [235] has stated that the position of the amide I band is 'subject to alteration when a change of state occurs in which H-bonding is broken [and]... variations in solution depending upon the polarity of the solvent'. Indeed, the position of this band has been observed at 1655 cm^{-1} in solid hexoamide but shifts to 1668 cm^{-1} and 1680 cm^{-1} in concentrated and dilute chloroform solution, respectively, and has been observed at 1672 cm^{-1} in methanol solution [235]. Evidently, the degree of intra and intermolecular hydrogen bonding in the solid is reduced on dilution in non-polar medium. However, the extent of the wavenumber shift of the C=O stretching band in a polar solvent (methanol) indicates the extent of polyacrylamide-solvent

hydrogen bonding interactions as it does in the results presented in this thesis. Consequently, the shift to high frequency of the carbonyl band indicates that the C=O functionality is involved in fewer intra and intermolecular hydrogen bonding interactions within the same molecule and with other polyacrylamide molecules in the complex than it is in solid polyacrylamide. It can therefore be assumed that the polyacrylamide molecule is involved in hydrogen bonding interactions in the interlayer of the clay platelet but that these interactions are predominantly of the polyacrylamide-water type and not of polyacrylamide-polyacrylamide.

This is contrary to the findings of Stutzmann and Siffert [153] (acetamide adsorption on montmorillonite) who observed a shift to lower frequency of the amide I band of acetamide (from 1670 to 1660 cm^{-1}) which would indicate increased hydrogen bonding of the acetamide in the bentonite complex than in the pure solid acetamide. The interpretation of the band shifts by Stutzmann and Siffert [153] is made more complicated by the anomalous high frequency position adopted by the amide I band in solid acetamide which implies few intramolecular interactions despite X-ray evidence to indicate it is associated [235].

These authors [153] also observed a shift of the C-N stretching band from 1380 in pure acetamide to 1400 cm^{-1} in the acetamide-montmorillonite complex. Although no discernible shift of the C-N stretching band to higher frequency can be observed in the spectrum of polyacrylamide of molecular weight 100k adsorbed from 1 gdm^{-3} aqueous solution onto dispersed bentonite (figure 6.3.3.4g), a small shift, to high frequency, in the position (~9 cm^{-1}) of the C-N stretching band has been observed in the spectrum of polyacrylamide of molecular weight 100k adsorbed from 5 gdm^{-3} and 3 gdm^{-3} (figure 6.3.3.4g). A similar, small shift in the C-N stretching band is observed at larger adsorbed

amounts of polyacrylamide (Mw 500k). The shift is somewhat more significant

($\sim$13 cm^{-1}) for the adsorption of polyacrylamide (Mw 7000k) from all solution

concentrations onto bentonite (figure 6.3.3.4i).

Stutzmann and Siffert [153] concluded that shifts of the carbonyl absorption

band to lower frequency and of the C-N absorption band to higher frequency,

coupled with the large shifts of the NH$_2$ stretching bands (mentioned

previously) indicate that considerable hydrogen bonding interaction occurs

between acetamide and itself and acetamide and water. In the results presented

in this thesis, it appears that hydrogen bonding is the mechanism of adsorption

of polyacrylamide but that the polyacrylamide-polyacrylamide interactions are

significantly reduced from those observed in the solid polymer and that the

predominant source of hydrogen bonding is via polyacrylamide-water

interactions.

Using infrared spectroscopy, Mortland and Tahoun [236] concluded that in

acidic montmorillonite systems, protonation of amides occurs predominantly on

the oxygen atom. The water molecules which surround the Al^{3+} exchange

cations are polarised to such an extent that the protons on the water molecules

become acidic. Mortland [114] has discussed the interaction of amides with clay

and shown that protonation of the carbonyl functionality causes a decrease in

the ν(C=O) absorption frequency. This is not the case in the Na$^+$, K$^+$, Ca^{2+}

mixed montmorillonite system presented here, as it is unlikely that the water

molecules are sufficiently polarised to make them acidic [121]. Consequently,

hydrogen bonding interactions are likely to both oxygen and nitrogen atoms of

the amide functionality of polyacrylamide.

From figure 6.3.3.4h and 6.3.3.4i it can be seen that, for higher molecular

weight polyacrylamide, the position of the carbonyl absorption follows exactly

the same pattern as that observed for polyacrylamide (Mw 500k), increasing to a higher wavenumber position as the concentration of polyacrylamide in solution (the adsorbed amount of polyacrylamide on the clay) increases.

Evidence of hydrogen bonding of the NH_2 functionality has been observed at higher frequency (shifts of 135 and 225 cm^{-1} of the NH_2 antisymmetric and symmetric stretching bands respectively are not those observed for 'free' NH_2 groups) and similarly, hydrogen bonding interactions may be observed due to shifts in band position of the amide II band. The position of the amide II band is known to be highly dependent upon the physical state and concentration of the amide molecule [234]. Indeed, Bellamy [235] discusses the downwards shift in frequency of this band on dilution due to breaking of hydrogen bonds. This shift is in the opposite direction to that of the NH stretching band on increasing hydrogen bonding. This is due to the bond becoming longer and easier to stretch as it forms hydrogen bonds causing the orbitals to adopt more p character which makes the bond more directional and harder to bend [236].

Unfortunately, it is very difficult to determine band shifts of the amide II band of polyacrylamide on adsorption onto bentonite, since its position in the pure solid polyacrylamide is so difficult to determine. In addition, the assessment of band shifts and changes in relative intensity becomes more confused when one considers that in addition to the amide I and II bands in this region, a band due to an H-O-H bending mode is also expected between 1650 and 1550 cm^{-1}. Consequently, changes to the amide II band can not be interpreted with any degree of accuracy. Hence, no explanation can be given to describe the various observable spectral changes (band shifts and relative intensity) in this region.

The final region of interest in the adsorption of polyacrylamide from solution onto dispersed bentonite, is the silicate stretching region (between 1450 and 850

239

cm^{-1}). As mentioned previously, this may be able to give some insight into the interaction between the polyacrylamide and the silicate lattice.

Figure 6.3.3.4j shows the infrared spectrum between 1450 and 850 cm^{-1} of the complex prepared from bentonite suspension and 5 gdm^{-3} polyacrylamide (Mw 7000k). Also observable in figure 6.3.3.4j are the synthetic spectrum and fitted bands which were obtained by curve fitting. The curve fitting was performed using the information provided by second derivative spectroscopy and Fourier self deconvolution (performed using κ =1.66, γ =35 cm^{-1} and a Bessel apodisation function). The result of FSD and SD are shown in figures 6.3.3.4k and 6.3.3.4l respectively.

Figure 6.3.3.4j Transmission spectrum, synthetic spectrum and component curve fitted bands of dried bentonite-polyacrylamide (7000k) complex prepared from 5 gdm^{-3} polyacrylamide solution.
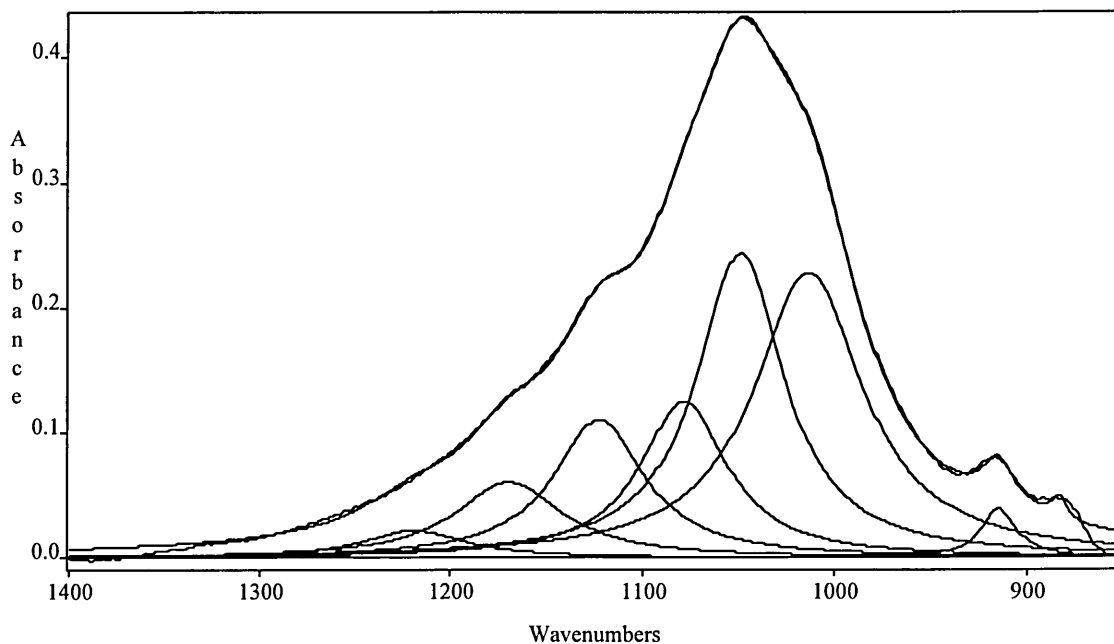
Figure 6.3.3.4k Fourier self deconvoluted spectrum of dry bentonite-polyacrylamide (7000k) complex prepared from 5 gdm^{-3} polymer solution.
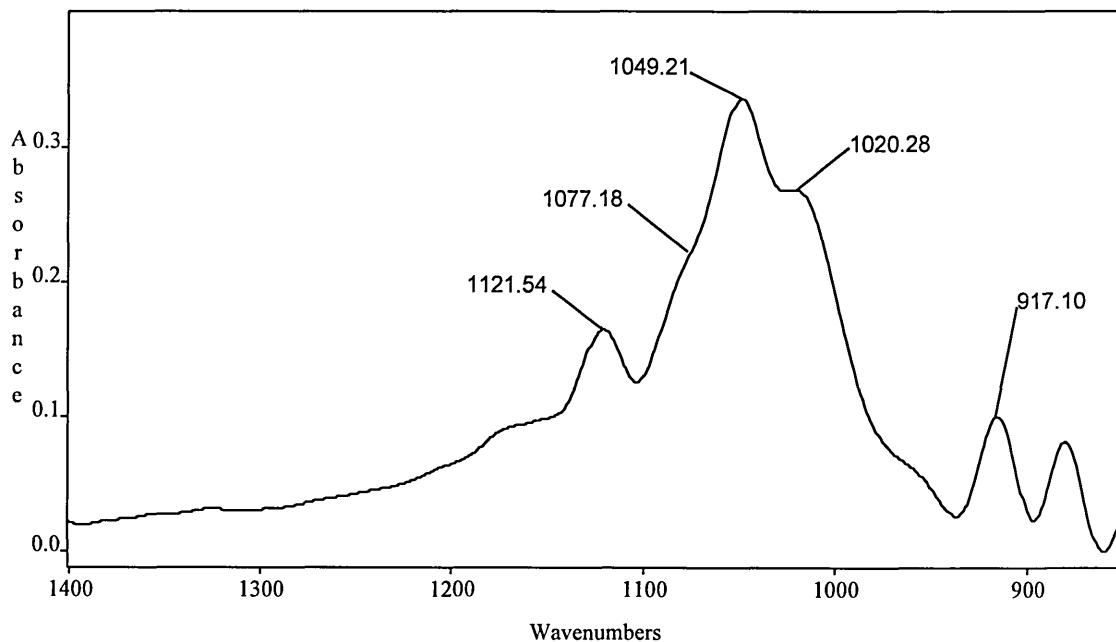
Figure 6.3.3.4l Second derivative spectrum of dry bentonite-polyacrylamide complex prepared from 5 gdm^{-3} polyacrylamide (7000k).
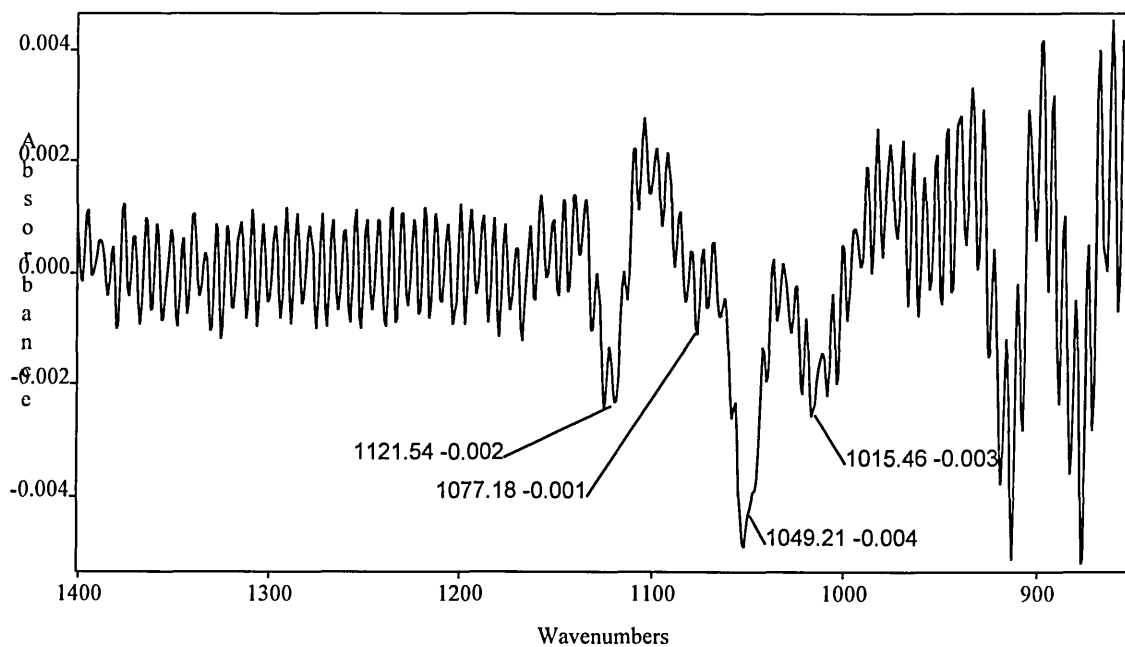
The positions of the main Si-O peaks have been determined in this way for all the polyacrylamide-bentonite complexes. A summary of the main band positions of all bentonite-polyacrylamide complexes, observed by curve fitting procedures is shown in table 6.3.3.4a.

Table 6.3.3.4a Summary of the main Si-O band positions of all bentonite-polyacrylamide complexes.

Mw (gmol^{-1})	Conc. (gdm^{-3})	Main Si-O band position (cm^{-1})			
100k	1.0	1123	1078	1045	1012
	3.3	1121	1078	1046	1009
	5.0	1122	1077	1046	1012
500k	1.0	1124	1078	1048	1011
	3.3	1124	1076	1047	1010
	5.0	1124	1078	1047	1009
7000k	1.0	1122	1078	1048	1013
	3.3	1124	1077	1048	1010
	5.0	1123	1078	1047	1010

By comparison of the values shown in table 6.3.3.4a above with the values obtained for pure bentonite at room temperature (table 5.3.2b) it is clear that the position of all Si-O bands are essentially unchanged in the spectra of bentonite-polyacrylamide complexes from that observed in pure bentonite at room temperature

It has been suggested that the strong binding of polyacrylamide onto montmorillonite exchanged with divalent cations is due to co-ordination

complex formation between the cations and amide groups of the polymer [236]. This contradicts the findings of Stutzmann and Siffert [153] who describe a chemisorption mechanism for acetamide on montmorillonite which requires protonation of the amide group by polarised water in the first hydration shell of the exchange cation. As mentioned previously, this mechanism is unlikely in the natural SWy-1 bentonite used in these experiments as the water molecules in the first hydration shell of Na^+, K^+ and Ca^{2+} exchange cations are unlikely to be sufficiently polarised to protonate the NH_2 group.

It is likely that polyacrylamide, if not directly adsorbed onto the exchange cation would form a water bridge (hydrogen bonding to the water of hydration which surrounds the interlayer cation) thus preventing the exchange cations from settling into the di-trigonal cavity of the silicate surface on heating to 200°C. This may be determined by analysing the effect of heating the complex on the position of the transient Si-O vibration. If the exchange cation is surrounded only by water, this will be removed at high temperatures manifesting itself as a shift to low frequency of the transient band as the cation settles into the di-trigonal cavity of the silicate sheet. If the polyacrylamide is directly bound to the cation (or bound via water bridges) then movement of the cation will be restricted and the transient Si-O band will not be shifted from its value quoted in table 6.3.3.4a.

Figure 6.3.3.4m shows the transmission infrared spectrum between 1450 and 850 cm^{-1} of the complex prepared from bentonite suspension and 5 gdm^{-3} polyacrylamide (Mw 100k) at 200°C.

Figure 6.3.3.4m Infrared transmission spectrum of dried bentonite-polyacrylamide (100k) complex prepared from 5 gdm^{-3} polyacrylamide solution at 200°C.
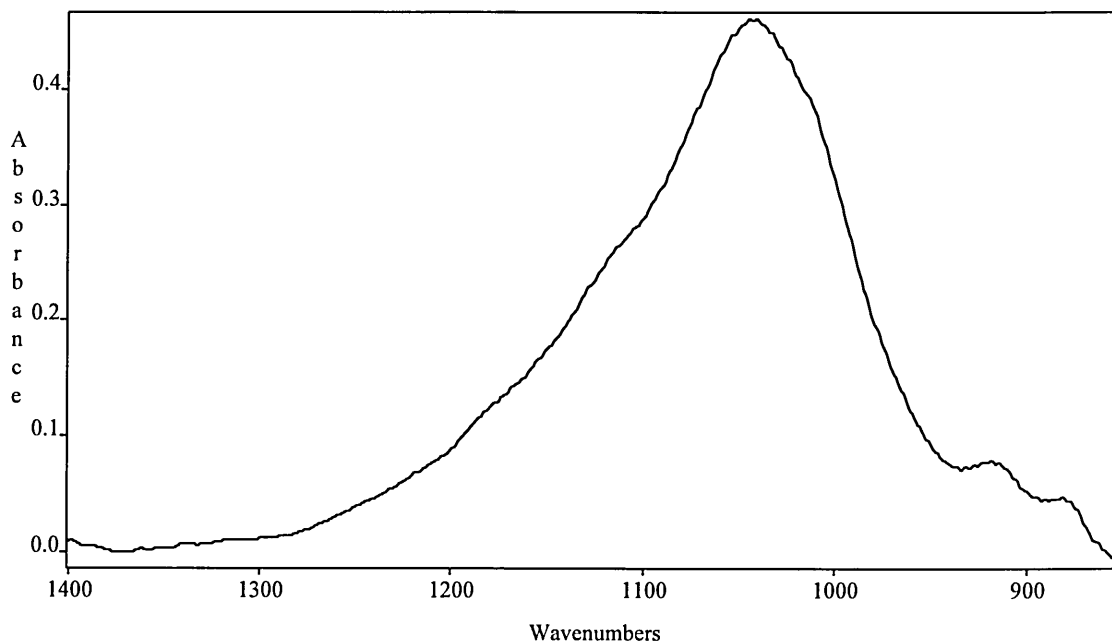
Fourier self deconvolution (using $\kappa = 1.70$, $\gamma = 35$ cm^{-1} and a Bessel apodisation function) and second derivative spectroscopy was performed on the spectra of bentonite-polyacrylamide complexes in this region and from the information received from these source, curves were fitted to the spectral lineshape.

The positions of the main Si-O peaks were determined in this way for all the polyacrylamide-bentonite complexes at 200°C and were found not to be changed (by more than ± 1 cm^{-1}) from the band positions in the spectrum of their corresponding bentonite-polyacrylamide complex at room temperature (table 6.3.3.4a). Large shifts to low frequency of the transient band (~8 cm^{-1}) would be expected if heating had caused a significant change to the complex, as is observed in the spectrum of pure bentonite heated to 200°C (table 5.3.2c).

244

These findings support the idea that polyacrylamide adsorption is dependent upon the cation (either by direct co-ordination or by water bridge) which therefore prevents the cation settling into the di-trigonal cavity on dehydration, i.e. when heating to 200°C.

Figure 6.3.3.4q shows the spectral region between 4000 and 2600 cm^{-1} of the transmission infrared spectrum of the complex prepared from bentonite suspension and 5 gdm^{-3} polyacrylamide (100k) at 200°C.

Figure 6.3.3.4q Infrared transmission spectrum of dried bentonite-polyacrylamide (7000k) complex prepared from 5 gdm^{-3} polyacrylamide solution at 200°C.
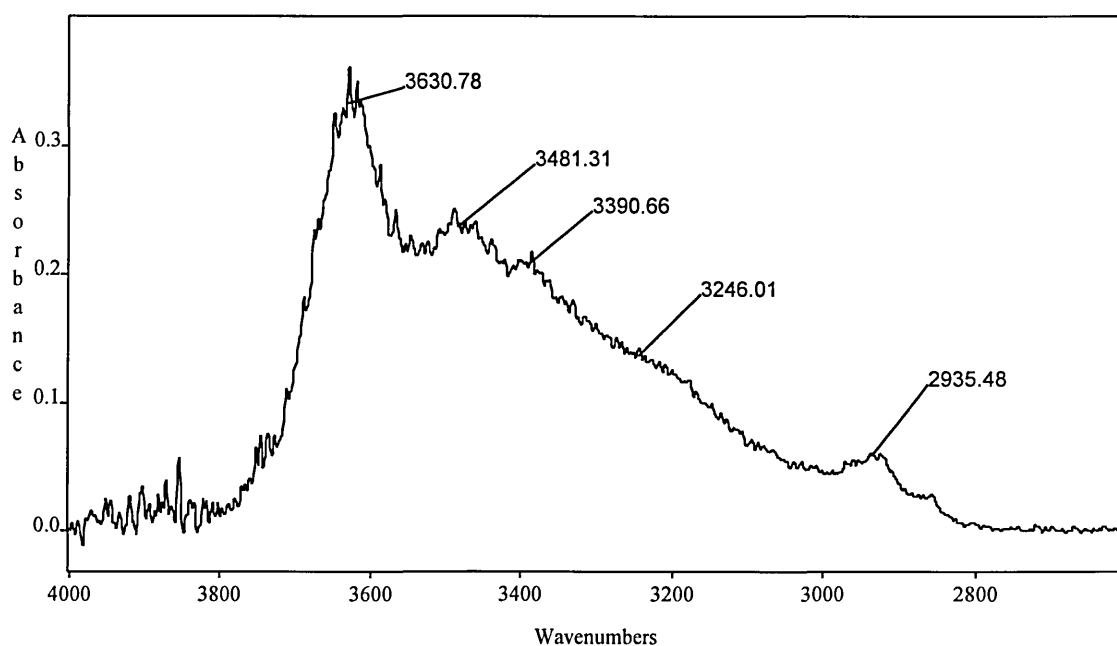
Evidently, some water is removed from the complex prepared from 5 gdm^{-3} polyacrylamide (7000k) solution at 200°C (figure 6.3.3.4q) compared to the spectrum of the same complex at room temperature (figure 6.3.3.4c). Removal of water from this region reveals, more clearly, the NH_2 antisymmetric and

symmetric bands shifted to 3480 and 3390 cm^{-1}, respectively. The band at ~3250 cm^{-1} which may be attributable to the overtone of the H-O-H bending mode, still remains. Thus, partial removal of water has very little effect on the spectrum other than reducing the intensity of the hydrogen bonded OH stretching band. This is indicative of a strongly hydrogen bonded, highly stable complex.

It should be noted that in every detail the spectra of complexes prepared from polyacrylamide adsorption on bentonite in the presence of 100 gdm^{-3} KCl solution were identical to those observed in the absence of KCl. The reasons for this are not wholly clear. However, it seems likely that despite reducing the adsorbed amount by flocculation, the partial cation exchange of K^+, for Na^+ and Ca^{2+} cations in the interlayer space is not significant enough to affect the adsorption behaviour.

6.4.   Conclusions

Aqueous solutions containing polyacrylamide of various molecular weight, in the concentration range of interest to water based oil well drilling fluids, have been shown to destabilise both self supporting and supported bentonite films. The presence of a flocculating agent (KCl) does not improve the durability of the film. Consequently, the applicability of polyacrylamide as an additive to help stabilise the wellbore and drilled cuttings suspended in solution (both comprising shale whose major constituent is bentonite) is doubtful. FTIR-ATR spectroscopy has shown that the bentonite film is dispersed by the aqueous solution before polyacrylamide is able to interact with the bentonite. Although it does not stabilise the bentonite film, it is able to form flocculated gel structures with the dispersed platelets which may offer partial or enhanced stability in the presence of other polymer additives.

The adsorption of polyacrylamide onto bentonite dispersed in aqueous solution has been studied using Kjeldahl nitrogen analysis, X-ray diffraction and transmission infrared spectroscopy.

The amount of polyacrylamide adsorbed on bentonite is determined by several factors, the most important of which, in low salinity solution, is the solid liquid ratio of the clay suspension since this determines the flocculation of the clay and therefore surface accessibility for polyacrylamide adsorption. Of lesser importance is the nature of the exchange cation on the clay since this also determines the state of bentonite dispersion. The true influence of the nature of the cation has not fully emerged from these results because the clay used was not homoionic and adsorption in electrolyte solution (which would be expected to ion exchange) showed no spectral differences.

In the presence of electrolyte (KCl), adsorption is significantly reduced due to collapse of the electrical double layer and subsequent platelet flocculation. Under such conditions, larger polyacrylamide molecules are inhibited from adsorption to a greater extent then smaller molecules.

The adsorption of polyacrylamide onto bentonite appears to increase with molecular weight. However, the adsorption of polyacrylamide of molecular weight 500k shows anomalous behaviour; in particular its adsorption from 1 gdm^{-3} solution appears to be severely inhibited. This has been attributed to a critical solution concentration in which polyacrylamide molecules form extensive intermolecular hydrogen bonding networks. The surface requirement for such a network cannot be fulfilled by the clay and consequently adsorption is low. Significantly, the CH_2 antisymmetric stretching band is shifted to lower frequency in the infrared spectrum of the complex prepared from this particular

polyacrylamide solution which may reflect the unique polyacrylamide conformation in solution.

Polyacrylamide adsorbs onto bentonite in aqueous solution and intercalates in the interlayer region. The range of adsorbed amounts (increasing with increasing molecular weight when solution concentrations do not influence other adsorption processes) has given an insight into the conformation of adsorbed polyacrylamide between the platelets. At low adsorbed amounts, d-spacings predict adsorption in a flat (stretched) conformation, whereas as the adsorbed amount increases, then the d-spacing increases above that which corresponds to flat conformation and it is assumed that the number and size of loops and tails in the polymer chain increases. This is probably due to entrained polymer being trapped between the platelets when the complex is dried. A flat adsorbed layer of polyacrylamide has a d-spacing slightly less than that calculated from the van der Waals radius of an analogous molecule. This seems to suggest that polyacrylamide keys into the di-trigonal cavity of the silicate layer surface, although no other evidence has been found to support this theory.

Additional infrared analysis has shown that inter and intramolecular (polyacrylamide-polyacrylamide) hydrogen bonding is significantly reduced in bentonite-polyacrylamide complexes compared to that in pure solid polyacrylamide. However, amide functionalities are susceptible to hydrogen bonding and evidence of hydrogen bonding, likely to be of the polyacrylamide-water type rather then polyacrylamide-polyacrylamide has been observed in the spectra of all bentonite-polyacrylamide. The narrowing of the infrared bands on adsorption compared to those observed in the spectrum of solid polyacrylamide is indicative of a reduction in the inter and intramolecular hydrogen bonding. In addition, shifts of the NH_2 stretching bands to higher frequency, of the amide I band to higher frequency and of the C-N stretching band to higher frequency

relative to their positions in the spectrum of solid polyacrylamide are all indicative of reduced polyacrylamide-polyacrylamide hydrogen bonding and therefore must represent polyacrylamide-water interactions.

No evidence of hydrogen bonding of polyacrylamide to the silicate surface has been observed. It is therefore highly likely that the polyacrylamide adsorbs via hydrogen bonding, the most likely of which is via a water bridge to the exchange cation. The reduced mobility of the exchange cation is evidenced in its inability to settle into the di-trigonal cavity of the silicate surface on heating. Indeed, the polyacrylamide-bentonite complexes formed by adsorption of polyacrylamide from aqueous solution onto dispersed bentonite have been shown to be stable up to 200°C, releasing only water from the clay at such elevated temperatures. This is indicative of a strongly bound complex in which the polymer is attached by multipoint hydrogen bonding (water bridges).

7.   ADSORPTION OF POLYALKYL GLYCOL ON BENTONITE

7.1.   Introduction

Another polymer that is commonly used as an additive to water based oil well drilling fluids is polyalkyl glycol (PAG), the structure of which can be seen in figure 4.9.2a. These polymers have been added to drilling muds in concentrations up to 100 gdm^{-3} and have been found, in conjunction with other additives such as ionic salts (particularly KCl), to significantly inhibit degradation of shales which comprise the wellbore wall and drilled cuttings [1, 8, 150, 151].

In chapter 3, the possible mechanisms by which polyalkyl glycols inhibit shale degradation were outlined [1, 8, 150, 151]. Nevertheless, the interaction of polyalkyl glycol with clay minerals is not fully understood and the behaviour of polyalkyl glycol in the drilling fluid is not clear. As a result, the interactions between polyalkyl glycol and bentonite have been studied by immersing clay mineral in the form of a free standing film (since this is considered representative of the bentonite which forms part of underground shale deposits [1]) in aqueous polyalkyl glycol and aqueous polyalkyl glycol/electrolyte solutions. Some work has been undertaken to study the adsorption of polyalkyl glycol onto bentonite dispersed in aqueous suspension (as in the drilling fluid) but much of this work has been covered by Rawson [3].

7.2.   Experimental

7.2.1.   Materials

SWy-1 bentonite was purified by sedimentation to obtain the <2μm fraction. Homoionic Na^+, and K^+ SWy-1 bentonite were prepared by the method outlined

in section 4.9.1 and used along with purified SWy-1 bentonite in its natural state (without cation exchange, containing predominantly Na^+, and small amounts of Ca^{2+} and K^+ exchange cations, as outlined in table 4.9.1). Aqueous bentonite suspensions were prepared by dispersing the bentonite in deionised water and allowing to 'age' by stirring for 12 hours.

Polyalkyl glycol with molecular weights 600 $gmol^{-1}$ (tradename DCP 101), 1200 $gmol^{-1}$ (tradename BREOX 50 A 50) and 1700 $gmol^{-1}$ (tradename BREOX 50 A 140) were used as supplied by Schlumberger Cambridge Research. Liquid polyalkyl glycol was either used without dilution (pure) or diluted in water prior to contact with free standing bentonite films. In all experiments deionised water (pH 7 and conductivity $<20~\mu Scm^{-1}$).

7.2.2.   Spectroscopy

7.2.2.1. Transmission - Free standing films

Free standing films were prepared by the method outlined in section 6.2.2.1. In each experiment, a small square (≥ 13 mm^2) weighing between 5 and 7 mg, was immersed in 50 cm^3 of aqueous polyalkyl glycol solutions with concentrations 100, 50, 5, 2.5 and 1 gdm^{-3} for the required time. The films were then dried in the nitrogen purge of the Mattson Polaris FTIR spectrometer. FTIR transmission spectra were then obtained with 4 cm^{-1} resolution, a triangular apodisation function, and 100 co-added scans. These experiments were repeated dissolving ionic salts (NaCl and KCl) in the aqueous polyalkyl glycol solution prior to immersion of the bentonite film in order to obtain a final salt concentration of 100 gdm^{-3}.

7.2.2.2. Transmission - Aqueous dispersions

Homoionic SWy-1 bentonite-polyalkyl glycol dispersions were prepared by adding aqueous solutions of PAG(600) to bentonite suspension in order to obtain 50 cm^3 of mixed suspension containing, polyalkyl glycol concentrations of 50, 5.0, 2.5 and 1 gdm^{-3} and bentonite concentrations of 20 gdm^{-3}.

These dispersions were equilibrated overnight at room temperature using a rotary sample mixer operating at 300 rpm. The dispersions were centrifuged at 20000 rpm and dried overnight at 40°C. The dried solids were dispersed in KBr disks and their transmission infrared spectrum acquired using the same conditions as described above.

7.2.2.3. ATR spectroscopy - Bentonite film

Bentonite films were prepared on the surface of the ZnSe Squarecol ATR prism as outlined in section 4.4.4. The cell was then sealed containing the bentonite coated ATR prism and the infrared spectrum of the supported air dried bentonite film acquired at room temperature. Each spectrum was acquired on a purged Mattson Polaris FTIR spectrometer with a resolution of 4 cm^{-1}, a triangular apodisation function and 512 co-added scans.

Without removing or repositioning the Squarecol cell from the sample compartment of the infrared spectrometer, the trough was filled with 2 cm^3 undiluted (pure) polyalkyl glycol (molecular weight 600 gmol^{-1}) or polyalkyl glycol, (molecular weight 600 gmol^{-1}) diluted in aqueous solution. Infrared spectra of the bentonite film (in contact with polyalkyl glycol solution) were obtained at 5 minute intervals on a Mattson Polaris FTIR spectrometer, using the same parameters as before.

7.2.2.4. ATR spectroscopy - Polyalkyl glycol

The infrared spectrum of pure (undiluted) polyalkyl glycol was obtained using Graseby Specac variable angle liquid ATR accessory, fitted with a 45° ZnSe ATR prism and a 12 μm spacer. The polymer was injected into the cell and the infrared spectrum acquired under ambient conditions using 256 scans at 4 cm^{-1} resolution. The infrared spectra of polyalkyl glycol diluted both with deionised water and with 100 gdm^{-3} aqueous KCl solution, were also acquired.

7.2.2.5 X-ray Diffraction

All basal spacings were measured between 4 and 20° 2θ using a Phillips 1050 diffractometer operating at 40 kV and 40 mA with Co K$_\alpha$ radiation. The d-spacing of SWy-1 bentonite free standing films and free standing films immersed in aqueous polyalkyl glycol or polyalkyl glycol/KCl solution were obtained from the dried film on a glass slide.

7.3.   Results and Discussion

7.3.1   Infrared spectroscopy of polyalkyl glycol and dilutions of polyalkyl
         glycol.

Polyalkyl glycol is an EO/PO polymer, having ethylene oxide and propylene oxide monomeric units randomly distributed along the chain. Figure 7.3.1a shows the ATR infrared spectrum of pure polyalkyl glycol ratioed against a clean ZnSe IRE. The absorbance bands have been tentatively ascribed using the literature assignments (table 7.3.1a) for ethylene glycol [238] and ethylene glycol mono ether [150].

253

Figure 7.3.1a the infrared spectrum of pure polyalkyl glycol.
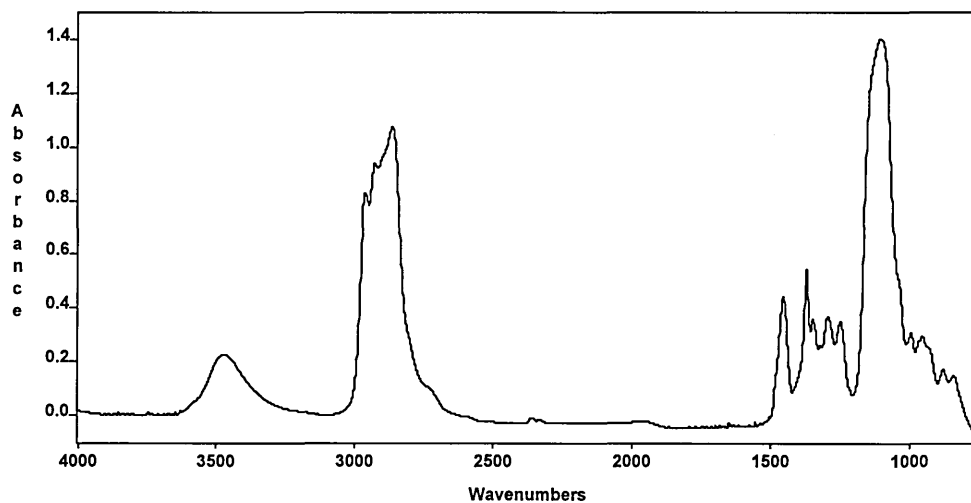
Table 7.3.1a Band assignments for polyethylene glycol.

Band position (cm^{-1})	Assignment
3475	H-bonded ν(OH)
2967	antisymmetric ν(CH$_3$)
2932	antisymmetric ν(CH$_2$)
2868	symmetric ν(CH$_3$) and ν(CH$_2$)
1459	δ(CH$_2$),antisymmetric δ(CH$_3$)
1374	w(OC$_2$H$_4$)
1351	symmetric δ(CH$_3$), w(CH$_2$)
1324	w(CH$_2$)
1109	ν(C-O-C)
1001	various ν(C-O)
957	various ν(C-O)

There is no band attributed to an OH deformation mode (1640-1650 cm^{-1}) in the spectrum of pure polyalkyl glycol indicating that there is no water impurity present in the pure sample.

Although polyalkyl glycol has been used pure (undiluted) in some experiments it has been more commonly mixed in aqueous solution and perhaps more importantly with 100 gdm^{-3} KCl solution. Molecules of the polyalkyl glycol type are known to change conformation in the presence of water and dissolved cations [99]. Consequently, the infrared spectrum of polyalkyl glycol on dilution in water and aqueous KCl solution is extremely important. Figure 7.3.1b shows the infrared spectrum of polyalkyl glycol diluted to 50% by weight in water and aqueous 100 gdm^{-3} KCl solution.

Figure 7.3.1b Infrared spectrum of polyalkyl glycol diluted to 50% by weight in water and aqueous 100 gdm^{-3} KCl solution.
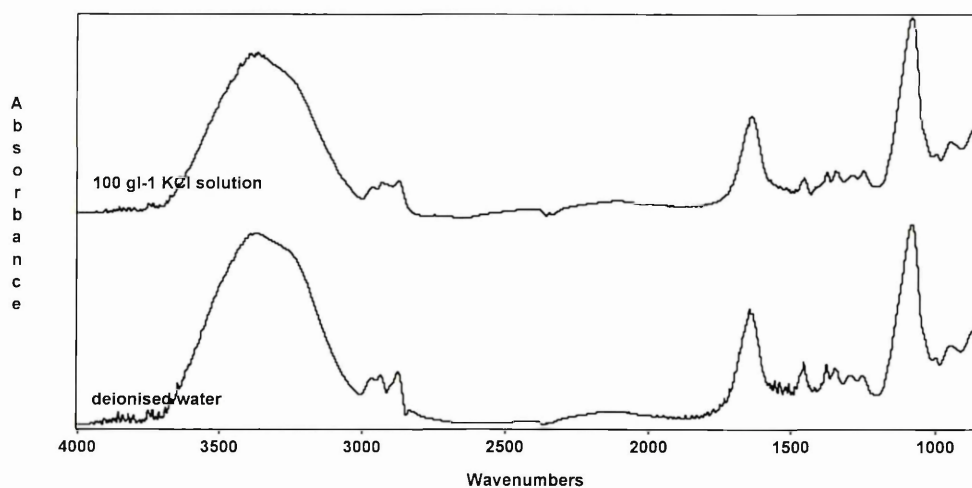
The spectra obviously show characteristic high intensity bands due to water. However, the band at 1374 cm^{-1} (figure 7.3.1c), attributed to an ν(OC) stretching mode of OC$_2$H$_4$ in pure polyalkyl glycol, is progressively shifted to higher frequency by ~8 cm^{-1} on increasing dilution.

Figure 7.3.1c Frequency shift of the v(OC) band on increasing dilution.
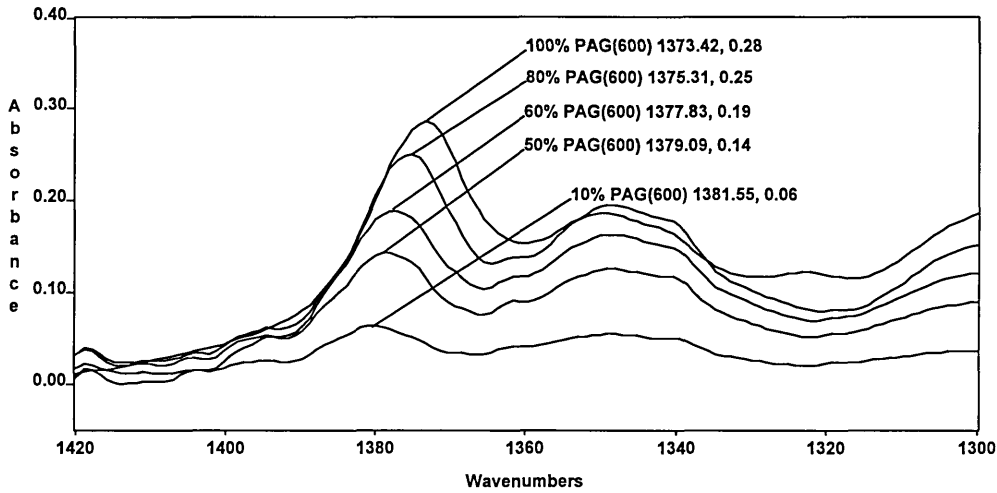
Graph 7.3.1c shows the shift in wavenumber position of the v(OC) band with increasing dilution in water. This corroborates the findings of Cliffe et al [1] who also noted this band shift to 1382 cm^{-1} on 6 % wt dilution of polyalkyl glycol in distilled water.

Graph 7.3.1c Shift in wavenumber position of the v(OC) band maximum with increasing dilution.
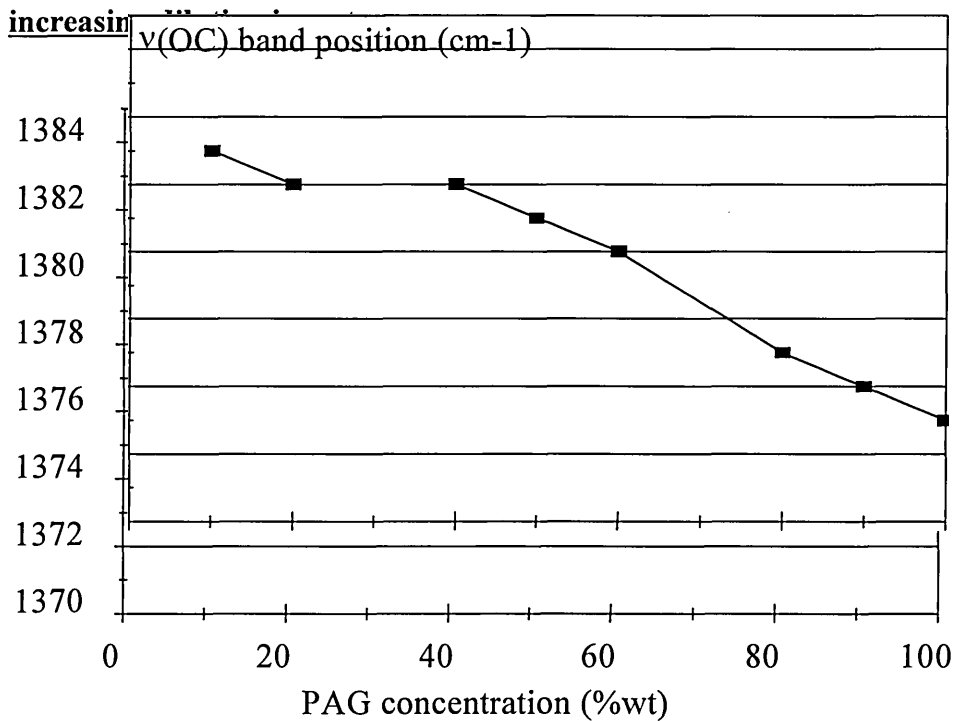
The same band shift is observed on dilution of polyalkyl glycol in the presence of 100 gdm^{-3} KCl solution. Hence, K$^+$ ions appear to have no influence on this band shift. This may instead be attributed to the interaction of water with the main chain ether oxygen atoms.

Another significant difference between the spectrum of pure polyalkyl glycol and its aqueous solution can be seen between 1250 and 1000 cm^{-1} (figure 7.3.1d). In this spectral region, the band attributed to C-O-C stretching in pure polyalkyl glycol appears to shift to low frequency on increasing dilution.

Figure 7.3.1d Infrared spectrum of the ν(C-O-C) band on increasing dilution.
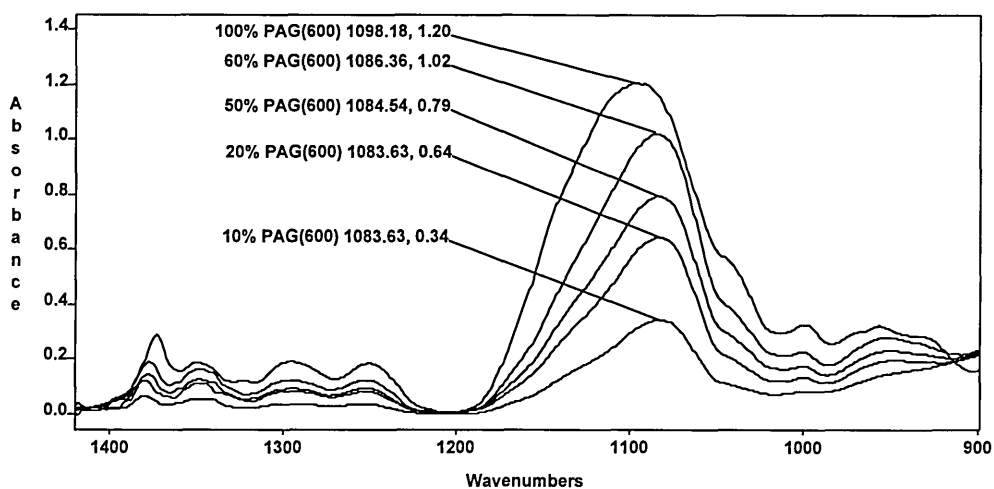
Graph 7.3.1d shows the shift in wavenumber position of the ν(C-O-C) band maximum with increasing dilution. Clearly, the 1098 cm^{-1} band of pure polyalkyl glycol is shifted to lower frequency (1082 cm^{-1} for dilution at ≤40% by weight).

Graph 7.3.1d Shift in wavenumber position of the v(C-O-C) band maximum with increasing dilution in water
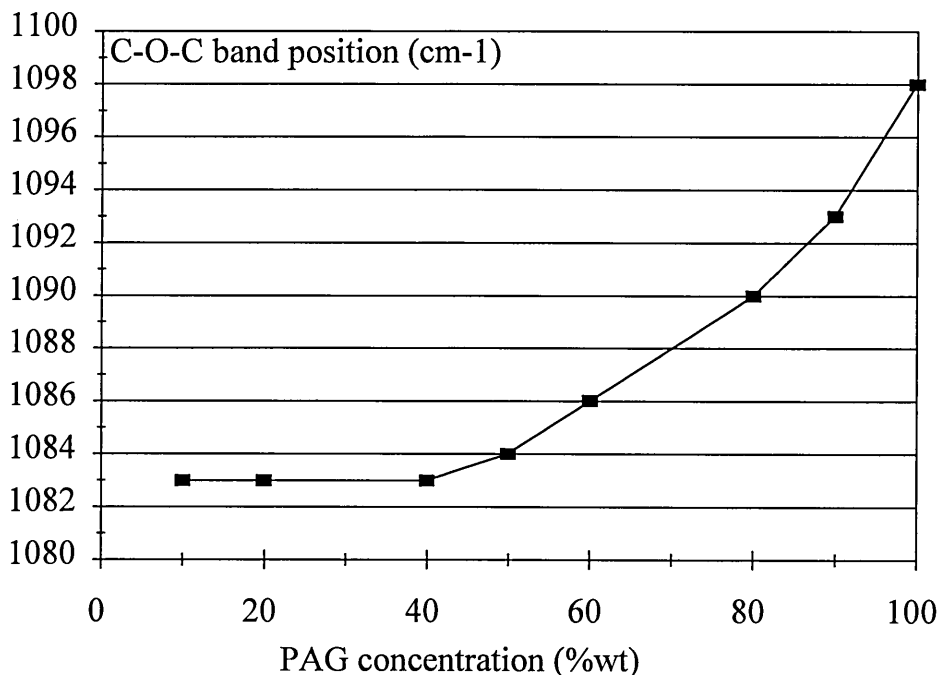
The observed band shift was not affected by KCl dissolved in solution. This effect is therefore associated with the hydration of the polyalkyl glycol molecule, in particular, the arrangement of water molecules around the ether oxygen atom.

Indeed, the shape of graph 7.3.1d appears to be indicative of the molecule reaching a maximum hydrated state between 40 and 50% by weight of polyalkyl glycol. This finding is consistent with the findings of Liu and Parsons [91] who observed a linear increase in the chemical shift of internal ethylene protons up to 50% by volume polyethylene glycol dilution in water. This was attributed to the change in segmental environment of the polyethylene glycol which does not change above a certain concentration of water. This was due to the formation of a stoichiometric hydrate containing three water molecules per ethylene oxide segment.

It should be noted, that the band centred at 1098 cm^{-1} (figure 7.3.1d) in the spectrum of pure polyalkyl glycol contains several components. It appears to have

a shoulder at high frequency and the half width of the band (~100 cm^{-1}) seems too large to be that of a single absorption. The apparent shift in the wavenumber position of the ν(COC) band may therefore be due to changes in relative intensity of the bands in this region. Detailed analysis of this spectral feature using Fourier self deconvolution was difficult as no prior knowledge of the number of component bands and their half widths existed. Additionally, the second derivative of this spectral feature was too noisy to be of value. Consequently, curve fitting to allow an understanding of the nature of band shifts and/or changes in relative intensity was not possible.

Both the 1073 and 1098 cm^{-1} bands in pure polyalkyl glycol appear to be diagnostic bands for the state of hydration of polyalkyl glycol in aqueous solution. Unfortunately, the band at 1098 cm^{-1} occurs in the same region as the strong ν(Si-O) absorptions (between 1150 and 950 cm^{-1}) of bentonite. Indeed, this ν(COC) band shifts to 1082 cm^{-1} on full polymer hydration and consequently directly coincides with the ν(Si-O) band in pure bentonite. This will obviously significantly hinder the analysis of the Si-O region of the bentonite spectrum (as was performed for polyacrylamide in chapter 6) in order to determine interactions of the polymer with the silicate lattice or with the exchange cations between the clay platelets.

7.3.2.   Adsorption Isotherms

Although adsorption isotherms provide information regarding the mechanism of polymer adsorption on clay mineral they have not been measured for the adsorption of polyalkyl glycol on bentonite in this study. However, the adsorption isotherms for the adsorption of polyalkyl glycol (Mw 600) have been studied previously [1, 3].

Cliffe et al [1] measured adsorption isotherms for polyol adsorbed on to bentonite dispersed in aqueous solution and onto bentonite pre formed into an air-dried free standing film. Polyol was concluded to have a high affinity for bentonite in both distilled water and KCl solution. In distilled water, comparable amounts adsorbed onto dispersed bentonite and bentonite films. However, adsorption was greater onto bentonite dispersed from aqueous KCl solution than onto free standing bentonite films from polyol/KCl solution, due probably to the accessibility of the interlayer surface of the bentonite platelets. Rawson [3], meanwhile, concluded that the maximum adsorbed amount of polyalkyl glycol (Mw 600) on homoionic Westone-L bentonite, increased as the swelling capacity of the exchange cation increased, i.e. in the order $Mn^{2+} > Na^+ > K^+ > Cs^+$.

The adsorbed amounts quoted by Rawson [3] ($\sim$90 mg g^{-1} clay on Na bentonite and 70 mg g^{-1} clay on K bentonite) are significantly lower than those observed by Cliffe et al [1] (200-300 mg g^{-1} clay from 20-30 gdm^{-3} polymer solution, but increasing linearly above this). This was attributed to washing the clay-polymer complexes in deionised water which would remove entrained polymer.

7.3.3.   X-ray diffraction

The d-spacing of homoionic Na and K bentonite free standing films have been determined by X-ray diffraction. Figure 7.3.3a shows the X-ray diffraction trace recorded for Na and K bentonite free standing films under ambient conditions. Table 7.3.3a displays the corresponding d-spacings

Figure 7.3.3a Diffraction traces recorded for Na and K bentonite free standing films under ambient conditions
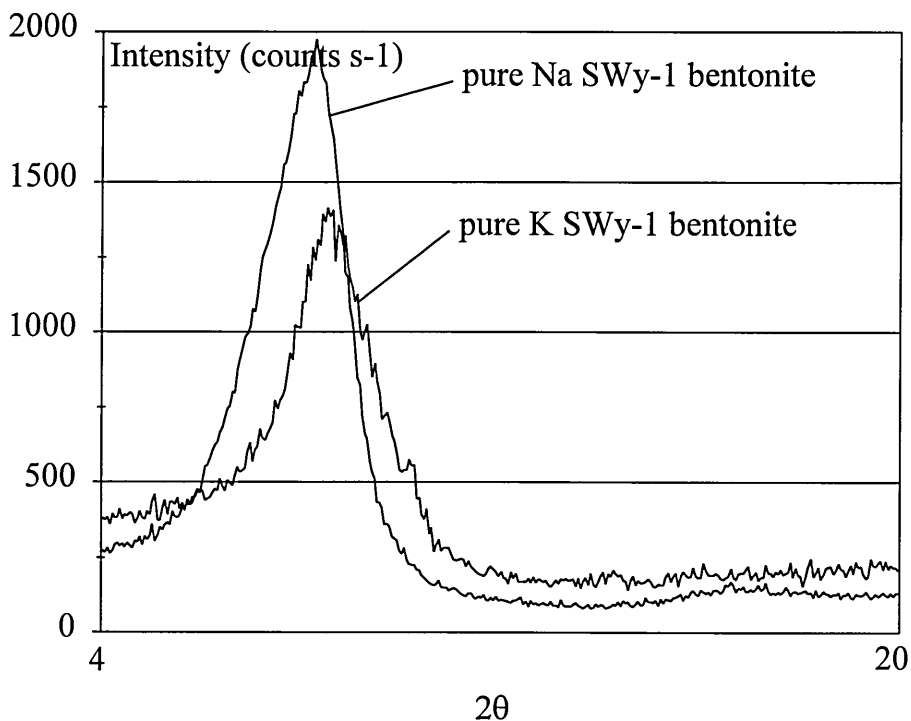
Table 7.3.3a d-spacing of Na^+ and K^+ SWy-1 bentonite free standing films.

M^+ SWy-1 bentonite	d-spacing (Å)
Na^+	12.5±0.3
K^+	11.9±0.3

The d-spacing of the K bentonite film is lower than that of the Na bentonite film, due to its low hydration energy (inability to form extended hydration spheres) and therefore its inability to swell [6]. Additionally, the maximum in the diffraction trace for K bentonite is broad and low, indicating that the platelets were not perfectly aligned to produce coherent diffraction.

7.3.3.1 Adsorption of polyalkyl glycol from solution onto Na bentonite free standing films

In agreement with the findings presented in chapter 6 for the adsorption of polyacrylamide from aqueous solution onto free standing natural bentonite films, immersion of films prepared from Na^+ SWy-1 bentonite in aqueous polyalkyl glycol (Mw 600 at ≤ 5 gdm^{-3}) caused the films to collapse. Consequently, they could not be retained and analysed using X-ray diffraction. Cliffe et al [1] also found that, for a 0.05% polyol loading in solution, the clay films disintegrated.

At higher PAG(600) loadings (50 gdm^{-3} or 100 gdm^{-3}), however, the Na bentonite films did not disintegrate. Films could be retrieved from these solutions and handled easily. This contrasts with the findings for polyacrylamide on SWy-1 bentonite free standing films where all films disintegrated.

Cliffe et al [1] studied the adsorption of polyalkyl glycol on both free standing films and dispersed bentonite, whereas Rawson [3], studied only the interaction of polyol with Na bentonite dispersed in aqueous solution. Both, however, discuss the dependence of interlayer spacing on the adsorbed amount of polyol, which in turn is critically dependent on the polymer solution concentration. Their observed d-spacings around 18.1Å and 14.2Å are attributed to the formation of ordered bi-layers and monolayers of polyalkyl glycol in the Na bentonite-polymer complex. This conclusion was based on the findings of other authors who have interpreted changes in d-spacings for clay-ethylene glycol [122, 123, 126] and clay-polyethylene glycol [117, 118, 121] complexes in the same way. Figure 7.3.3.1a shows the diffraction trace of the Na bentonite film after being placed in 100 and 50 gdm^{-3} polyalkyl glycol (Mw 600) and table 7.3.3.1a displays the d-spacings obtained from each diffraction trace.

Figure 7.3.3.1a Diffraction trace of stable Na bentonite films, immersion in 100 and 50 gdm^{-3} polyalkyl glycol (Mw 600) solution.
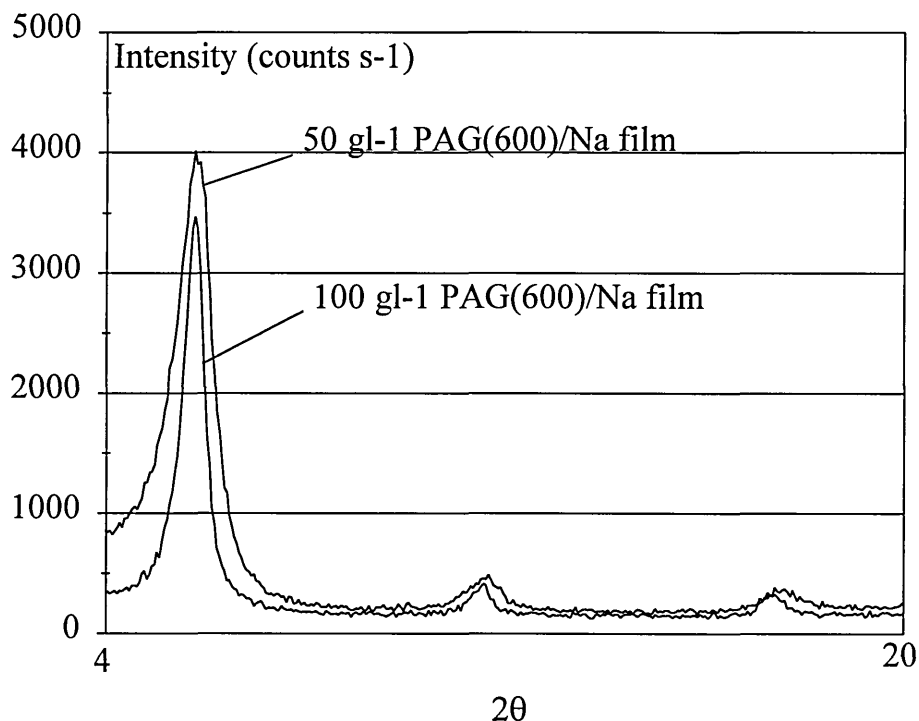
Table 7.3.3.1a d-spacing of Na bentonite films, intact, after being placed in 100 and 50 gdm^{-3} polyalkyl glycol (Mw 600) solution.

PAG(600) concentration (gdm^{-3})	d-spacing (Å)
100.0	18.1 ±0.2
50.0	18.2±0.2

It is interesting to note that these diffraction traces contain two higher order reflections and smooth intense maxima. This is indicative of highly ordered clay samples in which the c-axis (the axis of the basal spacing) are all oriented in the same direction.

A d-spacing of ~18Å corresponds to the formation of two layers of PAG(600) between the bentonite platelets. A basal spacing of 17.6Å in the X-ray diffraction trace of an air dried stable natural bentonite film immersed in 5% PAG(600) has been reported [1], which is slightly lower than reported here. It is noticeable, however, that further drying of the films by placing the film over P_2O_5 [1], caused a slight decrease of the basal spacing to 17.5Å. Consequently, it might be assumed that although the films used in this study have been dried in a nitrogen purge, they were stored under ambient conditions and placed in a diffractometer whose humidity level was not controlled. They may therefore have adsorbed water. Changes in relative humidity are known to affect the basal spacings of EG treated clay samples [128] so slight variations in humidity may account for the range of d-spacing observed for a 2 layer organic complex.

Clearly, in the absence of any other components in solution (see later), the formation of an organic bi-layer is imperative to the stabilisation of Na bentonite films in aqueous solutions of polyalkyl glycol. The formation of an organic bi-layer is related to the number of moles of polyalkyl glycol per unit volume of solution and to the concentration of bentonite (defined by the film weight).

In order to establish the effect of polyalkyl glycol concentration, the stabilisation of Na bentonite films has also been evaluated in aqueous polyalkyl glycol solutions of higher molecular weight, i.e. PAG(1200) and PAG(1700). Since at the same weight concentration, the number of moles per unit volume of higher molecular weight material offered to the clay film will be lower.

Figure 7.3.3.1b displays the diffraction trace of the only stable film prepared in polyalkyl glycol of higher molecular weight, that being at a solution concentration of 100 gdm^{-3} PAG(1200).

Figure 7.3.3.1b Diffraction trace of the stable Na bentonite film, after immersion in 100 gdm^{-3} polyalkyl glycol (Mw 1200) solution.
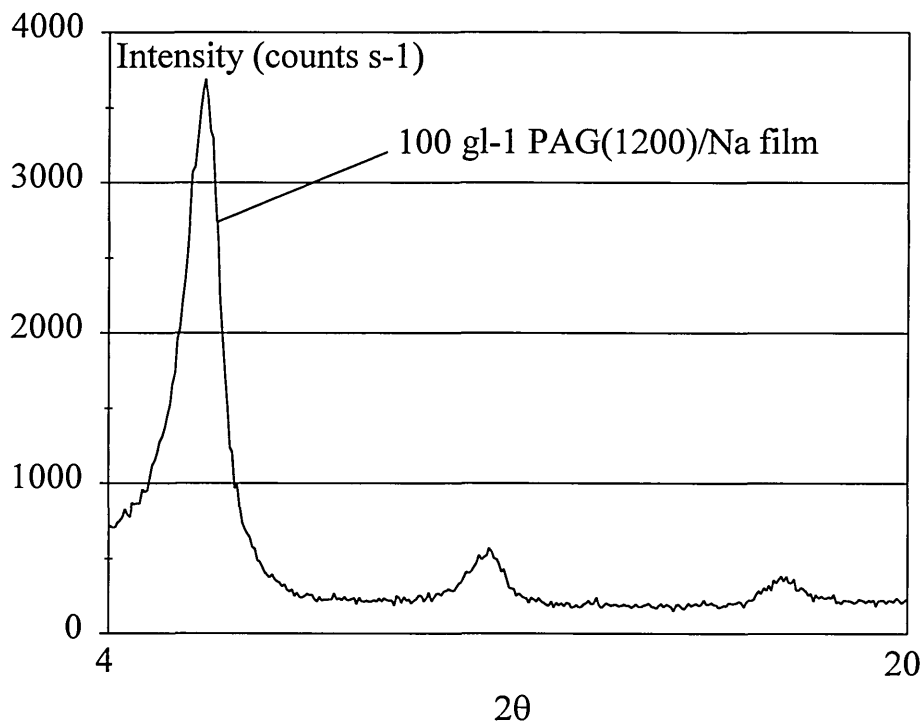
Again the bentonite platelets were well ordered and separated by ~ 8.0Å (d-spacing 17.9Å). This is again due to the formation of a polymer bi-layer between the platelets.

Na bentonite free standing film could not be stabilised in solutions containing PAG(1700), even at concentrations of 100 gdm^{-3} by weight. This confirms the conclusions of Cliffe et al [1] that Na bentonite film stabilisation is related to the number of moles of polyalkyl glycol per unit volume of solution. Table 7.3.3.1b shows the number of moles of polyalkyl glycol per unit volume at each concentration of each molecular weight.

Table 7.3.3.1b Number of moles of polyalkyl glycol per unit volume at each concentration of each molecular weight.

Concentration PAG (gdm^{-3})	No of moles of PAG per unit volume present by molecular weight (moldm^{-3})		
	Mw 600	Mw 1200	Mw 1700
100.0	1.6×10^{-1}*	8.3×10^{-2}*	5.9×10^{-2}
50.0	8.3×10^{-2}*	4.2×10^{-2}	2.9×10^{-2}
5.0	8.3×10^{-3}	4.2×10^{-3}	2.9×10^{-3}
2.5	4.2×10^{-3}	2.1×10^{-3}	1.5×10^{-3}
1.0	1.7×10^{-3}	8.3×10^{-4}	5.9×10^{-4}

* Indicates Na bentonite film stability

Allowances must be made for slight variations in film weight for different experiments but it appears that there is a critical minimum number of moles of polyalkyl glycol per unit volume of solution which is required to stabilise 5-7 mg Na bentonite films. This concentration is approximately 0.08 moldm^{-3}

There are many factors which might explain this observation. One plausible explanation is the role played by the functional groups (either the number of OH end groups or OCH$_2$CH(CH$_3$) main chain ether oxygen atoms) on the polyalkyl glycol chain. It should be noted that 0.08 moldm^{-3} of PAG(600) will have the same number of OH end groups as 0.08 moldm^{-3} of PAG(1200) or 0.08 moldm^{-3} of PAG(1700). This might indicate a critical number of OH end groups required to facilitate film stabilisation. However, an almost identical species, polyethylene glycol (Mw 600 gmol^{-1}) with OH end groups but OCH$_2$CH$_2$ main chain ether oxygen atoms instead does not stabilise the bentonite film in similar immersion experiments [1]. Additionally, other polyols without OH end groups

have also shown similar shale inhibitive action [1]. It therefore seems likely that the OH end groups are not important in the adsorption process.

The number of ether main chain oxygen atoms would not appear to explain this minimum critical number of moles of polymer per unit volume in solution since 0.08 moldm^{-3} of PAG(600) will have the same number of OH end groups as 0.08 moldm^{-3} of PAG(1200) but only half as many OCH$_2$CH(CH$_3$) ether main chain oxygen atoms. Hence, the most likely explanation is that, in the absence of other components in solution, the critical polymer concentration is related to the number of moles of polyol per unit volume of solution which are required to form a bi-layer between the platelets which will stabilise the film. These polymer layers may then restrict water molecules from forming extended hydration shells around the exchange cation thus preventing dispersion.

Although the influence of polymer concentration (moles per unit volume) in solution seems beyond doubt, many other factors may also influence the stability of bentonite free standing films. One such factor could be the relative rates of polymer adsorption. Large organic molecules may have lower diffusion rates in solution, consequently, the rate of adsorption will depend upon the molecular weight and the concentration of polymer species in solution. Hence, the larger molecules may require more time to adsorb which allows the bentonite platelets, which comprise the free standing film, to be hydrated and disperse, thus facilitating film rupture.

7.3.3.2 Adsorption of polyalkyl glycol from dilute solution onto K bentonite free standing films

The nature of the exchange cation is also extremely important to the stabilisation of the free standing films by polyalkyl glycol in solution. Evidence of this can be

found in a small contradiction between the results of Cliffe et al [1] and the results presented here. In these findings, films immersed in 5 gdm^{-3} (corresponds to 0.5% by weight) PAG(600) disintegrated. However, Cliffe et al [1] using the same polymer found films immersed at the same concentration to be stable. It is possible that the clay films used by Cliffe et al [1] contained significantly less clay solids than those used in this study and consequently, the PAG(600):clay loading ratio increased above the critical level which is required to stabilise the Na bentonite film. However, the size of films and hence mass of clay used in immersion tests [1] were not dissimilar to those used in these studies. A likely explanation for the contradiction is that their experiments [1] were performed on natural bentonite (without cation exchange, containing predominantly Na$^+$ but also lower amounts of Ca^{2+} and K$^+$ cations). The experiments presented here however, were performed on homoionic Na$^+$ exchanged SWy-1 bentonite. The presence of small amounts of K$^+$ and Ca^{2+} cations may critically affect the stabilisation mechanism. Indeed it was shown [1] that adsorption of PAG(600) onto K$^+$ exchanged clay produced stable films in PAG(600) solutions at concentration as low as 1% by weight.

These experiments have been repeated and, indeed, K$^+$ homoionic bentonite films are stable in PAG(600) solution at concentrations of 50, 5 and 1 gdm^{-3} (5, 0.5 and 0.1 % by weight). The diffraction traces of K bentonite films immersed in 50, 5 and 1 gdm^{-3} PAG(600) solutions are shown in figure 7.3.3.2a. Table 7.3.3.2a displays the d-spacings obtained from each diffraction trace.

Figure 7.3.3.2a Diffraction trace of stable K bentonite films, immersion in PAG(600) solutions.
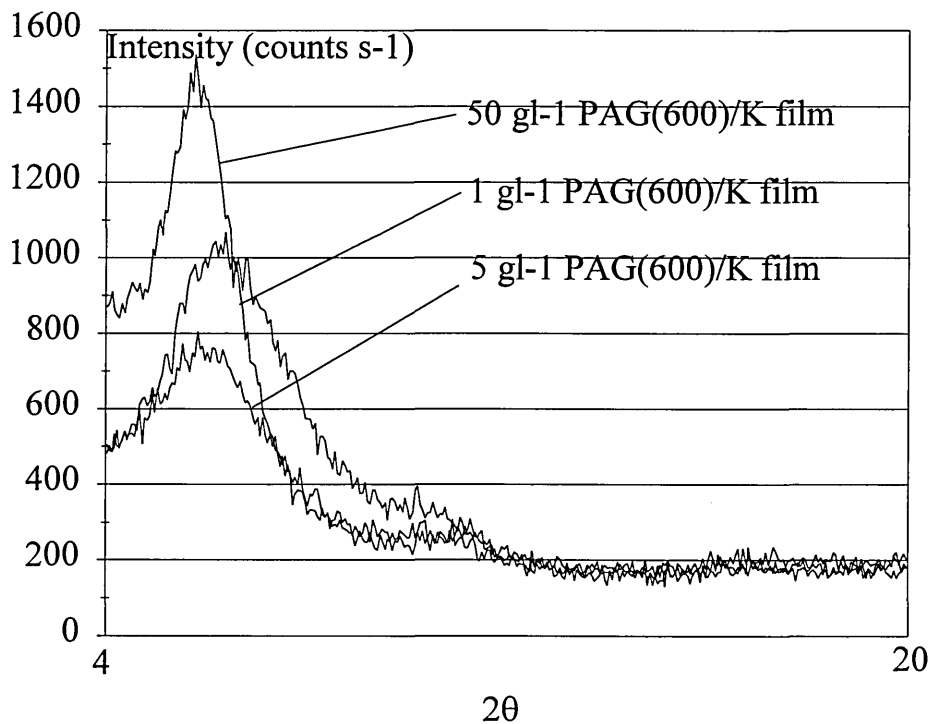
Table 7.3.3.2a The d-spacing of stable K bentonite films, after being placed in PAG(600) solutions.

PAG(600) concentration (gdm^{-3})	d-spacing (Å)
50.0	17.5±0.3
5.0	17.1±0.5
1.0	16.6±1.0

The stability of homoionic K$^+$ exchanged bentonite films in the presence of PAG(600), far exceeds that of homoionic Na$^+$ exchanged bentonite films for the same solution, being stable in PAG(600) solution at concentrations ≥ 1 gdm^{-3}.

In each film the interlayer has been swollen by adsorption of the polyol resulting in d-spacings corresponding to the formation of an organic double layer in the interlayer spacing at the two higher concentrations. These d-spacings for the double organic layer are slightly lower than those observed for polyol adsorbed in the interlayer of Na bentonite films ($\sim18\text{Å}$). This is probably due the lower hydration energy of the K^+ ion and therefore its inability to hydrate easily, thus preventing water adsorbing between and swelling the layers as it might in the Na bentonite. At the lowest concentration however, there is probably both single and double layer complexes formed. This results in a broad maxima whose position has a large error associated with it, existing between that corresponding to a purely single or purely double polymer layer complex. It is unlikely to be due to either a hydrated single layer complex (K^+ would probably not hydrate sufficiently), or a coiled polymer conformation (flexible, linear, nonionic polymers tend to uncoil on adsorption [11], adsorbing as flat layers). Figure 7.3.3.2a also shows that the platelets are disordered compared with the corresponding Na bentonite films. This may be related to the inability of the K bentonite to swell sufficiently to allow easy access for the adsorbing polymer. Broad diffraction traces for complexes between PAG(600) and various homoionic bentonites have revealed two basal spacings at approximately 18.0 and 14.2 Å on heating [3]. This corresponds to mixed complexes containing organic mono- and bi-layers between the platelets. It appears that the stabilisation of the K bentonite film does not require the polymer to form two organic layers between the platelets (as appears to be necessary in homoionic Na bentonite).

Cliffe et al [1] also identified the importance of K^+ exchangeable cations in the stabilisation of K^+ homoionic bentonite films by adsorption of PAG(600) from distilled water. The values of d-spacing quoted by Cliffe et al [1] were lower than those presented here, increasing from 13.8, to 15.2 Å, as the adsorbed amount increased from 17 to 28% by weight (corresponding to solution concentrations of

<5 gdm^{-3} and >40 gdm^{-3}). The most likely explanation is that in this study, mixed mono- and bi-layer complexes are formed (the influence of rehydration in the natural humid atmosphere is not likely to cause such large discrepancies). Cliffe et al [1] determined that the stability of the K bentonite-PAG(600) complex corresponds to the formation of a monolayer between the clay platelets, denoted by the diffraction peak at approximately 14.5Å and that K$^+$ inhibited the formation of two layer complexes. Indeed, the complex formed comprising a polymer bi-layer was not observed [1]. This contradicts the findings presented here where at all concentrations of PAG(600), evidence of mixed mono- and bi-layer complexes in the K bentonite film could be observed. The reason for this is not entirely clear but may be due to incomplete K$^+$ cation exchange in the bentonite used in this study. The presence of small amounts of Na$^+$ might allow the clay platelets to swell slightly more than if only K$^+$ cations were present, and hence will allow slightly more polymer to be adsorbed. The K bentonite used it should be noted however, had only a negligible K$^+$ content (table 4.9.1).

The effect of the exchange cation is nowhere more noticeable than in the adsorption of polyalkyl glycol of higher molecular weight onto K bentonite films. Na$^+$ homoionic bentonite films disintegrated when immersed in solutions of PAG(1700) at concentrations between 1 and 100 gdm^{-3}. However, when K$^+$ homoionic films are contacted with PAG(1700) in a comparable concentration range, all remain in tact. The diffraction traces of K bentonite films immersed in PAG(1700) solutions of concentrations between 1 and 50 gdm^{-3} are shown in figure 7.3.3.2b. Table 7.3.3.2b displays the d-spacings obtained from each diffraction trace.

**Figure 7.3.3.2b Diffraction trace of stable K bentonite films, after immersion in PAG(1700) solutions.**
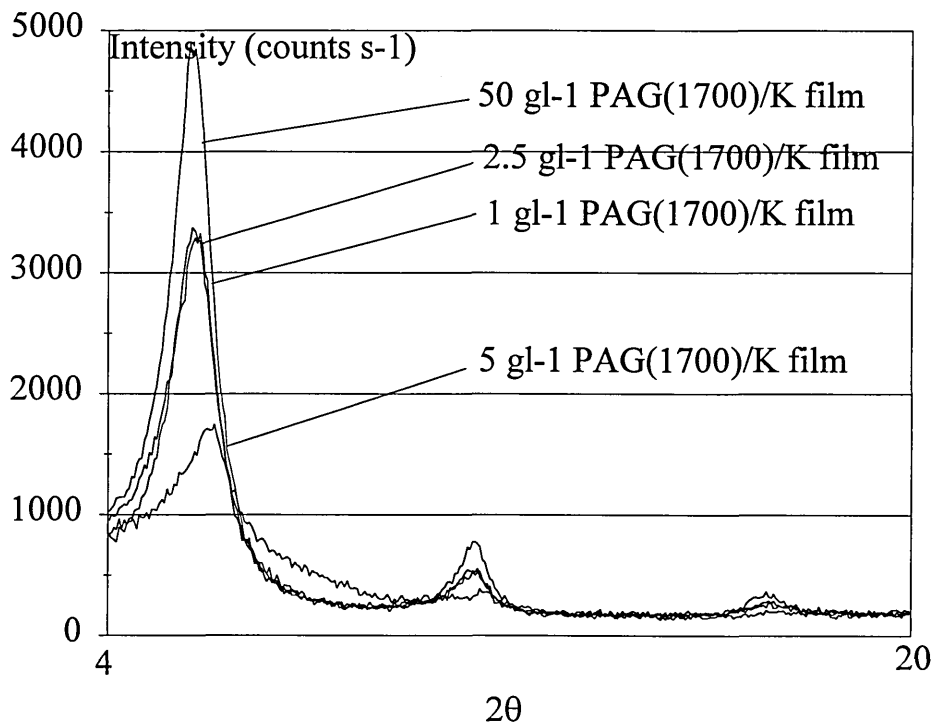
Table 7.3.3.2b d-spacing of stable K bentonite films, after immersion in PAG(1700).

PAG(1700) concentration (gdm^{-3})	d-spacing (Å)
50.0	18.1±0.2
5.0	17.5±0.2
2.5	18.0±0.2
1.0	18.1±0.2

These d-spacings all correspond to the formation of two polymer layers in the space between the K bentonite platelets, again in contradiction of the influence on d-spacing of K$^+$ as stated by Cliffe et al [1]. The traces observed in figure 7.3.3.2b are comparable to the traces obtained for the adsorption of PAG(600) onto Na

bentonite films (figure 7.3.3.1a) which are much more smooth, narrow and intense, than those obtained from the adsorption of PAG(600) onto K bentonite films (figure 7.3.3.2a) due to the orientation of platelets.

The shape of the diffraction traces may be indicative of a particular mechanism of adsorption. The ability of the bentonite platelets to stack directly on top of each other may be a function of the rate or ease of polymer adsorption. This depends on both the molecular weight of the polymer (faster for the lower molecular weight polymer than the higher molecular weight polymer) and the nature of the exchangeable cations (less impedance to adsorption when Na^+ are present than K^+ ions are present due to their relative swelling abilities).

Firstly, consider the K^+ exchanged bentonite; the K^+ ion can not easily hydrate and form extended hydration shells so adsorption between the platelets is more difficult than for the Na^+ exchanged bentonite as the clay will swell less. Consequently, the lower molecular weight polymer will diffuse quickly to the clay and adsorb quickly before dispersion is possible hence the mixed mono- and bi-layer complexes. However, the higher molecular weight polymer will diffuse more slowly to the clay allowing the bentonite more time to hydrate and disperse allowing easy access to the polymer resulting in bi-layer complexes only.

Now consider the Na^+ exchanged clay; Na^+ ions hydrate easily so only at high concentrations of low molecular weight polymer will adsorption occur quickly enough to prevent full dispersion of the platelets and hence, stabilise the film. Indeed, when the higher molecular weight polymer is used (even at high concentrations) the rate of diffusion to the clay is too slow to prevent dispersion and film rupture.

7.3.3.3   Adsorption of polyalkyl glycol from dilute solution onto Na bentonite

free standing films in the presence of electrolyte.

The presence of electrolyte in solution also affects polyalkyl glycol adsorption. Cliffe et al [1] proved in the presence of 7% KCl that the nature of the exchangeable counter cation is important in the stabilisation of bentonite films. Identical results were observed to those they had witnessed for the adsorption of PAG(600) from distilled water onto homoionic K bentonite films. Similar experimentation presented here (using 10% by weight KCl), showed general agreement with the results reported by Cliffe et al [1]. Figure 7.3.3.3a shows the diffraction traces of Na bentonite films immersed in PAG(600) solutions of concentrations between 1 and 50 gdm^{-3} containing 10% KCl. Table 7.3.3.3a displays the d-spacings obtained from each diffraction trace.

**Figure 7.3.3.3a Diffraction trace of stable Na bentonite films, after immersion in PAG(600)/10% KCl solutions.**
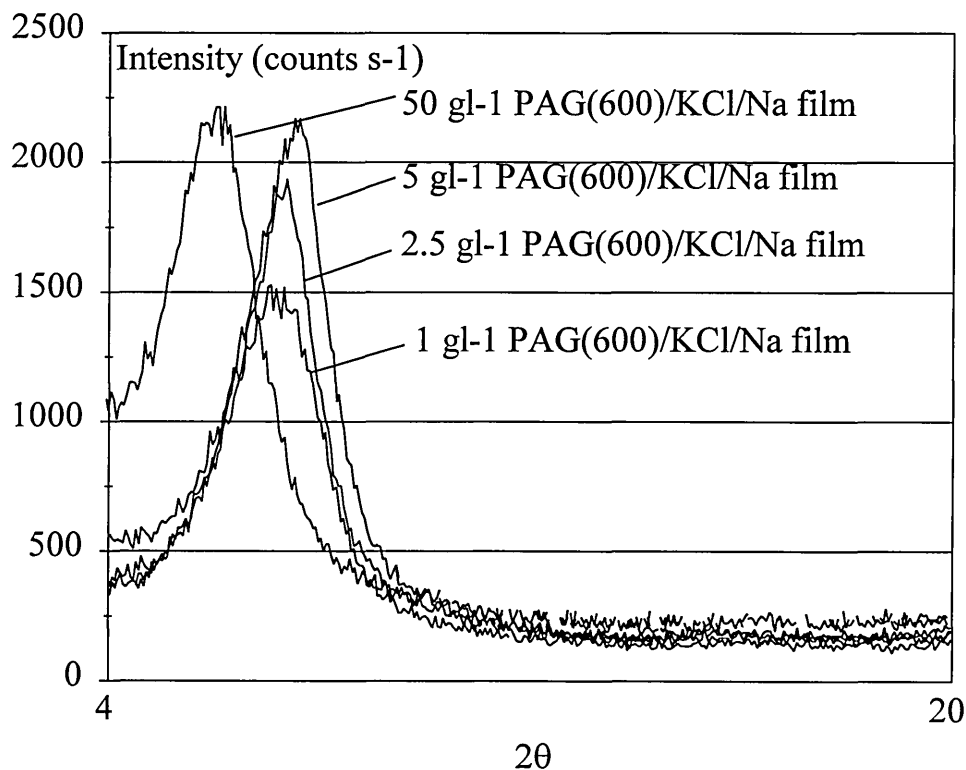
Table 7.3.3.3a d-spacing of stable Na bentonite films, after immersion in PAG(600)/10% KCl solutions.

PAG(600) concentration (gdm^{-3})	d-spacing (Å)
50.0	17.7±0.3
5.0	14.3±0.3
2.5	14.1±0.3
1.0	13.8±0.5

All Na bentonite films contacted with ≥1 gdm^{-3} PAG(600)/10% KCl solutions, remained intact. At concentrations ≥50 gdm^{-3} PAG(600) adsorbs into the interlayer region of the Na bentonite and forms a bi-layer complex which stabilises the clay film which was not observed by Cliffe et al [1]. However, at solution concentrations ≤5 gdm^{-3}, PAG(600) adsorbs and forms a mono-layer complex which stabilises the Na bentonite film. This in contrast to the previous findings where, in the absence of KCl, all Na bentonite free standing films were only stabilised by forming two layer complexes at concentrations ≥50 gdm^{-3} PAG(600).

It is not surprising that the adsorption of PAG(600) onto Na bentonite in the presence of KCl exhibits behaviour similar to that of PAG(600) adsorption onto K bentonite films. Rawson [3] concluded that K$^+$ ions in solution will exchange for those on the clay and that the presence of PAG(600) enhances the exchange of K$^+$ for Cs$^+$ ions on the clay. Hence, in these results, it seems likely to assume that, in the presence of KCl, exchange of K$^+$ for Na$^+$ will occur and consequently the Na bentonite film will adopt many of the characteristics of a K$^+$ exchanged film. Indeed, the diffraction traces are not very intense with ill defined maxima, similar to those of adsorption of PAG(600) onto K$^+$ exchanged bentonite films (figure

7.3.3.2a). However, the d-spacings observed for the adsorption onto Na bentonite from PAG(600)/KCl solution (except at a solution concentration of 50 gdm^{-3}) are slightly lower than those observed for the adsorption of PAG(600) onto K^{+} exchanged bentonite films (table 7.3.3.2a). This is indicative of the formation of only single layer polyol complexes in the interlayer region whereas mixed mono- and bi-layer complexes were observed in the adsorption directly onto homoionic K^{+} exchanged bentonite films. This may be due to an enhanced flocculating effect on the clay of excess of KCl in solution. This limits clay swelling so there is limited adsorption although the film is still stabilised. The formation of a bi-layer organic complex on a Na bentonite film from a 50 gdm^{-3} PAG(600)/10% KCl solution is less easy to explain but it may be an indication of the relative abilities of the lower molecular weight polyol, at this high concentration, and K^{+} to enter the interlayer space. It would seem likely that at such high concentrations the PAG(600) is able to quickly adsorb and hence form the two layer complex, before the system has been able to cation exchange significantly.

The adsorption of PAG(1700) onto Na bentonite films from KCl solution was studied to determine the effect of molecular weight on the adsorption characteristics in the presence of electrolyte. Figure 7.3.3.3b shows the diffraction traces of Na bentonite films immersed in PAG(1700) solutions of concentrations between 1 and 100 gdm^{-3}. Table 7.3.3.3b shows the d-spacings from each trace.

Figure 7.3.3.3b Diffraction trace of stable Na bentonite films, after immersion in PAG(1700)/10% KCl solution.
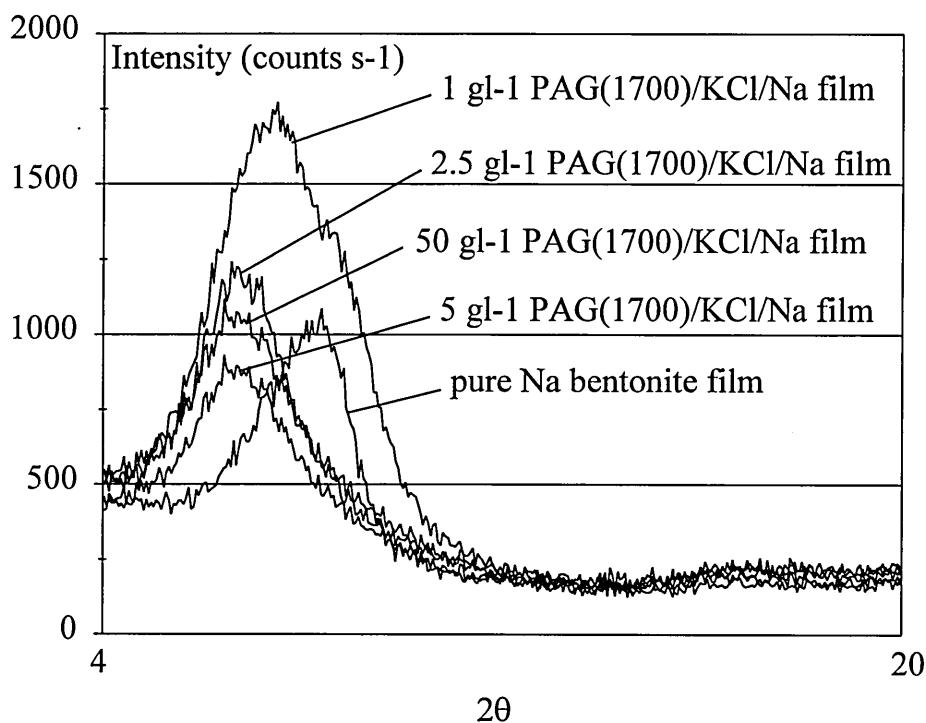
## Table 7.3.3.3b The d-spacing of stable Na bentonite films, after immersion in PAG(1700)/10% KCl solution.

PAG(1700) concentration (gdm^{-3})	d-spacing (Å)
50.0	15.8±0.5
5.0	15.5±0.5
2.5	15.2±0.6
1.0	13.8±1.0

Again, this result is unique, since in the absence of KCl, Na bentonite films were not stable in solutions of PAG(1700) at concentrations ≤ 100 gdm^{-3}. The position of the maxima and shape of the traces are quite unlike those observed in figure 7.3.3.2b for the adsorption of PAG(1700) onto K bentonite films, being more like

those observed for the adsorption of PAG(600) onto K bentonite films (figure 7.3.3.2a).

In order to explain the results, firstly, consider the d-spacing of 13.8Å seen in the trace of the Na bentonite film immersed in 1 gdm^{-3} PAG(1700)/KCl. The position of the maximum appears to be quite normal, corresponding to the formation of a single layer organic complex in the interlayer region. However, it appears to have quite a significant shoulder which is likely to correspond to the d-spacing of the natural unswelled clay. This indicates that a significant proportion of interlayer regions do not contain adsorbed polymer and therefore that complete formation of a single polyol layer between all the clay platelets in the film is not required for the film to remain robust and intact.

Secondly, consider the d-spacing observed between 15.2 and 15.8Å in the traces of films contacted with PAG(1700) solution at concentrations, ≥2.5 gdm^{-3}. These traces are broad, indicative of disoriented platelets and hence the difficulty of obtaining uniform adsorption in the presence of a highly flocculating environment. The d-spacings observed are not indicative of a dehydrated two layer complexes (which would be expected to have larger interlayer spacings around 17.0-17.5Å). Nor are they due to the formation of a coiled polymer layer between the platelets, since polymers of this type (flexible, linear, nonionic) are known to uncoil and adsorb in a flat conformation [11]. The more likely explanation is that each maximum corresponds to mixed one and two layer organic complexes. If these samples were to be heated as per Rawson et al [3], a d-spacing of approximately 14.4Å, corresponding to a single layer organic complex, might be observed as the second layer, considered to be more weakly bound [3], is removed. This work has not been performed here but the results would be interesting since the second layer in the complex formed in aqueous suspension can easily just sit between platelets.

In the case of adsorption onto bentonite films however, the polymer has to actively invade the interlayer region and therefore might be more strongly bound.

The shape and position of the traces (figure 7.3.3.3b) reflect the rate of PAG(1700) adsorption, K^+ cation exchange and the flocculating effect of the electrolyte solution. It appears that, using the higher molecular weight polymer in the presence of KCl does not degrade the film stability over the range of concentrations studied although it does seem to diminish its ability to adsorb. This is might due to both its slower rate of diffusion and the restriction to its adsorption in the confined space between the platelets in the presence of highly flocculating K^+ ions.

Although the influence of the K^+ ion is beyond doubt it is unclear whether the cation exchange of K^+ for Na^+ ions is the sole contributory factor in this stabilisation process or whether the presence of an excess of electrolyte in solution was also influential on the adsorption and stabilisation mechanism. Cliffe et al [1] believed that it was the specific interaction between K^+ and the polyol and not any salinity effects which enhanced the film stabilisation. Hence, the effect of electrolyte on the adsorption process was determined by using 10% NaCl as the flocculating electrolyte. Figure 7.3.3.3c displays the diffraction traces and table 7.3.3.3c lists the d-spacings obtained for the adsorption of PAG(600) onto Na bentonite films from solutions containing 10% by weight NaCl.

## Figure 7.3.3.3c Diffraction trace of stable Na bentonite films, after immersion in PAG(600)/10% NaCl.
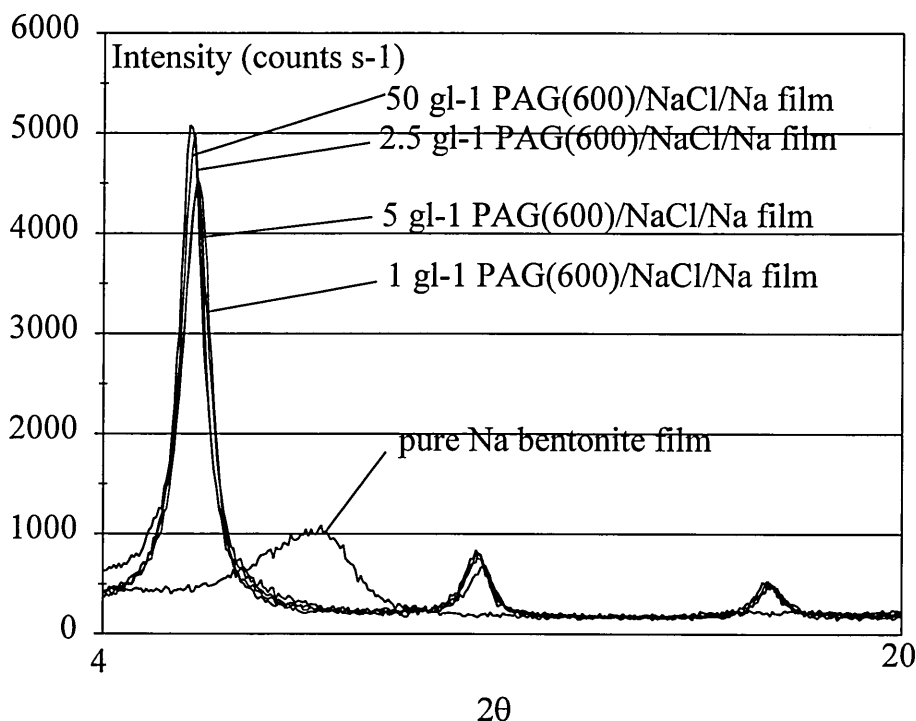
Table 7.3.3.3c d-spacing of stable Na bentonite films, after immersion in PAG(600)/10% NaCl.

PAG(600) concentration (gdm^{-3})	d-spacing (Å)
50.0	17.4±0.2
5.0	17.6±0.2
2.5	17.4±0.2
1.0	17.8±0.2

Clearly, NaCl has a profound effect on the stability of the Na bentonite films. In the absence of it (and other flocculents), bentonite films were only stable at concentrations ≥50 gdm^{-3}. However, in its presence, films were stable in solutions ≥1 gdm^{-3} PAG(600). Clearly, the presence of a flocculating electrolyte in solution,

regardless of its type, significantly increases the stability of Na bentonite films contacted with PAG(600). The d-spacings observed (17.4-17.8Å) are in good agreement with those observed by Cliffe et al [1] in the presence of 1 molar NaCl and correspond to adsorption of the polyol and formation of a two layer complex between the platelets.

These results, however, differ from those obtained for the adsorption of PAG(600) onto Na bentonite films in the presence of KCl (figure 7.3.3.3a). The d-spacings are larger and the traces are smooth and intense and show higher orders of reflection, all indicative of the relative ease of adsorption. It is known that Na^+ ions are more easily hydrated than as K^+ ions and consequently the extent to which the clay platelets can separate in the presence of Na^+ ions will be that much greater so film stability will be compromised. This seems more likely when one considers that the shape of diffraction traces obtained in the presence of Na^+ ions alone are smooth and highly intense whilst the shape of diffraction traces obtained in the presence of K^+ ions are broad and weak. This is indicative of the inability of the K^+ ions to allow swelling and hence hinder adsorption to give poorly oriented films and the ability of Na^+ ions to swell, allow adsorption and give well oriented films. It is noticeable that only one set of diffraction data for complex formation in the presence of K^+ ions showed intense smooth traces (figure 7.3.3.2b). These traces were for the adsorption of PAG(1700) onto K^+ exchanged bentonite without electrolyte solution. The ability of this system to swell may be due to the slower adsorption of the higher molecular weight polyol.

The stabilisation and resultant structure of the stable film is related to the polyol, the exchange cation and the presence of electrolyte. Consequently, given the key parameters of a system such as nature of exchange cation, nature and concentration of electrolyte and the nature, concentration and molecular weight of polyol, stabilisation may be predicted.

7.3.3.4 Kinetics of adsorption of polyalkyl glycol from dilute solution onto homoionic Na bentonite in the presence of electrolyte.

The adsorption of polyalkyl glycol onto free standing bentonite films has been studied by constraining several variables (such as molecular weight and nature of exchangeable cation) but keeping the time of immersion in the polyalkyl glycol solution to 12 hours (described as an overnight experiment). These experiments provide valuable information regarding the long term stability of the clay films under various conditions, however, little mechanistic information can be obtained. This information may be obtained by immersing individual Na^+ exchanged bentonite films in 50 gdm^{-3} polyalkyl glycol (with 10% wt KCl) solutions for various times.

The high and low molecular weight polyols are studied separately as the kinetics for the two are likely to be slightly different. Firstly, consider the kinetics of adsorption of PAG(600) from solution onto Na bentonite free standing films.

Figures 7.3.3.4a and 7.3.3.4b show the diffraction traces for Na bentonite films after immersion in 50 gdm^{-3} polyalkyl glycol (Mw 600)/10% KCl solution for times ≤30 minutes, and ≥60 minutes, respectively. Table 7.3.3.4b lists the corresponding d-spacings for Na bentonite films after immersion in the solution.

Figure 7.3.3.4a Diffraction trace of Na bentonite films, intact, after immersion in 50 gdm^{-3} polyalkyl glycol (Mw 600)/10% KCl for short times.

Intensity (counts s-1)
pure Na bentonite film
2mins:PAG(600)/KCl/Na film
5mins:PAG(600)/KCl/Na film
30mins:PAG(600)/KCl/Na film

2θ
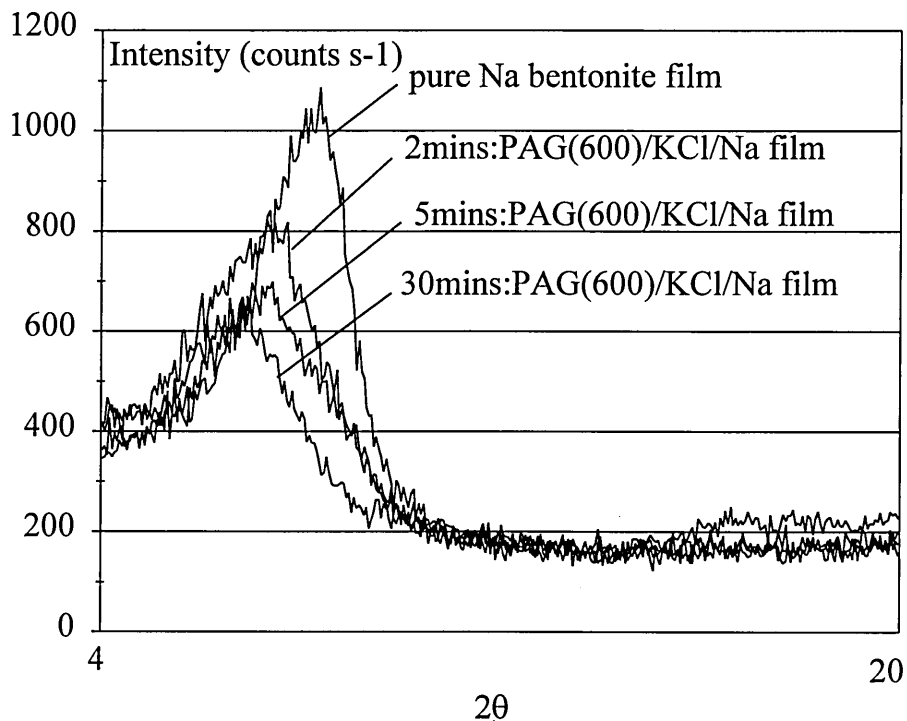
Figure 7.3.3.4b Diffraction trace of Na bentonite films, intact, after immersion in 50 gdm^{-3} polyalkyl glycol (Mw 600) /10% KCl for long times.

Intensity (counts s-1)
overnight:PAG(600)/KCl/Na film
120mins:PAG(600)/KCl/Na film
60mins:PAG(600)/KCl/Na film
pure Na bentonite film

2θ
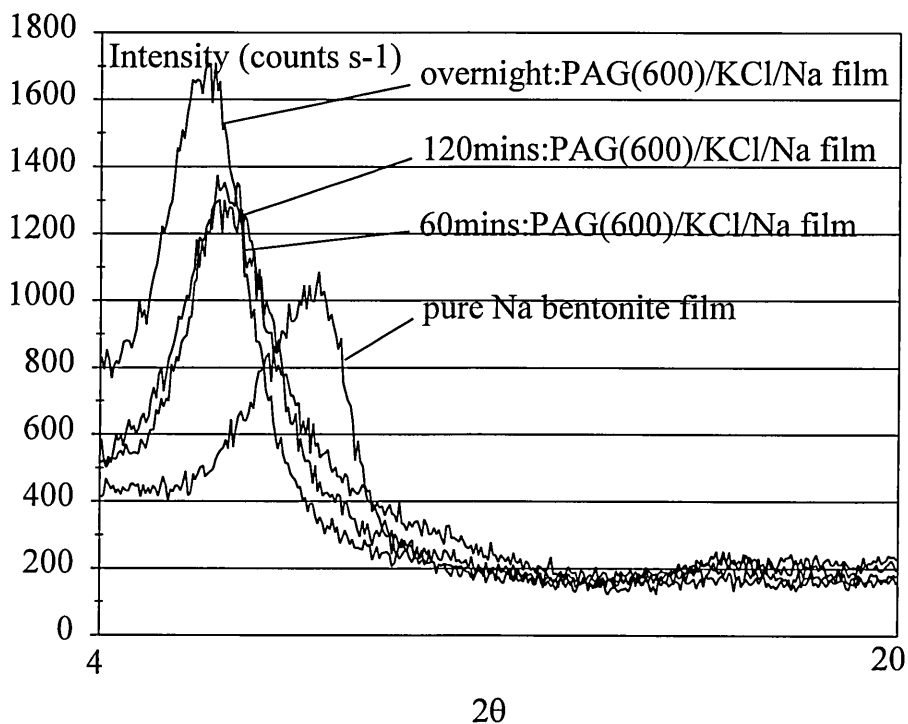
Table 7.3.3.4b The d-spacing of Na bentonite films, intact, after immersion in 50 gdm^{-3} polyalkyl glycol (Mw 600)/10% KCl for all times.

Time of contact (hrs)	d-spacing (Å)
0.03	14.1±0.6
0.08	14.0±0.6
0.25	14.4±0.5
0.5	14.9±0.5
1.0	15.9±0.4
2.0	16.0±0.4
12.0	17.5±0.4

As time progresses, the interlayer separation of the Na bentonite film increases indicative of an increase in the amount of adsorbed polyalkyl glycol in the interplatelet region. All the diffraction traces are broad and weak, symptomatic of the PAG(600)/K$^+$ system and is attributed to the inability of the K$^+$ to form extended hydration spheres (its inability to swell the clay) and the effect of a strongly flocculating electrolyte which inhibits the adsorption process.

After only two minutes immersion of the film in the PAG(600)/10% KCl solution, the diffraction maximum can be found at 14.1Å indicating formation of the single layer organic complex within two minutes of immersion. The speed at which this occurs is not surprising since if the adsorption process took any longer it would probably enable the Na bentonite to swell and disperse causing the film to disintegrate. In the diffraction trace of Na bentonite film immersed in PAG(600)/10% KCl for 2 minutes however, that there is a noticeable shoulder, the exact position of which can not be elucidated however, there are several explanations for its existence. One is that it corresponds to the unswelled Na

bentonite and therefore that the complex formed is a mixed zero and single organic layer system. Stable, mixed zero and single layer complexes have been observed previously in the adsorption of PAG(600) onto a K bentonite film from a very low concentration polymer solution (section 7.3.3.2). Other explanations such as the shoulder corresponding to the d-spacing of dehydrated Na bentonite (<12.5Å) or to the d-spacing of cation exchanged bentonite (K^+ for Na^+) in the interlayer (~11.9Å) are however no less plausible. The thermodynamic driving force for adsorption is by the desorption of water molecules from the clay [11] and cation exchange is a process is thought to occur, and indeed be enhanced, in the presence of PAG(600) [3].

Interestingly, after 2 minutes immersion the d-spacing does not increase dramatically although the shoulder does seem to disappear. In fact, up to 15 minutes immersion time, the d-spacing only increased to 14.4Å. This probably indicates a consolidation of the one layer complex as the polyol offered to the clay co-ordinates to available sites on the clay by continued displacement of adsorbed water.

Beyond immersion times of 15 minutes there is a slow increase in the d-spacing as the second layer adsorbs between the clay platelets. This second layer intercalates much more slowly than the first indicating that this process is controlled only by the rate of diffusion of the polymer throughout the system whereas the formation of the initial layer is much faster and has a much stronger driving force (entropy). This may account for the findings of Rawson [3] that the second layer is much more weakly bound than the first. It should be remembered that the stability of the second layer in complexes formed between PAG(600) and pre-formed Na bentonite films is not known but might be expected to be more stable than observed in complexes formed in aqueous suspension as the polymer has to physically adsorb between the platelets rather than just be trapped there by drying.

There appears to be no real thermodynamic driving force for the adsorption of a second layer of polyalkyl glycol between the platelets of the film. This probably explains the unwillingness of systems containing K^+ to form bi-layer complexes as easily as they are formed when the system contains only Na^+ ions. The Na^+ ions will swell easily so that when sufficient polymer is offered to the clay it is able to intercalate easily. K^+ however, does not swell the clay as easily as Na^+ and hence after adsorption of the first organic layer it becomes difficult to fully adsorb a second. Hence, many mixed mono- and bi-layer complexes are observed when polyalkyl glycol is adsorbed to bentonites in the presence of K^+.

This is extremely useful mechanistic information, however, as the molecular weight of the polyalkyl glycol used is low the adsorption process is too fast to be observed by these crude experiments and the key adsorption mechanism of the first layer can not be observed. As a result, by using PAG(1700) it is possible to slow the adsorption process down sufficiently to observe the formation of the first organic layer and therefore elucidate the adsorption mechanism. This assumes that the adsorption mechanism in each case is the same (which is not unlikely).

Figures 7.3.3.4c and 7.3.3.4d display the diffraction traces obtained from Na bentonite films after contacting with 50 gdm^{-3} polyalkyl glycol (Mw 1700) solution containing 10% KCl for times up to 30 minutes and over 60 minutes, respectively. Table 7.3.3.4d shows the change in d-spacing with time for this system

Figure 7.3.3.4c Diffraction trace of Na bentonite films, intact, after immersion in 50 gdm^{-3} polyalkyl glycol (Mw 1700) /10% KCl (short times).

Intensity (counts s-1)

pure bentonite
30mins:PAG(1700)/KCl/Na film
5mins:PAG(1700)/KCl/Na film
15mins:PAG(1700)/KCl/Na film

2θ
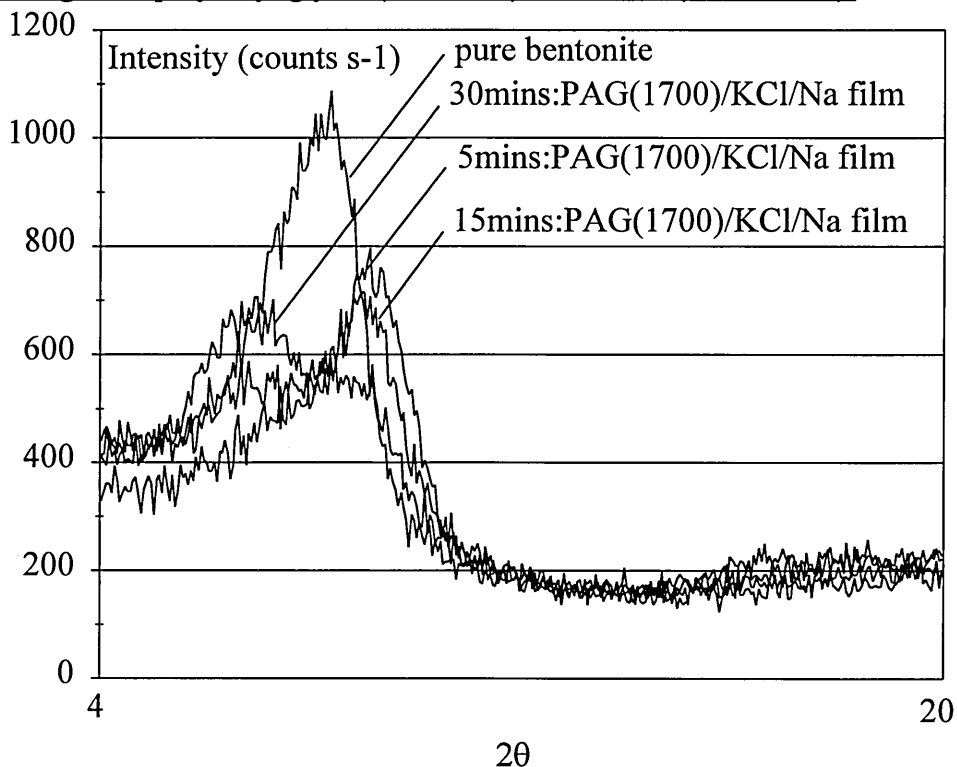
Figure 7.3.3.4d Diffraction trace of Na bentonite films, intact, after immersion in 50 gdm^{-3} polyalkyl glycol (Mw 1700) /10% KCl (long times).

Intensity (counts s-1)

overnight:PAG(1700)/KCl/Na film
120mins:PAG(1700)/KCl/Na film
60mins:PAG(1700)/KCl/Na film
pure Na bentonite film

2θ
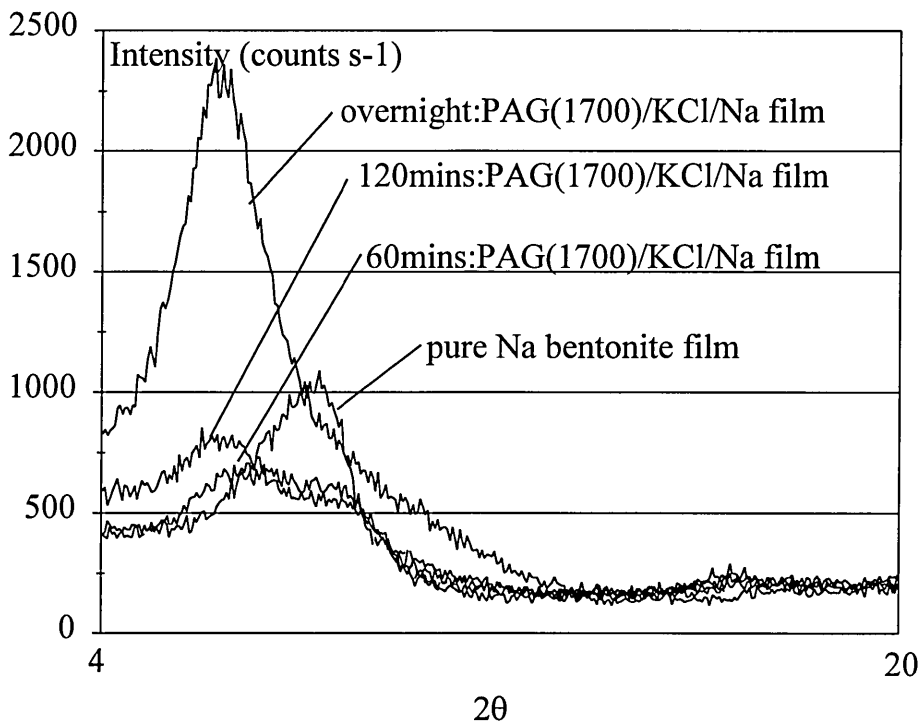
Table 7.3.3.4d The d-spacing of Na bentonite films, intact, after immersion in 50 gdm^{-3} polyalkyl glycol (Mw 1700) /10% KCl for all times.

Time of contact (hrs)	d-spacing (Å)
0.08	11.6±0.6
0.25	11.9, 14.4±1.0
0.5	12.0, 14.7±0.8
0.75	11.8, 14.8±0.6
1.0	12.2, 15.6±0.6
2.0	12.2, 16.1±0.5
12.0	16.1±0.3

These 'time of immersion' results show some similarities with those in figures 7.3.3.4a and 7.3.3.4b for the adsorption of low molecular weight PAG under similar conditions. As immersion time increases, the interlayer separation increases from 12.5Å in pure Na bentonite to 16.1Å (most likely due to a mixed single and double layer complex) after immersion of the Na bentonite film for 12 hours. The diffraction traces are broad and of low intensity, a trait, it appears, of adsorption of polyalkyl glycol in the presence of KCl.

There are, however, several differences from those results observed in figures 7.3.3.4a and 7.3.3.4b. Firstly, the Na bentonite film immersed for 2 minutes in the PAG(1700)/10% KCl solution was not stabilised and consequently disintegrated when attempts were made to retrieve it. This, it would seem, is indicative of the slower diffusion rate of the higher molecular weight polymer in solution compared to the lower molecular weight polymer and therefore its inability to stabilise the film quickly enough to prevent disintegration. The lower molecular weight polymer, stabilised the film within 2 minutes.

The second major difference from the results seen for the lower molecular weight system, is that no immediate jump to higher d-spacing, indicative of polymer adsorption between the platelets is observed in the diffraction traces. In fact, quite the opposite occurs and a drop in d-spacing to 11.6Å is observed. This value is lower than that observed in homoionic Na bentonite and may be attributed to the dehydration of the outer hydration shells of the Na^+ exchange cations in the interplatelet region by the polyalkyl glycol molecule and the subsequent collapse of the platelet spacings. This is not unsurprising since as explained in the literature [117, 118, 121], the driving force for adsorption of glycols to clay minerals is the removal of water from the interlayer region between the clay platelets. It might also be due to cation exchange of K^+ for Na^+ in the interlayer region since a d-spacing of 11.6Å is quite similar to that observed for homoionic K bentonite (direct exchange of one cation for the other would result in a drop in the d-spacing). It should be noted that whilst the observed diffraction maxima are attributed to the 11.6Å spacing, there is some PAG(1700) adsorption indicated by the long wing to the diffraction trace at low 2θ values.

This dehydration or cation exchange process is probably almost instantaneous (occurs inside 2 minutes) however, subsequent adsorption of the polymer will depend upon the molecular weight. The low molecular weight polymer had clearly adsorbed after 2 minutes however, even after 15 minutes immersion in PAG(1700) the d-spacing is only 11.9Å, again attributable to dehydration of hydrated Na^+ cations or cation exchange of K^+ for Na^+ in the interlayer space. After 15 minutes, a clear shoulder can be observed which corresponds to a d-spacing between approximately 14 and 15Å and is attributable to the formation of the first organic layer between the platelets. As the time of immersion increases then a diffraction maximum corresponding to a d-spacing of 14.7Å can be observed (after 30 minutes). This is the d-spacing of the one layer complex and becomes more prominent as the amount of polymer adsorbed between the clay platelets increases

with time. The position of this maximum then shifts to correspond to larger d-spacings as the time of immersion increases up to a maximum d-spacing of 16.1Å after 12 hours immersion. It is not clear whether this is a shift in band position or a change in the relative intensity of the maxima as the shoulder at 12.0Å reduces in intensity. Either way, it indicates that polymer adsorbs between all the platelets in the film when sufficient time is allowed for adsorption to occur. The position of the observed d-spacing after 12 hours immersion of Na bentonite films in PAG(1700)/10% KCl solution has previously been attributed to the formation of a mixed single and double layer organic complex in the interplatelet region.

It is interesting to note that the shoulder attributed to either dehydrated Na bentonite or K^+ exchanged Na bentonite can still be seen in the diffraction trace of a Na bentonite film immersed for 2 hours in PAG(1700)/10% KCl solution although it can not be seen in the diffraction trace of the film immersed for 12 hours. It appears that the clay immediately dehydrates or exchanges cations in readiness for the adsorption of polyalkyl glycol and if the delay before adsorption is too long the system will be able to rehydrate and the film will be unstable.

These experiments do not fully explain the adsorption mechanism, however, the reduction in the interlayer spacing, either by loss of water or cation exchange (K^+ for Na^+) on contact with polyalkyl glycol is beyond doubt. Further experimentation using various combinations of polyalkyl glycol, exchange cation and electrolyte would give a deeper insight to the actual adsorption mechanism.

7.3.4. Transmission infrared spectroscopy

X-ray diffraction provides a useful insight into the adsorption behaviour of polyalkyl glycol under a variety of conditions. FTIR spectroscopy may be used to complement this to give information regarding actual interactions and adsorption mechanism.

7.3.4.1 Homoionic Na^+ and K bentonite free standing films

The infrared transmission spectrum of homoionic bentonite free standing films (Na^+ and K^+) are shown in figure 7.3.4.1a. They are very similar to the spectrum of natural bentonite (without cation exchange) free standing film shown in figure 6.3.3.2a.

Figure 7.3.4.1a Infrared transmission spectra of free standing films of Na^+ and K^+ exchanged bentonite.
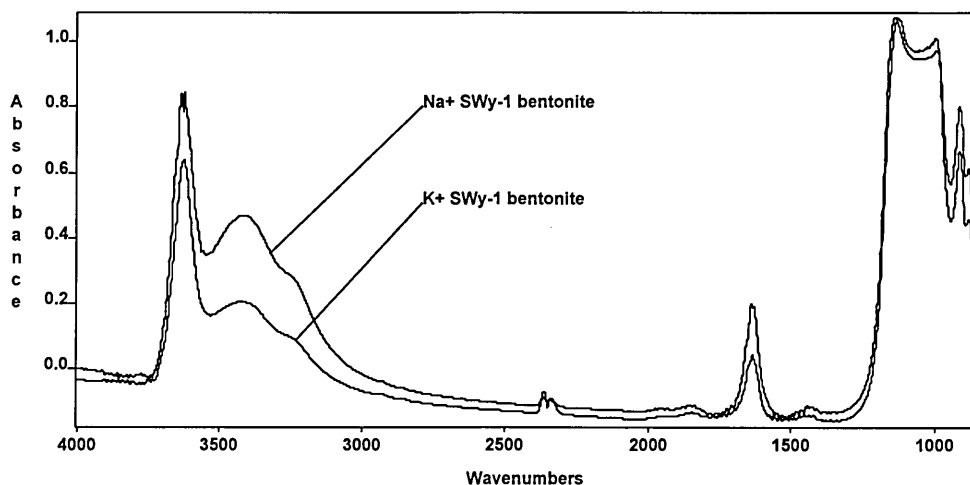
It should be noted, that each film used will have different thicknesses and consequently will have differing intensities (reflecting the amount of clay material placed in the spectrometer beam). In order to compare the infrared spectra obtained

291

from different films, it is important to normalise the relative intensities of particular spectral features against a spectral feature which is a characteristic of the clay and not expected to change from film to film or experiment to experiment.

The feature used in this study against which bands are normalised is the band at 3630 cm^{-1} attributed to the structural OH stretching modes, since the intensity of this band should be indicative of the amount of bentonite present. Possible problems with using this band have been raised. In chapter 5, the dehydration of bentonite by heating to 200°C, reduced the intensity of the band at 3630 cm^{-1}. This was attributed to the removal of water and subsequent settling of the exchange cation into the di-trigonal cavity of the silicate layer surface. However, this effect is not expected to be significant in these experiments since the adsorption of glycol (see later) and the dehydration mechanism are thought to involve the exchange cation, which, as a result, will remain in the interlayer space, and be prevented from settling into the di-trigonal cavity (chapter 5). As a consequence, negligible reduction in the intensity of the band attributed to structural OH (at 3630 cm^{-1}) should be observed. Table 7.3.4.1a shows the variation in absorbance ratios A(3630)/A(3440) and A(3630)/A(1640) of the bands in Na^{+} and K^{+} exchanged bentonite.

Table 7.3.4.1a Absorbance ratios A(3630)/A(3440) and A(3630)/A(1640) of the bands in Na^{+} and K^{+} exchanged bentonite.

absorbance ratio	Na^{+} SWy-1 bentonite	K^{+} SWy-1 bentonite
3630/3440*	1.5	3.1
3630/1640*	2.4	3.6

* The wavenumber position of the bands attributed to the hydrogen bonded OH stretching modes and the H-O-H bending mode are quite complicated. The band maximum centred around 3440 cm^{-1} is composed of several bands due to the antisymmetric and symmetric OH stretching vibrations of interlayer water [34] and is found at 3406 cm^{-1} in Na^+ SWy-1 bentonite and at 3431 cm^{-1} in K^+ SWy-1 bentonite. Similarly the position of the band at ~1640 cm^{-1} varies depending upon the degree of bound and adsorbed water [34] (bound water resides in the inner hydration sphere) and is found at 1636 cm^{-1} and 1638 cm^{-1} in Na^+ SWy-1 and K^+ SWy-1 respectively. Table 7.3.3b displays these assignments following Bishop et al [34].

Table 7.3.4.1b Band assignments for molecular water in the infrared spectrum of bentonite after Bishop et al [34].

Band position (cm^{-1})	Assignment
~3620	ν_3 antisymmetric stretch (bound)
3550-3520	ν_1 symmetric stretch (bound)
~3450	ν_3 antisymmetric stretch (adsorbed)
3400-3350	ν_1 symmetric stretch (adsorbed)
~3250	$2\nu_2$ H-O-H bending overtone
~1650	ν_2 H-O-H bending (adsorbed)
1617-1630	ν_2 H-O-H bending (bound)

Both the ν_1 and ν_2 bands are highly dependent on the nature of the cation [34]; ν_1 shifting to lower frequency and ν_2 shifting to higher frequency with increasing polarising strength of exchange cation. Consequently, the wavenumber positions of both spectral features is a complex balance between the amount of adsorbed water and the nature of the exchange cation. It is with this complexity in mind that

infrared spectroscopy has been used to help determine the nature of the interactions occurring between polyalkyl glycol and homoionic Na and K bentonite free standing films.

7.3.4.2 Adsorption of polyalkyl glycol from dilute solution onto Na bentonite free standing films

Free standing Na bentonite films form two layer organic complexes when stabilised by PAG(600) at solution concentrations ≥ 50 gdm^{-3} (table 7.3.3.1b). Figures 7.3.4.2a and b show the transmission infrared spectra of stable Na bentonite free standing films following immersion in 100 and 50 gdm^{-3} PAG (Mw 600) solutions.

Figure 7.3.4.2a Infrared spectra of stable Na bentonite films, after immersion in 100 and 50 gdm^{-3} polyalkyl glycol (Mw 600) solution.
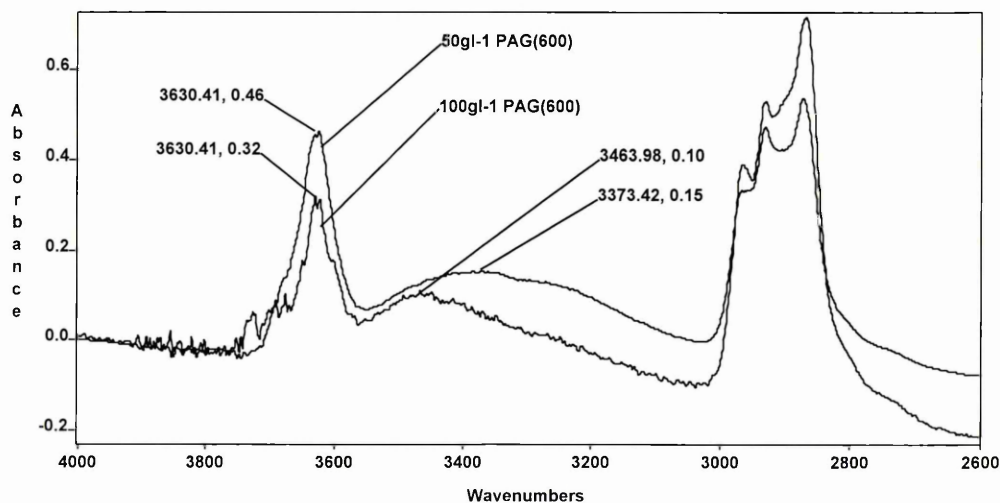
Figure 7.3.4.2b Infrared spectra of stable Na bentonite films, after immersion in 100 and 50 gdm^{-3} polyalkyl glycol (Mw 600) solution.
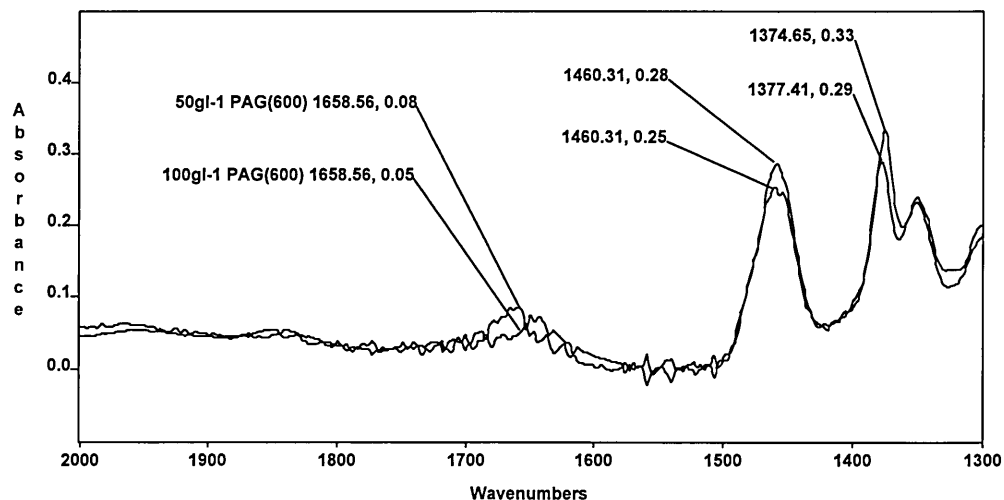
Comparison of the spectra obtained from a homoionic Na bentonite free standing film before and after immersion in PAG(600), shows that the immersed films have been significantly dehydrated. Theng [11] explained the entropic gain associated with the displacement of water from the clay mineral surface on adsorption of neutral polymers. The entropic gain incurred from the displacement of water associated with the polymer (section 7.3.1) should also not be forgotten as a possible driving force for adsorption. Table 7.3.4.2b displays the absorbance ratios A(3630)/A(3440) and A(3630)/A(1640) from the infrared spectra of Na$^+$ exchanged bentonite films, intact after being immersed in 100 gdm^{-3} and 50 gdm$^-$^{3} PAG(600) solution.

Table 7.3.4.2b Absorbance ratios from FTIR spectra of stable Na bentonite films after immersion in 100 and 50 gdm⁻³ PAG(600) solution.

absorbance ratio	100 gdm⁻³ PAG(600)	50 gdm⁻³ PAG(600)
3630/3440*	3.0	3.1
3630/1640*	6.0	5.7
3630/2932	0.5	1.0

*The actual positions of the spectral maxima around 3440 and 1640 cm⁻¹ are related to the extent of hydration and consequently, the bands are shifted from their positions in Na bentonite at 3406 cm⁻¹ and 1636 cm⁻¹, respectively.

Both absorbance ratios A(3630)/A(3440) and A(3630)/A(1640) are significantly increased from their values in a Na bentonite film prior to immersion (1.53 and 2.38 respectively). This increase in the absorbance ratios A(3630)/A(3440) and A(3630)/A(1640) may be attributed solely to the removal of adsorbed water. The removal of water from the clay by adsorption of polyalkyl glycol has been reported previously in this thesis and also by Cliffe et al [1] in the infrared spectra of polyol treated clay films and by Rawson [3] in the NMR study of clay-polyol suspensions. The dehydration of clay minerals by ethylene glycol [122, 123, 125] and polyethylene glycol [117, 118, 121] has been observed by many workers. However, experiments presented later in this chapter will give strong indications as to possible mechanisms and rates of water removal when contacted with polyalkyl glycol solutions at various concentrations.

It is interesting to initially study the effect of PAG(600) adsorption on the Na bentonite films alone. Previously, it was observed (figure 7.3.3.1a and table 7.3.3.1a) that PAG(600) adsorbed onto Na bentonite films from aqueous solution

stabilised the film, only at concentrations ≥ 50 gdm^{-3}. The complex formed in this adsorption process had a d-spacing of ~18.1Å corresponding to two organic layers adsorbed between the platelets.

As mentioned, the positions of the spectral maxima associated with OH stretching modes and H-O-H bending modes are related to the extent of hydration. In the spectrum of the Na bentonite film immersed in 100 gdm^{-3} PAG(600) solution, the spectral maximum in the OH stretching region appears to be shifted, being found at ~3464 cm^{-1}. This particular region of the spectrum is too complex to determine the exact position of individual spectral bands. As a result, band shifts may occur but they are likely to be apparent shifts due to changes in the relative intensity of all the bands in this region as water is removed in the dehydration process.

One explanation for this apparent band shift is that dehydration, by the desorption of adsorbed water [34], on adsorption of the polyalkyl glycol molecule, causes the band maximum to be predominantly influenced by the antisymmetric and symmetric stretching vibrations of bound water [34], at 3620 and between 3550 and 3520 cm^{-1}. Consequently, changes in relative intensities cause an apparent shift to high frequency. It should be noted however, that in the presence of PAG(600), which itself has OH end groups and therefore a band, associated with the OH stretching mode, at 3475 cm^{-1}, the position of the spectral maximum may be shifted to higher frequency. The position of this band would not be expected to change from that in pure polyalkyl glycol as no evidence exists [1] that OH end groups are involved in the interaction of polyalkyl glycol onto bentonite. This ν (OH) band associated with the polyol would make a more significant contribution to the spectral intensity as the influence of molecular water is reduced by dehydration of the clay) and consequently, shifts to high frequency of this spectral maximum may be observed.

As the Na bentonite films immersed in 50 and 100 gdm^{-3} PAG(600) solution both formed organic bi-layer complexes, it might be expected that their infrared spectra would be similar. However, the position of the spectral maximum associated with OH stretching modes is observed at lower frequency in the spectrum of the Na bentonite film immersed in 50 gdm^{-3} PAG(600) solution, being found at 3372 cm^{-1} compared to 3406 cm^{-1} in the spectrum of the Na bentonite film prior to immersion.

These observed effects are likely to be related to the amount of adsorbed polyalkyl glycol as indicated by the absorbance ratio, A(3630)/A(2932) shown in table 7.3.4.2b. For 100 gdm^{-3} PAG(600) a much lower absorbance ratio A(3630)/A(2932) is observed than for 50 gdm^{-3} PAG(600). This is indicative, as expected, of increased PAG(600) adsorption onto the Na bentonite film from the solution of higher polymer concentration. Despite both systems forming two layer organic complexes, the complex prepared from the lower concentration, 50 gdm^{-3}, PAG(600), solution contains less adsorbed polymer and more adsorbed water than that prepared from the 100 gdm^{-3} PAG(600) solution. It appears that when insufficient polymer is available to fully co-ordinate to sites around exchange cations in the interlayer space, the remaining co-ordination sites are filled by re-adsorbing water. The idea of re-hydrated organic double layers was established in section 7.3.3.1 where lower than expected d-spacings were attributed to low humidity and drying.

Stabilisation did not occur on immersion of Na bentonite films in ≤ 5 gdm^{-3} PAG(600) solutions. This is due to the low solution concentration of polymer which restricts the amount of adsorbed polymer, thus enabling water to re-hydrate the system to such an extent it caused film degradation.

Additionally, at lower frequency (figure 7.3.4.2b) there is a shift of the band associated with the H-O-H bending mode, from 1636 cm^{-1} in Na bentonite spectrum prior to immersion, to 1658 cm^{-1} in the spectra of the films stabilised in 50 and 100 gdm^{-3} PAG(600). This is not due to bands associated with PAG(600) (the spectrum of PAG(600) does not have bands in this region), hence it must be due entirely to environmental changes of the water in the interlayer. In homoionic Na bentonite the band attributed to the H-O-H bending mode has an absorption band associated with it at ~1650 cm^{-1} (due to adsorbed water [34]) and an absorption band between 1617-1630 cm^{-1} (associated bound water [34]). Consequently, a shift to low frequency would be expected on dehydration. Indeed, dehydration of clay by heating does cause a shift to lower frequency of this particular maximum [34]. However, hydrogen bonding interactions between PAG(600) and water in the interlayer causes a stiffening of the bending mode thus causing the band shift to high frequency. As explained earlier, bound water can still be observed in the infrared spectra of Na bentonite films immersed in PAG(600). This would appear to indicate that the adsorbed polyalkyl glycol interacts directly with the water bound to the exchange cation via a water bridge as postulated by Cliffe et al [1]. Other water observed in the infrared spectra of PAG(600) treated Na bentonite films is likely to be predominantly that of re-adsorbed water, filling co-ordination sites which have not been occupied by adsorbed polymer.

This adsorption mechanism gives a significant indication towards the mechanism of film (and therefore wellbore stability). At high PAG(600) concentration in solution (~100 gdm^{-3}) there is sufficient adsorbed polymer to fill most or all the co-ordination sites around the cation (these sites being bound water molecules) to prevent re-hydration of the cations and dispersion of the platelets. At lower PAG(600) concentrations in solution (~50 gdm^{-3}) there is sufficient polymer adsorption to fill enough co-ordination sites to prevent extensive cation hydration

(although rehydration is observed). Again the Na bentonite film is not dispersed

and is stable. However, in ≤ 5 gdm^{-3} PAG(600) concentration solution there is

insufficient polymer adsorption to fill the co-ordination sites around the exchange

cation (inner sphere bound water) which will not prevent extensive cation

hydration. As a result, the bentonite platelets become dispersed and the film is

unstable.

Further evidence of the extent of re-hydration of the interplatelet region following

PAG(600) being adsorbed in the interlayer can be observed in the spectral region

between 1420 and 1300 cm^{-1}. Figure 7.3.4.2c shows the infrared spectrum of Na

bentonite films intact after contact with 100 and 50 gdm^{-3} PAG(600) solution, in

this region.

Figure 7.3.4.2c Infrared spectra of stable of Na bentonite films after

immersion in 100 and 50 gdm^{-3} polyalkyl glycol (Mw 600) solution.
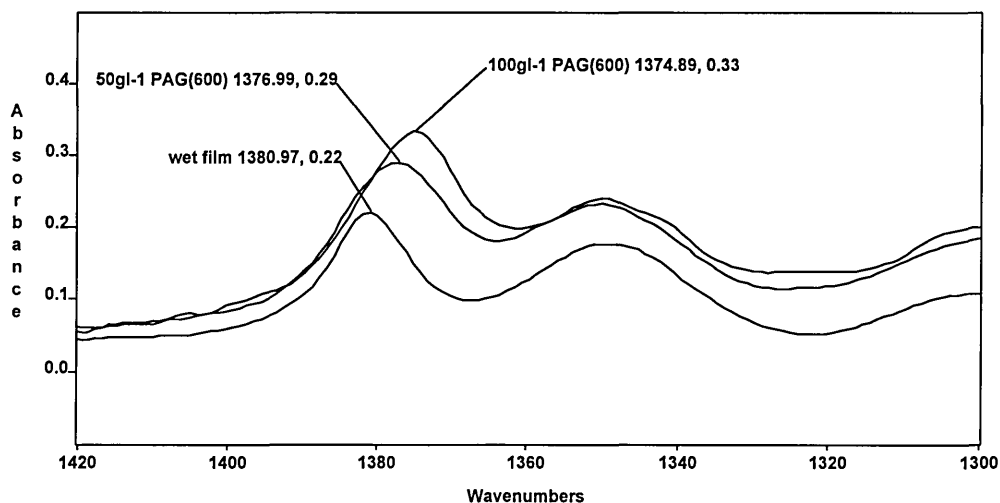
When both films are removed from solution (wet) and placed in the spectrometer,

the wavenumber position of the band attributed to the v(OC) band of polyalkyl

glycol is at 1381 cm^{-1}. This is the position it would be expected to be seen in a

10% by weight dilution of PAG(600) in deionised water. When the films are dry the position of the band is shifted to lower frequency, depending upon the concentration of PAG(600) in solution, being found at 1377 and 1375 cm^{-1} in the spectra of Na bentonite films contacted with 50 gdm^{-3} and 100 gdm^{-3} PAG(600) solutions, respectively. It was shown previously (section 7.3.1) that the ν(OC) band shifted to higher frequency on increasing dilution of polyalkyl glycol in deionised water and 100 gdm^{-3} KCl solution. Hence, as the films dry, loosely adsorbed water is displaced, and the polyalkyl glycol molecule experiences fewer PAG-water interactions and more PAG-PAG interactions. Despite both systems having two organic layer between the platelets, the Na bentonite film contacted with 100 gdm^{-3} PAG(600) shows more PAG-PAG interactions than in the Na bentonite film contacted with 50 gdm^{-3} PAG(600) (which conversely shows more PAG-water interactions). This indicates that when less polymer is offered to the clay, less adsorbs, consequently, water is then able to re-hydrate the system and swell the clay.

Cliffe et al [1] used this band shift to show that interactions between PAG(600) chains in the interlayer become significant as they adsorb and become oriented and concentrated between the platelets. These weak interactions were partially attributed to the stabilisation observed, as PEG(600) did not exhibit similar results and does not exhibit the same stabilisation traits.

In the absence of other components, the stabilisation of Na bentonite films by higher molecular weight polyalkyl glycol was only previously observed (figure 7.3.3.1b) using 100 gdm^{-3} PAG(1200). The infrared spectra obtained were very similar to those observed in the infrared spectrum of a Na bentonite film immersed in a 50 gdm^{-3} solution of PAG(600). This is attributed to the number of moles of polyalkyl glycol per unit volume in each solution being the same (both solutions contain 0.08 moldm^{-3}, table 7.3.3.1b). It is possible that this particular number of

moles per unit volume is approximately the minimum number required in solution to stabilise the film against rehydration. Re-adsorption of water does occur but not sufficiently to disperse the Na^+ platelets and destabilise the film. In the presence of PAG(1700) it would appear that insufficient moles of polymer were present per unit volume of solution to adsorb and stabilise the film.

7.3.4.3   Adsorption of polyalkyl glycol from dilute solution onto homoionic K bentonite free standing films

Homoionic K bentonite films have been shown to be stabilised by PAG(600) solutions (section 7.3.4.2) over the whole range of polymer concentrations (≥ 1 gdm^{-3}). The infrared spectra of these stable films are shown in figures 7.3.4.3a and 7.3.4.3b. Table 7.3.4.4b shows the variation of the absorbance ratios A(3630)/A(3440), A(3630)/A(1640) and A(3630)/A(2932) in these spectra.

Figure 7.3.4.3a Infrared spectra of K bentonite films, intact, after being placed in polyalkyl glycol (Mw 600) solution.
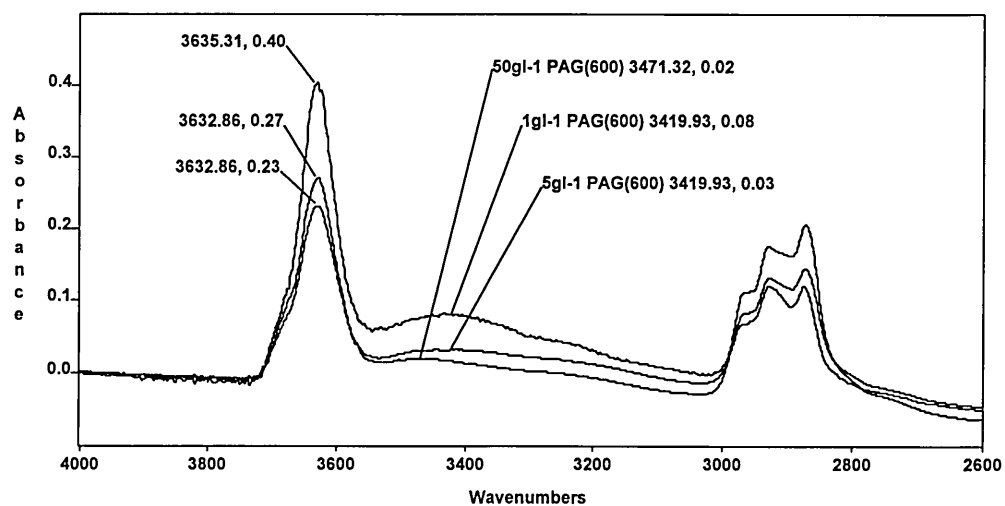
Figure 7.3.4.3b Infrared spectra of stabilised K bentonite films after being placed in polyalkyl glycol (Mw 600) solution.
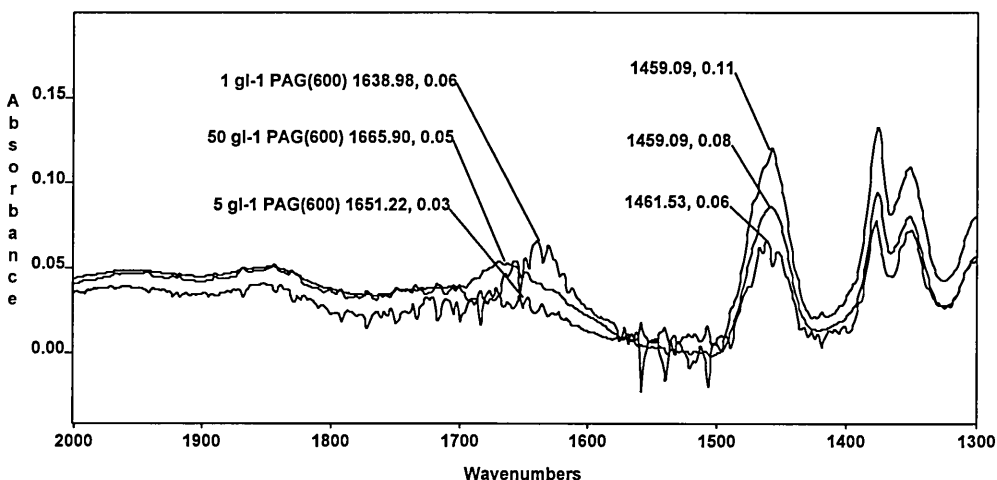
Table 7.3.4.3b Absorbance ratios from the infrared spectra of bands in stable K bentonite films, after immersion in PAG(600) solution.

absorbance ratio	50 gdm^{-3} PAG(600)	5 gdm^{-3} PAG(600)	1 gdm^{-3} PAG(600)
3630/3420	12.9	7.5	5.0
3630/1640	9.6	8.4	6.6
3630/2932	1.5	1.8	3.3

*The actual position of these bands is dependent upon the extent of dehydration.

As the solution concentration of PAG(600) increases, so the adsorbed amount increases, as determined by the decrease in the absorbance ratio A(3630)/A(2932). The d-spacings observed for these systems (figure 7.3.3.2a) also increased with increasing polymer solution concentration from a 16.6Å (mixed single and double layer complex), up to 17.5Å (double layer complex) at the highest solution concentration. Similarly, as the adsorbed amount increases, the extent of

dehydration of the clay increases, as determined by the increasing absorbance ratios A(3630)/A(3440) and A(3630)/A(1640).

The position of the spectral maximum attributed to hydrogen bonded OH (figure 7.3.4.3a) is found at higher wavenumber (3471 cm^{-1}) in the spectrum of the K bentonite film contacted with the highest concentration (50 gdm^{-3}) of PAG(600) solution, compared to 3431 cm^{-1} in the spectrum of K bentonite prior to immersion. This is very similar to the spectrum of Na bentonite immersed in 100 gdm^{-3} PAG(600) in figure 7.3.4.2a and can therefore be attributed to the removal of adsorbed water enabling the spectral maximum to be dominated by the presence of bound water at higher wavenumber.

The position of this band however, is found at lower wavenumber (3420 cm^{-1}) in the spectrum of K bentonite films contacted with 5 and 1 gdm^{-3} PAG(600) solution. This band position is lower in frequency than observed in the spectrum of K bentonite prior to immersion and is similar to that observed for the Na bentonite film stabilised in 50 gdm^{-3} PAG(600). Again this is likely to be due to slight rehydration of the clay after polymer adsorption (but not to the same extent as was observed previously) despite forming only mixed one and two organic layers between the platelets.

Unfortunately, the exact adsorbed amounts in each case have not been calculated but it appears that the stability of the K bentonite to re-hydration is not dependent on the formation of two organic layers between the platelets [1] and that even at low PAG(600) solution concentrations (1 gdm^{-3}) re-hydration is possible without destabilising the bentonite film. This is clearly due to the inability of the K^+ exchange cation to form extended hydration shells and hence, its reduced ability to cause interplatelet swelling compared to Na^+ cations.

Band shifts are also observed at lower frequency. In the spectrum of the K bentonite film immersed in 50 gdm^{-3} solution of PAG(600), the position of the band attributed to the H-O-H bending mode is found at higher wavenumber (1667 cm^{-1}) than in a homoionic K bentonite film prior to immersion (attributed to the hydrogen bonding of the polyalkyl glycol molecule to the primary hydration sphere surrounding the exchange cation). As the concentration of the solution into which the K bentonite film is immersed is reduced, then the position of the band is found shifted less from its position in the homoionic K bentonite. This is attributed to re-adsorbed water occupying unfilled co-ordination sites and dominating this spectral region. The extent of rehydration of the interlayer region, can also be followed by studying the position of the ν(OC) band between 1420 and 1300 cm^{-1} (figure 7.3.4.3c).

Figure 7.3.4.3c Infrared spectra of stabilised K bentonite films after immersion in polyalkyl glycol (Mw 600) solution.
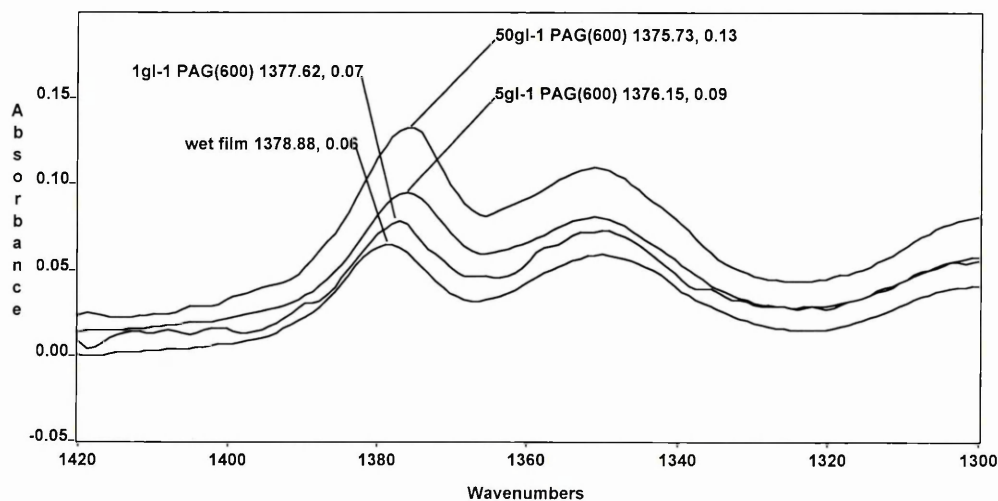
In figure 7.3.4.3c, (the spectra of Na bentonite films contacted with polyalkyl glycol of molecular weight 600), as the concentration of PAG(600) in solution increases, then the ν(OC) band shifts to lower frequency in the spectrum of the

305

stabilised film. Again, this indicates an increase in the number of PAG-PAG

interactions (and consequent decrease in the number of PAG-H$_2$O interactions) as

the polymer concentrates between the clay platelets, i.e. as the amount adsorbed

(solution concentration) increases and as the extent of re-hydration is inhibited.

The influence of molecular weight may be analysed and the infrared spectra of K

bentonite films stabilised in PAG(1700) solutions are shown in figures 7.3.4.3d

and 7.3.4.3e. In the spectra of the K bentonite films immersed in the PAG (1700)

the polymer dehydrates the clay as can be clearly seen in the absorbance ratios

A(3630)/A(3440) and A(3630)/A(1640) in table 7.3.4.3e.

Figure 7.3.4.3d Infrared spectra of stabilised K bentonite films after being

placed in polyalkyl glycol (Mw 1700) solution.
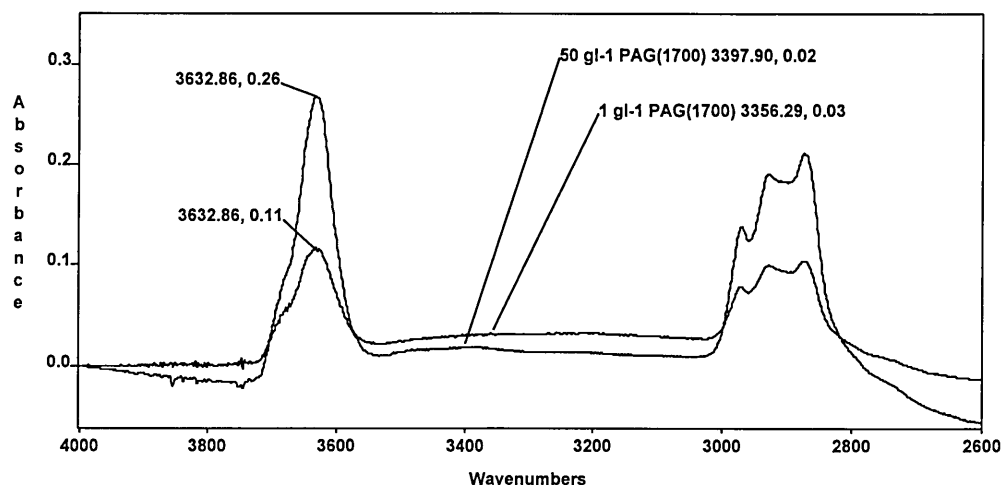
Figure 7.3.4.3e Infrared spectra of K bentonite films, intact, after being placed in polyalkyl glycol (Mw 1700) solution.
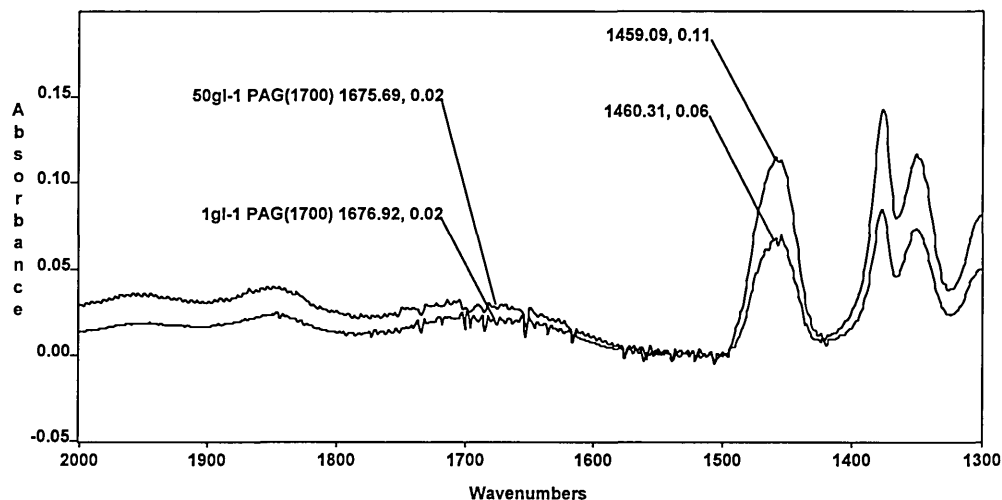
Table 7.3.4.3e Absorbance ratios from the spectra of stabilised K bentonite films after immersion in polyalkyl glycol (Mw 1700) solutions.

absorbance ratio	50 gdm^{-3} PAG(1700)	5 gdm^{-3} PAG(1700)	2.5 gdm^{-3} PAG(1700)	1 gdm^{-3} PAG(1700)
3630/3440*	10.0	9.5	5.5	3.44
3630/1640*	12.7	9.5	8.2	4.5
3630/2932	1.1	1.0	1.6	1.7

*The actual position of these bands is dependent upon the extent of dehydration.

As expected, the absorbance ratio A(3630)/A(2932) decreases with increasing solution concentration of PAG(1700), i.e. as the amount of polymer adsorbed on the clay increases and concurrently, the extent of dehydration increases.

In the infrared spectrum of the K$^+$ exchanged bentonite film immersed in the highest concentration (50 gdm^{-3}) PAG(1700) solution, the position of the spectral

maximum in the hydrogen bonded OH stretching region is at 3397 cm^{-1}. This is much lower in frequency than observed for a K bentonite film prior to immersion or a K bentonite film immersed in PAG(600). It is actually closer to the value observed (3373 cm^{-1}) in figure 7.3.4.2a for a Na bentonite stabilised in 50 gdm^{-3} PAG(600) solution. This is due to significant rehydration of the complex. However, in the presence of K$^+$ interlayer cations, the film is less able to disperse and destabilise than it is when Na$^+$ counter cations are present, consequently, the clay film is stable, despite the presence of a considerable amount of re-adsorbed water. Similarly, in the spectrum of a K bentonite film immersed in lower concentration solutions (1 gdm^{-3}) of PAG(1700) the band maximum is located at 3356 cm^{-1}, again attributable to re-adsorbed water. This is even lower than observed in the spectrum of Na bentonite film immersed in 50 gdm^{-3} PAG(600) and is probably due to the slower rate of adsorption of the higher molecular weight polyol which does not inhibit re-adsorption as effectively as the lower molecular weight polyol. It should be noted that despite the presence of a significant amount of re-adsorbed water, the film remains stable which, as before, is attributable to the low swelling capacity of the K$^+$ exchangeable cation.

In figure 7.3.4.3e, the absorption band attributed to the H-O-H bending mode has been significantly reduced in intensity and is very broad, containing both bound and adsorbed water corroborating the findings of the higher frequency region. The position of the maximum (although quite difficult to pinpoint exactly) appears to have been shifted to slightly higher wavenumber (1649 cm^{-1}) in all cases. This is indicative of a stiffening of the H-O-H bending mode due to the interaction of PAG(1700) with bound water surrounding the exchange cation.

7.3.4.4 Adsorption of polyalkyl glycol from dilute solution onto Na bentonite free standing films in the presence of electrolyte.

Electrolyte in solution, and in particular the nature of the electrolyte in solution, has a significant influence on the adsorption process (section 7.3.3.3 and [1]). Immersed Na bentonite films in all PAG(600) solutions were stabilised in the presence of 10% KCl. Obviously, the presence of 10% KCl solution whether by virtue of its strongly flocculating effect and/or by cation exchange with Na^+ on the clay appears to have a profound effect on the adsorption of PAG(600) forming a two layer organic complex with a Na bentonite film at a 50 gdm^{-3} solution concentration and a single layer complex at lower solution concentrations, ≤ 5 gdm^{-3}. The infrared spectra of these complexes are shown in figures 7.3.4.4a and 7.3.4.4b. Table 7.3.4.4b clearly shows both the increase in adsorbed amount (decrease in A(3630)/(2932)) and the increase in the dehydration of the clay (increases in A(3630)/A(3440) and A(3630)/A(1640)) with increased solution concentration.

Figure 7.3.4.4a Infrared spectra of stabilised Na bentonite films after immersion in polyalkyl glycol (Mw 600)/10% KCl.
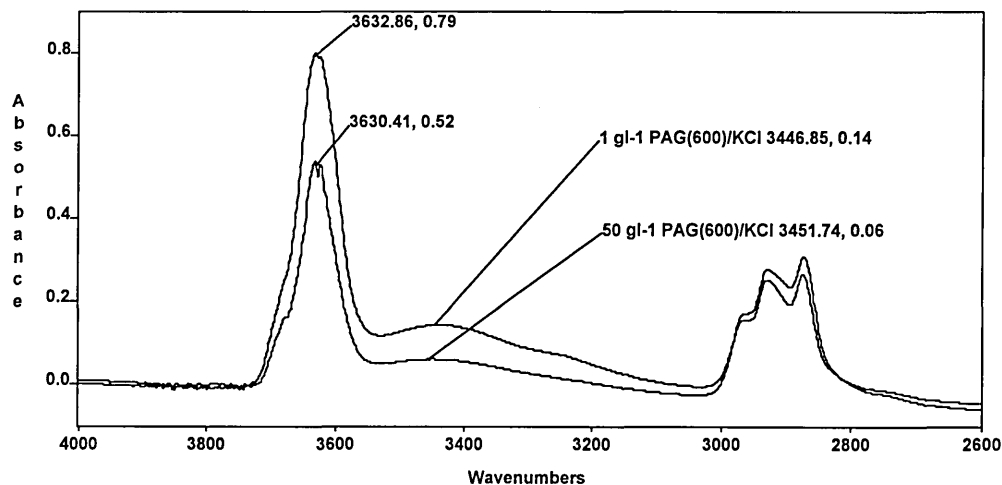
Figure 7.3.4.4b Infrared spectra of stabilised Na bentonite films after immersion in polyalkyl glycol (Mw 600)/10% KCl.
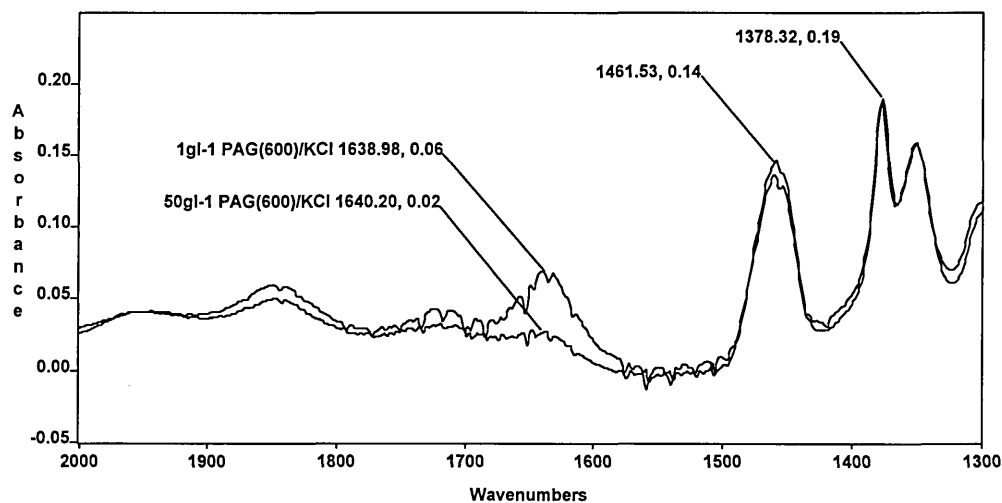
Table 7.3.4.4b Absorbance ratios from the infrared spectra of stable Na bentonite films, after immersion in PAG(600)/10% KCl solution.

absorbance ratio	50 gdm^{-3} PAG(600)	5 gdm^{-3} PAG(600)	2.5 gdm^{-3} PAG(600)	1 gdm^{-3} PAG(600)
3630/3440*	9.8	8.4	5.9	6.0
3630/1640*	26.1	14.6	12.7	11.2.0
3630/2932	1.9	2.9	3.0	3.4

*The actual position of these bands is dependent upon the extent of dehydration.

From figure 7.3.4.4a, it is clear that the shift in the band maximum associated with the various hydrogen bonded OH stretching modes in Na bentonite following immersion in PAG(600)/10% KCl solutions is approximately the same (3448 cm^{-1} ±3 cm^{-1}), regardless of the polymer concentration. This is not at nearly so high a frequency (3463 cm^{-1}) as observed for Na bentonite immersed in 100 gdm^{-3} PAG(600) but at a much higher frequency than observed for Na bentonite

immersed in 50 gdm^{-3} PAG(600) (3372 cm^{-1}) as seen in figure 7.3.4.2a. Evidently, KCl helps stabilise the film even at low PAG(1700) solution concentrations. The resultant spectra appear to exhibit features more like those observed for Na bentonite immersed in 100 gdm^{-3} PAG(600) in which re-hydration by water adsorbing onto unfilled co-ordination sites is very limited. However, this is not at quite as high a frequency as observed in the infrared spectrum of K bentonite films immersed in 50 gdm^{-3} PAG(600) (figure 7.3.4.3a) where the observed value was 3471 cm^{-1}, but at much higher frequency than observed in 1 gdm^{-3} PAG(600) (figure 7.3.4.3a) where the observed value was 3420 cm^{-1}. Clearly, the influence of K^{+} cations is again in evidence but this result also shows the effect of having a large excess of flocculating electrolyte in solution which collapses the electrical double layer and impedes clay swelling.

The position of this band reflects the dehydration of the bentonite followed by adsorption of a single polyalkyl glycol layer via a water bridge to the first hydration sphere surrounding the exchange cations. The stability of this complex will then depend upon the subsequent inhibition to re-hydration of the interlayer region, whether by virtue of the formation of a second organic layer between the clay platelets, by partial cation exchange of Na^{+} by K^{+} or by a flocculating electrolyte.

Additionally, in figure 7.3.4.4b, the spectrum of a Na bentonite film immersed in 50 gdm^{-3} PAG(600) solution shows the spectral maximum associated with the H-O-H bending mode located at higher frequency (1649 cm^{-1}) than in homoionic Na bentonite prior to immersion. This band has been observed shifted to 1649 cm^{-1} previously for the adsorption of PAG(600) and PAG(1700) onto Na^{+} and K bentonite and attributed to the stiffening of the H-O-H bending mode of water in the inner co-ordination sphere around the exchange cation as the polyalkyl glycol hydrogen bonds to it.

At lower concentrations (≤ 5 gdm^{-3}) of PAG(600) the position of the spectral maximum attributed to the H-O-H bending mode of water does not appear to be shifted significantly from that of 1640 cm^{-1} in homoionic Na bentonite, being found at 1639 cm^{-1} ± 4 cm^{-1}. The absence of a band shift may be indicative of a low absorbed amount (these systems formed only one layer complexes). Indeed, the absorbance ratio A(3630)/A(2932) is much higher (3.2 ± 0.3) for solution concentrations ≤ 5 gdm^{-3} of PAG(600) than for solution concentration ≥ 50 gdm^{-3} (A(3630)/A(2932) is 1.9). This is due to hindered polyalkyl glycol adsorption in KCl solution as the electrolyte will both collapse the electrical double layer causing flocculation and allow cation exchange of K^{+} for Na^{+} ions in the interlayer which inhibits swelling. As a result, re-adsorption of water is not suppressed and the amount of adsorbed water on the clay is sufficiently large to mask the expected shift.

Clearly, complexes formed between Na bentonite and PAG(600) in the presence of 10% KCl are significantly re-hydrated. Indeed, the ν(OC) band is located at 1378 cm^{-1} in the spectra of Na bentonite films immersed in ≤ 5 gdm^{-3} PAG(600)/10%KCl solutions. This indicates a high degree of hydration of the polymer in the interlayer region in these particular films. At the highest concentration (50 gdm^{-3}) of PAG(600), the ν(OC) band is located at slightly lower frequency (1376 cm^{-1}) which corresponds to a slightly less hydrated complex. This is not unexpected since it does exist as a two layer complex and the absorbance ratios A(3630)/A(3440) and A(3630)/A(1640) are higher for this system than those observed for the other complexes.

Stabilised Na bentonite films in PAG(1700)/10% KCl solution formed mixed layer complexes (zero/one layer at 1 gdm^{-3} PAG(1700), one/two layer at ≥ 2.5 gdm^{-3} PAG(1700)). The FTIR spectra of these films are shown in figures 7.3.4.4c and 7.3.4.4d.

Figure 7.3.4.4c Infrared spectra of stable Na bentonite films after immersion in PAG(1700)/10% KCl solutions.
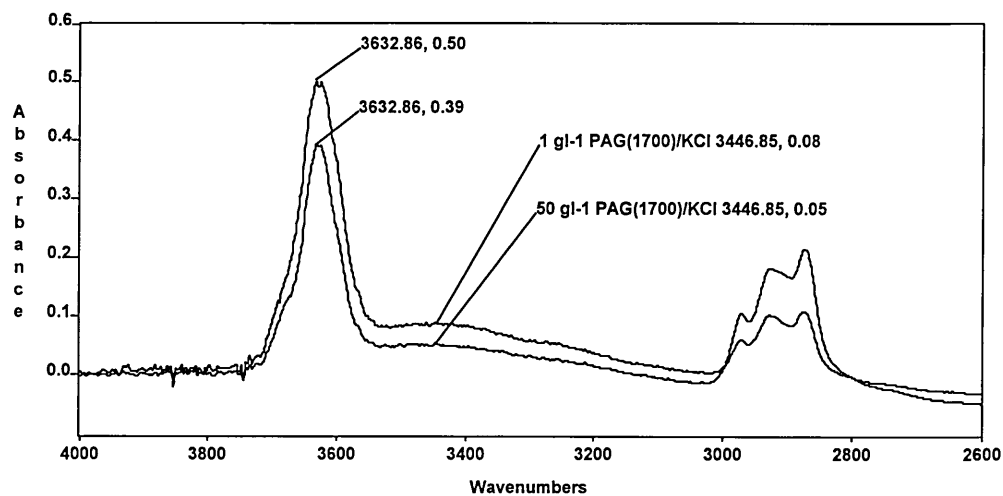

Figure 7.3.4.4d Infrared spectra of stable Na bentonite films after immersion in PAG(1700)/10% KCl solutions.
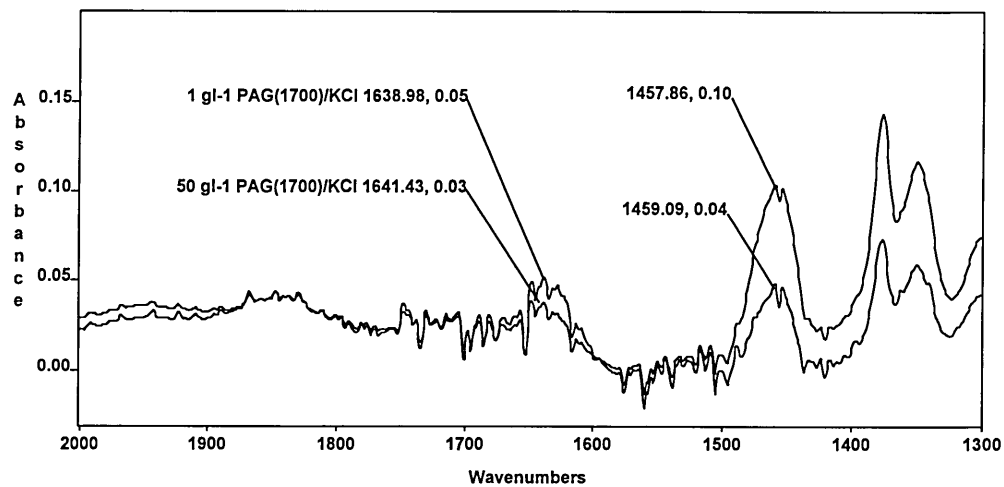
Again the clay can clearly be seen to be dehydrated, a feature which increases with increasing solution concentration. The relevant absorbance ratios, A(3630)/A(3440), A(3630)/A(1640) and A(3630)/A(2932) are shown in table 7.3.4.4d.

Table 7.3.4.4d Absorbance ratios from the infrared spectra of stable Na bentonite films after immersion in PAG(1700)/10% KCl.

absorbance ratio	50 gdm^{-3} PAG(1700)	5 gdm^{-3} PAG(1700)	2.5 gdm^{-3} PAG(1700)	1 gdm^{-3} PAG(1700)
3630/3440*	4.2	4.5	4.4	4.3
3630/1640*	9.0	8.3	5.8	6.3
3630/2932	1.8	1.7	2.7	4.9

*The actual position of these bands is dependent upon the extent of dehydration.

Clearly, as the polymer solution concentration increases, the adsorbed amount increases (decreasing A(3630)/A(2932) with increasing polymer solution concentration). The dehydration of the clay can be seen in the decrease in the absorbance ratio, A(3630)/A(1640) with increasing adsorbed amount. The dehydration of the clay is not so easily observable however with increasing adsorbed amount in the absorbance ratio A(3630)/A(3440) (probably due to the presence of re-adsorbed water in the complex).

The position of the spectral maximum associated with hydrogen bonded OH stretching modes (located at 3444 cm^{-1} ±4 cm^{-1} in all spectra) may also be attributed to re-adsorbed water in the complex. This behaviour is very similar to that observed in the spectra of Na bentonite films immersed in PAG(600) in the presence of 10% KCl at solution concentrations ≤5 gdm^{-3}.

Re-adsorbed water also appears to influence the infrared spectra at lower frequency (figure 7.3.4.4d). The band attributed to the H-O-H bending mode can be observed at 1638 cm^{-1} ± 4 cm^{-1}, regardless of the polymer solution concentration. This, again, is similar behaviour to that observed in the adsorption

of PAG(600) onto Na bentonite from ≤ 5 gdm^{-3} polymer solution containing 10% KCl (figure 7.3.4.4b).

The extent of water re-adsorption can be correlated to the position of the ν(OC) band in figure 7.3.4.4e.

Figure 7.3.4.4e Infrared spectra of stable Na bentonite films after immersion in PAG(1700)/10% KCl solution.
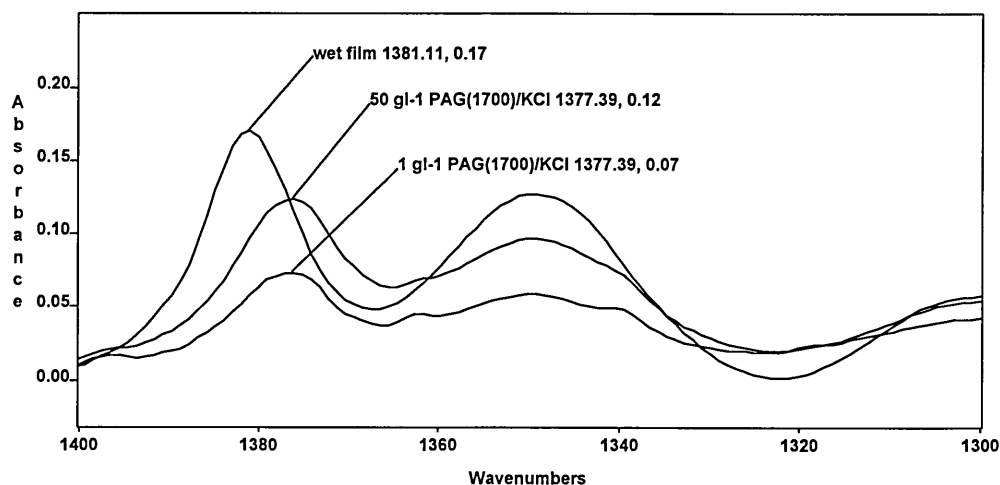
The ν(OC) band is located at 1377 cm^{-1} in the spectra of all dried Na bentonite films following immersion in PAG (1700)/10% KCl solutions. This is indicative of a relatively high degree of hydration, which supports the theory that the presence of the flocculating cation is able to suppress Na bentonite dispersion to such an extent that a highly hydrated complex may form and stabilise the film

It should be noted that apart from the ν(OC) band at ~1380 cm^{-1} the position of absorption bands attributed to adsorbed polyol are unchanged from their positions in the spectrum of the dilute solutions (figure 7.3.1b). The change in position of the ν(OC) band is due to hydration of the polymer chain. The implication is that despite the number of organic layers, the nature of the exchange cation and the

presence of electrolyte, the conformation of the adsorbed polymer is always the same and, in keeping with the theory [11] of adsorption of linear flexible nonionic polymers, is flat.

In order to establish the relative influences, on the stabilisation of Na bentonite films by adsorption of polyalkyl glycol, of the flocculating effect of electrolyte in solution and of the nature of the exchange cation, Na bentonite films were stabilised (forming two layer complexes at all concentrations (figure 7.3.3.3c)) in PAG(600) solutions.

Figure 7.3.4.4f and 7.3.4.4g show the infrared spectra of these complexes and table 7.3.4.4g, the absorbance ratios A(3630)/A(3440), A(3630)/A(1640) and A(3630)/A(2932).

Figure 7.3.4.4f Infrared spectra of stable Na bentonite films after immersion in PAG(600)/10% NaCl solutions.
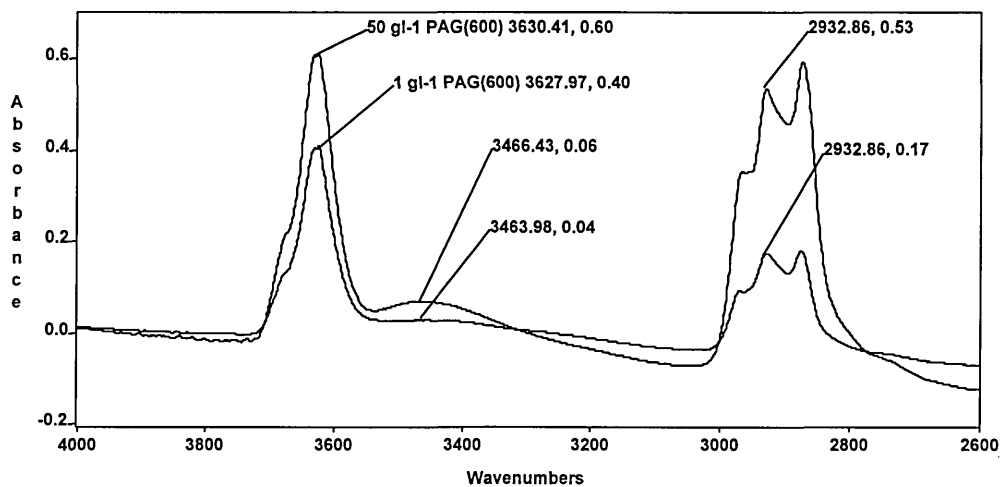
Figure 7.3.4.4g Infrared spectra of stable Na bentonite films after immersion in PAG(600)/10% NaCl solutions.
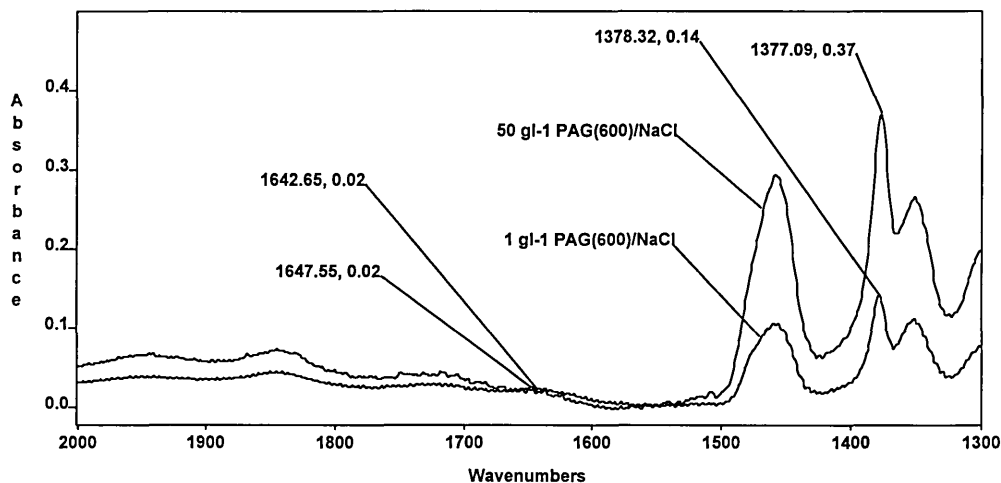
Table 7.3.4.4g Absorbance ratios from the infrared spectra of stable Na bentonite film after immersion in PAG(600)/10% NaCl solution.

absorbance ratio	50 gdm^{-3} PAG(600)	5 gdm^{-3} PAG(600)	2.5 gdm^{-3} PAG(600)	1 gdm^{-3} PAG(600)
3630/3440*	10.7	11.0	10.5	9.8
3630/1640*	23.1	22.7	19.4	19.1
3630/2932	2.2	2.3	2.4	2.4

*The actual position of these bands is dependent upon the extent of dehydration.

As the solution concentration increases, then the adsorbed amount, as determined by the absorbance ratio A(3630)/A(2932), appears to slightly increase.

Again, as was observed previously for the adsorption of PAG(1700) onto Na bentonite in the presence of 10% KCl, the dehydration of the clay can be seen in the decrease in the absorbance ratio A(3630)/A(1640) with increasing adsorbed amount. The dehydration of the clay is less easily observable with increasing

317

adsorbed amount in the absorbance ratio A(3630)/(3440) which appears to stay reasonably unchanged regardless of adsorbed amount.

The behaviour of this system is similar to the stabilisation of Na bentonite films in the presence of 100 gdm^{-3} PAG(600) only. Indeed, the position of the spectral maximum attributed to the hydrogen bonded OH stretching mode is shifted to high frequency being found at 3465 cm^{-1} ± 4 cm^{-1}. This apparent shift (or change in relative intensity) has previously been attributed to the dehydration of the clay on polymer adsorption causing the intensity of the bands due to adsorbed water to be reduced and hence the spectral maximum in this region being influenced more significantly by the bands associated with inner hydration sphere water (bound water). The extent of the band shift is determined by the extent of dehydration, adsorption and then re-hydration

Further evidence of this can be seen in the infrared spectra in figure 7.3.4.4g. The position of the band attributed to H-O-H bending mode may be observed at 1649 cm^{-1} ±3 cm^{-1}. This shift from its position (1636 cm^{-1}) in a Na bentonite film prior to immersion is attributed to the stiffening of the H-O-H bending mode of bound water in the inner hydration sphere of the cation due to hydrogen bonding of polyalkyl glycol to it. This band shift is not always observable because it is sometimes masked by the re-adsorption of water into the interlayer space. In this case however, in the presence of Na^{+} cations the clay is able to swell sufficiently to enable the polyalkyl glycol to adsorb and form the two layer organic complex which inhibits re-adsorption of water.

7.3.4.5 Kinetics of adsorption of polyalkyl glycol from dilute solution onto homoionic Na bentonite in the presence of electrolyte.

The effect on the infrared spectra of varying the time of immersion of the bentonite film in polyol solution has also been studied. Firstly consider the smaller polyalkyl glycol molecule. Figure 7.3.4.5a and 7.3.4.5b show the infrared spectra of Na bentonite films immersed for various times in 50 gdm^{-3} PAG(600)/10% KCl solution. The absorbance ratios A(3630)/A(3440), A(3630)/A(1640) and A(3630)/A(2932) and the corresponding d-spacings (from figure 7.3.3.4b) are shown in table 7.3.4.5b.

Figure 7.3.4.5a Infrared spectra of stable Na bentonite films after immersion in a 50 gdm^{-3} PAG(600)/10% KCl solution for various times.
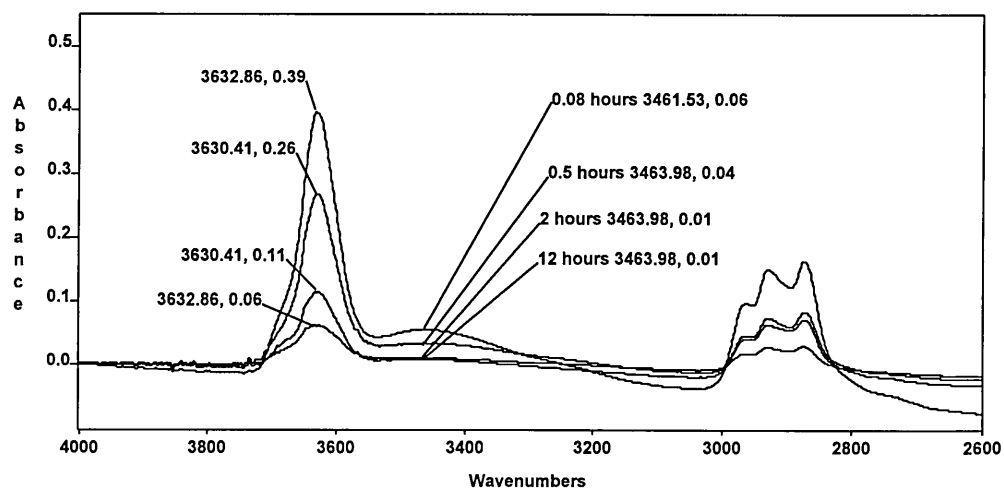
Figure 7.3.4.5b Infrared spectra of stable Na bentonite films after immersion in a 50 gdm^{-3} PAG(600)/10% KCl solution for various times.
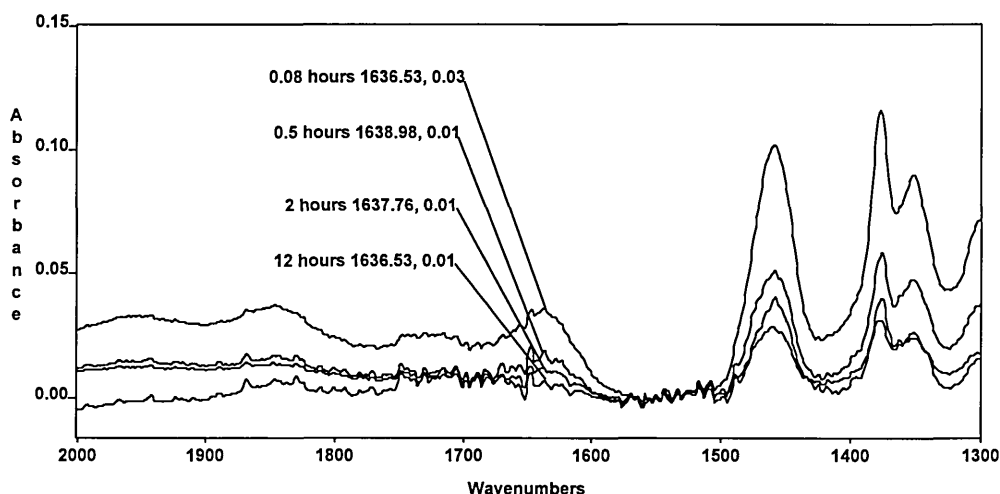
Table 7.3.4.5b Absorbance ratios from the FTIR spectra of stable Na bentonite films after immersion in 50 gdm^{-3} PAG(600)/10% KCl solution for various times.

	Time of soak (hours)						
	0.03	0.08	0.25	0.5	1.0	2.0	12.0
d-spacing (Å)	14.1	14.0	14.4	14.9	15.9	16.0	17.5
absorbance ratios							
3630/3440*	5.0	6.1	6.1	6.0	6.0	7.5	9.8
3630/1640*	10.5	11.9	11.8	11.4	12.3	13.7	16.1
3630/2932	3.0	2.6	2.5	2.3	2.3	2.1	1.9

*The actual position of these bands is dependent upon the extent of dehydration.

Clearly, the absorbance ratios A(3630)/A(3440) and A(3630)/A(1640) increase with increasing immersion time in the solution, indicative of dehydration of the bentonite film. After only two minutes the ratios A(3630)/A(3440) and

320

A(3630)/A(1640) have increased to 5.0 and 10.1 respectively, compared to their values of 1.5 and 2.4 in the spectrum of the film prior to immersion. These ratios then increase slowly with increasing immersion time as the first adsorbed layer consolidates and the clay slowly dehydrates, i.e. with the slow increase in adsorbed polymer (diffusion controlled) between the platelets (denoted by the decrease in the absorbance ratio A(3630)/A(2932) with immersion time).

Additionally, from figures 7.3.4.5a and 7.3.4.5b it is possible to observe the change in the position of spectral maxima attributed to water in the interlayer with increasing immersion time. After only 2 minutes the position of the spectral maximum associated with hydrogen bonded OH stretching modes (figure 7.3.4.5a) is shifted (3461 cm^{-1}) from its position in Na bentonite prior to immersion (3406 cm^{-1}). Thereafter, this band (attributed to removal of adsorbed water and the subsequent domination of this spectral region by water directly bound to the exchange cation) is located at 3461 cm^{-1} ±3 cm^{-1} in the infrared spectra of Na bentonite films immersed in 50 gdm^{-3} PAG(600)/10% KCl solution for increasing lengths of time up to 12 hours. This implies that the important adsorption process for stabilisation (formation of a water bridge between the polyalkyl glycol and inner hydration sphere water around the cation) has occurred after only two minutes.

Additionally, the position of the spectral maxima associated with the H-O-H bending modes appears to be shifted to 1637 cm^{-1} after two minutes immersion in 50 gdm^{-3} PAG(600)/10% KCl for various times (figure 7.3.4.5b). This shift has been observed previously for the adsorption of polyalkyl glycol onto Na and K bentonite films and is attributed to the stiffening of the H-O-H bending mode of water in the inner co-ordination sphere around the exchange cation as the polyalkyl glycol hydrogen bonds to it.

The extent of hydration of the complexes formed can be seen in the position of the v(OC) band as shown in figure 7.3.4.5c.

Figure 7.3.4.5c Infrared spectra of stable Na bentonite films after immersion in 50 gdm^{-3} PAG(600)/10% KCl solution for various times.
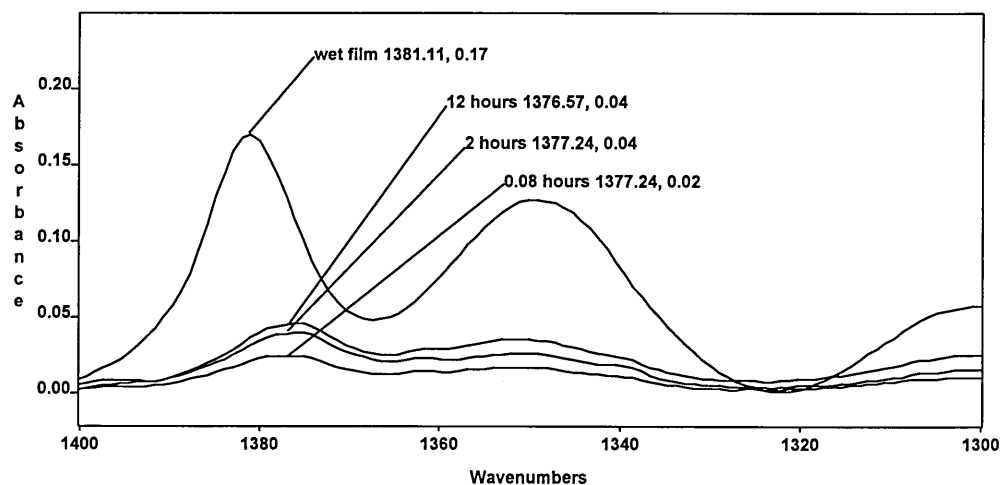

The position of the band attributed to v(OC) is located at 1377 cm^{-1} in the spectra of Na bentonite film immersed in PAG(600)/10% KCl for two minutes, and times up to 2 hours and at 1377 cm^{-1} after immersion of the film in solution for 12 hours. This is indicative of the formation of a relatively hydrated, stable film after only two minutes and perhaps a slight increase in the number of PAG-PAG interactions as polyalkyl glycol concentrates between the platelets (formation of the second layer) and dehydrates the clay further with increased immersion time.

In the presence of PAG(1700) however, XRD evidence suggests the initial formation of a dehydrated or cation exchanged system followed by the adsorption of polyol between the platelets. Figures 7.3.4.5c and 7.3.4.5d show the infrared spectra of Na bentonite films immersed for various times in a 50 gdm^{-3} PAG(1700)/10% KCl solution. Table 7.3.4.5d shows the absorbance ratios

A(3630)/A(3440) A(3630)/A(1640) and A(3630)/A(2932) from these spectra and

the d-spacings from table 7.3.3.4d.

Figure 7.3.4.5c Infrared spectra of stable Na bentonite films after immersion in PAG(1700)/10% KCl solution for various times.
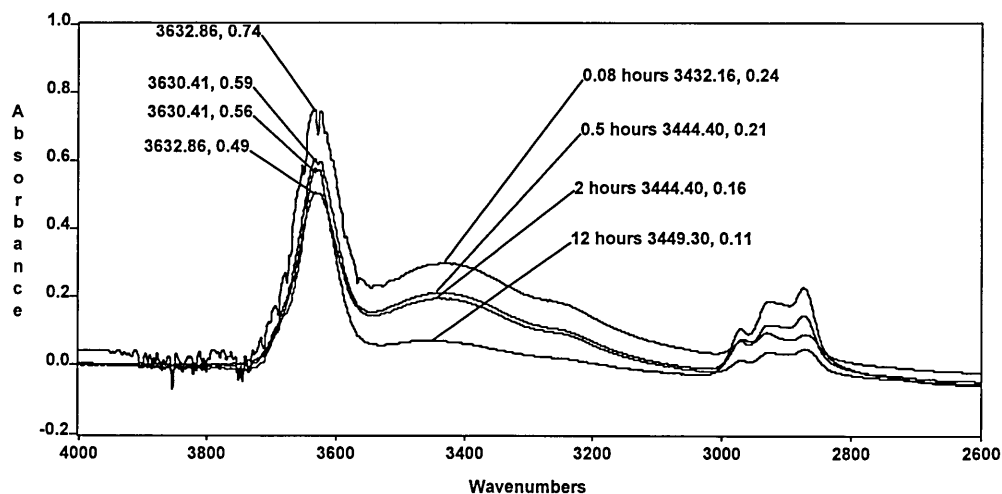
Figure 7.3.4.5d Infrared spectra of stable Na bentonite films after immersion in PAG(1700)/10% KCl solution for various times.
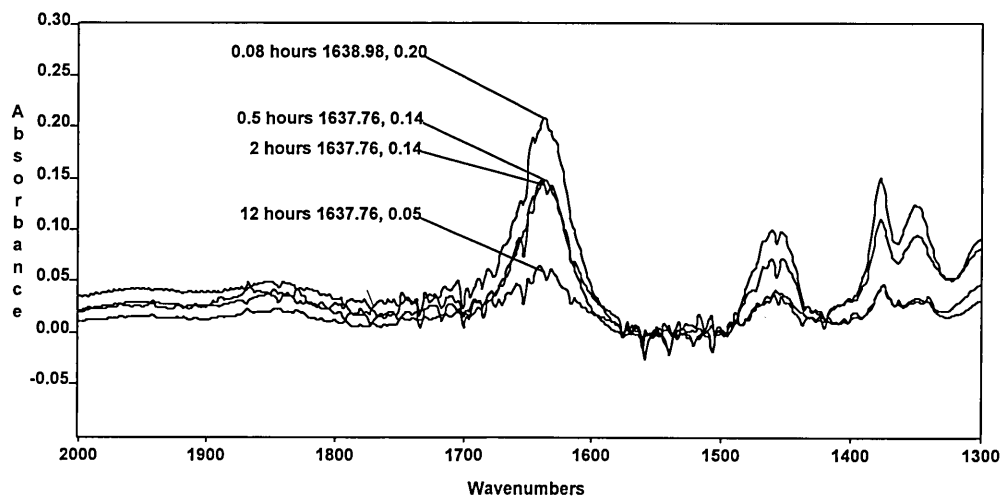
Table 7.3.4.5d Absorbance ratios from the infrared spectra of stable Na bentonite films after immersion in a 50 gdm^{-3} PAG(1700)/10% KCl solution for various times.

	Time of soak (hours)						
	0.08	0.25	0.5	0.75	1.0	2.0	12.0
d-spacing (Å)	11.6	11.9	14.7 12.0sh	14.8 11.8sh	15.6 12.2sh	16.1 12.2sh	16.1
absorbance ratio							
3630/3440*	3.0	2.7	2.6	3.1	2.6	3.4	4.3
3630/1640*	3.1	2.8	3.7	3.4	6.3	4.0	6.3
3630/2932	14.5	13.8	13.5	8.9	6.7	5.1	4.9

*The actual position of these bands is dependent upon the extent of dehydration.

The absorbance ratio A(3630)/(2932) decreases as the time of immersion of the Na bentonite film in the 50 gdm^{-3} PAG(1700) /10% KCl solution increases, indicative of an increase in the amount of polyalkyl glycol adsorbed.

The initial dehydration of the clay can be clearly seen after 5 minutes as the absorbance ratios A(3630)/(3440) and A(3630)/(1640) both increase to 3.0 and 3.1, respectively, compared to 1.5 and 2.4 in the homoionic Na bentonite film. The subsequent dehydration of the clay is very slow with the absorbance ratios A(3630)/(3440) and A(3630)/(1640) increasing gradually as the time of immersion increases. This is not unexpected, as the d-spacings suggest that the clay initially dehydrates or undergoes cation exchange. As polymer adsorbs between the platelets, the d-spacing increases and at the same time, the interlayer regions which do not have adsorbed polymer re-hydrate (indicated by the shoulder at 12.2Å) and so the stable complex exists with mixed zero and one layer of PAG(1700) between

the platelets. As time progresses, more polymer adsorbs between the platelets and the d-spacing gradually increases corresponding to the formation of a mixed 1 and 2 layer complex.

The position of the spectral maxima associated with hydrogen bonded OH stretching modes (figure 7.3.4.5c) corroborates these findings. After 5 minutes the band is found at 3433 cm^{-1} shifted from its position of 3406 cm^{-1} in Na bentonite prior to immersion. This shift is due to the dehydration of the clay and hence the spectral maximum being dominated by the bands associated with bound water. Previously, however, (in sections 7.3.4.2 and 7.3.4.3 for example) this feature has been observed shifted to >3450 cm^{-1}. The explanation for this could be that the position of this spectral maximum is almost identical to that observed in homoionic K bentonite (at 3431 cm^{-1}) and that these films have undergone significant cation exchange of K^{+} for Na^{+}. This would explain the observed d-spacing of 11.6 and 11.9Å after immersion of the film in the 50 gdm^{-3} PAG(1700) /10% KCl solution for 5 and 15 minutes, respectively. This is not unlikely as Rawson [3] indicated that K^{+} exchange for Cs^{+} was enhanced by the presence of polyalkyl glycol of molecular weight <1000 gmol^{-1}.

This initial dehydration and/or cation exchange process cannot be seen in the X-ray diffraction or infrared results when the complex is formed between Na bentonite film and the low molecular weight polyalkyl glycol in the presence of KCl because the polymer adsorbs too quickly for the intermediate (cation exchanged/dehydrated) system to be observed. The adsorption of the higher molecular weight polyalkyl glycol (Mw 1700) however, is slower so the intermediate can be observed. The clay is prevented from dispersing (destabilisation) by the presence of the strongly flocculating electrolyte in solution. After 30 minutes immersion, the position of the spectral maxima associated with hydrogen bonded OH stretching modes in the infrared spectra of the film has

shifted to 3446 cm^{-1} where it may be observed ($\pm$ 3 cm^{-1}) in the spectra of films immersed for all times up to 12 hours.

In addition, the spectral maxima associated with the H-O-H bending modes after immersion of Na bentonite films in 50 gdm^{-3} PAG(1700)/ 10% KCl for all times (figure 7.3.4.5d) is located at 1640 cm^{-1} $\pm$3 cm^{-1}. This position is very similar to that observed in homoionic Na and K bentonite prior to immersion and is due to the relative extents of cation exchange and dehydration.

Further evidence regarding the degree of hydration of the complex can be found in figure 7.3.4.5e (in the spectral region between 1420 and 1300 cm^{-1}). The position of the ν(OC) band is found at 1374 cm^{-1} in the spectrum of Na bentonite film immersed in PAG(1700)/10% KCl for 5 minutes. This band then shifts to slightly higher frequency, being found at 1377 cm^{-1} for times $\geq$30 minutes immersion of the Na bentonite film in 50 gdm^{-3} PAG (1700)/10% KCl solution up to 12 hours.

Figure 7.3.4.5e Infrared spectra of stable Na bentonite films after immersion in 50 gdm^{-3} PAG(1700)/10% KCl solution for various times.
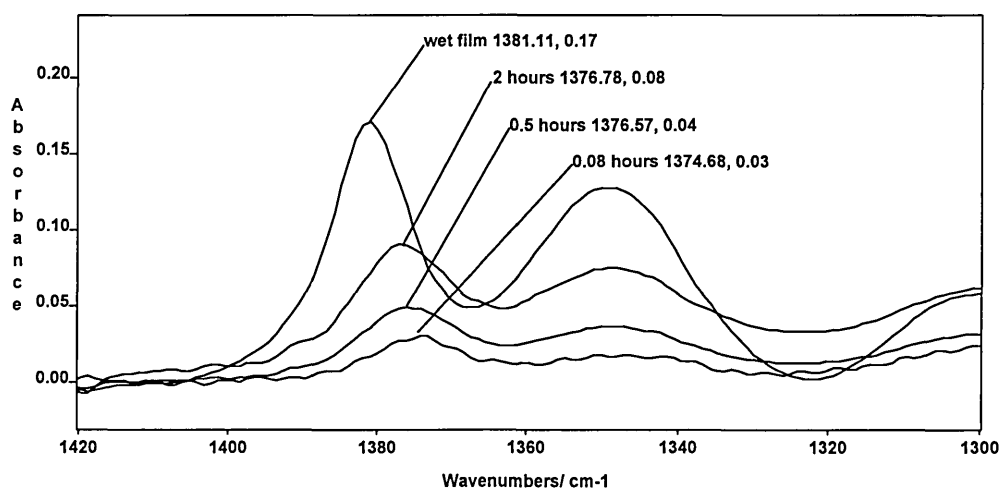
This would appear to indicate that on initial adsorption, the number of PAG-H$_2$O interactions in the interlayer is extremely small (after 5 and 15 minutes

326

immersion). However, as more polymer adsorbs, there is competition for adsorption sites between the polymer and water which is able to re-hydrate the system. Consequently, the number of PAG-H$_2$O interactions increases. This extent of re-adsorption depends on the ability of both the polymer and exchange cation to become hydrated. Clearly, the PAG(1700) molecule is not as effective as PAG(600) at preventing re-hydration.

X-ray diffraction evidence suggests that after 12 hours immersion, the system exists as a mixed 1/2 layer complex and that hydration is possible because not all the inner co-ordination sphere water around the exchange cation is used for hydrogen bonding to the polymer. In the presence of KCl solution, cation exchange and collapse of the electrical double layer restricts swelling. However in the absence of K$^+$ ions (in solution or on the clay) it is likely that the Na bentonite-PAG(1700) complex re-hydrates as the exchange cations are able to form extended hydration spheres and therefore disperse the platelets, thus de-stabilising the film.

7.3.4.6 Adsorption of polyalkyl glycol from dilute solution onto Na bentonite dispersed in aqueous suspension.

X-ray diffraction traces obtained by Rawson [3] from the dried centrifuged solids of Na bentonite suspension mixed with PAG(600) showed the formation of one and two layer complexes depending on the solution concentration of PAG(600) [3]; at concentrations ≥ 5 gdm^{-3} PAG(600) the two layer complex is formed, at concentrations ≤ 2.5 gdm^{-3} PAG(600), the single layer complex is formed. Figure 7.3.4.6a shows the infrared spectra of complexes formed between Na bentonite and polyalkyl glycol (Mw 600) in aqueous suspension.

Figure 7.3.4..6a Infrared spectra of complexes formed between Na bentonite and polyalkyl glycol (Mw 600) in aqueous suspension.
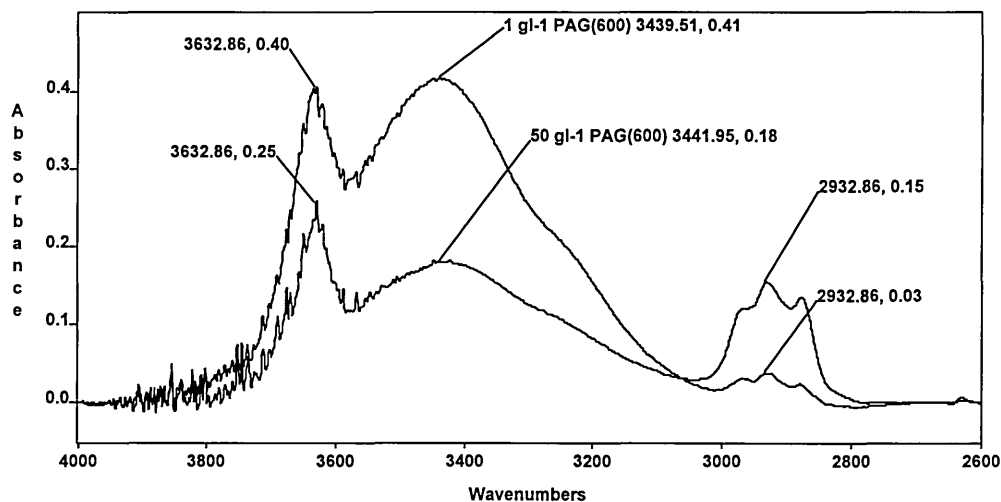
The position of the spectral maximum attributed to the hydrogen bonded OH stretching frequency is located at 3440 cm^{-1} ±3 cm^{-1} for all the spectra of complexes formed between PAG(600) and Na bentonite in aqueous suspension. This is very close to its value in homoionic Na bentonite prior to contact with the polyol. Indeed, the relative intensities of the spectral features (shown by A(3630)/A(3440) in table 7.3.4.6a) seems to indicate that the systems are not dehydrated.

Table 7.3.4.6a Absorbance ratios from the infrared spectra of complexes prepared from Na bentonite and PAG(600) in aqueous suspension.

absorbance ratio	50 gdm^{-3} PAG(600)	5 gdm^{-3} PAG(600)	2.5 gdm^{-3} PAG(600)	1 gdm^{-3} PAG(600)
3630/3440	1.4	1.0	0.9	1.0
3630/2932	1.7	3.7	8.6	13.3

328

The decrease in the absorbance ratio A(3630)/A(2932) with increasing polymer solution concentration indicates increased adsorbed amount. It should be remembered however, that for Na bentonite the absorbance ratio A(3630)/A(3440) is ~1.5. It therefore appears that the complexes formed between Na bentonite and PAG(600) are more hydrated than homoionic Na bentonite alone. This could be due to the method of adsorption, since in aqueous suspension the platelets are widely dispersed and polymer may pass easily between them. On drying polymer may be trapped between the platelets without actually being physically adsorbed. Consequently, the exchange cations and polymer may have any amount of water associated with them, as the complex can be highly hydrated since it does not have to exhibit stability. As a result, the adsorption of polymer is controlled only by the ease of hydration of the cation (ability to swell the clay) and the polymer solution concentration.

Further evidence of the highly hydrated nature of the complex can be found by analysis of the v(OC) band a in figure 7.3.4.6b.

Figure 7.3.4.6b Infrared spectra of complexes formed between Na bentonite and polyalkyl glycol (Mw 600) in aqueous suspension.
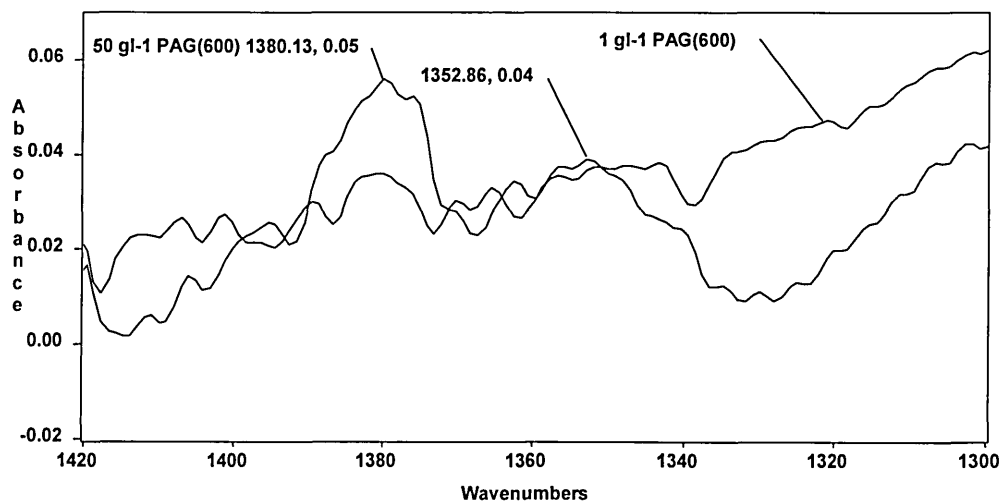
The bands in this region are extremely weak, in fact they are impossible to observe in the spectrum of the complex prepared from Na bentonite and 1 gdm^{-3} PAG(600) in aqueous suspension. The band can, however, be seen in the spectrum of the complex prepared from Na bentonite and 50 gdm^{-3} PAG(600) in aqueous suspension, located at 1380 cm^{-1}. This corresponds to the position of the band in the spectrum of a highly dilute solution of polyalkyl glycol in water (20% by weight), i.e. many PAG-H_2O interactions.

7.3.5.   ATR infrared spectroscopy

FTIR transmission spectroscopy and X-ray diffraction have been used (here and [1]) to study the stabilisation of free standing bentonite films by adsorption of polyalkyl glycol. However, ATR FTIR has been used to study the stabilisation of bentonite films supported on the surface of a ZnSe IRE *in-situ*. This method has previously been used to study the adsorption of water soluble polymers [204] and pyridine [205] onto homoionic bentonite clay films.

7.3.5.1   Adsorption onto Na bentonite films (supported on a ZnSe ATR crystal) of polyalkyl glycol from the pure liquid polymer.

Figure 7.3.5.1a shows the infrared spectrum of the ZnSe Squarecol ATR prism coated on each sampling face with an air dried bentonite film and ratioed against the ATR prism with clean sampling faces.

Figure 7.3.5.1a The infrared spectrum of the ZnSe Squarecol ATR prism coated on each sampling face with an air dried bentonite film
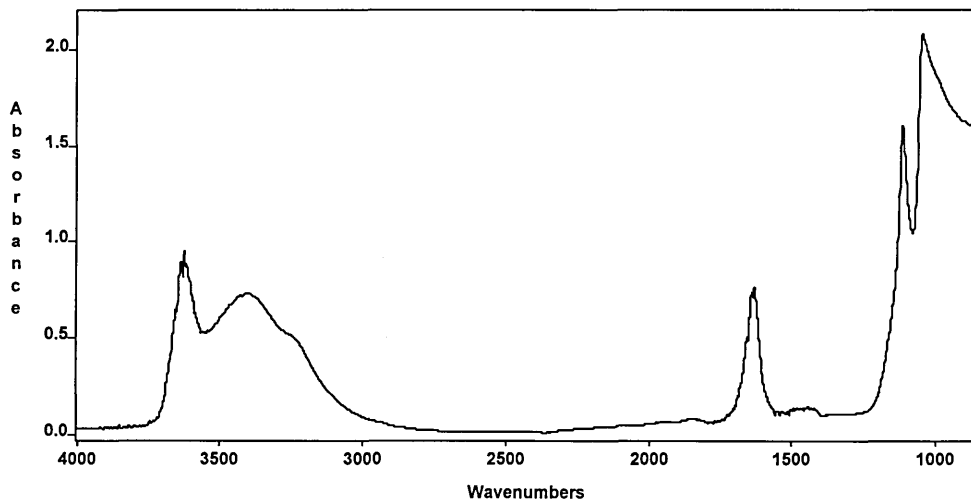
This spectrum is very similar to the infrared spectrum of the free standing Na bentonite film in figure 7.3.4.1a and the infrared spectrum of the Na bentonite film supported on the Si Squarecol ATR prism in figure 6.3.3.3a. As a result it will have the same features and assignments of the bentonite infrared spectrum described in table 5.3.1. The infrared spectrum of the Na bentonite film supported on a ZnSe prism does not exhibit the strange absorption band profile below 1500 cm^{-1} observed in the spectrum of bentonite film supported on the Si prism because the infrared window of ZnSe is much wider than that of silicon. The spectrum only shows 'cut off' below approximately 1200 cm^{-1} due to the intense Si-O vibrations of the bentonite film.

The addition of pure polyalkyl glycol (Mw 600) to the trough of the Squarecol cell containing bentonite coated optics has a profound effect on the infrared spectrum. Figure 7.3.5.1b shows the evolution of the infrared spectra with time.

Figure 7.3.5.1b The evolution of infrared spectra after addition of pure PAG(600) to Na bentonite coated ZnSe ATR prism.
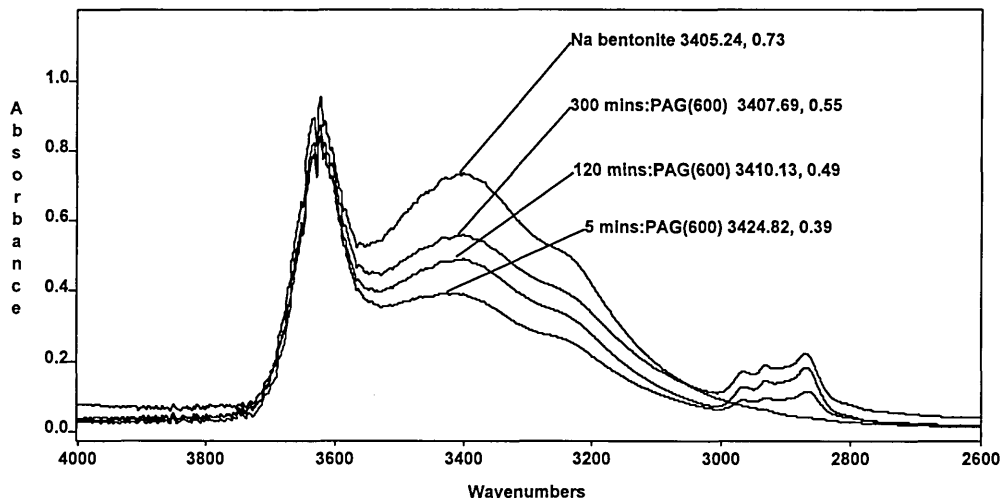
The band attributed to the structural OH stretching mode at 3630 cm^{-1} appears to be largely unaffected by the presence of PAG(600). This is in contrast to the experiments where the introduction of 1 gdm^{-3} aqueous polyacrylamide (Mw 7000k) to the cell immediately caused the height of the band at 3630 cm^{-1} to reduce to zero, consistent with dispersion and destabilisation of the film (section 6.3.3.3). Consequently, it can be assumed that in the presence of pure polyalkyl glycol (Mw 600) the Na bentonite is not dispersed and the film therefore, is stabilised.

More interestingly, 5 minutes after the introduction of the pure polyalkyl glycol to the cell the spectral maximum associated with hydrogen bonded OH stretching modes has decreased in intensity compared to its value in the Na bentonite film. However, as the contact time of the polymer with the Na bentonite film increases, the intensity of this spectral maximum appears to increase. This behaviour can also be observed in the intensity of the band attributed to the H-O-H bending mode of water in figure 7.3.5.1c.

Figure 7.3.5.1c The evolution of infrared spectra after addition of pure PAG(600) to Na bentonite coated ZnSe ATR prism.
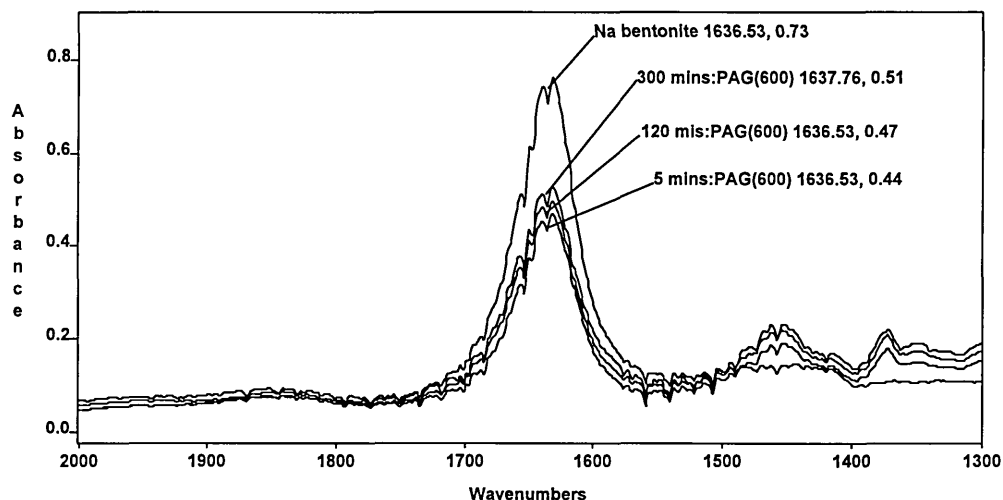
Table 7.3.5.1c shows the change in the absorption ratios A(3630)/A(3440), A(3630)/A(2932) and A(3630)/A(2932) as the contact time of the polymer with the supported Na bentonite film increases.

Table 7.3.5.1c Absorbance ratios from the infrared spectra of a supported Na bentonite, at various times after contact with PAG(600).

Absorbance ratio	Time of contact (hours)						
	0	0.08	1.0	2.0	3.0	4.0	5.0
3630/3440	1.2	2.3	2.0	1.8	1.7	1.7	1.6
3630/1640	1.2	2.0	1.9	1.9	1.8	1.8	1.7
3630/2932	∞	9.8	6.2	6.2	5.9	5.2	4.6

Clearly, as the contact time increases then the amount of PAG(600) sampled by the evanescent field appears to increase, as indicated by the decrease in the

absorbance ratio A(3630)/A(2932). As the bentonite film remains in tact then the only plausible explanation is that PAG(600) is diffusing or adsorbing into the Na bentonite film.

Following the initial detection of PAG(600) in the infrared spectrum, after only 5 minutes contact time of the polyalkyl glycol with the Na bentonite film, there is an initial dehydration of the clay (which provides the entropic driving force for adsorption). This denoted by the increase in the absorbance ratios A(3630)/A(3440) and A(3630)/A(1640) from that of the Na bentonite film prior to contact (at time zero). Following the initial dehydration, the clay appears to re-hydrate and the absorbance ratios A(3630)/A(3440) an A(3630)/A(1640) tend back to their observed values in Na bentonite. No water is associated with the polyol molecule prior to adsorption, hence desorbed water from the clay must re-adsorb into the interlayer region either around exchange cations or around the polymer. Evidence that the polymer does not become significantly hydrated can be observed in the position of the v(OC) band in figure 7.3.5.1d.

Figure 7.3.5.1d Evolution of infrared spectra after the addition of pure PAG(600) to Na bentonite coated ZnSe ATR prism.
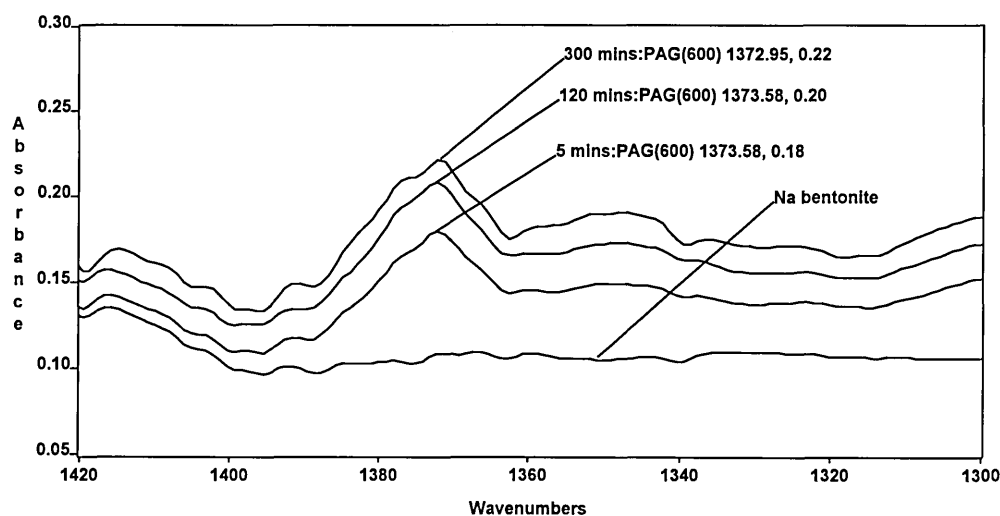
Clearly, the ν(OC) band is located at 1373 cm^{-1}, the same as its position in pure PAG(600), indicating almost exclusive PAG-PAG interactions and no PAG-H$_2$O interactions. Hence, rehydration of the clay film must be by re-adsorbed water on the exchange cation.

7.3.5.2 Adsorption onto Na bentonite films supported on a ZnSe ATR crystal of polyalkyl glycol from a dilute aqueous polymer solution.

Whilst the results from the adsorption of pure polyalkyl glycol (Mw 600) onto a Na bentonite film supported by an ATR prism are very interesting, the real time, *in-situ* study of PAG(600) adsorption onto supported Na bentonite films from aqueous solution is of greater technological importance. Figure 7.3.5.2a shows the infrared spectrum 5 minutes after addition of 50 gdm^{-3} PAG(600) to the Squarecol cell containing Na bentonite coated ZnSe ATR optics.

Figure 7.3.5.2a Infrared spectrum 5 minutes after addition of 50 gdm^{-3} PAG(600) to Na bentonite coated ZnSe ATR prism
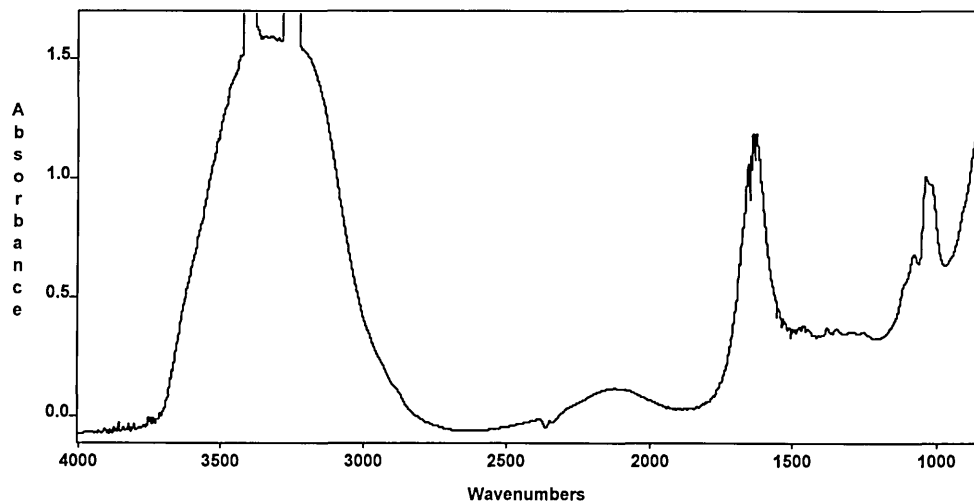
The spectrum is completely dominated by the presence of highly intense absorption bands due to water. Billingham et al [204] subtracted the background spectra of clay or of clay/polymer/solvent. However it is extremely difficult to subtract the background spectrum of water with sufficient accuracy in order to reveal the subtle shifts in spectral maxima due to environmental changes to the water in the interlayer. However, between 1400 and 850 cm^{-1}, the bands attributed to silicate stretching modes may be observed (figure 7.3.5.2b).

Figure 7.3.5.2b FTIR-ATR spectrum 5 minutes after addition of 50 gdm^{-3} PAG(600) to Na bentonite coated ZnSe IRE.
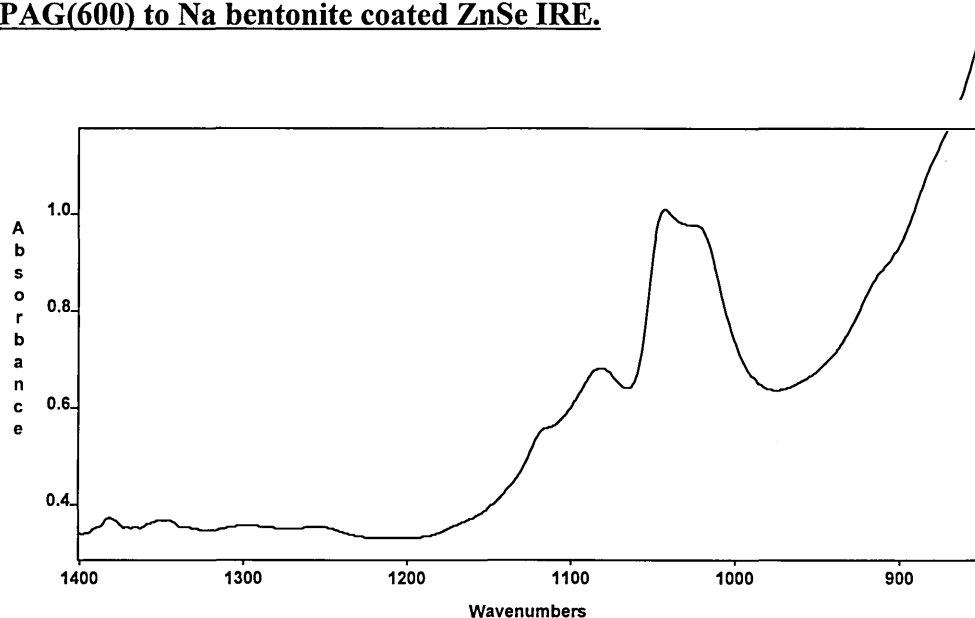
The shape of the infrared spectrum of the Na bentonite film contacted with 50 gdm^{-3} PAG(600) in the region between 1400 and 850 cm^{-1} is almost identical to that observed in figure 5.3.4a of the ATR spectrum of an aqueous bentonite suspension. However, two small differences exist between the two spectra. Firstly, the spectrum of water has not been subtracted from the spectrum shown in figure 7.3.5.2b and secondly, the presence of bands at 1381 and 1350 cm^{-1} attributed to the ν(OC) and ν(CH$_2$) wagging modes of PAG(600) can be detected in figure 7.3.5.2b due to the presence of PAG(600) in the system.

The intensity of the main Si-O absorption band maxima seen in figure 7.3.5.2b is much lower than observed in the supported film prior to addition of polymer solution (figure 7.3.5.1a). It may be assumed therefore, that the film has become detached from the surface of the ATR prism where it is sampled by the evanescent field. Evidently, water has been able to fully hydrate the Na bentonite film so that the solution comprises 50 gdm^{-3} PAG(600) and fully dispersed Na bentonite. Although a solution concentration of 50 gdm^{-3} PAG(600) was previously observed to stabilise a free standing film of Na bentonite, this does not take into account the experimental differences in this ATR study where the volume of solution is much less (in the 2 cm^3 volume of solution used only 0.00017 moles of PAG exist) and the mass of bentonite much greater than used in the studies using bentonite free standing films. The stability of the Na bentonite film/PAG(600) system has been proved to be controlled by the critical number of polymer moles per unit volume in solution:clay loading ratio. Clearly, the number of moles of PAG in solution is insufficient to stabilise the film. For this reason, and because polyethylene glycol does not stabilise clay mineral films [1] the findings of Billingham et al [204] seem hard to believe.

7.3.5.3 Adsorption onto Na bentonite films supported on a ZnSe ATR prism of polyalkyl glycol from a dilute aqueous electrolytic solution.

Despite the inability of the 50 gdm^{-3} PAG(600) solution to stabilise the Na bentonite films supported on the ZnSe IRE, stabilisation was observed *in-situ* in the presence of a 50 gdm^{-3} PAG(600)/KCl solution by the ATR method. This is not surprising as the stability of Na bentonite free standing films is not controlled by the polymer concentration in solution alone and that the presence of KCl inhibits film destabilisation. Figure 7.3.5.3a shows the infrared spectra 5 minutes and 2 hours after addition of 50 gdm^{-3} PAG(600)/10% KCl solution to Na bentonite films coated ZnSe ATR optics in the Si-O stretching region.

Figure 7.3.5.3a infrared spectra 5 minutes and 2 hours after addition of 50 gdm^{-3} PAG(600)/10% KCl solution to Na bentonite coated ZnSe IRE.
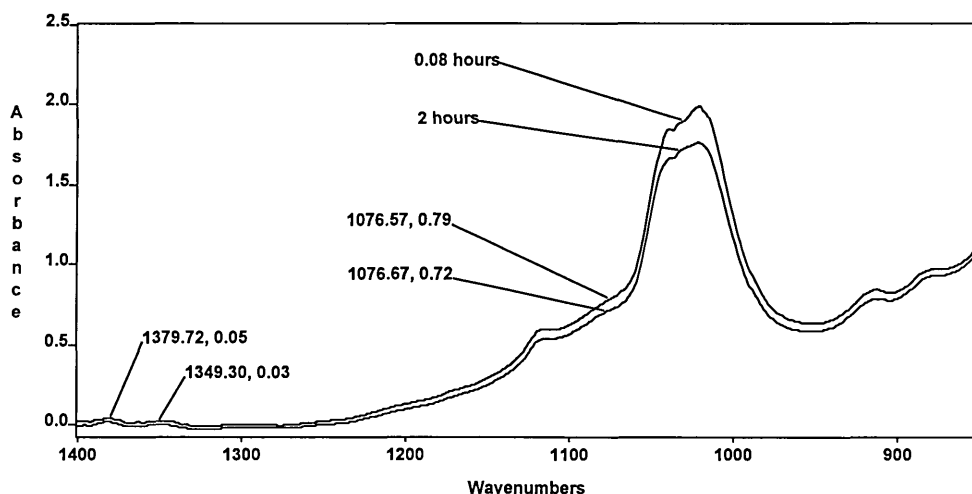
The extent to which water dominates the spectra is considerably reduced in the presence of KCl. Indeed, the bands at 918 cm^{-1} (due to structural OH deformation) and 887 cm^{-1} (attributed also to structural OH deformation) could not be located in figure 7.3.5.2b but are quite clear in figure 7.3.5.3a. Additionally, the intensity of the absorbance bands associated with Si-O stretching modes are extremely high even after 120 minutes contact. This clearly indicates that the Na bentonite film remains predominantly intact at the surface of the ATR prism. Although the small reduction in intensity of the main maxima between 5 and 120 minutes does seem to indicate a small reduction in the amount of bentonite at the surface over the course of the experiment.

Despite the film being stabilised at the surface of the ATR crystal however, the shape of the Si-O spectral region is unusual, exhibiting a shoulder at ~1076 cm^{-1}. This band may be due to the absorption band attributed to the C-O-C stretching mode of polyalkyl glycol (found at 1082 cm^{-1} in the spectrum of PAG(600) diluted to 40% by weight) as PAG(600) adsorbs between the clay platelets nearer to the surface of the IRE, to be sampled by the evanescent field.

338

Indeed, evidence of PAG(600) can be seen by the presence of the bands at 1380 and 1349 cm^{-1} attributed to $v(OC)$ and $v(CH_2)$ wagging modes, respectively. It may also be due to perturbations of the silicate lattice by the exchange cation having adsorbed on it polyalkyl glycol. The position of the shoulder at 1076 cm^{-1} in the spectra after both 5 minutes and 120 minutes contact of the Na bentonite film with the PAG(600)/ 10% KCl solution is very similar to that seen in figure 5.3.8a of homoionic Ca^{2+} bentonite suspended in water. The position of this band for the Ca^{2+} bentonite was explained in terms of the Ca^{2+} ion existing close to the surface of the clay mineral in aqueous suspension. Na^+ and K^+ show bands at even higher frequency as they are able to hydrate more easily than Ca^{2+} and be fully removed from the clay surface. When aqueous bentonite suspensions dry or are flocculated by electrolyte then this band shifts to low frequency (chapter 5). Consequently, the observed position of this band in figure 7.3.5.3a, may be due to flocculating electrolyte on a partially dispersed Na bentonite film, or even due to the Na^+ or K^+ cations being held close to the silicate surface, but not able to sit in the di-trigonal cavity, due to adsorption of polyol around them.

7.4.   Conclusions

Information has been obtained which helps to explain the nature of the interaction of polyalkyl glycol with Na and K bentonite films and the mechanism of bentonite film stabilisation. Polyalkyl glycol has a high affinity for Na and K SWy-1 bentonite and the interaction appears to be via a water bridge between the polymer and exchange cation on the clay mineral; i.e. between the polyalkyl glycol and the first hydration shell of water surrounding the cation. The mechanism involves the dehydration of loosely bound water in the interlayer region from the clay surface and the outer hydration shells around the cation, thus providing the thermodynamic (entropic) driving force for adsorption. The subsequent

stabilisation of the film depends on the ability of the components in the system to prevent rehydration. This depends on the nature, molecular weight and number of moles per unit volume of the polyalkyl glycol, the clay loading, the nature of the exchange cation on the clay and the nature and presence of electrolyte in solution.

In the absence of other components in solution, X-ray diffraction has shown that polyalkyl glycol will stabilise Na bentonite films which are immersed within it by forming two organic layers in the space between the clay platelets. The formation of a PAG double layer (and hence stability) depends critically on the ratio of the concentration of polymer (number of moles per unit volume) in solution:clay loading (in the form of the film). In this work it was found that a minimum critical polyalkyl glycol solution concentration of 0.08 moldm^{-3} was required to stabilise Na bentonite clay films, weighing between 5 and 7 mg. Attention must therefore be paid to the molecular weight of the polymer used since at identical w/w loadings, a higher molecular weight polymer may be unable to stabilise the film as fewer moles of polymer would be present per unit volume. Consequently, PAG(600) was able to stabilise the clay film at solution concentrations of 50 and 100 gdm^{-3}, PAG(1200) was able to stabilise the film at a solution concentration of 100 gdm^{-3} and PAG(1700) was not observed to stabilise the films.

Kinetic measurements (using FTIR and X-ray diffraction) have also indicated that the relative rates of adsorption of large and small PAG molecules, is also important to the stabilisation mechanism. Larger molecules take a little longer to diffuse and adsorb to the surface of the clay and so at very short times the film may not be stable.

In-situ measurements using FTIR-ATR support the theory that, in the absence of other components in solution, the number of moles of polymer per unit volume is critical to film stability. Indeed, supported Na bentonite films could not be

stabilised by 50 gdm^{-3} polyalkyl glycol solution alone as it introduces only 0.00017 moles of PAG(600) in the 2 cm^3 trough of the Squarecol cell, which is insufficient to facilitate stabilisation. In fact, the infrared spectra showed that the bentonite which comprises the film became hydrated and existed as an aqueous suspension of dispersed bentonite (losing contact with the surface of the ATR crystal).

In such systems, the ability of polyalkyl glycol to stabilise the film is related to the amount adsorbed and the ability of the clay-polymer complex to resist rehydration of the exchange cation. Since if the cation is able to hydrate, then the clay will swell and disperse.

It is also possible to inhibit swelling of the clay by introducing an electrolyte into the polymer solution. This causes the electrical double layer to collapse and causes flocculation of the clay. Infrared and X-ray diffraction data of Na bentonite films immersed in polyol solutions in the presence of KCl clearly show the effect of the electrolyte. The ratio of the number of moles of PAG per unit volume:clay loading is not the limiting factor controlling Na bentonite film stabilisation as they are observed to be stable at solution concentrations as low as 0.0017 moldm^{-3}, i.e. at all concentrations (between 1.0 and 50 gdm^{-3}) of all the molecular weights (between 600 and 1700 gmol^{-1}) polyalkyl glycol samples studied. Similar, enhanced stabilisation of such clay films has also been observed in PAG(600) solution concentrations as low as 0.0017 moldm^{-3}, when the strongly flocculating electrolyte is NaCl.

FTIR-ATR evidence is consistent with these findings. Indeed, the intensity of the main ν(Si-O) stretching bands remained relatively unchanged over the timescale of the experiment (2 hours) when 50 gdm^{-3} PAG(600)/ 10% KCl solution was introduced to the 2cm^3 trough of the Squarecol cell.

The formation of the clay polymer complexes has been shown using X-ray diffraction and infrared spectroscopy to occur in distinct phases.

1. The mechanism of stabilisation is believed to be via dehydration of the clay (this provides the thermodynamic driving force for adsorption), by removal of outer sphere water of hydration around the exchange cations. The infrared spectra clearly show that water has been removed from the clay on contact with the polymer and in the FTIR-ATR study of adsorption of pure polyalkyl glycol onto the clay film water desorption was observed *in-situ*

2. Following the desorption of water there is an almost instantaneous adsorption of polymer. Infrared evidence indicates that the polyalkyl glycol molecules adsorb to the clay and the X-ray diffraction evidence indicates that the adsorption occurs between the clay platelets. The interaction is thought to be via hydrogen bonding (water bridges) to the inner sphere water of hydration around the cations (denoted by an increase in the d-spacing). The position of the H-O-H bending mode of water in the spectra of clay films contacted with polyalkyl glycol has been observed shifted to high frequency compared to its position in the spectrum of the untreated clay. This has been attributed to the stiffening of the H-O-H bending mode of water in the inner hydration sphere surrounding the exchange cation as it hydrogen bonds to the polyalkyl glycol.

3. Subsequently, there is a slow diffusion controlled process which involves the consolidation of the first organic layer on vacant sites around the cation and then, if the clay is able to swell sufficiently (i.e. in the presence of Na^+ ions), the formation of the second layer. The second layer has been observed to be weakly bound in adsorption studies on dispersed montmorillonite clays [3] and would be expected to be easily removed by heating or repeated washing. The ease of removal in such experiments may be related to the ease of intercalation (direct

adsorption may not be necessary for the polymer to reside between the clay platelets). In these studies however, the second layer is not expected to be so easily removed as a driving force (possibly enthalpic) must exist for the polymer to adsorb into the confined geometry of the interlayer.

The process of adsorption of the second polymer layer is in competition with the process of exchange cation rehydration by desorbed water and other water present in solution. The readsorption of water in the interlayer has been observed *in-situ* to be almost exclusively at the exchange cation using FTIR ATR spectroscopy. The position of the hydrogen bonded OH stretching mode in the spectra of free standing bentonite films immersed in PAG solution is shifted form its position in untreated bentonite. The extent of the shift generally depends on the amount of polymer adsorbed and consequently, the extent to which the polymer restricts re hydration of the interlayer.

The extent of hydration in the interlayer can also be established from the position of the $v(OC)$ band of the PAG molecule. The position of this band has been observed to be progressively shifted to high frequency in the spectra of dilutions of polyalkyl glycol in water and aqueous KCl solutions (down to 40% weight dilutions). This has been attributed to the interaction of water with the ether oxygen atoms of the polyalkyl glycol molecule.

Consequently, when PAG concentrates between the clay platelets, the band will shift from its position in the spectrum of the diluted PAG to reflect the increased number of PAG-PAG interactions. Hence, when PAG adsorbs onto clay films the position of the $v(OC)$ band reflects the restriction of water to the (found between 1374 and 1377 cm^{-1}). However, when PAG adsorbs onto fully hydrated and dispersed bentonite, water and polymer may exist together between the platelets

(the system does not need to be stabilised like a clay film) and the position of the band (at ~1380 cm^{-1}) reflects the relative number of PAG- H_2O interactions.

In the presence of K^+ in solution, the respective shape and nature of the diffraction profiles appears to indicate an additional further stabilisation mechanism. Kinetic measurements have revealed that in addition to dehydration of the system, cation exchange of K^+ for Na^+ may also occur initially in these systems. The enhanced stabilising effect of the K^+ cation has also been observed in the stabilisation of K+ bentonite films over the whole range of concentrations studied.

8. COMPETITIVE ADSORPTION OF POLYALKYL GLYCOL AND POLYACRYLAMIDE ON BENTONITE

8.1. Introduction

Thus far, the adsorption of individual polymer components such as polyacrylamide (chapter 6) and polyalkyl glycol (chapter 7) onto bentonite has been studied in some detail. One of the interesting features of the adsorption behaviour of both polymers has been the influence of other components in solution. Indeed, the effect of dissolved electrolyte in solution has been found to significantly affect the amount of polymer adsorbed and the stability of free standing films contacted with aqueous polymer solutions.

The effect of multiple components in solution on the adsorption behaviour of any other single component is extremely important, as water based oil well drilling fluids are multicomponent systems containing various polymer additives, minerals and dissolved salts. Consequently, it is imperative to determine the adsorption behaviour of any single polymer component from a solution containing several components [1, 4, 5, 9].

As a result, a preliminary study into the adsorption of polymer onto pre-formed free standing bentonite films from aqueous solution containing both polyacrylamide and polyalkyl glycol has been undertaken in order to establish the shale inhibition properties of such polymer systems. It should be noted that the effect of electrolyte on such stabilisation mechanisms has not been evaluated here, but could form the basis of any future work.

Infrared spectroscopy and X-ray diffraction have been used to determine the adsorption properties of one polymer in the presence of another. This is

extremely important in determining the mechanisms by which these fluids might stabilise the reactive shales which comprise the wellbore.

6.2.   Experimental

8.2.1   Materials

Homoionic Na^+ SWy-1 bentonite was used as outlined in section 7. 2.1. Sections 6.2.1 and 7.2.1 outline the use of polyacrylamide and polyalkyl glycol respectively.

8.2.2.   Spectroscopy

8.2.2.1   Transmission -   Free standing films

Free standing films were prepared and used by the method outlined in sections 6.2.2.1 and 7.2.2.1. Here, however, films were immersed in mixed aqueous polyalkyl glycol (molecular weight 600 and 1700 $gmol^{-1}$) and polyacrylamide (molecular weight 7000k $gmol^{-1}$) solutions overnight (for a minimum of 12 hours). The solutions contained polyacrylamide at concentrations 5.0, 3.3 and 1.0 gdm^{-3} and polyalkyl glycol at concentrations 50, 5.0, 2.5 and 1.0 gdm^{-3}. The infrared transmission spectra were acquired as outlined in sections 6.2.2.1 and 7.2.2.1.

8.2.2.2   ATR spectroscopy - Bentonite film

Na bentonite films were prepared on the surface of the ZnSe Squarecol ATR prism as outlined in section 4.4.4. The cell was assembled and infrared spectra acquired after filling the trough with 2 cm^3 mixed solution containing 50 gdm^{-3}

polyalkyl glycol (Mw 600 gmol^{-1}) and 5.0 gdm^{-3} polyacrylamide (Mw 7000k).

The spectra were acquired at 5 minute intervals as outlined in section 7.2.2.3.

8.2.2.3.   X-ray diffraction

Basal spacings of Na bentonite films after immersion in solution of aqueous

polyalkyl glycol/polyacrylamide were measured as outlined in sections 6.2.2.4

and 7.2.2.5.

8.3   Results and Discussion

8.3.1   X-ray diffraction.

As previously, X-ray diffraction was used to analyse the clay-polymer

complexes prepared from Na$^+$ SWy-1 montmorillonite free standing films and

polymer adsorbed from aqueous solutions containing both polyacrylamide and

polyalkyl glycol. These experiments provide information regarding the nature of

the adsorbed species and the site of adsorption, i.e. whether the polymer

adsorption occurs between clay platelets.

It is important to consider the effects of the high and low molecular weight

polyalkyl glycol separately as they have been shown, in chapter 7, to exhibit

slightly different stabilisation characteristics.

It was shown previously, in the absence of electrolyte, that Na bentonite films

were stabilised only by polyalkyl glycol (Mw 600) solutions at PAG(600)

concentrations $\geq$50 gdm^{-3} (section 7.3.3.1). Similarly, in the absence of

electrolyte Na bentonite films were stabilised only by mixed polyalkyl

glycol/polyacrylamide polymer solution which contained PAG(600) at a

concentration of 50 gdm^{-3}. The concentration of polyacrylamide appears not to affect the stabilisation process.

Figure 8.3.1a shows the X-ray diffraction traces of Na bentonite films which remained intact following immersion in solutions containing 50 gdm^{-3} polyalkyl glycol (Mw 600) and 5.0, 3.3 and 1.0 gdm^{-3} polyacrylamide (Mw 7000k). Table 8.3.1a shows the d-spacings corresponding to the diffraction maxima in these traces.

Figure 8.3.1a Diffraction traces of Na$^+$ SWy-1 bentonite films, intact, following immersion in PAG(600)/PAM(7000k) solutions at various concentrations.

Table 8.3.1a d-spacings from diffraction maxima in figure 8.3.1.1a.

50 gdm^{-3} PAG(600)/ xPAM(7000k) concentration	d-spacing
x= 5.0	17.2
x= 3.3	17.4
x= 1.0	17.4

Many of the features of the diffraction traces such as their shape their smoothness, the presence of higher orders of reflection and the position of the maxima (the d-spacings) are very similar to those observed in section 7.3.3.1 for PAG(600) adsorption onto Na bentonite films in the absence of any other additives. This would tend to suggest that the principle component in the solution which facilitates stabilisation of the free standing bentonite film is the polyalkyl glycol.

In this mixed polymer study, the diffraction profiles have maxima which correspond to d-spacings of ~17.3Å which has been identified as two flat lying polyalkyl glycol layers between the platelets. Additionally, the concentrations of polymer required to stabilise the film (>50 gdm^{-3} polyalkyl glycol) appears to be independent of polyacrylamide (Mw 7000k) concentration which would indicate that the polyacrylamide has no involvement in the stabilisation process. This does not seem unlikely when one considers the relative abilities of each molecule to stabilise the clay films on their own. Polyacrylamide (Mw 7000k) alone in solution at concentrations ≤5 gdm^{-3} cannot stabilise free standing films of bentonite, whereas ≥50 gdm^{-3} polyalkyl glycol (Mw 600) can (chapters 6 and 7). The relative sizes of the molecules and the relative numbers of moles per unit volume of solution must also be considered. The polyacrylamide (Mw

7000k) molecule is several orders of magnitude larger than the polyalkyl glycol (Mw 600) molecule so as a result will be able to adsorb much more quickly than the amide polymer. This ties up adsorption sites on the clay mineral which polyacrylamide might adsorb to (both polymers adsorb via water bridges to water directly bound to the exchange cation in the interlayer space) which would inhibit adsorption. The adsorbed polyalkyl glycol might then present a hydrophobic surface to the polyacrylamide molecules in solution further inhibiting adsorption of PAM [168]. Additionally, it should be noted that there are significantly more moles of polyalkyl glycol (Mw 600) in solution (2×10^{-3} moldm^{-3} at its maximum concentration) compared to only 7×10^{-7} moldm^{-3} of PAM (7000k) at its highest solution concentration (5 gdm^{-3}).

The stabilisation of Na$^+$ SWy-1 bentonite films by solutions containing PAG(1700) and PAM(7000k) however, does not follow the behaviour observed in the presence of polyalkyl glycol (molecular weight 1700 gmol^{-1}) alone.

Previously, in section 7.3.3.1, it was shown that Na bentonite films were not stabilised in the presence of PAG(1700) alone. All films immersed in such solutions (at concentrations ≤100 gdm^{-3}) collapsed and could not be retained for analysis. Indeed, in general, most films immersed in mixed solutions containing both PAG(1700) and PAM (7000k) collapsed. However, Na$^+$ SWy-1 bentonite films were stabilised in solutions containing concentrations 50 gdm^{-3} PAG(1700) and ≤3.3 gdm^{-3} PAM(7000k). Figure 8.3.1b shows the diffraction traces of Na bentonite films which remained intact following immersion in solutions containing 50 gdm^{-3} polyalkyl glycol (Mw 1700) and 3.3 and 1.0 gdm^{-3} polyacrylamide (Mw 7000k). Table 8.3.1b shows the d-spacings corresponding to the diffraction maxima.

Figure 8.3.1b Diffraction traces of Na$^+$ SWy-1 bentonite films intact following immersion in PAG(1700)/PAM(7000k) solutions at various concentrations.

Intensity (counts s-1)

50 gl-1 PAG(1700)/3.3 gl-1 PAM(7000k)/Na film

50 gl-1 PAG(1700)/1.0 gl-1 PAM(7000k)/Na film

2θ

Table 8.3.1b d-spacings from diffraction maxima in figure 8.3.1.1b.

50 gdm^{-3} PAG(600)/ x gdm^{-3} PAM(7000k) concentration	d-spacing (Å)
x= 3.3	17.1
x= 1.0	17.2

This result is quite unexpected and clearly indicates that the presence of polyacrylamide (7000k) at relatively low solution concentration, provides additional stability to the Na bentonite film, which PAG(1700) is unable to offer alone. This would seem to indicate that the polyacrylamide molecule must be involved in the adsorption process. This tends to agree with the findings of other

workers [1, 4, 9] who have indicated that glycol in the presence of PHPA has a greater propensity for stabilising reactive shales which comprise the borehole than glycol alone.

It is unclear however, from these findings, what the involvement of polyacrylamide is, and in fact, what the exact nature of the adsorbed species is. The smooth, sharp traces, evidence of higher orders of reflection and the position of the diffraction maxima tend to suggest that the adsorbed species is more likely to be polyalkyl glycol. In such circumstances the interlayer spacing corresponds to the formation of a two layer organic complex in the region between the clay platelets. However, PAG (1700) does not stabilise Na bentonite films on its own in solution and the observed d-spacings are only slightly higher than those observed for PAM(7000k) adsorbed onto dispersed Na bentonite (section 6.3.2.1) of ~16.6Å.

Clearly, solutions containing polyacrylamide (Mw 7000k) at concentrations $\leq 3.3 \text{gdm}^{-3}$ appears to enhance the stabilisation of Na bentonite films in the presence of 50 gdm^{-3} polyalkyl glycol (Mw 1700). Similar improved stabilisation is not observed when the polyacrylamide is added to solutions containing polyalkyl glycol (Mw 600). This is not to say that it does not exhibit its stabilising mechanism in such solutions it may be that its magnitude is small compared to the magnitude of stabilisation provided by PAG(600). No direct conclusions may be made form these results however, infrared analysis of these bentonite film-polyacrylamide complexes (section 8.3.2) provides further evidence of the nature of the adsorbed species and the nature of their interaction with the clay platelets

8.3.2   Transmission infrared spectroscopy.

In order to establish the mechanism of enhanced stabilisation by PAM(7000k) the infrared spectra of films stabilised in solutions containing PAG(600) and PAG(1700) have been acquired. Again, it is instructive to consider the two molecular weights of glycol molecule separately as they exhibit slightly differing stabilisation characteristics.

Firstly, consider the stabilisation of Na bentonite films by PAG(600) in the presence of PAM(7000k). From section 7.3.4.2 it is clear that an aqueous solution containing 50 gdm^{-3} PAG(600) alone stabilises Na bentonite films by dehydrating the clay and the subsequent formation of two polymer layers between the clay platelets. It seems likely that in aqueous solutions containing 50 gdm^{-3} PAG(600) and PAM (7000k) at concentrations between 1.0 and 5.0 gdm^{-3} (section 8.3.1) stabilisation is by the same mechanism.

The infrared evidence would tend to suggest this. Comparison of figures 7.3.4.2a and figure 7.3.4.2b (the infrared spectra between 4000 and 2600 cm^{-1} and 2000 and 1300 cm^{-1} respectively, of Na bentonite films stabilised by 50 gdm^{-3} PAG(600) solution) with figures 8.3.2a and 8.3.2b the analogous spectra for the Na bentonite films stabilised by 50 gdm^{-3} PAG(600) solution containing between 1.0 and 5.0 gdm^{-3} PAM(7000k) shows this quite clearly.

Figure 8.3.2a Infrared spectra of Na bentonite films, intact, after immersion in 50 gdm^{-3} PAG(600) and PAM(7000k) solutions at various concentrations.

Figure 8.3.2b Infrared spectra of Na bentonite films, intact, after being placed in 50 gdm^{-3} PAG(600) and PAM(7000k) solutions at various concentrations.

As in figures 7.3.4.2a and 7.3.4.2b, the films immersed in mixed PAG(600) PAM(7000k) solution exhibit absorbance ratios A(3630)/A(3440) and A(3630)/A(1640) significantly higher than observed in a homoionic Na bentonite film before immersion. Table 8.3.2a displays the absorbance ratios

A(3630)/A(3440) A(3630)/A(1640) and A(3630)/A(2932) from the infrared spectra shown in 8.3.2a and 8.3.2b.

Table 8.3.2a Absorbance ratios from the spectra in figures 8.3.2a and 8.3.2b.

absorbance ratio	5.0 gdm^{-3} PAM(7000k)	3.3 gdm^{-3} PAM(7000k)	1.0 gdm^{-3} PAM(7000k)
3630/3440*	2.5	7.8	12.0
3630/1640*	4.8	7.8	12.0
3630/2932	1.5	1.6	1.7

* The actual position of these bands is dependent upon the extent of dehydration.

Clearly, the Na bentonite films become dehydrated (the ratios A(3630)/A(3440) and A(3630)/A(1640) in a homoionic Na bentonite film are 1.53 and 2.38, respectively) for the same reasons as explained in chapter 7. However, it would appear that the extent of dehydration is controlled by the concentration of PAM(7000k) in solution. As the concentration PAM(7000k) in solution becomes less so the amount of polymer adsorbed becomes slightly lower (indicated by the increase in the absorbance ratio A(3630)/A(2932)). This might indicate a slight reduction in the amount of adsorbed polyacrylamide or in the amount of adsorbed polyalkyl glycol. Concurrently, the extent of dehydration increases and as a result, the likelihood of film stabilisation increases. This is not surprising as dehydration was identified as the driving force and first key stage of polyalkyl glycol adsorption and hence film stabilisation by reducing the capability of the cations to rehydrate (chapter 7).

It seems likely that there is an additional mechanism which aids stabilisation of the film whether it be by inhibiting clay dispersion, by aiding dehydration or by enhancing polyalkyl glycol adsorption which appears to depend critically on an optimum amount of polyacrylamide in solution.

At low concentrations of polyacrylamide in solution, dehydration appears to be enhanced compared to when polyacrylamide is absent (table 7.3.4.2b). However, as the concentration of polyacrylamide in solution becomes higher, the film is able to become more hydrated and may not be stabilised as effectively. At higher concentrations of polyacrylamide in solution, the film becomes completely destabilised and disintegrates.

In section 6.3.3.4, evidence of polyacrylamide adsorption onto aqueous dispersions of mixed cation bentonite was observed in all spectral regions. Between 4000 and 2600 cm^{-1}, relatively strong bands attributed to the antisymmetric and symmetric stretching modes of NH_2 interacting with the water of hydration surrounding the exchange cations were observed at approximately 3475 and 3390 cm^{-1}, respectively. Similarly, between 2000 and 1300 cm^{-1}, the amide I band (attributed to the C=O stretching mode) is observed at around 1670 cm^{-1}, again due to hydrogen bonding interactions with water surrounding the exchange cation. However, in both figures 8.3.2a and 8.3.2b, there is no evidence of the direct interaction of polyacrylamide with the clay, indeed there is no evidence of polyacrylamide at all.

It may be possible that direct adsorption between the polyacrylamide and the Na bentonite does occur but that the complexity of the spectra masks identifying spectral features. The spectra contain bands attributable to bentonite and an organic component which could be polyacrylamide or polyalkyl glycol (or both) and consequently, the identifying polyacrylamide bands may not be observed.

This is however, hard to believe as some evidence of the relatively intense NH_2 antisymmetric and symmetric bands and the Amide I band would be expected in the spectra particularly after the clay is dehydrated, and the intensity of bands attributed to bentonite in the spectrum are significantly diminished. Hence, it is more likely that direct interaction between the polyacrylamide and the water of hydration around the exchange cations does not occur. This does not seem unlikely when one considers the relative sizes and concentrations of each polymer. The very small polyalkyl glycol molecules are competing with much larger polyacrylamide molecules for the same adsorption sites in a restricted geometry. Consequently, the ability of the polyacrylamide to access the adsorption sites will be significantly less compared to that of the polyalkyl glycol molecules. Additionally, the number of moles of polyalkyl glycol per unit volume of solution is significantly higher than that of polyacrylamide which will influence the adsorption behaviour as mentioned previously. Then once the polyalkyl glycol molecules have adsorbed the entropic driving force to replace the glycol polymer by the amide polymer will be much smaller than the driving force to replace water molecules by polyacrylamide molecules and the adsorption process is unlikely to proceed. Additionally, adsorbed polyalkyl glycol will present a hydrophobic surface to the polyacrylamide molecules which may well inhibit polyacrylamide adsorption [168].

Whilst the enhanced stabilising effect of PAM(7000k) can be seen when it is added to 50 gdm^{-3} PAG(600) solution, the effect is most notable in solutions containing PAG(1700). Figures 8.3.2c and 8.3.2d show the infrared spectra obtained between 4000 and 2600 cm^{-1} and 2000 and 1300 cm^{-1} respectively, of Na bentonite films stabilised by 50 gdm^{-3} PAG(1700) solutions containing PAM(7000k) at solution concentrations of 1.0 and 3.3 gdm^{-3}. As mentioned previously a solution containing 50 gdm^{-3} PAG(1700) and 5.0 gdm^{-3} PAM(7000k) did not stabilise the Na bentonite film.

Figure 8.3.2c FTIR spectra of Na bentonite films, intact, after immersion in 50 gdm⁻³ PAG(1700)/PAM(7000k) solutions at various concentrations.

Figure 8.3.2d FTIR spectra of Na bentonite films, intact, after immersion in 50 gdm⁻³ PAG(1700)/PAM(7000k) solutions at various concentrations.

The pattern here is almost identical to that observed previously in 50 gdm⁻³ PAG(600) solution. However, it would seem that the ability of the film to become hydrated when the concentration of PAM(7000k) in solution is 5.0 gdm⁻³ is sufficient to cause it to become destabilised. Otherwise, when the concentration of PAM(7000k) in solution is 3.3 or 1.0 gdm⁻³ the Na bentonite

films are dehydrated compared to that observed in homoionic bentonite prior to immersion (table 8.3.2c).

Table 8.3.2a Absorbance ratios from spectra in figures 8.3.2c and 8.3.2d.

absorbance ratio	3.3 gdm^{-3} PAM(7000k)	1.0 gdm^{-3} PAM(7000k)
3630/3440*	3.2	5.8
3630/1640*	3.2	5.8
3630/2932	1.8	2.4

* The actual position of these bands is dependent upon the extent of dehydration.

Again, as the concentration of polyacrylamide in solution decreases, so the extent of dehydration increases. In the absence of PAM(7000k) however, the films cannot be stabilised (section 6.3.3.2). This is further evidence to suggest that a critical polyacrylamide concentration in solution exists, above and below which, the film is able to become hydrated and disintegrate.

It is likely that, at high solution concentrations, the polyacrylamide is able to compete with the polyalkyl glycol more effectively for adsorption sites on the clay and will thus inhibit the stabilisation mechanism of polyalkyl glycol. This may be by flocculating the clay to such an extent that it prevents polyol ingress between the platelets or maybe by virtue of the viscosity it imparts to solution preventing polyalkyl glycol access to the clay. However, when the flocculating effect of the polyacrylamide in solution is not present (i.e. at zero polyacrylamide loading) the PAG(1700) is not able to prevent the clay platelets from becoming dispersed, and the film will become unstable.

As before, there is no evidence of polyacrylamide adsorption (direct interaction) on the clay. The spectra shown in figures 8.3.2c and 8.3.2d are very similar to those observed in figures 8.3.2a and 8.3.2b respectively. This would again tend to imply that the polyacrylamide does not directly interact with the clay and that the stabilisation it provides is purely by virtue of its concentration preventing the clay platelets from becoming highly dispersed (up to a critical concentration value above which it hinders the stabilisation mechanism).

8.3.3.   ATR infrared spectroscopy

Competitive adsorption of polyethylene glycol (PEG), polyacrylic acid (PAA) and polycation (FL15) on supported Na bentonite clay films has been studied previously, using FTIR-ATR [204]. In section 7.3.5.2, the adsorption of polyalkyl glycol from aqueous solution onto supported Na bentonite films were studied *in-situ* using FTIR-ATR spectroscopy. After only 5 minutes, the addition of a 50 gdm^{-3} solution of PAG(600) to the Squarecol cell containing Na bentonite coated optics caused the bentonite to become fully hydrated and to no longer exist as a robust film (figure 7.3.5.2b). It was not until the experiment was performed adding 10% KCl to the polyalkyl glycol solution that the film was induced to retain its integrity.

The experiment was repeated but PAM(7000k) solution was added to provide a concentration of 5.0 gdm^{-3} of polyacrylamide in the polyalkyl glycol solution as a replacement for KCl. Figure 8.3.3a shows the infrared spectra 5 minutes and 2 hours after addition of the 50 gdm^{-3} PAG(600)/5.0 gdm^{-3} PAM(7000k) solution to the Na bentonite coated on ZnSe ATR optics in the region between 1400 and 850 cm^{-1}.

Figure 8.3.3a ATR spectra of bentonite film contacted with 50 gdm^{-3} PAG(600)/5.0 gdm^{-3} PAM(7000k) solution at various times.

Clearly, after 5 minutes the bentonite has not become widely dispersed and the film appears to be stable. This is a marked improvement on the situation observed in the presence of PAG(600) only (figure 7.3.5.2b). However, after 2 hours the spectrum resembles that of hydrated bentonite (section 5.3.4) indicating that it has become dispersed and the film has lost its integrity. This seems to imply that polyacrylamide is not as efficient at enhancing stability as 10% KCl and supports previous findings in which 10% KCl enabled Na bentonite films to be stabilised even at very low (1.0 gdm^{-3}) solution concentrations of polyalkyl glycol. Polyacrylamide made an observable impact only in 50 gdm^{-3} polyalkyl glycol solutions.

Obviously, the concentration of polyacrylamide used has not been optimised to provide optimum stability and this test is quite subjective since the relative amounts of bentonite on the surface of the IRE in each case has not been quantified. However, it does seem that the film is stabilised for longer in the presence of polyalkyl glycol and polyacrylamide solution than it is in the presence of polyalkyl glycol solution alone.

8.4.   Conclusions

Polyacrylamide (Mw 7000k) in solution has been shown to aid the stabilisation of Na bentonite films immersed in polyalkyl glycol solutions. The effect is smaller than the enhanced stabilisation provided by electrolyte in such solutions and has only been physically observable in solutions containing polyalkyl glycol (Mw 1700). Infrared evidence however, suggests that the effect also manifests itself in solutions containing polyalkyl glycol (Mw 600) but its effect is too small compared to the effect of the low molecular weight glycol and is not observed.

The effectiveness of polyacrylamide (Mw 7000k) depends as critically on its concentration in solution. At low concentration, it appears highly effective at enhancing the stabilisation of the film by polyalkyl glycol. However, as the concentration increases then its ability to aid film stabilisation diminishes and it begins to cause the film to destabilise.

The presence of polyacrylamide has not been observed in the infrared spectra of films stabilised by solutions containing polyacrylamide and polyalkyl glycol. This indicates that there is no specific interaction between the clay and polyacrylamide when used at low concentrations. Indeed, the shape and the position of maxima in the X-ray diffraction traces appear to indicate that Na bentonite films were stabilised only by the adsorption of polyalkyl glycol between the platelets. This is not surprising considering the both the smaller size of the polyalkyl glycol molecule which is able to diffuse quickly to adsorption sites and access the constricted geometry between the platelets and its much higher solution concentration (number of moles per unit volume). This would tend to indicate that polyacrylamide is not directly involved in the adsorption. In fact, it is likely that the polyalkyl glycol adsorbs via hydrogen bonding to water

directly bound to adsorption sites around the exchange cation which leaves the polyacrylamide very few sites on which it might adsorb. It would also imply that the polyalkyl glycol presents a hydrophobic surface within the interlayer which inhibits both water rehydration and polyacrylamide adsorption.

It would appear that at low concentrations, polyacrylamide prevents the clay platelets from dispersing sufficiently on contact with the aqueous solution to inhibit destabilisation of the film. This might be by virtue of its ability to slightly flocculate the clay (prevent them dispersing prior to polyalkyl glycol adsorption) or the viscosity it imparts to the solution. It thus allows the clay to be dehydrated by adsorption of polyalkyl glycol and the film to be stabilised. Polyacrylamide appears not to hinder polyalkyl glycol adsorption at such low concentrations, however, as its concentration increases it may prevent adsorption by a number of mechanisms:

i) Increased flocculation of the Na bentonite, preventing polyalkyl glycol access to the confined geometry of the interlayer space.

ii) Slowing the rate of polyalkyl glycol adsorption which might decrease the rate of adsorption and therefore increase the time to stabilise the film. The clay platelets would then have more time to disperse and therefore rupture the film.

iii) Competing for the same adsorption sites (inner hydration sphere water surrounding exchange cations in the interlayer) therefore reducing the ability of polyalkyl glycol to adsorb, and allowing the platelets to disperse, destabilising the film.

Evidently, in water based drilling muds considerable attention must paid to the effectiveness of one polymer to stabilise the wellbore wall in the presence of another and how this changes as the concentrations of various components change as they are slowly depleted from the drilling fluid.

8.   COMPETITIVE ADSORPTION OF POLYALKYL GLYCOL AND POLYACRYLAMIDE ON BENTONITE

8.1.   Introduction

Thus far, the adsorption of individual polymer components such as polyacrylamide (chapter 6) and polyalkyl glycol (chapter 7) onto bentonite has been studied in some detail. One of the interesting features of the adsorption behaviour of both polymers has been the influence of other components in solution. Indeed, the effect of dissolved electrolyte in solution has been found to significantly affect the amount of polymer adsorbed and the stability of free standing films contacted with aqueous polymer solutions.

The effect of multiple components in solution on the adsorption behaviour of any other single component is extremely important, as water based oil well drilling fluids are multicomponent systems containing various polymer additives, minerals and dissolved salts. Consequently, it is imperative to determine the adsorption behaviour of any single polymer component from a solution containing several components [1, 4, 5, 9].

As a result, a preliminary study into the adsorption of polymer onto pre-formed free standing bentonite films from aqueous solution containing both polyacrylamide and polyalkyl glycol has been undertaken in order to establish the shale inhibition properties of such polymer systems. It should be noted that the effect of electrolyte on such stabilisation mechanisms has not been evaluated here, but could form the basis of any future work.

Infrared spectroscopy and X-ray diffraction have been used to determine the adsorption properties of one polymer in the presence of another. This is

extremely important in determining the mechanisms by which these fluids might stabilise the reactive shales which comprise the wellbore.

6.2. Experimental

8.2.1 Materials

Homoionic Na^+ SWy-1 bentonite was used as outlined in section 7. 2.1. Sections 6.2.1 and 7.2.1 outline the use of polyacrylamide and polyalkyl glycol respectively.

8.2.2. Spectroscopy

8.2.2.1 Transmission - Free standing films

Free standing films were prepared and used by the method outlined in sections 6.2.2.1 and 7.2.2.1. Here, however, films were immersed in mixed aqueous polyalkyl glycol (molecular weight 600 and 1700 $gmol^{-1}$) and polyacrylamide (molecular weight 7000k $gmol^{-1}$) solutions overnight (for a minimum of 12 hours). The solutions contained polyacrylamide at concentrations 5.0, 3.3 and 1.0 gdm^{-3} and polyalkyl glycol at concentrations 50, 5.0, 2.5 and 1.0 gdm^{-3}. The infrared transmission spectra were acquired as outlined in sections 6.2.2.1 and 7.2.2.1.

8.2.2.2 ATR spectroscopy - Bentonite film

Na bentonite films were prepared on the surface of the ZnSe Squarecol ATR prism as outlined in section 4.4.4. The cell was assembled and infrared spectra acquired after filling the trough with 2 cm^3 mixed solution containing 50 gdm^{-3}

polyalkyl glycol (Mw 600 gmol^{-1}) and 5.0 gdm^{-3} polyacrylamide (Mw 7000k).
The spectra were acquired at 5 minute intervals as outlined in section 7.2.2.3.

8.2.2.3.   X-ray diffraction

Basal spacings of Na bentonite films after immersion in solution of aqueous
polyalkyl glycol/polyacrylamide were measured as outlined in sections 6.2.2.4
and 7.2.2.5.

8.3   Results and Discussion

8.3.1   X-ray diffraction.

As previously, X-ray diffraction was used to analyse the clay-polymer
complexes prepared from Na$^+$ SWy-1 montmorillonite free standing films and
polymer adsorbed from aqueous solutions containing both polyacrylamide and
polyalkyl glycol. These experiments provide information regarding the nature of
the adsorbed species and the site of adsorption, i.e. whether the polymer
adsorption occurs between clay platelets.

It is important to consider the effects of the high and low molecular weight
polyalkyl glycol separately as they have been shown, in chapter 7, to exhibit
slightly different stabilisation characteristics.

It was shown previously, in the absence of electrolyte, that Na bentonite films
were stabilised only by polyalkyl glycol (Mw 600) solutions at PAG(600)
concentrations ≥ 50 gdm^{-3} (section 7.3.3.1). Similarly, in the absence of
electrolyte Na bentonite films were stabilised only by mixed polyalkyl
glycol/polyacrylamide polymer solution which contained PAG(600) at a

concentration of 50 gdm^{-3}. The concentration of polyacrylamide appears not to affect the stabilisation process.

Figure 8.3.1a shows the X-ray diffraction traces of Na bentonite films which remained intact following immersion in solutions containing 50 gdm^{-3} polyalkyl glycol (Mw 600) and 5.0, 3.3 and 1.0 gdm^{-3} polyacrylamide (Mw 7000k). Table 8.3.1a shows the d-spacings corresponding to the diffraction maxima in these traces.

Figure 8.3.1a Diffraction traces of Na$^+$ SWy-1 bentonite films, intact, following immersion in PAG(600)/PAM(7000k) solutions at various concentrations.

Table 8.3.1a d-spacings from diffraction maxima in figure 8.3.1.1a.

50 gdm^{-3} PAG(600)/ xPAM(7000k) concentration	d-spacing
x= 5.0	17.2
x= 3.3	17.4
x= 1.0	17.4

Many of the features of the diffraction traces such as their shape their smoothness, the presence of higher orders of reflection and the position of the maxima (the d-spacings) are very similar to those observed in section 7.3.3.1 for PAG(600) adsorption onto Na bentonite films in the absence of any other additives. This would tend to suggest that the principle component in the solution which facilitates stabilisation of the free standing bentonite film is the polyalkyl glycol.

In this mixed polymer study, the diffraction profiles have maxima which correspond to d-spacings of ~17.3Å which has been identified as two flat lying polyalkyl glycol layers between the platelets. Additionally, the concentrations of polymer required to stabilise the film (>50 gdm^{-3} polyalkyl glycol) appears to be independent of polyacrylamide (Mw 7000k) concentration which would indicate that the polyacrylamide has no involvement in the stabilisation process. This does not seem unlikely when one considers the relative abilities of each molecule to stabilise the clay films on their own. Polyacrylamide (Mw 7000k) alone in solution at concentrations $\leq$5 gdm^{-3} cannot stabilise free standing films of bentonite, whereas $\geq$50 gdm^{-3} polyalkyl glycol (Mw 600) can (chapters 6 and 7). The relative sizes of the molecules and the relative numbers of moles per unit volume of solution must also be considered. The polyacrylamide (Mw

7000k) molecule is several orders of magnitude larger than the polyalkyl glycol (Mw 600) molecule so as a result will be able to adsorb much more quickly than the amide polymer. This ties up adsorption sites on the clay mineral which polyacrylamide might adsorb to (both polymers adsorb via water bridges to water directly bound to the exchange cation in the interlayer space) which would inhibit adsorption. The adsorbed polyalkyl glycol might then present a hydrophobic surface to the polyacrylamide molecules in solution further inhibiting adsorption of PAM [168]. Additionally, it should be noted that there are significantly more moles of polyalkyl glycol (Mw 600) in solution ($2x10^{-3}$ moldm^{-3} at its maximum concentration) compared to only $7x10^{-7}$ moldm^{-3} of PAM (7000k) at its highest solution concentration (5 gdm^{-3}).

The stabilisation of Na$^+$ SWy-1 bentonite films by solutions containing PAG(1700) and PAM(7000k) however, does not follow the behaviour observed in the presence of polyalkyl glycol (molecular weight 1700 gmol^{-1}) alone.

Previously, in section 7.3.3.1, it was shown that Na bentonite films were not stabilised in the presence of PAG(1700) alone. All films immersed in such solutions (at concentrations $\leq$100 gdm^{-3}) collapsed and could not be retained for analysis. Indeed, in general, most films immersed in mixed solutions containing both PAG(1700) and PAM (7000k) collapsed. However, Na$^+$ SWy-1 bentonite films were stabilised in solutions containing concentrations 50 gdm^{-3} PAG(1700) and $\leq$3.3 gdm^{-3} PAM(7000k). Figure 8.3.1b shows the diffraction traces of Na bentonite films which remained intact following immersion in solutions containing 50 gdm^{-3} polyalkyl glycol (Mw 1700) and 3.3 and 1.0 gdm^{-3} polyacrylamide (Mw 7000k). Table 8.3.1b shows the d-spacings corresponding to the diffraction maxima.

Figure 8.3.1b Diffraction traces of Na⁺ SWy-1 bentonite films intact following immersion in PAG(1700)/PAM(7000k) solutions at various concentrations.


Table 8.3.1b d-spacings from diffraction maxima in figure 8.3.1.1b.

50 gdm^{-3} PAG(600)/ x gdm^{-3} PAM(7000k) concentration	d-spacing (Å)
x= 3.3	17.1
x= 1.0	17.2

This result is quite unexpected and clearly indicates that the presence of polyacrylamide (7000k) at relatively low solution concentration, provides additional stability to the Na bentonite film, which PAG(1700) is unable to offer alone. This would seem to indicate that the polyacrylamide molecule must be involved in the adsorption process. This tends to agree with the findings of other

workers [1, 4, 9] who have indicated that glycol in the presence of PHPA has a greater propensity for stabilising reactive shales which comprise the borehole than glycol alone.

It is unclear however, from these findings, what the involvement of polyacrylamide is, and in fact, what the exact nature of the adsorbed species is. The smooth, sharp traces, evidence of higher orders of reflection and the position of the diffraction maxima tend to suggest that the adsorbed species is more likely to be polyalkyl glycol. In such circumstances the interlayer spacing corresponds to the formation of a two layer organic complex in the region between the clay platelets. However, PAG (1700) does not stabilise Na bentonite films on its own in solution and the observed d-spacings are only slightly higher than those observed for PAM(7000k) adsorbed onto dispersed Na bentonite (section 6.3.2.1) of ~16.6Å.

Clearly, solutions containing polyacrylamide (Mw 7000k) at concentrations $\leq 3.3 gdm^{-3}$ appears to enhance the stabilisation of Na bentonite films in the presence of 50 gdm^{-3} polyalkyl glycol (Mw 1700). Similar improved stabilisation is not observed when the polyacrylamide is added to solutions containing polyalkyl glycol (Mw 600). This is not to say that it does not exhibit its stabilising mechanism in such solutions it may be that its magnitude is small compared to the magnitude of stabilisation provided by PAG(600). No direct conclusions may be made form these results however, infrared analysis of these bentonite film-polyacrylamide complexes (section 8.3.2) provides further evidence of the nature of the adsorbed species and the nature of their interaction with the clay platelets

8.3.2   Transmission infrared spectroscopy.

In order to establish the mechanism of enhanced stabilisation by PAM(7000k) the infrared spectra of films stabilised in solutions containing PAG(600) and PAG(1700) have been acquired. Again, it is instructive to consider the two molecular weights of glycol molecule separately as they exhibit slightly differing stabilisation characteristics.

Firstly, consider the stabilisation of Na bentonite films by PAG(600) in the presence of PAM(7000k). From section 7.3.4.2 it is clear that an aqueous solution containing 50 gdm^{-3} PAG(600) alone stabilises Na bentonite films by dehydrating the clay and the subsequent formation of two polymer layers between the clay platelets. It seems likely that in aqueous solutions containing 50 gdm^{-3} PAG(600) and PAM (7000k) at concentrations between 1.0 and 5.0 gdm^{-3} (section 8.3.1) stabilisation is by the same mechanism.

The infrared evidence would tend to suggest this. Comparison of figures 7.3.4.2a and figure 7.3.4.2b (the infrared spectra between 4000 and 2600 cm^{-1} and 2000 and 1300 cm^{-1} respectively, of Na bentonite films stabilised by 50 gdm^{-3} PAG(600) solution) with figures 8.3.2a and 8.3.2b the analogous spectra for the Na bentonite films stabilised by 50 gdm^{-3} PAG(600) solution containing between 1.0 and 5.0 gdm^{-3} PAM(7000k) shows this quite clearly.

Figure 8.3.2a Infrared spectra of Na bentonite films, intact, after immersion in 50 gdm⁻³ PAG(600) and PAM(7000k) solutions at various concentrations.

Figure 8.3.2b Infrared spectra of Na bentonite films, intact, after being placed in 50 gdm⁻³ PAG(600) and PAM(7000k) solutions at various concentrations.

As in figures 7.3.4.2a and 7.3.4.2b, the films immersed in mixed PAG(600)

PAM(7000k) solution exhibit absorbance ratios A(3630)/A(3440) and

A(3630)/A(1640) significantly higher than observed in a homoionic Na

bentonite film before immersion. Table 8.3.2a displays the absorbance ratios

A(3630)/A(3440) A(3630)/A(1640) and A(3630)/A(2932) from the infrared spectra shown in 8.3.2a and 8.3.2b.

Table 8.3.2a Absorbance ratios from the spectra in figures 8.3.2a and 8.3.2b.

absorbance ratio	5.0 gdm^{-3} PAM(7000k)	3.3 gdm^{-3} PAM(7000k)	1.0 gdm^{-3} PAM(7000k)
3630/3440*	2.5	7.8	12.0
3630/1640*	4.8	7.8	12.0
3630/2932	1.5	1.6	1.7

* The actual position of these bands is dependent upon the extent of dehydration.

Clearly, the Na bentonite films become dehydrated (the ratios A(3630)/A(3440) and A(3630)/A(1640) in a homoionic Na bentonite film are 1.53 and 2.38, respectively) for the same reasons as explained in chapter 7. However, it would appear that the extent of dehydration is controlled by the concentration of PAM(7000k) in solution. As the concentration PAM(7000k) in solution becomes less so the amount of polymer adsorbed becomes slightly lower (indicated by the increase in the absorbance ratio A(3630)/A(2932)). This might indicate a slight reduction in the amount of adsorbed polyacrylamide or in the amount of adsorbed polyalkyl glycol. Concurrently, the extent of dehydration increases and as a result, the likelihood of film stabilisation increases. This is not surprising as dehydration was identified as the driving force and first key stage of polyalkyl glycol adsorption and hence film stabilisation by reducing the capability of the cations to rehydrate (chapter 7).

It seems likely that there is an additional mechanism which aids stabilisation of the film whether it be by inhibiting clay dispersion, by aiding dehydration or by enhancing polyalkyl glycol adsorption which appears to depend critically on an optimum amount of polyacrylamide in solution.

At low concentrations of polyacrylamide in solution, dehydration appears to be enhanced compared to when polyacrylamide is absent (table 7.3.4.2b). However, as the concentration of polyacrylamide in solution becomes higher, the film is able to become more hydrated and may not be stabilised as effectively. At higher concentrations of polyacrylamide in solution, the film becomes completely destabilised and disintegrates.

In section 6.3.3.4, evidence of polyacrylamide adsorption onto aqueous dispersions of mixed cation bentonite was observed in all spectral regions. Between 4000 and 2600 cm^{-1}, relatively strong bands attributed to the antisymmetric and symmetric stretching modes of NH_2 interacting with the water of hydration surrounding the exchange cations were observed at approximately 3475 and 3390 cm^{-1}, respectively. Similarly, between 2000 and 1300 cm^{-1}, the amide I band (attributed to the C=O stretching mode) is observed at around 1670 cm^{-1}, again due to hydrogen bonding interactions with water surrounding the exchange cation. However, in both figures 8.3.2a and 8.3.2b, there is no evidence of the direct interaction of polyacrylamide with the clay, indeed there is no evidence of polyacrylamide at all.

It may be possible that direct adsorption between the polyacrylamide and the Na bentonite does occur but that the complexity of the spectra masks identifying spectral features. The spectra contain bands attributable to bentonite and an organic component which could be polyacrylamide or polyalkyl glycol (or both) and consequently, the identifying polyacrylamide bands may not be observed.

This is however, hard to believe as some evidence of the relatively intense NH_2 antisymmetric and symmetric bands and the Amide I band would be expected in the spectra particularly after the clay is dehydrated, and the intensity of bands attributed to bentonite in the spectrum are significantly diminished. Hence, it is more likely that direct interaction between the polyacrylamide and the water of hydration around the exchange cations does not occur. This does not seem unlikely when one considers the relative sizes and concentrations of each polymer. The very small polyalkyl glycol molecules are competing with much larger polyacrylamide molecules for the same adsorption sites in a restricted geometry. Consequently, the ability of the polyacrylamide to access the adsorption sites will be significantly less compared to that of the polyalkyl glycol molecules. Additionally, the number of moles of polyalkyl glycol per unit volume of solution is significantly higher than that of polyacrylamide which will influence the adsorption behaviour as mentioned previously. Then once the polyalkyl glycol molecules have adsorbed the entropic driving force to replace the glycol polymer by the amide polymer will be much smaller than the driving force to replace water molecules by polyacrylamide molecules and the adsorption process is unlikely to proceed. Additionally, adsorbed polyalkyl glycol will present a hydrophobic surface to the polyacrylamide molecules which may well inhibit polyacrylamide adsorption [168].

Whilst the enhanced stabilising effect of PAM(7000k) can be seen when it is added to 50 gdm^{-3} PAG(600) solution, the effect is most notable in solutions containing PAG(1700). Figures 8.3.2c and 8.3.2d show the infrared spectra obtained between 4000 and 2600 cm^{-1} and 2000 and 1300 cm^{-1} respectively, of Na bentonite films stabilised by 50 gdm^{-3} PAG(1700) solutions containing PAM(7000k) at solution concentrations of 1.0 and 3.3 gdm^{-3}. As mentioned previously a solution containing 50 gdm^{-3} PAG(1700) and 5.0 gdm^{-3} PAM(7000k) did not stabilise the Na bentonite film.

Figure 8.3.2c FTIR spectra of Na bentonite films, intact, after immersion in 50 gdm^{-3} PAG(1700)/PAM(7000k) solutions at various concentrations.

Figure 8.3.2d FTIR spectra of Na bentonite films, intact, after immersion in 50 gdm^{-3} PAG(1700)/PAM(7000k) solutions at various concentrations.

The pattern here is almost identical to that observed previously in 50 gdm^{-3} PAG(600) solution. However, it would seem that the ability of the film to become hydrated when the concentration of PAM(7000k) in solution is 5.0 gdm^{-3} is sufficient to cause it to become destabilised. Otherwise, when the concentration of PAM(7000k) in solution is 3.3 or 1.0 gdm^{-3} the Na bentonite

films are dehydrated compared to that observed in homoionic bentonite prior to immersion (table 8.3.2c).

Table 8.3.2a Absorbance ratios from spectra in figures 8.3.2c and 8.3.2d.

absorbance ratio	3.3 gdm^{-3} PAM(7000k)	1.0 gdm^{-3} PAM(7000k)
3630/3440*	3.2	5.8
3630/1640*	3.2	5.8
3630/2932	1.8	2.4

* The actual position of these bands is dependent upon the extent of dehydration.

Again, as the concentration of polyacrylamide in solution decreases, so the extent of dehydration increases. In the absence of PAM(7000k) however, the films cannot be stabilised (section 6.3.3.2). This is further evidence to suggest that a critical polyacrylamide concentration in solution exists, above and below which, the film is able to become hydrated and disintegrate.

It is likely that, at high solution concentrations, the polyacrylamide is able to compete with the polyalkyl glycol more effectively for adsorption sites on the clay and will thus inhibit the stabilisation mechanism of polyalkyl glycol. This may be by flocculating the clay to such an extent that it prevents polyol ingress between the platelets or maybe by virtue of the viscosity it imparts to solution preventing polyalkyl glycol access to the clay. However, when the flocculating effect of the polyacrylamide in solution is not present (i.e. at zero polyacrylamide loading) the PAG(1700) is not able to prevent the clay platelets from becoming dispersed, and the film will become unstable.

As before, there is no evidence of polyacrylamide adsorption (direct interaction) on the clay. The spectra shown in figures 8.3.2c and 8.3.2d are very similar to those observed in figures 8.3.2a and 8.3.2b respectively. This would again tend to imply that the polyacrylamide does not directly interact with the clay and that the stabilisation it provides is purely by virtue of its concentration preventing the clay platelets from becoming highly dispersed (up to a critical concentration value above which it hinders the stabilisation mechanism).

8.3.3.   ATR infrared spectroscopy

Competitive adsorption of polyethylene glycol (PEG), polyacrylic acid (PAA) and polycation (FL15) on supported Na bentonite clay films has been studied previously, using FTIR-ATR [204]. In section 7.3.5.2, the adsorption of polyalkyl glycol from aqueous solution onto supported Na bentonite films were studied *in-situ* using FTIR-ATR spectroscopy. After only 5 minutes, the addition of a 50 gdm^{-3} solution of PAG(600) to the Squarecol cell containing Na bentonite coated optics caused the bentonite to become fully hydrated and to no longer exist as a robust film (figure 7.3.5.2b). It was not until the experiment was performed adding 10% KCl to the polyalkyl glycol solution that the film was induced to retain its integrity.

The experiment was repeated but PAM(7000k) solution was added to provide a concentration of 5.0 gdm^{-3} of polyacrylamide in the polyalkyl glycol solution as a replacement for KCl. Figure 8.3.3a shows the infrared spectra 5 minutes and 2 hours after addition of the 50 gdm^{-3} PAG(600)/5.0 gdm^{-3} PAM(7000k) solution to the Na bentonite coated on ZnSe ATR optics in the region between 1400 and 850 cm^{-1}.

Figure 8.3.3a ATR spectra of bentonite film contacted with 50 gdm⁻³ PAG(600)/5.0 gdm⁻³ PAM(7000k) solution at various times.

Clearly, after 5 minutes the bentonite has not become widely dispersed and the film appears to be stable. This is a marked improvement on the situation observed in the presence of PAG(600) only (figure 7.3.5.2b). However, after 2 hours the spectrum resembles that of hydrated bentonite (section 5.3.4) indicating that it has become dispersed and the film has lost its integrity. This seems to imply that polyacrylamide is not as efficient at enhancing stability as 10% KCl and supports previous findings in which 10% KCl enabled Na bentonite films to be stabilised even at very low (1.0 gdm⁻³) solution concentrations of polyalkyl glycol. Polyacrylamide made an observable impact only in 50 gdm⁻³ polyalkyl glycol solutions.

Obviously, the concentration of polyacrylamide used has not been optimised to provide optimum stability and this test is quite subjective since the relative amounts of bentonite on the surface of the IRE in each case has not been quantified. However, it does seem that the film is stabilised for longer in the presence of polyalkyl glycol and polyacrylamide solution than it is in the presence of polyalkyl glycol solution alone.

8.4.   Conclusions

Polyacrylamide (Mw 7000k) in solution has been shown to aid the stabilisation of Na bentonite films immersed in polyalkyl glycol solutions. The effect is smaller than the enhanced stabilisation provided by electrolyte in such solutions and has only been physically observable in solutions containing polyalkyl glycol (Mw 1700). Infrared evidence however, suggests that the effect also manifests itself in solutions containing polyalkyl glycol (Mw 600) but its effect is too small compared to the effect of the low molecular weight glycol and is not observed.

The effectiveness of polyacrylamide (Mw 7000k) depends as critically on its concentration in solution. At low concentration, it appears highly effective at enhancing the stabilisation of the film by polyalkyl glycol. However, as the concentration increases then its ability to aid film stabilisation diminishes and it begins to cause the film to destabilise.

The presence of polyacrylamide has not been observed in the infrared spectra of films stabilised by solutions containing polyacrylamide and polyalkyl glycol. This indicates that there is no specific interaction between the clay and polyacrylamide when used at low concentrations. Indeed, the shape and the position of maxima in the X-ray diffraction traces appear to indicate that Na bentonite films were stabilised only by the adsorption of polyalkyl glycol between the platelets. This is not surprising considering the both the smaller size of the polyalkyl glycol molecule which is able to diffuse quickly to adsorption sites and access the constricted geometry between the platelets and its much higher solution concentration (number of moles per unit volume). This would tend to indicate that polyacrylamide is not directly involved in the adsorption. In fact, it is likely that the polyalkyl glycol adsorbs via hydrogen bonding to water

directly bound to adsorption sites around the exchange cation which leaves the polyacrylamide very few sites on which it might adsorb. It would also imply that the polyalkyl glycol presents a hydrophobic surface within the interlayer which inhibits both water rehydration and polyacrylamide adsorption.

It would appear that at low concentrations, polyacrylamide prevents the clay platelets from dispersing sufficiently on contact with the aqueous solution to inhibit destabilisation of the film. This might be by virtue of its ability to slightly flocculate the clay (prevent them dispersing prior to polyalkyl glycol adsorption) or the viscosity it imparts to the solution. It thus allows the clay to be dehydrated by adsorption of polyalkyl glycol and the film to be stabilised. Polyacrylamide appears not to hinder polyalkyl glycol adsorption at such low concentrations, however, as its concentration increases it may prevent adsorption by a number of mechanisms:

i) Increased flocculation of the Na bentonite, preventing polyalkyl glycol access to the confined geometry of the interlayer space.

ii) Slowing the rate of polyalkyl glycol adsorption which might decrease the rate of adsorption and therefore increase the time to stabilise the film. The clay platelets would then have more time to disperse and therefore rupture the film.

iii) Competing for the same adsorption sites (inner hydration sphere water surrounding exchange cations in the interlayer) therefore reducing the ability of polyalkyl glycol to adsorb, and allowing the platelets to disperse, destabilising the film.

Evidently, in water based drilling muds considerable attention must paid to the effectiveness of one polymer to stabilise the wellbore wall in the presence of another and how this changes as the concentrations of various components change as they are slowly depleted from the drilling fluid.

9. INTERACTIONS OCCURRING AT THE BENTONITE/ WATER/ POLYMER INTERFACE.

9.1. Conclusions

Oil based muds have many advantages over their water based counterparts (as outlined in chapter 1), the most important being that they are extremely adept at inhibiting shale hydration thus maintaining borehole stability. Whilst the drilling industry prefers to use oil based muds, water based drilling muds have been used extensively. This is mainly because water based drilling muds are relatively inexpensive and much more environmentally acceptable since they use less toxic components in their formulation. The obvious drawback to using water based muds is that they are able to easily hydrate, swell and disperse the shales which comprise the borehole causing it to become unstable.

The swelling of clay minerals by the hydration of exchangeable cations which reside in the interlayer is well known and in this study, perturbations in the structure of the silicate lattice have been observed using FTIR transmission, microscopy and ATR-FTIR spectroscopy. A band at ~1086 cm^{-1} in the infrared spectrum of fully hydrated bentonite attributed to the silicate stretching mode, perpendicular to the plane of the silicate lattice, is perturbed due to the proximity of the exchange cation to the silicate lattice. Consequently, since the nature of the exchange cation, the effect of flocculating electrolyte and the extent of hydration/dehydration of the clay has an enormous influence on the position of the cation between the platelets they also influence perturbations of the silicate lattice, and hence the position of the band.

Obviously, the nature of the exchange cation has an influence on the perturbations felt by the silicate lattice. The band was indeed more developed in

the spectrum of aqueous homoionic bentonite suspensions exchanged with cations (such as Na^+) which are more easily hydrated than in the spectrum of bentonite exchanged with cations which are less easily hydrated (Ca^{2+}). The Na^+ cations form extended double layers and has very little influence on the silicate lattice. The Ca^{2+} cation however, is unable to form extended double layers and therefore resides close to the silicate layer. Consequently, the position of the $\nu(Si-O)$ band in the spectrum of aqueous Ca bentonite is at lower frequency than in the spectrum of aqueous Na bentonite, indicating increased perturbation of the silicate lattice.

Dehydration of such aqueous homoionic bentonite suspensions also has an influence on the silicate lattice. As the exchange cations lose their hydration shells they will move closer to the surface of the bentonite platelets. Cations which are small (such as Na^+ and K^+) are able to settle into the di-trigonal cavity of the silicate surface and cause perturbation of the silicate lattice (observed as a shift of the $\nu(Si-O)$ to low frequency). Larger cations such as Ca^{2+} are unable to settle into the cavity and exist close to the platelet surface and consequently exert less influence on the silicate lattice.

Not surprisingly, flocculating electrolyte also causes the exchange cation to perturb the silicate lattice structure since increasing the ionic strength of an aqueous homoionic bentonite suspension will cause the double layer surrounding the exchange cation to collapse. This will cause the cation to approach the silicate surface and in the case of sufficiently small cations enter and settle in the di-trigonal cavity. This process has been observed by following the change in frequency of the silicate stretching mode perpendicular to the clay surface.

Clearly, the hydration and swelling of clay minerals which comprise underground shale deposits is a problem when a drilling fluid is used whose continuous phase is water. The swelling of the clay is related to the extent of hydration, nature of the exchange cations present in its interlayer and the presence of flocculating electrolyte (the performance of water based drilling fluids is highly dependent on the nature of underground salt deposit through which it drills). Hence, it is possible to inhibit swelling slightly by adding dissolved salts such as KCl and $CaCl_2$ which flocculate the clay by cation exchange (replacing cations which hydrate easily with cations which hydrate and swell the clay less easily) and also by collapsing the electrical double layer.

The effect of electrolyte is not sufficient to maintain borehole stability and, as a result, many polymeric additives such as polyacrylamide and polyalkyl glycols are added to the system. Knowledge of the mechanism and nature of the interaction between the polymer (which comprises the drilling fluid) and the clay mineral (which comprises the borehole and drilled cuttings) is therefore extremely useful in determining the effectiveness of a particular system at stabilising the wellbore.

In this study, polyacrylamide in aqueous solution has been shown to be wholly ineffective at stabilising thin films of bentonite, whether they be free standing (unsupported) or supported by a rigid structure. Indeed, measurements imply that in the presence of aqueous polyacrylamide solution, the bentonite film disperses before the polyacrylamide is able to interact. The presence of flocculating electrolyte in solution (10% wt KCl) made no improvement in the stabilisation. Evidently, polyacrylamide is not an additive which, when added to the water based drilling fluid, is considered likely to exhibit shale inhibition properties to any great extent.

Polyacrylamide does, however, appear to form highly flocculated gel structures with clay mineral material (chapter 6) which has been hydrated and dispersed from the clay mineral film. Consequently, polyacrylamide may help to enhance stabilisation of the wellbore (particularly in the presence of other polymers which stabilise the wellbore) and also to flocculate drilled cuttings.

In the absence of electrolyte, the ratio of solid clay:liquid in the suspension is critical to the adsorption behaviour since it controls the surface accessibility for polymer adsorption. The influence of exchange cation on this process has not fully emerged from this study but is expected to play an important role, as it will control the state of bentonite dispersion.

In the presence of electrolyte (10% wt KCl), adsorption of polyacrylamide is significantly reduced due to flocculation of the clay mineral by collapse of the double layer, the effect not surprisingly, being more noticeable for polyacrylamide of higher molecular weight. The effect of cation exchange (replacing cations which swell easily by K^+ which hydrates less therefore swells less) is also be important in such systems.

Polyacrylamide is easily able to intercalate between dispersed bentonite platelets in aqueous suspension and consequently increases the platelet separation (d-spacing) with increasing adsorbed amount. The mechanism of such adsorption has been shown in chapter 6 to be by polyacrylamide-water hydrogen bonding and that the polymer adopts a flat conformation (as is expected of a linear, flexible, nonionic polymer). Few polyacrylamide-polyacrylamide interactions are observed, particularly when the amount adsorbed is low (at low solution concentrations). The actual interaction is thought to be not by hydrogen bonding via water attached to the silicate layer of the clay mineral but via a water bridge between the polyacrylamide and the first hydration shell surrounding the

exchange cation in the interlayer space. At higher concentrations of polymer in solution the adsorption of polyacrylamide becomes more complicated with the polymer adsorbing in more coiled conformation. This is probably attributable to vast amounts of entrained polymer between the platelets which becomes lodged between the platelets and which is not actually adsorbed.

Clearly, polyacrylamide is a useful additive to use in a water based drilling fluid as it will enhance stabilisation of the wellbore and it will also flocculate dispersed cuttings, aiding their removal from the wellbore. Polyacrylamide is not, however, a very interesting additive. Polyalkyl glycols are much more interesting and they have been used quite extensively in the industry due to their ability to stabilise shale deposits effectively.

In chapter 7 the stabilisation of clay mineral films and hence underground shale deposits by polyalkyl glycol has been found to depend upon a wide range of variables in the system such as nature of the exchange cation, presence and nature of electrolyte ratio of concentration of polymer to clay loading in suspension. Whilst the actual mechanism of interaction has been established, changes in the variables can make quite important differences to the stabilisation.

The exact nature of the interaction appears to be via a water bridge between the main chain ether oxygen atoms on the polyol and the first hydration shell of water surrounding the exchange cation. The mechanism involves the dehydration of loosely bound water in the interlayer region from the clay surface and the outer hydration shells around the cation thus providing the thermodynamic (entropic) driving force for adsorption. The subsequent stabilisation of the film then depends on the ability of the components in the system to prevent rehydration.

In the absence of any other components, the stabilisation of a Na bentonite film is wholly dependent upon the ratio of concentration of polymer (number of moles per unit volume) to clay loading in suspension. In such circumstances the stabilisation of the film requires the formation of a double organic layer between the clay platelets. The formation of such a complex occurs from solutions containing at least 0.08 $moldm^{-3}$ in two distinct stages. Firstly, the almost instantaneous formation of the first polyol layer surrounding the cation by desorption of adsorbed water molecules, which is an entropy driven process. The second layer forms much more slowly and appears to be diffusion controlled. This layer is thought to be quite weakly bound and would be expected to be easily removed. The ability for this system to stabilise the film is related to the rate of formation of the complex, the flocculating effect of high concentrations of polyol and the ability of the polymer to resist rehydration of the exchange cations.

Film stabilisation is enhanced by the presence of K^+ cations. Indeed, homoionic K bentonite films, may be stabilised by as little as 0.0017 $moldm^{-3}$ polyalkyl glycol. The stabilisation of such systems is attributed to both the flocculating effect of the polymer and also the ease with which the exchange cation may hydrate ($Na^+ > K^+$) causing the platelets to swell and disperse the clay film. Hence the relative abilities of the Na^+ and K^+ cations to hydrate is extremely important to the stabilisation process.

The ability of the exchange cation to stabilise the film may also be enhanced by the presence of a highly flocculating electrolyte. In the presence of KCl, a Na^+ exchanged film may be stabilised at polymer concentrations as low as 0.0017 $moldm^{-3}$. In these systems, the mechanism of adsorption again appears to be by dehydration of the exchange cation. However, there may also be some influence from the exchange of K^+ ions in solution for Na^+ cations in the interlayer. The

effect of the highly flocculating medium also enhances stabilisation by collapsing the electrical double layer and preventing the platelets from dispersing. Similarly, in the presence of NaCl, Na bentonite films may be stabilised by the dehydration of the film and subsequent adsorption of the polymer to resist rehydration of the exchange cations at solution concentrations as low as 0.0017 moldm^{-3}. This is made possible by the enhanced effect of the flocculating electrolyte.

The rate at which the polymer adsorbs is also a major factor in the stabilisation of the film. Once the bentonite has been dehydrated, sufficient polymer must adsorb onto the clay to inhibit significant rehydration and subsequent dispersion of the platelets. As a result, the ability for a lower molecular weight polyol to stabilise the film will be greater than that of the higher molecular weight polymer because it is able to adsorb more quickly.

It is important to remember that water based drilling fluids are not single component systems and that the ability of a single component to enhance borehole stability may be enhanced by the presence of another [1, 4, 5, 9]. Indeed, as the effectiveness of polyalkyl glycol in stabilising the wellbore has been seen to be vastly improved in the presence of KCl, so its effectiveness in the presence of polyacrylamide is slightly improved.

The stabilising effect of polyacrylamide is not noticeable in the presence of polyalkyl glycol of low molecular weight as the polyol is able (in the concentration ranges studied here) to stabilise the film and hence the wellbore quite easily. Higher molecular weight polyols do not stabilise the wellbore quite so well and consequently, in their presence, polyacrylamide is able to enhance the stabilisation mechanism.

Polyacrylamide does not actually adsorb to the clay mineral surface in the presence of polyalkyl glycol. Several reasons for this exist. Firstly, the disparity of molecular weights allows the smaller polyol molecule to adsorb into the restricted geometry between the platelets in the clay film. The rate of this adsorption is much faster for such a small molecule (as observed in the absence of polyacrylamide). Secondly, once the polyol molecule has adsorbed it inhibits polyacrylamide adsorption both by occupying suitable adsorption sites on the clay and by presenting a hydrophobic surface to the polyacrylamide.

The ability for polyacrylamide to enhance stabilisation of clay mineral films (and hence wellbores) is critically controlled by its concentration in solution. At low concentrations it is either able to weakly flocculate the clay or its viscosity is able to inhibit the clay platelets from becoming dispersed. This allows polyalkyl glycol to adsorb and fully stabilise the clay film structure. At higher concentrations in solution it inhibits polyol adsorption by restricting its access to the clay interlayer. This might be by increasing the flocculation, slowing the rate of polyol adsorption or by competing more strongly for adsorption sites.

Evidently the effectiveness of the drilling fluid to stabilise the wellbore in such circumstances will be critically controlled by the concentration of polyacrylamide in solution. Clearly this is not a preferred situation, as the concentration of polyacrylamide in solution will constantly be changing as polymer is depleted from the fluid by adsorption to drilled cuttings. As a result, this particular system would not be employed alone as a drilling fluid. More likely would be that the low molecular weight polyalkyl glycol would be used along with the polyacrylamide as a system to more effectively stabilise the borehole [1, 4].

9.2.   Future Work

Clearly, X-ray diffraction and infrared spectroscopy are techniques which are extremely useful in characterising the 'where' and the 'how' of polymer adsorption onto clay minerals. Evidently then, the vast range of drilling fluid components and variety of underground formations leaves the scope for this work almost indefinable. Whilst the nature and composition of underground deposits will change from drilling site to drilling site, the options for changes to the polymer components is enormous. The advantages of using these techniques is that they may be applied to both simple and complex mixtures of polymers and by elucidating the adsorption characteristics of each individually, the effectiveness of one polymer in the presence of others (or other components in solution) may be established. These methods may then be used to evaluate the effect on the shale inhibition properties of slight changes to the polymer structure, beyond merely molecular weight differences as described in this work (it is known that PAG(600) exhibits much greater shale inhibition properties than PEG(600) [1]) or changes to other components such as electrolyte.

Evidently, the use of bentonite free standing films in this study has provided a good approximation to the wellbore in as much that it provides a measure of the ease with which a compacted clay may be dispersed. Of further interest would be to characterise this film and compare it to actual shale deposits or indeed to use very thin (microtombed) layers of shale deposits to mimic as closely as possible the actual wellbore conditions.

In addition to these techniques, it has been shown that FTIR-ATR is a powerful tool which may be applied to the study of stabilisation of the drilled wellbores. Consequently, for polymeric solutions (simple muds) which stabilise the wellbore and inhibit clay/shale dispersion (and hence a bentonite film supported

on the surface of an ATR prism) in the way that polyalkyl glycol has been shown to, the use of bentonite coated optics provides great scope for a wide range of *in-situ* studies.

Another of the principle advantages of using the Squarecol cell containing a bentonite coated ZnSe IRE, is that this particular cell is able to firstly, be heated, and secondly to have solution flowed through it. Such conditions would approximate much more closely to the physical action of the water based drilling fluid on the wellbore than the static case considered in this work.

[1] Cliffe S., Dolan B. and Reid P. I., Mechanism of Shale Inhibition by Polyols in Water Based Drilling Fluids, SPE International Symposium on Oilfield Chemistry, 28960, San Antonio, Texas, 1995.

[2] Bailey L., Keall M., Audibert A. and Lecourtier J., Effect of Clay/Polymer Interactions on Shale Stabilisation During Drilling, *Langmuir,* 10(5), 1544-1549, 1994.

[3] Rawson J. O., The Physicochemical Studies of Clay Polymer Interactions, PhD Thesis, Sheffield Hallam University, 1995.

[4] Amanullah Md., Marsden J. R. and Shaw H. F., An Experimental Study of the Swelling Behaviour of Mudrocks in the presence of Water-based Mud Systems, *Journal of Canadian Petroleum Technology*, 36, 45-50, 1997.

[5] Gray G. R. and Darley H. C. H., Composition and Properties of Oil Well Drilling Fluids, 4th ed., Gulf Publishing Co., Houston, 1980.

[6] Reid P. I., Oil Based Drilling Fluids, Schlumberger Cambridge Research, Internal Exercise, Session 2.5-2.6, 1994.

[7] Ballard T. J., Bearce S. P. and Lawless T. A., Shale Inhibition with Water Based Muds: The Influence of Water Transport Through Shales, *The Proceedings of the fifth International Symposium on Chemistry in the Oil Industry,* The Royal Society of Chemistry, 38-55, 1994.

[8] Reid P. I., Elliot G. P., Minton R. C., Chambers B. D. and Burt D. A., Reduced Environmental Impact Drilling Performance with Water-Based Muds Containing Glycols, SPE/EPA Exploration and Production Environmental Conference, 25989, San Antonio, Texas, 1993.

[9] Bailey L., Reid P. I. and Sherwood J. D., Mechanisms and Solutions for Chemical Inhibition of Shale Swelling and Failure, *The Proceedings of the fifth International Symposium on Chemistry in the Oil Industry,* The Royal Society of Chemistry, 13-27, 1994.

[10] Worrall W. E., Clays and Ceramic Raw Materials, 2nd ed., Elsevier, London, 1986.

[11] Theng B. K. G., Formation and Properties of Clay-Polymer Complexes, Elsevier, Amsterdam, 1979.

[12] Grim R. E., Applied Clay Mineralogy, International Series in the Earth Sciences, McGraw-Hill, New York, 1962.

[13] Grim R. E., Clay Mineralogy, 2nd ed., McGraw-Hill, New York, 1968.

[14] Van Olphen H., An Introduction to Clay Colloid Chemistry, 2nd ed., John Waters, New York, 1977.

[15] Hofmann U., Endell K. and Wilm D., Kristallstruktur und Quellung und Montmorillonite, *Z. Kristallogr.,* 86, 340-348, 1933.

[16] Magdefrau E. and Hofmann U., Die Kristallstruktur des Montmorillonite, *Z. Kristallogr.,* 98, 299-323, 1937.

[17] Hendricks S. B., Lattice Structure of Clay Minerals and Some Properties of Clays, *J. Geol.,* 50,276-290,1942.

[18] Edelman C. H. and Faverjee J. C. L., On the Crystal Structure of Montmorillonite and Halloysite, *Z. Kristallogr.,* 102, 417-431, 1940.

[19] Plee D., Borg F., Gatineau L. and Fripiat J. J., High-Resolution Solid-State ^{27}Al and ^{29}Si Nuclear Magnetic Resonance Study of Pillared Clays, *J. Amer. Chem. Soc.,* 107, 2362-2369, 1985.

[20] Grim R. E. and Kulbicki G., Montmorillonite: High Temperature Reactions and Classification, *Amer. Mineral.,* 46, 1329-1369, 1961.

[21] Güven N., Smectites; in Hydrous Phyllosilicates, Bailey S. W. ed., Mineralogical Society of America, Washington DC, 497-559, 1988.

[22] Landgraf K. F., Distinction Between Cheto and Wyoming Type of Montmorillonites by the Effect of Organic Interlayers on the Optical Refraction, *Chem. Erde,* 38, 97-104, 1979.

[23] Landgraf K. F., Distinction Between Cheto and Wyoming Type of Montmorillonites by the Relative Intensities of the (001) Series of Glycol Complexes, *Chem. Erde,* 38, 233-244, 1979.

[24] Solomon D. H. and Hawthorne D. G., Chemistry of Pigments and Fillers, John Wiley, New York, Ch. 1, 1983.

[25] Bukka K., Miller J. D. and Shabtai J., FTIR Study of Deuterated Montmorillonites: Structural Features Relevant to Pillared Clay Stability, *Clays and Clay Minerals,* 40(1), 92-102, 1992.

[26] van Olphen H. and Fripiat J. J., Data Handbook for Clay Minerals and Other Non-Metallic Minerals, Pergamon Press, New York, 1979.

[27] Peigneur P., Maes A and Cremers A., Heterogeneity of Charge Density Distribution in Montmorillonite as Inferred from Cobalt Adsorption, *Clays and Clay Minerals,* 23,71-75, 1975.

[28] Robertson R. H. S. and Ward R. M., The Assay of Pharmaceutical Clays, *J. Pharm. Pharmacol.,* 3, 27-35, 1951.

[29] Sposito G. and Prost R., Structure of Water on Smectites, *Chem. Rev.,* 82, 553-573, 1982.

[30] Prost R., Interactions between Adsorbed Water Molecules and the Structure of Clay Minerals: Hydration Mechanism of Smectites, *Proc. Int. Clay Conf.,* Clay Minerals Society, Mexico City, 351-359, 1975.

[31] Farmer V. C., Water on Particle Surfaces; in Chemistry of Soil Constituents, Greenland D. G. and Hayes M. H. B. eds., Wiley, New York, 1978

[32] Russell J. D. and Farmer V. C., Infrared Spectroscopic Study of the Dehydration of Montmorillonite and Saponite, *Clay Min. Bull.,* 5, 443-464, 1964.

[33] Johnston C. T., Sposito G, and Erickson C., Vibrational Probe Studies of Water Interactions with Montmorillonite, *Clays and Clay Minerals*, 40, 722-730, 1992.

[34] Bishop J. L., Pieters C. M. and Edwards J. O., Infrared Spectroscopic Analyses on the Nature of Water in Montmorillonite, *Clays and Clay Minerals,* 42, 702-716, 1994.

[35] Poisignon C., Cases J. M. and Fripiat J. J., Electrical-Polarisation of Water Molecules Adsorbed by Smectites: An Infrared Study, *J. Phys. Chem.,* 82, 1855-1860, 1978.

[36] Eisenberg D. and Kauzmann W., The Structure and Properties of Water, Oxford University Press, New York, 1969.

[37] Shulz J. W., On the Raman Spectra of Water and Concentrated Solutions of Alkali Halides, PhD Thesis, Brown University, 1957.

[38] Farmer V. C. and Russell J. D., Interlayer Complexes in Layer Silicates: The Structure of Water in Lamellar Ionic Solutions, *Trans. Farad. Soc.,* 67, 2737-2749, 1971.

[39] Low P. F., The Swelling of Clay: III. Dissociation of exchangeable Cations, *Soil Sci. Soc. Amer. J.,* 45, 1074-1078,1981.

[40] Sposito G., Prost R. and Gaultier J-P., Infrared Spectroscopic Study of Adsorbed Water on Reduced-Charge Na/Li Montmorillonites, *Clays and Clay Minerals,* 31(1), 9-16, 1983.

[41] Shewring N. I. E., Jones T. G. J., Maitland G. and Yarwood J., Fourier Transform Infrared Spectroscopic Techniques to Investigate Surface Hydration Processes on Bentonite, *J. Coll. Int. Sci.,* 176, 308-317, 1995.

[42] Malek Z., Balek V., Garfinkel-Shweky D. and Yariv S., The Study of the Dehydration and Dehydroxylation of Smectites by Emanation Thermal Analysis, *Journal of Thermal Analysis*, 48, 83-92, 1997

[43] Lerot L. and Low P. F., Effect of Swelling on the Infrared Absorption Spectrum of Montmorillonite, *Clays and Clay Minerals,* 24, 191-199, 1976.

[44] Gan H. and Low P. F., Spectroscopic Study of Ionic Adjustment s in the Ionic Double Layer of Montmorillonite, *J. Coll. Int. Sci.,* 161, 1-5, 1993.

[45] Yan L., Roth C. B. and Low P.F., Changes in the Si-O Vibrations of Smectite Layers Accompanying the Sorption of Water, *Langmuir*, 12, 4421-4429, 1996.

[46] MacEwan D. M. C. and Wilson M. J., Interlayer and Intercalation Complexes of Clay Minerals, in Crystal Structures of Clay Minerals and their X-ray Identification, Brindley G. W. and Brown G. eds., Mineralogical Society, London, 1980.

[47] Pons C. H., Tchoubar C. and Tchoubar D., Organisation des Molécules d'Eau à la Surface des Feuillets dans un Gel du Montmorillonite-Na, *Bull. Soc. Franç. Minér.,* 103, 452-456, 1980.

[48] Bradley W. F., Grim R. E. and Clark G. F., A Study of the Behaviour of Montmorillonite on Wetting, *Z. Kristallogr.,* 97, 260-270, 1937.

[49] Mooney R. W., Keenan A. G. and Wood L. A., Adsorption of Water by Montmorillonite. II. Effect of Exchangeable Ions and Lattice Swelling as Measured by X-ray Diffraction, *J. Am. Chem. Soc.,* 74(6), 1371-1374, 1952.

[50] Glaeser R. and Méring J., Homogeneous Hydration Domains of the Smectites, *C.r. hebd. Séanc. Acad. Sci.,* Paris, 267, 436-466, 1968.

[51] Ormerod E. C. and Newman A. C. D., Water Sorption on Ca-Saturated Clays: II. Internal and External Surfaces of Montmorillonite, *Clay Minerals,* 18, 289-299, 1983.

[52] Ben-Rhaiem H. Tessier D. and Pons C. H., Comportment Hydrique et Évolution Structurale et Texturale des Montmorillonites au Cours d'un Cycle de Dessication-Humectation: Partie I. Cas des Montmorillonite Calciques, *Clay Minerals,* 21, 9-29, 1986.

[53] Quirk J. P. and Aylemore L. A. G., Domains and Quasi-Crystalline Regions in Clay Systems, *Soil Sci. Soc. Amer. Proc.,* 35, 652-654, 1971.

[54] Norrish K., Manner of Swelling of Montmorillonites, *Nature,* 173, 256-257, 1954.

[55] Denis J. H., Keall M. J., Hall P. L. and Meeten G. H., Influence of Potassium Concentration on the Swelling and Compaction of Mixed (Na/K) Ion-Exchanged Montmorillonite, *Clay Minerals,* 26, 255-268, 1991.

[56] Slade P. G., Quirk J. P. and Norrish K., Crystalline Swelling of Smectite Samples in Concentrated NaCl Solutions in Relation to Layer Charge, *Clays and Clay Minerals,* 39, 234-238, 1991.

[57] Slade P. G. and Quirk J. P., The Limited Crystalline Swelling of Smectites in $CaCl_2$, $MgCl_2$ and $LaCl_3$ Solutions, *J. Coll. Int. Soc.,* 144, 18-26, 1991.

[58] Laird D. A., Shang C. and Thompson M. L., Hysteresis in Crystalline Swelling of Smectites, *J. Coll. Int. Soc.,* 171, 240-245, 1995.

[59] Ravina I. and Low P. F., Change of b-Dimension with Swelling of Montmorillonite, *Clays and Clay Minerals,* 25, 201-204, 1977.

[60] Odom J. W. and Low P. F., Relation between Swelling, Surface Area and b-Dimension of Na-Montmorillonites, *Clays and Clay Minerals,* 26, 345-351, 1978.

[61] Langmuir I., The Role of Attractive and Repulsive Forces in the Formation of Tactoids, Thixotropic Gels, Protein Crystals and Coacervates, *J. Chem. Phys.,* 6, 873-896, 1938.

[62] Derjaguin B. V., On the Repulsive Forces Between Charged Colloid Particles and On the Theory of Slow Coagulation and Stability of Lyophobe Sols, *Trans. Farad. Soc.,* 36, 203-215, 1940.

[63] Verwey E. J. W. and Overbeek J. Th. G., Theory of the Stability of Lyophobic Colloids, Elsevier, New York, 1948.

[64] Hemwall J. B. and Low P. F., The Hydrostatic Repulsive Force in Clay Swelling, *Soil Sci.,* 82, 135-145, 1956.

[65] Low P. F. and Margheim J. F., The Swelling of Clay: I. Basic Concepts and Empirical Equations, *Soil Sci. Soc. Am. J.,* 43, 473-481, 1979.

[66] Low P. F., The Swelling of Clay: II. Montmorillonites, *Soil Sci. Soc. Am. J.,* 44, 6667-6676, 1980.

[67] Miller S. E. and Low P. F., Characterisation of the Electrical Double Layer of Montmorillonite, *Langmuir,* 6, 572-578, 1990.

[68] Viani B. E., Low P. F. and Roth C. B., Direct Measurement of the Relation between Interlayer Force and interlayer Distance in the Swelling of Montmorillonite, *J. Coll. Int. Sci.,* 96, 229-244, 1983.

[69] Mulla D. J. and Low P. F., The Molar Absorptivity of Interparticle Water in Clay-Water Systems, *J. Coll. Int. Sci.,* 95, 51-60, 1983.

[70] Low P. F. Nature and Properties of Water in Montmorillonite-Water Systems, *Soil Sci. Soc. Am. J.,* 43, 651-658, 1979.

[71] Sun Y., Lin H. and Low P. F., The Non-Specific Interaction of Water with the Surfaces of Clay Minerals, *J. Coll. Int. Sci.,* 112, 556-564, 1986.

[72] Low P. F., The Clay-Water Interface, *Proc. Intrnatl. Clay Conf.,* Denver Colorado, 1985, Schulz L. G., van Olphen H. and Mumpton F. A. eds., The Clay Minerals Society, Indiana, 247-256, 1987.

[73] Low P. F., Interparticle Forces in Clay Suspensions: Flocculation, Viscous Flow and Swelling, in CMS Workshop Lectures Vol. 4, Clay-Water Interface and its Rheological Implications, Güven N. and Pollastro R. M. eds., The Clay Minerals Society, Colorado, 1989.

[74] Israelichvelli J. N. and Adams G. E., Measurement of Forces Between two Mica Surfaces in Aqueous Electrolyte Solutions in the Range 0-100 nm, *J. Chem. Soc. Farad. Trans. I,* 74, 975-1001, 1978.

[75] Pashley R. M., Hydration Forces between Mica Surfaces in Aqueous Electrolyte Solutions, *J. Coll. Int. Sci.* 80, 153-162, 1981.

[76] Israelichvelli J. N. and Pashley R. M., Molecular Layering of Water at Surfaces and Origin of Repulsive Forces, *Nature,* 306, 249-250, 1983.

[77] Pashley R. M. and Quirk J. P., The Effect of Cation Valency on DLVO and Hydration Forces Between Macroscopic Sheets of Muscovite Mica in Relation to Clay Swelling, *Colloids and Surfaces*, 9, 1-17, 1984.

[78] Skipper N. T., Refson K. and McConnell J. D. C., Computer Simulation of Interlayer Water in 2-1 Clays, *J. Chem. Phys.,* 94, 7434-7445, 1991.

[79] Chang F-R. C., Skipper N. T. and Sposito G., Computer Simulation of Interlayer Molecular Structure in Sodium Montmorillonite Hydrates, *Langmuir,* 11, 2734-2741, 1995.

[80] Chang F-R. C., Skipper N. T. and Sposito G., Monte Carlo and Molecular Dynamics Simulations of Electrical Double-Layer Structure in Potassium-Montmorillonite Hydrates, *Langmuir*, 14, 1201-1207, 1998.

[81] Delville A., Structure of Liquids at a Solid Interface: An Application to the Swelling of Clay by Water, *Langmuir,* 8, 1796-1805, 1992.

[82] Karaborni S., Smit B., Heidug W., Urai J. and van Oort E., The swelling of Clays: Molecular Simulations of the Hydration of Montmorillonite, *Science*, 271, 1102-1104, 1996.

[83] Hunter R. J., Foundations of Colloid Science, Vol. 1., Oxford University Press, Oxford, 1992.

[84] Napper D. H., Polymeric Stabilisation of Colloidal Dispersions, Academic Press, London, 1983.

[85] Burchill S., Hall P. L., Harrison R., Hayes M. H. B., Langford J. I., Livingstone W. R., Smedley R. J., Ross D. K. and Tuck J. J., *Clay Minerals,* 18, 373-397, 1983.

[86] Cowie J. M. G., Polymers: Chemistry and Physics of Modern Materials, 2nd edn., Blackie, Chapman and Hall, 1991.

[87] Flory P. J., Principles of Polymer Chemistry, Cornell University Press, Ithaca, New York, 1953.

[88] Flory P. J. and Krigbaum W. R., Statistical Mechanics of Dilute Polymer Solutions, *J. Phys. Chem.,* 18, 1086-1094, 1950.

[89] Phillipova O. E., Kuchanov S. I., Topchieva I. N. and Kabonov V. A., Hydrogen Bonds in Dilute Solutions of Polyethylene Glycol, *Macromolecules,* 18, 1628-1633, 1985.

[90] Lusse S. and Arnold K., The Interaction of Poly(ethylene glycol) with Water Studied by ^{1}H and ^{2}H NMR Relaxation Time Measurements, *Macromolecules*, 29, 4251-4257, 1996.

[91] Liu K-J. and Parsons J. L., Solvent Effects on the Preferred Conformation of Poly (ethylene glycols), *Macromolecules*, 2(5) 529-533, 1969.

[92] Kjellander R. and Florin E., Water Structure and Changes in Thermal Stability of the System Polyethylene Oxide-Water, *J. Chem. Soc., Faraday Trans. I*, 77, 2053-2077, 1981.

[93] Khoultchaev K. K., Kerekes R. J. and Englezos P., The Role of Poly (ethylene oxide)-Water Solution Phase Behaviour in the Retention of Fibre Fines and Clay, *The Canadian Journal of Chemical Engineering*, 75, 161-166, 1997.

[94] Chaiko D. J., Aggregation of Polyethylene Oxide in Aqueous Solutions, *Abs. Papers Amer. Chem. Soc.*, 207, 65, 1994.

[95] Bednar B., Li Z., Huang Y., Chang L-C. P. and Morawetz H., Fluorescence Study of the Factors Affecting the Complexation of Poly (acrylic acid) with Poly (oxyethylene), *Macromolecules*, 18, 1829, 1985.

[96] Maltesh C., Somasundaran P., Pradip, Kulkarni R. A. and Gundiah S., Effects of Degree of Hydrolysis of Polyacrylamide on Its Interactions with Poly(ethylene oxide) and Poly(vinylpyrrolidone), *Macromolecules*, 24, 5775-5778, 1991.

[97] Poonia N. S. and Bajaj A. V., Co-ordination Chemistry of Alkali and Alkaline Earth Cations, *Chem. Rev.*, 79, 389-445, 1979.

[98] Cobranchi D. P., Garland B. A., Masiker M. C., Eyring E. E., Firman P. and Petrucci S., Relaxation Kinetics and Infrared Spectra of the Complexation of Lithium Ion by Triethylene and by Tetraethylene Glycol in Acetonitrile, *J. Phys. Chem.*, 96, 5836-5865, 1992.

[99] Bauer C. B. and Rogers R. D., Structural Analyses of Group 2 Metal/Polyethylene Glycol Complexes, *Abs. Papers Amer. Chem. Soc.,* 207, 472, 1994.

[100] Fleer G. J. and Lyklema J., in Adsorption from solution at the solid-liquid interface, Parfitt G. D. and Rochester C. H. eds., Academic Press, 153-220, 1983.

[101] Scheutjens J. M. H. M., and Fleer G. J., Some Implications of Recent Polymer Adsorption Theory, in The Effect of Polymers on Dispersion Properties, Tadros Th. F. ed., Academic Press, New York, 144-168, 1982.

[102] Ash S. G., Polymer Adsorption at the Solid-liquid Interface in: *Colloid Science Vol. 1, Specialist Periodical Reports,* The Chemical Society, London, 103-122, 1973.

[103] Elaissari A., Haouam A., Huguenard C. and Pefferkorn E., Kinetic Factors in Polymer Adsorption at Solid/Liquid Interfaces. Methods of Study of the Adsorption Mechanism, *J. Coll. Int. Sci.,* 149, 68-83, 1992.

[104] Tadros Th. F., Polymer Adsorption and Dispersion Stability, in The Effect of Polymers on Dispersion Properties, Tadros Th. F. ed., Academic Press, New York, 1-38, 1982.

[105] Killmann E., Conformation and Thermodynamics of Adsorbed Macromolecules at the Liquid/Solid Interface, *Polymer,* 17, 864-868, 1976.

[106] Cosgrove T., Heath T. G., Ryan K. and Crowley T. L., Neutron Scattering from Adsorbed Polymer Layers, *Macromolecules,* 20, 2879-2882, 1987.

[107] Silberberg A., The Adsorption of Flexible Macromolecules. Part I. The Isolated Macromolecule at a Plane Interface, *J. Phys. Chem.,* 66, 1872-1883, 1962.

[108] Cosgrove T., Griffiths P. C. and Lloyd P. M., Polymer Adsorption. The Effect of the Relative Sizes of Polymer and Particle, *Langmuir,* 11, 1457-1463, 1995.

[109] Furusawa K., Shou Z. and Nagahashi N., Polymer Adsorption on Fine Particles; The Effect of Particle Size and its Stability, *Coll. Polymer Sci.,* 270, 212-218, 1992.

[110] Hesselink F. Th., in Adsorption from solution at the solid-liquid interface, Parfitt G. D. and Rochester C. H. eds., Academic Press, 277-412, 1983.

[111] Somasundaran P. and Kunjappu J. T., In-Situ Investigation of Adsorbed Surfactants and Polymers on Solids in Solution, *Colloids and Surfaces,* 37, 245-268, 1989.

[112] Miller J. D. and Kellar J. J., Quantitative In-Situ Analysis of Collector Adsorption Reactions by FTIR Internal Reflection Spectroscopy, in Challenges in Mineral Processing, Ch. 6, Symp. Proc., California, 1988, Sastry K. V. S. and Fuerstenau M. C. eds., Society of Mining Engineers, California, 109-129, 1988.

[113] Morris H. H. and Brooks L. E., Pigmentation of Paper Goods, Pigment Handbook, Vol. 2, Patton T. C. ed., 205-213, Wiley, New York, 1974.

[114] Mortland M. M. Clay Organic Complexes and Interactions, *Advances in Agronomy,* 22, 75-117, 1970.

[115] Parfitt G. D. and Rochester C. H., in Adsorption from solution at the solid-liquid interface, Parfitt G. D. and Rochester C. H. eds., Academic Press, 3-47, 1983.

[116] Theng B. K. G., Clay-Polymer Interactions and Perspectives, *Clays and Clay Minerals,* 1, 1-10, 1982.

[117] Parfitt G. D. and Greenland D. J., The Adsorption of Poly(ethylene glycols) on Clay Minerals, *Clay Minerals,* 8, 305-315, 1970.

[118] Parfitt G. D. and Greenland D. J., Adsorption of water by Montmorillonite-Poly(ethylene glycol) Adsorption Products, *Clay Minerals,* 8, 317-324, 1970.

[119] Theng B. K. G., Formation and Properties of Clay-Polymer Complexes, Elsevier, Amsterdam, 1979.

[120] Brindley G. W., Ethylene Glycol and Glycerol Complexes of Smectites and Vermiculites, *Clay Minerals,* 6, 237-259, 1966.

[121] Theng B. K. G., The Chemistry of Clay Organic Reactions, Adam Hilger, London, 1974.

[122] Bradley W. F., Molecular Associations Between Montmorillonite and some Poly-Functional Organic Liquids, *J. Am. Chem. Soc.,* 67, 975-981, 1945.

[123] MacEwan D. M. C., Complexes of Clays with Organic Compounds I. Complex Formation Between Montmorillonite and Halloysite and Certain Organic Liquids, *Trans. Farad. Soc.,* 44, 349-367, 1948.

[124] Dowdy R. H. and Mortland M. M. Alcohol-Water Interactions on Montmorillonite Surfaces: II Ethylene Glycol, *Soil Science,* 105(1), 36-43, 1967.

[125] Tettenhorst R., Beck C. W. and Brunton G., Montmorillonite-Polyalcohol Complexes, *Clays and Clay Minerals,* 9, 500-519, 1962.

[126] Mackenzie R. C. Complexes of Clays with Organic Compounds. Pt II. Investigation of the Ethylene Glycol-Water-Montmorillonite System Using the Karl Fischer Reagent, *Trans. Farad. Soc.,* 44, 368-375, 1948.

[127] Reynolds R. C. An X-ray Study of an Ethylene Glycol-Montmorillonite Complex, *Am. Mineralogist,* 50, 990-1001, 1965.

[128] Hsieh Y. P., Effects of Relative Humidity on the Basal Expansion of Mg-Smectite Equilibrated with Ethylene Glycol at Low Vapour Pressure, *Clays and Clay Minerals,* 37(5), 459-463, 1989.

[129] McNeal B. L., Effect of Exchangeable Cations on Glycol Retention by Clay Minerals, *Soil Science,* 97, 96-102, 1964.

[130] Mortland M. M. and Erickson A. E., Surface Reactions of Clay Minerals, *Soil Sci. Soc. Am. Proc.,* 20, 476-479, 1956.

[131] Jonas E. C. and Thomas G. L., Hydration Properties of K-Deficient Micas, *Clays and Clay Minerals,* 8, 183-192, 1960.

[132] Kunze G. W. Anomalies in the Ethylene Glycol Solvation Technique Used in X-ray Diffraction, *Clays and Clay Minerals* 3, 88-93, 1955.

[133] Volzone C., Cavalieri A. L. and Porto-Lopez J. M., Modifications of Unit Cell Parameters in Bentonite-Ethylene Glycol Complexes, *Materials Research Bulletin,* 23, 935-942, 1988.

[134] Brunton G., Tettenhorst R. and Beck C. W., Montmorillonite-Polyalcohol Complexes II, *Clays and Clay Minerals,* 11, 105-116, 1963.

[135] Eltantaway I. M. and Arnold P. W. Ethylene Glycol Sorption by Homoionic Montmorillonites, *J. Soil Sci.,* 25(1), 99-110, 1974.

[136] Dyal R. S. and Hendricks S. B., Total Surface of Clay in Polar Liquids as Characteristic Index, *Soil Sci.,* 69, 421-432, 1950.

[137] Eltantaway I. M. and Arnold P. W. Reappraisal of Ethylene Glycol Mono-Ethyl Ether (EGME) Method for Surface Area Estimations of Clays, *J. Soil Sci.,* 24(2), 232-238, 1973.

[138] Grandjean J., Interaction of Poly(ethylene glycol) Monoalkyl Ethers with Synthetic Saponites in Aqueous Suspensions: A Multinuclear Magnetic Resonance Study, *Langmuir,* 14, 1037-1040, 1998.

[139] Nguyen T. T., Raupach M. and Janik L. J., Fourier Transform Infrared Study of Ethylene Glycol Monoethyl Ether on Montmorillonite: Implications for Surface Area Measurements of Clays, *Clays and Clay Minerals,* 35(1), 60-67, 1987.

[140] Theng B. K. G., The Chemistry of Clay-Organic Reactions, Adam Hilger, London, 1974.

[141] Zhao X., Urano K. and Ogasawara S., Adsorption of Polyethylene Glycol from Aqueous Solution on Montmorillonite, *Colloid Polym. Sci.,* 267, 899-906, 1989.

[142] Moudgil B. M., Behl S. and Kulkarni N. S, Measurement of Heat of Adsorption of Polyethylene Oxide on Dolomite, Silica and Alumina by Microcalorimetry, *J. Coll. Int. Sci.,* 148(2), 337-342, 1992.

[143] Trens P. and Denoyl R., Conformation of Poly(ethylene glycol) Polymers at the Silica/Water Interface: A Microcalorimetric Study, *Langmuir,* 9, 519-522, 1993.

[144] Ruiz-Hitzky E. and Casal B., Crown Ether Intercalation with Phyllosilicates, *Nature,* 276, 596-597, 1978.

[145] Casal B., Aranda P., Sanz J. and Ruiz-Hitzky E., Interlayer Adsorption of Macrocyclic Compounds (Crown-Ethers and Cryptands) in 2:1 Phyllosilicates: II Structural Features, *Clay Minerals,* 29, 191-203, 1994.

[146] Ruiz-Hitzky E. and Aranda P., Polymer-Salt Intercalation Complexes in Layer Silicates, *Adv. Mater.,* 11, 545-547,1990.

[147] Wu J. and Lerner M. M., Structural, Thermal and Electrical Characterisation of Layered Nanocomposites Derived from Na-Montmorillonite and Polyethers, *Chem. Mater,* 5, 835-838, 1993.

[148] Rubio J. and Kitchener J. A., The Mechanism of Adsorption of Poly (Ethylene Oxide) Flocculent on Silica, *J. Coll. Int. Sci.,* 57, 132-142, 1976.

[149] Behl S .and Moudgil M., Mechanisms of Poly(Ethylene Oxide) Interactions with Dolomite and Apatite, *J. Coll. Int. Sci.,* 161,443-449, 1993.

[150] Aston M. S. and Elliott G. P., Water-Based Glycol Drilling Muds: Shale Inhibition Mechanisms, SPE European Petroleum Conference, 28818, London, 1994.

[151] Downs J. D., van Oort E., Redman D. I., Ripley D. and Rothman B., A New Concept in Water-Based Drilling Fluids for Shales, SPE Offshore Europe Conference, 28960, Aberdeen, 1993.

[152] Mortland M. M., Urea Complexes with Montmorillonite: an Infrared Study., *Clays and Clay Minerals,* 6, 143-146, 1966.

[153] Stutzmann Th. and Siffert B., Contribution to the Adsorption Mechanism of Acetamide and Polyacrylamide on to Clays, *Clays and Clay Minerals,* 25, 392-406, 1977.

[154] Espinasse P. and Siffert B., Acetamide and Polyacrylamide Adsorption onto Clays: Influence of the Exchangeable Cation and the Salinity of the Medium, *Clays and Clay Minerals,* 27, 279-284, 1979.

[155] Bottero J. Y., Bruant M., Cases J. M., Canet D. and Fiessinger F., Adsorption of Nonionic Polyacrylamide on Sodium Montmorillonite: Relation between Adsorption ζ Potential, Turbidity, Enthalpy of Adsorption Data and ^{13}C-NMR in Aqueous Solution, *J. Coll. Int. Sci.,* 124(2), 515-527, 1988.

[156] Schamp N. and Huylebroeck J., Adsorption of Polymers on Clays, *J. Polymer Sci.* Symp., 42(2), 553-562,1973.

[157] Volpert E., Selb J., Candau F., Green N., Argillier J. F. and Audibert A., Adsorption of Hydrophobically Associating Polyacrylamides on Clay, *Langmuir* 14, 1870-1879, 1998.

[158] Argillier J-F., Audibert A., Lecourtier J., Moan M. and Rousseau L., Solution and Adsorption Properties of Hydrophobically Associating Water Soluble Polyacrylamides, *Colloids and Surfaces A*, 113, 247-257, 1996.

[159] Lee L. T., Rahbari R., Lecourtier J. and Chauveteau G., Adsorption of Polyacrylamides on the Different Faces of Kaolinite, *J. Coll. Int. Sci.,* 147(2), 351-357, 1991.

[160] Griot O. and Kitchener J. A., Surface Silanol Groups in the Flocculation of Silica Suspensions by Polyacrylamide II. Surface Changes of Silica Suspensions on Ageing, *Trans. Farad. Soc.,* 61, 1032-1038, 1965.

[161] Pefferkorn E., Nabzar L. and Carroy A., Adsorption of Polyacrylamide to Na Kaolinite: Correlation between Clay Structure and Surface Properties, *J. Coll. Int. Sci.,* 106(1), 94-103, 1985.

[162] Atesok G., Somasundaran P. and Morgan L. J., Charge Effects in the Adsorption of Polyacrylamides on Sodium Kaolinite and its Flocculation, *Powder Technology,* 54, 77-83, 1988.

[163] Atesok G., Somasundaran P. and Morgan L. J., Adsorption Properties of Ca^{2+} on Na-Kaolinite and Its Effect on Flocculation Using Polyacrylamides, *Colloids and Surfaces,* 32, 127-138, 1988.

[164] Lee L. T., Lecourtier J. and Chauveteau G., Influence of Calcium on Adsorption Properties of Enhanced Oil Recovery Polymers, Ch. 11, *ACS Symposium Series,* 396, 224-240, 1989.

[165] Lee L. T. and Somasundaran P., Adsorption of Polyacrylamide on Oxide Minerals, *Langmuir,* 5, 854-860, 1989.

[166] Lecourtier J., Lee L. T. and Chauveteau G., Adsorption of Polyacrylamides on Siliceous Minerals, *Colloids and Surfaces,* 47, 219-231, 1990.

[167] Page M., Lecourtier J., Noïk C. and Foissy A., Adsorption of Polyacrylamides and of Polysaccharides on Siliceous Materials and Kaolinite: Influence of Temperature, *J. Coll. Int. Sci.,* 161(1), 450-454, 1993.

[168] Broseta D. and Medjahed F., Effects of Substrate Hydrophobicity on Polyacrylamide Adsorption, *J. Coll. Int. Sci.,* 170, 457-465, 1995.

[169] Song S., Ke J., Han B., Yang G. and Yan H., Enthalpy of Adsorption and Adsorption Isotherms of Polyacrylamide on Sea Sand, *Journal of Thermal Analysis,* 45, 7-12, 1995.

[170] Audibert A., Bailey L., Hall P., Keall M. and Lecourtier J., The role of Clay/Polymer Interactions in Clay Stabilisation During Drilling, Physical Chemistry of Colloids and Interfaces in Oil Production, 6th Research Conference on Exploration-Production, Saint-Raphaël, France, 1991.

[171] Bocquenet Y. and Siffert B., Polyacrylamide Adsorption onto Kaolinite and Illite in the Presence of Sodium Dodecylbenzenesulfonate, *Colloids and Surfaces,* 9, 147-161, 1984.

[172] Chauveteau G., Lecourtier J. and Lee L. T., Reduction of Polymer Adsorption on Reservoir Rocks, *Revue De L'Institut Français Du Pétrole,* 43(4) 533-543, 1988.

[173] Siffert B. and Bocquenet Y., Polyacrylamide Adsorption onto Kaolinite in the Presence of Sodium Dodecylbenzenesulfonate in Saline Medium, *Colloids and Surfaces,* 11, 137-143, 1984.

[174] Michaels A. S. and Morelos O., Polyelectrolyte Adsorption by Kaolinite, *Industrial and Engineering Chemistry,* 47(9),1801-1809, 1955.

[175] Banwell C. N., Fundamentals of Molecular Spectroscopy, 3rd ed., McGraw-Hill, 1983.

[176] Herzberg G., Infrared and Raman Spectra of Polyatomic Molecules, Van Nostrand, Princeton, New Jersey, 1945.

[177] Hollas J. M., Modern Spectroscopy, John Wiley, New York, 1988.

[178] Potts W. J. Jr. Chemical Infrared Spectroscopy, Vol. 1: Techniques, John Wiley, New York, 1963.

[179] Atkins P. W., Molecular Quantum Mechanics, 2nd ed., Oxford University Press, 1989.

[180] Griffiths P. R. and de Haseth J. A., Fourier Transform Infrared Spectroscopy, Wiley, New York, 1986.

[181] Chamberlain J. E., The Principles of Interferometric Spectroscopy, Wiley, New York, 1979.

[182] Farmer V. C., The Infrared Spectra of Minerals, Mineralogical Society, London, 1974.

[183] Kauppinen J. K., Moffatt D. J., Mantsch H. H. and Cameron D. G., Fourier Self Deconvolution: A Method for Resolving Intrinsically Overlapped Bands, *Applied Spectroscopy,* 35, 271-276, 1981.

[184] Mantsch H. H and Moffatt D. J., Computer Aided Methods for the Resolution Enhancement of Spectral Data with Special Emphasis on Infrared Spectra, NATO ASI Ser C, Recent Experimental and Computational Advances in Molecular Spectroscopy, 406, 113-124, 1993.

[185] Kauppinen J. K., Moffatt D. J., Cameron D. G. and Mantsch H. H., Noise in Fourier Deconvolution, *Applied Optics,* 20, 1866-1879, 1981.

[186] James D. I. Maddams W. F. and Tooke P. B., The Use of Fourier Deconvolution in Infrared Spectroscopy. Part I: Studies with Synthetic Single Peaks, *Applied Spectroscopy*, 41, 1362-1370, 1987.

[187] Smeller L., Goossens K. and Heremans K., How to Minimise Certain Artefacts in Fourier Self-Deconvolution, *Applied Spectroscopy*, 49, 1538-1542, 1995.

[188] Economou I. G., Cui Y. and Donohue M. C., Hydrogen bonding in Polymer Solvent Mixtures, *Macromolecules*, 24, 5058-5067 1991.

[189] Seshadri K. S. and Jones R. N., The Shapes and Intensities of Infrared Absorption Bands- An Overview, *Spectrochimica Acta*, 19, 1013-1085, 1963.

[190] Russell J. D. and Farmer A. R., Infrared Methods, in Clay Mineralogy: Spectroscopic and Chemical Determinative Methods, Wilson M. J. ed., Chapman and Hall, London, 1994.

[191] Farmer V. C. and Russell J. D., Effects of Particle Size and Structure on the Vibrational Frequencies of Layer Silicates, *Spectrochimica Acta*, 22, 389-398, 1966.

[192] Brown G and Brindley G. W., X-ray Diffraction Procedures for Clay Mineral Identification, in Crystal Structures of Clay Minerals and their X-ray Identification, Brindley G. W. and Brown G. Eds., Mineralogical Society, London, 1980.

[193] Craciun C., Influence of the Fe^{3+} for Al^{3+} Substitution on the IR Spectra of Montmorillonite Minerals, *Spectroscopy Lett.*, 17, 579-590, 1984.

[194] Madejová J., Putyera K. and Cicel B., Proportion of Central Atoms in Octahedra of Smectites Calculated From Infrared Spectra, *Geol. Carpathica Ser. Clays*, 43, 117-120, 1992.

[195] Madejová J., Komadel P. and Cicel B., Infrared Study of Octahedral Site Populations in Smectites, *Clay Minerals*, 29, 319-326, 1994.

[196] Serratosa J. M. and Bradley W. F., Determination of the Orientation of OH Bond Axes in Layer Silicates by Infrared Absorption, *J. Phys. Chem.,* 62, 1164-1167, 1958.

[197] Farmer V. C. and Russell J. D., The Infrared Spectra of Layer Silicates, *Spectrochimica Acta,* 20, 1149-1173, 1964.

[198] Roush P. B., The Design Handling and Applications of Infrared Microscopes, ASTM Special Technical Publications 949, 1985.

[199] Messerschmidt R. G. and Harthcock M. A., Infrared Microspectroscopy Theory and Applications, Practical Spectroscopy Series Vol 6.

[200] Harrick N. J., Surface Chemistry from Spectral Analysis of Totally Internally Reflected Radiation, *J. Phys. Chem.* 64, 1110, 1960.

[201] Harrick N. J., Internal Reflection Spectroscopy, Harrick Scientific Corp., Wiley Interscience, New York, 1967.

[202] Mirabella F. M. Jr., Internal Reflection Spectroscopy, *Appl. Spec. Rev.,* 21(1,2), 45-178, 1985.

[203] Muller G., Abraham K. and Schaldach M., Quantitative ATR Spectroscopy-Some Basic Considerations, *Applied Optics,* 20(7), 1182-1190, 1981.

[204] Billingham J., Breen C. and Yarwood J., Adsorption of Polyamine, Polyacrylic Acid and Polyethylene Glycol on Montmorillonite: An In Situ Study using ATR-FTIR, *Vibrational Spectroscopy,* 14, 19-34, 1997.

[205] Billingham J. Breen C. and Yarwood J., In Situ Determination of Bronsted/Lewis Acidity on Cation Exchanged Clay Mineral Surfaces by ATR-IR, *Clay Minerals,* 31, 513-522, 1996.

[206] Miller J. D., Kellar J. J. and Cross W. M., Infrared Spectroscopy for In-Situ Characterisation of Surface Reactions, in Advances in Coal and Mineral Processing Using Flotation, Ch. 4, Proc. Eng. Found. Conf., Chander S. and Klimpel R. R. eds., Society for Mining, Metallurgy and Exploration Inc., Florida, 33-44, 1989.

[207] Mielczarski J., In-Situ ATR-IR Spectroscopic Study of Xanthate Adsorption on Marcasite, *Colloids and Surfaces*, 17, 251-271, (1986)

[208] Mielczarski J., Cases J. M., Bouquet E., Barres O. and Delon J. F., Nature and Structure of Adsorption Layer on Apatite Contacted with Oleate Solution. 1. Adsorption and Fourier Transform Infrared Reflection Studies, *Langmuir*, 9, 2370-2382, 1993.

[209] Hunter D. B. and Bertsch P. M., In Situ Measurements of Tetraphenylboron Degradation Kinetics on Clay Mineral Surfaces by IR, *Environ. Sci. Technol.*, 28, 686-691, 1994.

[210] Raupach M. and Janik L. J., The Orientation of Ornithine and 6-Aminohexanoic Acid Adsorbed on Vermiculite from Polarized IR ATR Spectra, *Clays and Clay Minerals*, 24, 127-133, 1976.

[211] Guzonas D. A., Hair M. L., and Tripp C. P., Measurement of Monolayers Adsorbed on Mica, in FTIR Spectroscopy in Colloid and Interface Science, Ch. 14, *ACS Symp. 447*, 237-250, 1990.

[212] Banga R., Vibrational Spectroscopy and Atomic Force Microscopy Studies of Silane Adsorption onto Silica and Glass, PhD Thesis, Sheffield Hallam University, 1995.

[213] Kuys K. K. and Roberts N. K., In Situ Investigation of the Adsorption of Styrene Phosphonic Acid on Cassiterite by FTIR-ATR Spectroscopy, *Colloids and Surfaces,* 24, 1-17, 1987.

[214] Sperline R. P., Song Y. and Freiser H., Fourier Transform Infrared Attenuated Total Reflection Spectroscopy Linear Dichroism Study of Sodium Dodecyl Sulfate Adsorption at the Al_2O_3/Water interface Using Al_2O_3-Coated Optics, *Langmuir,* 8, 2183-2191, 1992.

[215] Couzis A. and Gulari E., Adsorption of Sodium Laurate from Its Aqueous Solution onto an Alumina Surface. A Dynamic Study of the Surface-Surfactant Interaction Using Attenuated Total Reflection Fourier Transform Infrared Spectroscopy, *Langmuir,* 9, 3414-3421, 1993.

[216] Nunn N. S., FTIR and Rheological Studies of Surfactant Adsorption onto Silica, PhD Thesis, University of Durham, 1993.

[217] Parry D. B. and Harris J. M., Attenuated Total Reflection FT-IR Spectroscopy to Measure Interfacial Reaction Kinetics at Silica Surfaces, *Applied Spectroscopy,* 42, 997-1004, 1988.

[218] Cross W. M. Kellar J. J. and Miller J. D., Conformation of Adsorbed Species in the Alumina/Sodium Dodecyl Sulfate/Water System as Determined by In-Situ FTIR/IRS, XVIIth International Mineral Processing Congress, Preprints Vol. 2, Fine Particles Processing Flotation, Dresden, 319-338, 1991.

[219] Yalamanchilli M. R., Kellar J. J. and Miller J. D., In-Situ FT-IR Internal Reflection Spectroscopy of Collector Adsorption Phenomena in Soluble-Salt Flotation Systems, XVIIth International Mineral Processing Congress, Preprints Vol. 5, Processing of Potash Ores, Dresden, 131-142, 1991.

[220] Sperline R. P., Muralidharan S. and Freiser H., In-Situ Determination of Species Adsorbed at a Solid-Liquid Interface by Quantitative Infrared Attenuated Total Reflectance Spectrophotometry, *Langmuir*, 3, 198-202, 1987.

[221] Haller G. L. and Rice R. W., A Study of Adsorption on Single Crystals by Internal Reflectance Spectroscopy, *J. Phys. Chem.*, 74(25), 4386-4393, 1970.

[222] Cullity B. D., Elements of X-Ray Diffraction, 2nd ed., Addison-Wesley Pub. Co., Massachusetts, 1978.

[223] Moore D. M. and Reynolds R. C. Jr., X-ray Diffraction and the Identification and Analysis of Clay Minerals, Oxford University Press, New York, 1989.

[224] MacEwen D. M. C., Identification of the Montmorillonite Group of Minerals by X-rays, *Nature,* 154, 577-578, 1944.

[225] Giles H. L., Hurley P. W. and Webster H. W. M., Simple Approach to the Analysis of Oxides, Silicates and Carbonates Using X-Ray Fluorescence Spectrometry, *X-Ray Spectrometry*, 24, 205-218, 1995.

[226] Ngyugen T. T., Janik L. J. and Raupach M., Diffuse Reflectance Infrared Fourier Transform (DRIFT) Spectroscopy in Soil Studies, *Aust. J. Soil Res.,* 29, 49-67, 1991

[227] Margulies L., Rozen H. and Banin A., Use of X-ray Powder Diffraction and Linear Dichroism Methods to Study the Orientation of Montmorillonite Clay Particles, *Clays and Clay Minerals,* 36, 476-479, 1988.

[228] Jones T. G. J., Hughes T. L. and Tompkins P. G., European Patent Application EP 0 507 405 A2, October , 1992.

[229] Cebula D. J., Thomas R. K., Middleton S., Ottewill R. H. and White J. W., Neutron Diffraction from Clay-Water Systems, *Clays and Clay Minerals,* 27, 39-52, 1979.

[230] Farmer V. C., in Data Handbook of Clay Minerals and Other Non-Metallic Minerals, van Olphen H. and Fripiat H. H. eds., Pergamon Press, Oxford, 1979.

[231] Jones T. G. J., Design of a High Temperature/High Temperature ATR Cell: Application to Monitoring Cement Hydration, Schlumberger Cambridge Research, Internal Scientific Report, SCR/SR/1994/023/WPC/U.

[232] Jones T.G.J., Schlumberger Cambridge Research, Private Communication.

[233] Kulicke W. M., Kniewske R. and Klein J., Preparation, Characterisation, Solution Properties and Rheological Behaviour of Polyacrylamide, *Prog. Polym. Sci.,* 8, 373-468, 1982.

[234] Bellamy L. J., The Infrared Spectra of Complex Molecules, Vol. 2, 2nd ed., Chapman and Hall, London, 1980.

[235] Bellamy L. J., The Infrared Spectra of Complex Molecules, Vol. 1, 3rd ed., Chapman and Hall, London, 1975.

[236] Mortland M. M. and Tahoun S. A., Complexes of Montmorillonite with Primary, Secondary and tertiary Amides: II, *Soil Science,* 102, 314-321, 1966.

[237] Silverstein R. M., Bassler G. C. and Morrill T. C., Spectrometric Identification of Organic Compounds, 4th ed. John Wiley, New York, 1981.

[238] Snyder R. G. and Zerbi G. Vibrational Analysis of Ten Simple Aliphatic Ethers: Spectra, Assignments, Valence Force Field and Molecular Conformations, *Spectrochim. Acta*, 23A, 391-437, 1967.

CONFERENCES ATTENDED

1. SCI: Second UK Colloid and Surface Science Student Meeting

   University of Nottingham

   18-21 April 1993

2. Infrared and Raman Discussion Group: Martin and Willis Prize Meeting

   University of Nottingham

   12 April 1994

3. Faraday Discussion 98: Polymer at Interfaces

University of Bristol

12-14 September 1994

4. Infrared and Raman Discussion Group: Martin and Willis Prize Meeting

   Rutherford Appleton Laboratory

   5-6 April 1995

5. SCI: Third UK Colloid and Surface Science Student Meeting

   University of Hull

   16-19 July 1995